EFFECTS OF SECONDARY BINDING MOTIFS IN ARYLETHYNYL ANION RECEPTORS

by

LISA MARIE EYTEL

A DISSERTATION

Presented to the Department of Chemistry and Biochemistry
and the Graduate School of the University of Oregon
in partial fulfillment of the requirements
for the degree of
Doctor of Philosophy

June 2019

DISSERTATION APPROVAL PAGE

Student: Lisa Marie Eytel

Title: Effects of Secondary Binding Motifs in Arylethynyl Anion Receptors

This dissertation has been accepted and approved in partial fulfillment of the requirements for the Doctor of Philosophy degree in the Department of Chemistry and Biochemistry by:

Ramesh Jasti	Chairperson
Darren W. Johnson	Advisor
Michael M. Haley	Advisor
Victoria DeRose	Core Member
Ellen K. Scott	Institutional Representative

and

Janet Woodruff-Borden	Vice Provost and Dean of the Graduate School

Original approval signatures are on file with the University of Oregon Graduate School.

Degree awarded June 2019

DISSERTATION ABSTRACT

Lisa Marie Eytel

Doctor of Philosophy

Department of Chemistry and Biochemistry

June 2019

Title: Effects of Secondary Binding Motifs in Arylethynyl Anion Receptors

Anions are abundant throughout our environmental and biological systems. These negatively charged and weakly coordinating species play crucial roles as ingredients in soil fertilizers and regulators of cellular processes. Supramolecular interactions, like anion-π, weak-σ, and hydrogen bonding, offer a convenient method to identify and quantify a variety of anions. However, we struggle to design selective molecular receptors due to the inherently complex thermodynamic and kinetic processes involved in host-guest interactions.

2,6-bis(anilinoethynyl) receptors and the mono(anilinoethynyl) derivatives offer an easily modified scaffold for studying the influence of supporting secondary interactions on anion selectivity. Two mono-urea receptors with the ability to bind anions via anion-pi, aryl CH-hydrogen bonds, or weak-sigma interactions were synthesized. Association constants with halide anions Cl-, Br-, and I-, were measured by 1H NMR spectroscopy and UV-Vis spectroscopy titrations. The receptors aggregated to form a 2-to-1 host-guest complex, with a different mechanism of complexation based on the supporting interaction of the aromatic core. Three additional bis-urea receptors with different secondary-binding motifs were synthesized and found to bind three disparate oxoanions at similarly high-affinities in non-polar solvents. In polar solvents, however,

the receptors bound each oxoanion in a predictable manner based on the acidity of the conjugate acid of the guest. This understanding is applied through an array of differentially substituted receptors for anions of environmental and biological interests.

This dissertation contains previously published and unpublished co-authored material.

CURRICULUM VITAE

NAME OF AUTHOR: Lisa Marie Eytel

GRADUATE AND UNDERGRADUATE SCHOOLS ATTENDED:

University of Oregon, Eugene
Russell Sage College, Troy

DEGREES AWARDED:

Doctor of Philosophy, Chemistry, 2019, University of Oregon
Bachelor of Science, Chemistry, 2014, Russell Sage College
Bachelor of Science, Forensic Science, 2014, Russell Sage College

AREAS OF SPECIAL INTEREST:

Physical Organic Chemistry
- Supramolecular chemistry
- Host-guest chemistry

Science Pedagogy
- Chemical education practices
- Organic chemistry education practices
- K-12 STEM teaching methods
- Teaching science communication

PROFESSIONAL EXPERIENCE:

Graduate Research Assistant, Department of Chemistry and Biochemistry
University of Oregon, Eugene, Oregon, 2014-2019

Graduate Teaching Assistant, Department of Chemistry and Biochemistry
University of Oregon, Eugene, Oregon, 2014-2019.

Graduate Education Mentor, Science Literacy Program
University of Oregon, Eugene, Oregon, 2018-2019

GRANTS, AWARDS, AND HONORS:

Scientific Teaching Education Fellow, Summer Institutes on Scientific Teaching
University of Oregon, Eugene, Oregon, 2018-2019

Science Literacy Program Graduate Education Mentor Fellow, Science Literacy Program, University of Oregon, Eugene, Oregon, 2018-2019

Science Literacy Program Graduate Fellow of General Chemistry, Science Literacy Program, University of Oregon, Eugene, Oregon, 2016

National Science Foundation Graduate Research Fellows Program Honorable Mention, 2016

Graduate Student Award for Excellence in the Teaching of Chemistry, Organic Chemistry, Department of Chemistry and Biochemistry, University of Oregon, Eugene, Oregon, 2015

Summa cum Laude, Russell Sage College, Troy, New York, 2014

Project Honors in Chemistry, Russell Sage College, 2014

Degree Honors in Chemistry and Forensic Science, Russell Sage College, 2014

ACS Division of Organic Chemistry Undergraduate Award, Russell Sage College, 2014

Russell Sage College Library Research Award, The Sage Colleges, 2014

Greater Seattle Business Association (GSBA) Scholar, 2011

PUBLICATIONS:

Eytel, L. M.; Fargher, H. A.; Haley, M. M. and Johnson, D. W. "The road to aryl CH···anion binding was paved with good intentions: fundamental studies, host design, and historical perspectives in hydrogen bonding." *Chem. Commun.*, 2019, *Advance Article.*

Eytel, L. M.; Brueckner, A. C.; Lohrman, J. A.; Haley, M. M.; Cheong, P. H.-Y. and Johnson, D.W. "Conformationally flexible arylethynyl bis-urea receptors bind disparate oxoanions with similar, high affinities." *Chem. Commun.*, 2018, **54**, 13208-13211.

Eytel, L.M.; Gilbert, A.K.; Görner, P.; Zakharov, L.N.; Johnson, D.W.; Haley, M.M. "Do CH-Anion and Anion-π Interactions Alter the Mechanism of 2:1 Host-Guest Complexation in Arylethynyl Monourea Anion Receptors?" *Chem. Eur. J.*, **2017**, *23*, 4051-4054. Selected as *Very Important Paper*.

ACKNOWLEDGMENTS

Two pages is not enough room to express my thanks to every person who has influenced my career to this point. I first must express my sincerest gratitude to the Department of Chemistry and Biochemistry faculty and staff members I have had the pleasure of interacting with and learning from over the past five years. I must give a special shout-out to my two bosses, Darren W. Johnson and Mike Haley. Darren, your gentle guidance and patience with me over these past five years was the true key to my completing this work. Thank you for continuously pushing me to be a better scientist, mentor, and teacher while also supporting me during some tough times. Mike, thank you for having faith in my abilities and pushing me to be in lab when I would rather be doing something else. To my labmates, of which there are too many to list, thank you for acting as sounding boards, editors, critics, mentors, therapists, and friends over the past five years. I also could not have found a "home" without the opportunity to rotate in Vickie DeRose's and Ramesh Jasti's labs, so thank you for providing me those learning opportunities as a young first year. Additionally, I would not have even considered a PhD without constant encouragement and push from the professors at Russell Sage College, but particularly my first mentor, Dr. Tom Gray. Thank you for believing I was worth your time.

To Elly Vandegrift, Nicola Barber, and the participants of the Science Literacy Program and the Summer Institutes on Scientific Teaching: Thank you for allowing me to engage in pedagogical development as a graduate student and for teaching me how to teach so I can create a community of learners in my future classrooms. To the professors I had a pleasure of teaching under, including Mike Koscho, Deb Exton, and the teaching

labs staff, thank you for allowing me to learn from your teaching experiences and providing me a platform to practice my craft in front of your students. A special thanks must also be given to Janet Macha, Kathy Noakes, Christi Mabinouri, Leah O'Brien, Jennifer Jess, Julie Haack, Diane Lachenmeier, and Kiran Virani-Edwards for their administrative assistance, candy bowls, and listening ears during many procrastination sessions over the past five years.

During my time at the UO, I was deeply engaged with a variety of professional organizations that provided me with friendships, community, and a sense of self-worth outside of the laboratory. To all those I had the opportunity to work with over the years, I cannot say "thank you" enough. I especially want to thank UOWGS, LGBT+ in STEM, and WPSP. I would not have survived this graduate program without the support and outreach opportunities I found through the UO Women in Graduate Science, so thank you to every volunteer and participant who made my three years as an outreach co-chair possible. To my family of Willamette Pass Ski Patrol: Thank you for embracing me as a member of the WPSP community and for showing me how to be a better person, medic, and skier over the years. The knowledge and friendships gained on and off the slopes of Willamette Pass will not soon be forgotten.

Last, but certainly not least, I want to thank my friends who have been there to offer hugs, join me in laughter, reminisce in rejection, push through the pain on the rock wall, eat and drink together, and simply sludge through this phase of life with me: Celeste Manka, Katelyn Peat, Loni Kringle, Mindy Ingebretson-Wolowicz, Tanesha Beebe, Rachel Shepard, Katie Bode, Kory Plakos, Thais de Faria, Sarah Casper, Annie Gilbert, Rusty Percivel Eytel, and many many more.

This dissertation is dedicated to the friends who became family over the years. Thank you for inspiring me to be better.

TABLE OF CONTENTS

Chapter Page

LIST OF FIGURES

Figure Page

CHAPTER II

Figure Page

CHAPTER III

CHAPTER IV

Figure Page

LIST OF TABLES

LIST OF SCHEMES

CHAPTER I

THE ROAD TO ARYL CH---ANION BINDING WAS PAVED WITH GOOD INTENTIONS: FUNDAMENTAL STUDIES, HOST DESIGN, AND HISTORICAL PERSPECTIVES IN CH HYDROGEN BONDING

Chapter I is composed from a focus review published in *Chem. Commun.*, 2019, *Advance Article*. I co-authored the review with Hazel A. Fargher, with editorial assistance from Prof. Michael M. Haley and Prof. Darren W. Johnson. The work in Chapter II includes co-authored, previously published material published in *Chem. Eur. J.*, volume 23, 2017, with contributions from Annie K. Gilbert, Paul Görner, Dr. Lev N. Zakharov, Prof. Darren W. Johnson, and Prof. Michael M. Haley. Chapter III contains work co-authored with Alexander C. Brueckner, Dr. Jessica A. Lohrman, Prof. Michael M. Haley, Prof. Paul H.-Y. Cheong, and Prof. Darren W. Johnson. This work was previously published in *Chem. Commun.*, volume 54, 2018. The work in chapter IV is unpublished work with contributions from Dr. Blakely W. Tresca, Anne-Lise Emig, Leif Winstead, Prof. Michael M. Haley, and Prof. Darren W. Johnson. Chapter V is also contains unpublished work with editorial contributions from Prof. Eleanor V. H. Vandegrift.

General Introduction

The focus of this dissertation is on the use of differentially-substituted aryl urea receptors for anion detection. The main supporting interaction involved in the host-guest

complexes described herein is hydrogen bonds donated through the urea N-H groups. However, the secondary binding-motifs contributed by the aromatic core that makes-up the center of the sensing scaffolds can influence the binding behavior too. These supporting interactions can be weaker than or as strong as the main urea hydrogen bonding anchors. This dissertation teases apart the influence of these supporting interactions, with a focus on the use of aryl CH hydrogen bonds, in an effort to design selective and turn-on fluorescent anion receptors.

Introduction to Sensing Anions via Hydrogen Bonding

Anionic species play diverse and complex roles in environmental, industrial, and biological systems, which necessitates chemical methods for detecting, sensing, sequestering, and selectively binding these negatively charged species to understand their fate, transport, and modes of action. As examples in the environment, anions are often found as natural and anthropogenic sources of pollution. Arsenate (AsO_4^{3-}) contamination in Bangladeshi wells has caused one of the largest mass-poisonings in history, affecting an estimated 85 million people.[1] Nitrate (NO_3^-) and dihydrogen phosphate ($H_2PO_4^-$) are essential for plant growth and are used in fertilizers to increase crop yield; however, over-application of these anions can be extremely detrimental to the environment, reaching surrounding bodies of water through agricultural run-off and promoting eutrophication.[2] As an example in industrial processes, anions such as sulfate (SO_4^{2-}) also serve as major contaminants, and can thereby inhibit the effective vitrification of radioactive waste.[3]

In organisms, anions are essential for numerous biological processes. Chloride (Cl^-) is used to regulate membrane transport and control nervous system function, and the misregulation of chloride is linked with serious diseases such as cystic fibrosis.[4] The hydrosulfide anion (HS^-) is currently being studied for its therapeutic potential as a signaling agent at low concentrations, but, at high concentrations, it is a deadly toxin and requires detailed monitoring in applications where exposure to the anion or its conjugate base (hydrogen sulfide, H_2S) exists.[5] Anions are even implicated in systems beyond our own planet. While perchlorate (ClO_4^-) serves as a rocket fuel additive and can lead to water contamination problems near terrestrial military bases (such as the Joint Base on Cape Cod, MA) and near flare manufacturing plants throughout California, perchlorate was also unexpectedly detected in soil on Mars.[6,7] This finding perhaps hints at past microbial life on the Red Planet,[7a] and may suggest a future environmental cleanup challenge during terraforming by future humans seeking to populate other locations within the solar system.[7b]

To understand, and potentially to monitor, the complicated roles that anions play in these many systems, the complex modes of action between an anionic "guest" and a molecular "host" has received increasing attention. Anions present several challenges as targets for molecular/ion recognition, including: (*i*) Anions tend to be harder to bind by traditional electrostatic interactions because they are larger, more polarizable, and more diffuse than comparable cations. (*ii*) Anions exist in a diversity of molecular geometries, ranging from spherical (the halides) to planar (nitrate) to octahedral (SiF_6^{2-}), among other forms.[8a] (*iii*) Anions typically serve as weak to moderate bases, so their speciation can be pH dependent. As a result, proton transfer might occur rather than, e.g., hydrogen bond

formation during their interactions with a host. (*iv*) Anions tend to be highly solvated and particularly mobile, especially in polar protic solvents. Despite these challenges, supramolecular host-guest systems have emerged over the past few decades as a way to continuously monitor anions through reversible, non-covalent interactions.[8] Molecular design and anion binding motifs can be used to modify and tailor host receptors for specific anion guests.[9] Given the widespread use of hydrogen bonding in Nature, it is no surprise that a very popular approach that strongly mimics how proteins bind substrates is through the use of hydrogen bonding.[9d,10]

Our Native Oregonian and famous sister school Beaver, Linus Pauling, predicted the significance of the hydrogen bond well before confirmation of its influence on the structure of DNA or the folding of proteins.[11-13] In fact, despite decades of debate on the hydrogen bond, much of Pauling's quite simple description of the hydrogen bond in *The Nature of the Chemical Bond* still drives today's more inclusive, lengthy formal definition.[10,14] Pauling defines a hydrogen bond quite succinctly as occurring "under certain conditions [when] an atom of hydrogen is attracted by rather strong forces to two atoms, instead of only one, so that it may be considered to be acting as a bond between them".[14]

Pauling's definition reflects the traditional perspective of the hydrogen bond seen in structural biology, where the total interaction of the hydrogen bond is predominantly electrostatic and the distance between the donor and acceptor is less than the sum of the van der Waals radii.[10,15] This classical definition of the hydrogen bond also reflects what many are taught in introductory chemistry courses: X–H···A reflects the strongly polar

hydrogen bond donor groups X–H (X = O, N, or halogen) on one side and hydrogen bond acceptor atoms A (A = O, N, halogen, etc.) on the other (Fig. 1a).

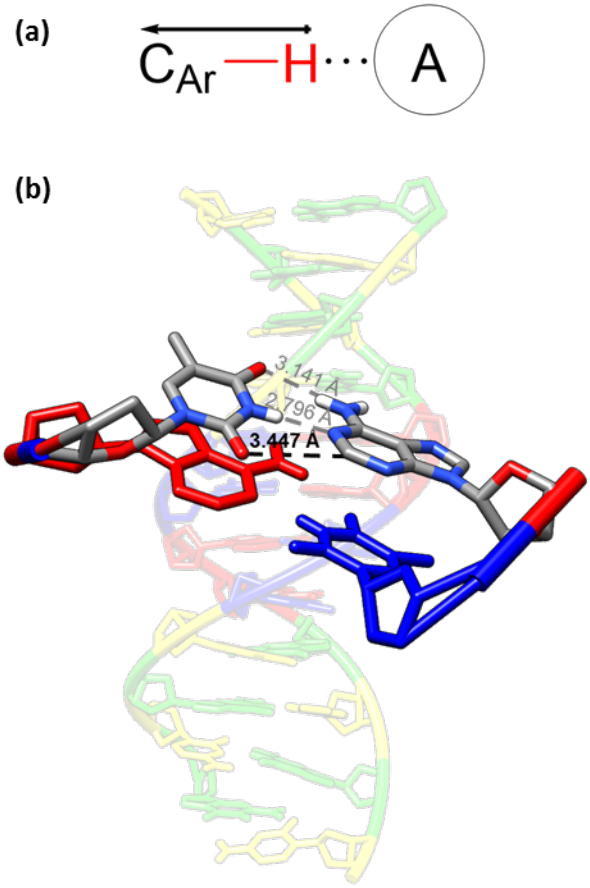

Figure 1. (a) A representation of a polarized aryl CH hydrogen bonding interaction with an anion and (b) a highlight of the adenine·thymine dimer with the traditional and non-traditional hydrogen bonding interactions highlighted.[13] PDB ID: 4HLI[60]

The definition and classification of a hydrogen bond has evolved quite a bit since the early observations and predictions of this attractive interaction, and a knowledge of this evolving history is perhaps useful in understanding the relatively recent emergence of CH bonds as hydrogen bond donors in molecule and anion recognition.[15] In fact, the fields of host-guest chemistry and anion recognition now regularly employ acidic CH hydrogens as H-bond donors, and the resultant interactions have often been deemed

"weak" hydrogen bonds (irrespective of some stricter definitions we may learn in introductory organic chemistry courses).[8,9,10,14] These and related emergent hydrogen bonding interactions are now well-recognized, in part due to an improved understanding of the interplay of the various attractive forces that comprise these interactions, including electrostatics, van der Waals forces, covalency, and degree of polarization.[10,15,16]

History and Definition of the CH···X Hydrogen Bond

The first indication of the existence of a possible CH hydrogen bond (HB) appears to have occurred in 1935, around the same time as studies emerged about more traditional hydrogen bonds.[11,12] However, these non-traditional CH hydrogen bonds were largely ignored until the early 1960s when D. June Sutor first published a systematic approach to define the existence of CH hydrogen-bonds in crystal structures.[17] Her survey of crystal structures with "'short' intermolecular and intramolecular C···O contacts" was the first step toward defining this weak interaction but was limited in scope to molecules containing C–H···O contacts.[17]

A few years later, Donohue challenged the Sutor definition of these short contacts as hydrogen bonds, in part suggesting the 2.6 Å contact was too long to be considered significant.[18] With this dismissal—which appeared in a book celebrating the life and work of Linus Pauling and received almost no critical response—progress in the field halted until almost two decades later when Taylor and Kennard published a comprehensive survey of the neutron scattering data of 113 structures from the Cambridge Structural Database containing short C–H···X contacts.[19] In that work, they conclusively corroborated Sutor's observations of the existence of C–H···O hydrogen

bond and systematically defined the properties of C–H···X HBs. They also expanded the definition of these short contacts to include general C–H···X interactions, where X = N, O, and Cl. They continued to postulate that "the C–H···X hydrogen bond may be a significant factor in determining the minimum energy packing arrangements of small organic molecules that contain nitrogen".[19] A recent review by Schwalbe provides a wonderful analysis of Sutor's role in the discovery, controversy, and ultimate vindication of the importance of the CH hydrogen bond.[20] Shortly after her death in 1990, Desiraju dedicated "The C–H···O Hydrogen Bond: Structural Implications and Supramolecular Design" to Dr. Sutor's memory.[21]

Nineteen years after the Taylor and Kennard work, Desiraju and Steiner published their book *The Weak Hydrogen Bond: In Structure and Biology*, wherein they further described the nature of the CH hydrogen bond.[10] This weak hydrogen bond would then differ from classical "strong" hydrogen bonds defined as X–H···A, where A and X are assumed to be highly electronegative (e.g., O, N) and can approach each other closely, with the HBs observed between H_2O molecules in crystalline ice serving as an example.[15] Similarly, in defining the weak hydrogen bond, A and X are only of moderate electronegativity (e.g., CH hydrogen bonds where X is C). The definition and properties presented by Steiner et al. provided the following standard definition guiding current research in the field of supramolecular anion receptors:

> "A X–H···A interaction is a hydrogen bond if i) it constitutes a local bond and ii) X–H acts as a proton donor to A: in the case of X–H + B: → X–H···:B. This definition implies a dipole-dipole interaction with a directional dependence."[10,15]

While this clear definition of the hydrogen bond emerged in the late 1990s and the field of crystal engineering was transformed in the mid-1990s by the CH···X interaction, the field of supramolecular anion receptor chemistry did not begin to fully utilize or

characterize this interaction in the solution-state until the mid-2000s.[22,23] Recent work has shown that, when properly polarized by electron-withdrawing groups, CH HB donors can form hydrogen bonds similar in strength to those seen in more traditional HB donors.[9d,24] These studies have also revealed several advantages in using CH HBs, including a greater resistance to proton transfer and pH-dependent host speciation, a greater affinity for softer anions in certain cases, and an overall additive effect to achieve strong binding (much like in the adenine·thymine base-pairs in the double helical backbone of DNA, Fig. 1b).[13]

Before we highlight current efforts in supramolecular anion receptors that utilize aryl CH hydrogen bonds as supporting interactions, we must first acknowledge the other, often competing and synergistic, supramolecular interactions at play in many such host-guest complexes. For this review, we focus on the interactions between an aromatic host and an anionic guest, but we will briefly touch on other competing forces, as well as solvent and entropic effects. Synthetic organic anion receptors commonly incorporate six main intermolecular and/or intramolecular interactions, alongside hydrophobic/solvophobic effects: ion pairing forces, dipole-anion forces, hydrogen bonding, halogen bonding, weak-σ interactions, and anion-π interactions (Fig. 2).[8,9,25] All of these binding forces rely on an attractive force between two or more atoms of differing electrostatic potentials. Interestingly, aryl CH hydrogen bonds, halogen bonding, weak-σ interactions, and anion-π interactions are all dependent on electron-withdrawing functional groups to create a positive electrostatic potential within the molecule to "catch" the anion.[9] In fact, the use of electron-withdrawing groups to flip the quadrupole

moment in a phenyl ring to create a receptor capable of anion-π type interactions is how our group first stumbled into aryl CH hydrogen bonds.[26]

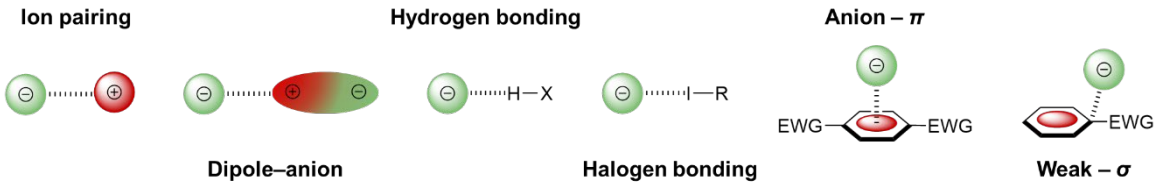

Figure 2. Depiction of common intrermolecular binding forces at play in host–anionic guest systems

Aryl CH Hydrogen Bonding in Anion Receptors

In some of our early studies on anion recognition, published in 2008 with collaborator Ben Hay and then-doctoral student Orion Berryman, we designed a series of sterically-geared electronegative triaryl-substituted triethylbenzene receptors with different dinitro-substitution patterns on the aryl substituents (**1** and **2**, Fig. 3).[26] In designing these receptors we sought to experimentally probe the continuum between weak-σ interactions and anion-π interactions in neutral aromatic hosts;[27] at the time of this research, the anion-π literature was heavily weighted towards computational studies, with a few solution-state studies of receptors that often featured other competing binding forces (e.g., ion-pairing or hydrogen bonding).[27c] One key finding that fell out of these halide binding studies was not a direct measurement of the strength of the anion-π or the weak-σ interactions; rather, it was the surprising appearance of downfield shifts in ^{1}H NMR spectroscopy titration studies that indicated the possibility of a different binding force at play: aryl CH hydrogen bonding. The substitution pattern of the dinitro groups allowed for discrimination between competing arene-anion and CH-anion binding interactions, since the 3,5-dinitro substituted receptor **2** was predicted to block aryl CH···X^{-} hydrogen bonding sterically, while the 2,4-dinitro substituted receptor **1** allowed

for two CH hydrogen bonds from the two weakly acidic *ortho* hydrogens within the anion binding pocket (Fig. 3).[26]

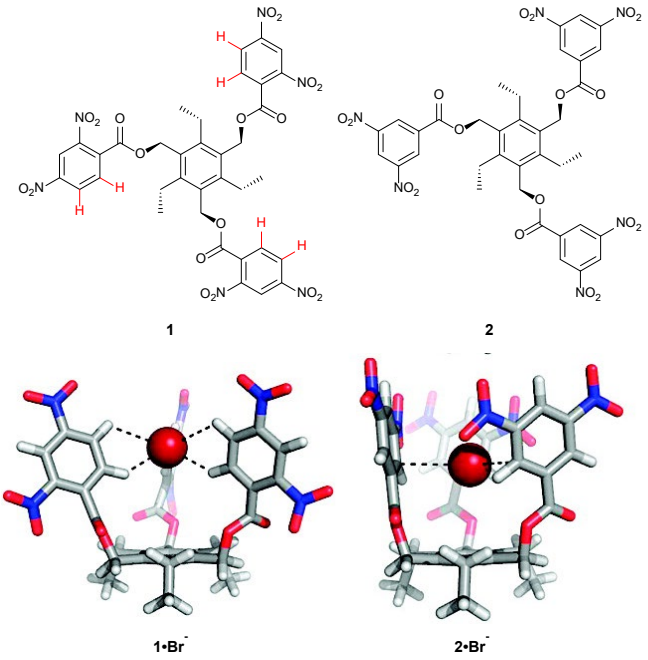

Figure 3. Optimized geometries of **1**·Br^- and **2**·Br^-. The 2,4-dinitro substituted triethylbenzene receptor **1** binds its guest via aryl CH hydrogen bonds versus the weak–σ binding mode depicted in the 3,5-dinitro substituted receptor **2**. Figure adapted with permission of the American Chemical Society from ref. 26. Copyright 2008.

A key contemporary experimental investigation at the time also explored the aryl CH···X^- interaction, as reported by Sessler, Hay, Lee, and coworkers in the context of a series of strapped calix[4]pyrroles.[28] These systems—designed to bind chloride—contained either a phenyl, pyrrole, or furan moiety in the bridge/strap (Fig. 4). When compared to the unsubstituted calix[4]pyrrole, the phenyl and pyrrole straps (**3** and **4**, respectively) increased the affinity toward chloride by one and two orders of magnitude, respectively; however, the furan strapped system (**5**) showed an order of magnitude lower binding than the phenyl strapped system.[28] This study was one of the first experimental

examples to show the significance of the aryl CH···X⁻ hydrogen bond as a supporting interaction for anion binding in synthetic hosts.

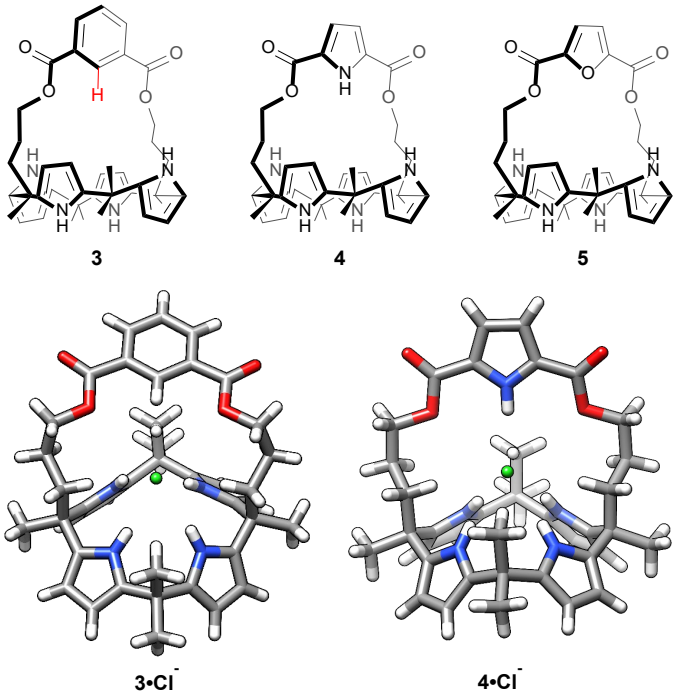

Figure 4. Series of strapped calix[4]pyrroles designed to bind chloride and the crystal X-ray diffraction structures of the Cl^- complex. The key CH···Cl^- interaction is clearly depicted in the **3**·Cl^- crystal structure (bottom). The added aryl CH hydrogen bond interaction available in the phenyl-strapped system **3** binds Cl^- stronger than an unsubstituted calix[4]pyrrole and the furan-strapped system **5**.

Shortly after these two studies were published, Colleti and Re performed high level computations to determine the strength of binding of the halide ions (F^-, Cl^-, Br^-, and I^-) to benzene.[29] Their results suggested bifurcated aryl CH···X^- hydrogen bonds of intermediate strength to be the preferred binding mode of F^-, Cl^-, Br^-, and I^- with benzene. However, a stronger, singular aryl CH···X^- HB dominated the fluoride- benzene interaction. This study, in combination with the previous solution-state analyses, appeared to rekindle interest in using aryl CH···X^- hydrogen bonding as an additional supporting interaction in complex host-guest systems.[9]

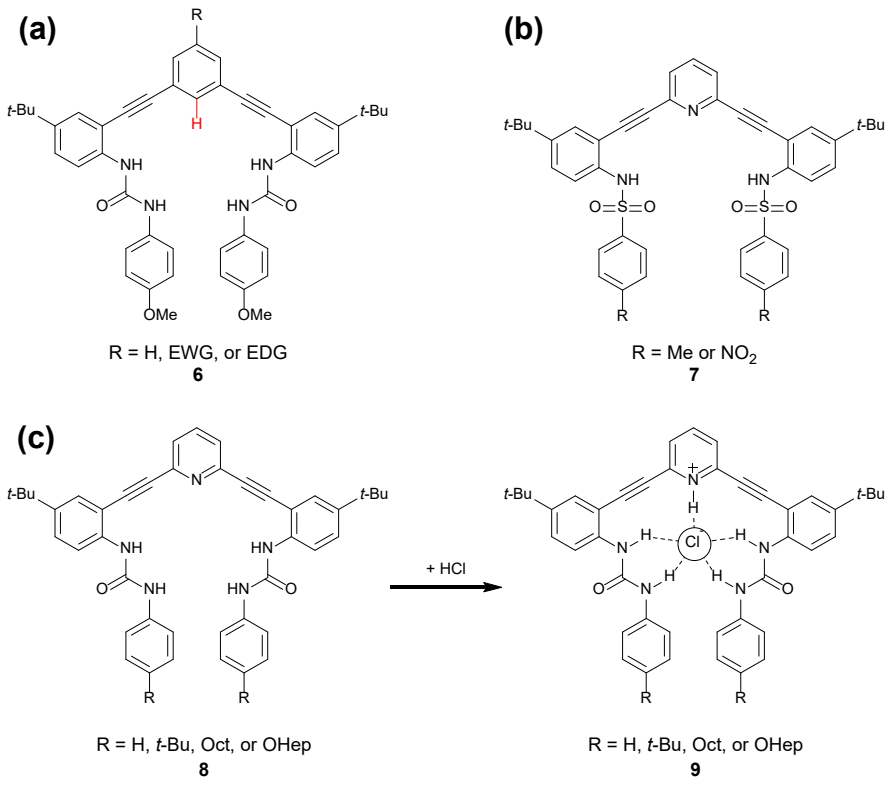

Figure 5. (a) Generic scaffold of the phenylethynyl bis-urea anion receptors our lab has used to investigate aryl CH hydrogen bonding; (b) bis-sulfonamide scaffold **7**; and (c) original pH sensitive pyridine (**8**) to pyridinium (**9**) anion binding receptors.

This series of earlier studies also helped inspire the longstanding collaboration between the Johnson and Haley labs at the University of Oregon in designing arylethynyl urea anion receptors, with a recent focus on phenylethynyl hosts (e.g. **6**, Fig. 5a). This scaffold serves as a modified version of our original pyridylethynyl bis-urea and bis-sulfonamide receptors in which the core pyridine/pyridinium is replaced with a phenyl ring that is not subject to proton transfer (**7**, Fig. 5b).[30] Our traditional pyridine and pyridinium-based receptors (**8** and **9**, Respectively, Fig. 5c) showed a pH dependency, limiting the scope of the anions we could bind and making studies at a physiological pH more challenging due to competing proton transfer processes between host, anions, and solvent.[31] To overcome these limitations, we asked: did protonated pyridine need to be

present in these receptor scaffolds? Graduate students at the time Calden Carroll, and later Blake Tresca, realized that the *para*-position on the aromatic core of the scaffold provided an easily functionalizable, fortuitous handle for polarizing the CH HB and studying substituent effects. In transitioning from a pyridine to a phenyl core, the opportunity to utilize aryl CH hydrogen bonding to bind anions was realized: by functionalizing the *para*-position on the core benzene ring with an electron-withdrawing substituent, the acidity of the aryl CH pointing into the binding pocket could be tuned as a hydrogen bond donor (Fig. 6, **10**).[32]

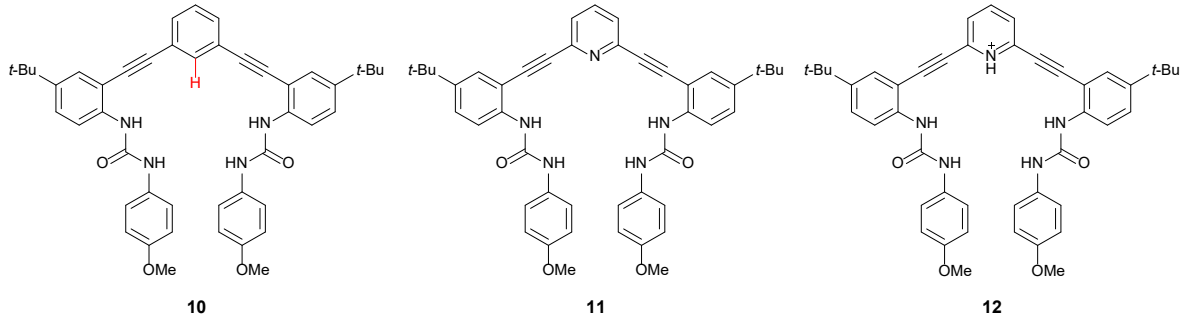

Figure 6. The three anion receptors that brought our lab into its current generation of aryl CH hydrogen bond studies. Tresca et al. compared the binding affinities of the phenyl- (**10**), pyridine- (**11**), and pyridinium-core (**12**) receptors to realize the potential of the supporting aryl CH HB in our scaffolds.

Similar to Sessler and coworkers' research with strapped calix[4]pyrroles, Tresca et al. compared the affinity of halides with this phenyl-based receptor to those of the pyridine and pyridinium receptors (Fig. 6, **11** and **12**).[32] Receptor **12** showed the strongest binding for Cl^-, attributed to the strong NH^+ hydrogen bond combined with ion-pairing interactions.[32] Phenyl-core receptor **10** featured an aryl CH HB in the binding pocket, which was further polarized by ortho-substituted alkynes. The resulting host-guest complex was not quite as stable as the complex with the pyridinium core when binding Cl^-, as it showed a binding affinity an order of magnitude lower than **12**. In comparison

to receptor **11**, scaffold **10** also showed an order of a magnitude stronger affinity toward Cl^-, which was attributed to the repulsion of the nitrogen lone pair toward anions in the binding pocket of **11**. ^{1}H NMR titration studies showed a downfield shift of the internal proton resonance, indicating the participation of the aryl CH hydrogen bond in **10**·Cl^-, and a crystal structure analysis of **10**·Cl^- showed short contacts between the aryl CH and Cl^- at 3.579(3) Å, demonstrating the clear participation of the aryl CH HB in this scaffold (Fig. 7).[32]

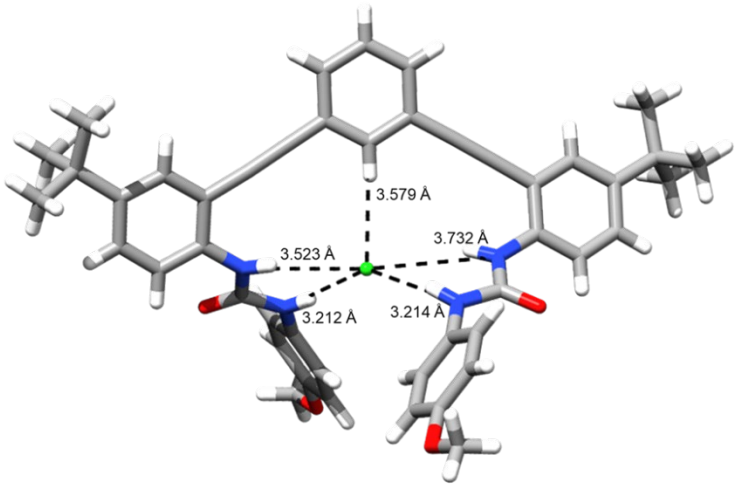

Figure 7. X-ray crystal structure of phenylethynyl bis-urea receptor **10** binding Cl^- through urea NH and aryl CH hydrogen bonds.

The arylethynyl bis-urea scaffolds reported from our group are inherently flexible and capable of binding anions in a variety of conformations, with the aryl CH HBs acting as supporting anion binding motifs to traditional urea NH HBs or anion-π interactions.[32,33] This is not an uncommon approach in designing anion receptors.[8a] As a related approach to these flexible hosts, many others have shown that moderate to strong anion binding is also possible with multiple aliphatic and/or aryl CH HBs in pre-organized macrocyclic receptors.[34,9b-9d] For example, triazolophane macrocycle receptors

bind anions solely through aryl CH hydrogen bonds and serve as an early example of shape persistent hosts for anions, also reported in 2008.[35] Flood et al. exploited the large diploe moment of 1,4-disubstituted 1,2,3-triazole groups linked by 1,3-disubstituted aromatic groups to pre-organize at least six acidic, polarized aryl CH groups pointing into the center of the macrocyclic ring (Fig. 8, **13**). This series of neutral macrocycles showed selective binding toward halides utilizing only aryl CH hydrogen bonding, establishing the significance and strength of the aryl CH···X^- interaction to bind anions in solution and the solid state.[35]

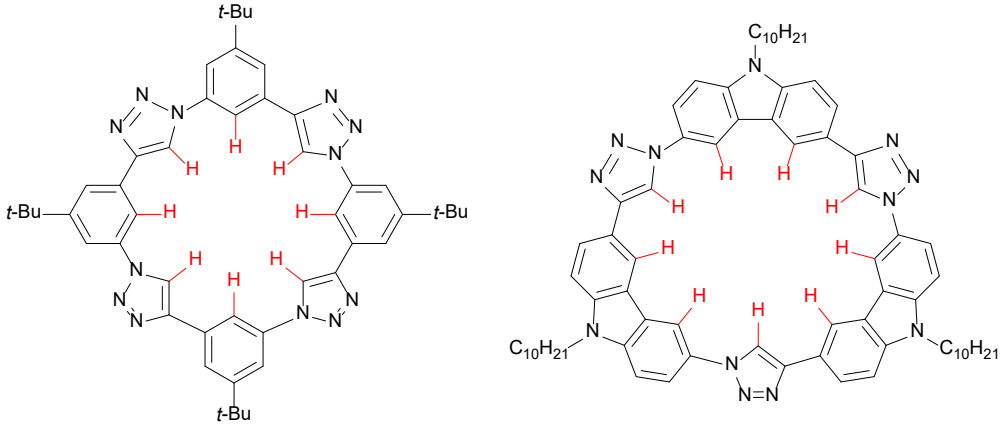

Figure 8. Triazolophane macrocycle **13** and related tricarbazolo triazolophane macrocycle **14** bind anionic guests solely through aryl CH hydrogen bonds.

Since that first triazolophane publication in 2008, the Flood group has reported a multitude of elegant differentially-substituted triazolophanes and their anion-binding properties.36 In one spectacular example in 2016, Lee et al. replaced the phenyl linkers in the macrocycle with carbazole groups to create a rigid receptor (Fig. 8, 14) easily synthesized (in one pot) and in high yields (70% on an 8-gram scale). This tricarbazolo triazolophane structure showed highly cooperative binding with high affinities toward larger, more diffuse, and notoriously weakly-coordinating anions, such as SbF6– and

PF6– in 20% MeOH in CHCl3 or the per-deutero equivalent. Strong π-stacking within this system also appeared to play a significant role in the self-assembly of this shape-persistent macrocycle into slip-stacked sandwiches in solution and at the liquid/solid interface, forming 2D crystalline honeycomb and flower polymorphs. Despite these supporting intermolecular interactions, host binding toward the anions results solely due to the activated aryl CH hydrogen bonds.[36] The uniqueness of the triazole subunit – a conjugated ring that is easy to synthesize through "click" chemistry with a highly activated CH groups – has led to its incorporation into a variety of other anion-binding scaffolds, including foldamers,[38] pyrrolyl-based triazolophane macrocycles,[39] strapped calix[4]pyrroles,[40] and anion-responsive self-assembled bis(triazole)benzamide receptors,[41] among others.[42]

Another approach to incorporate aryl CH hydrogen bond donors lies in ring-strained hydrocarbon macrocycles featuring aryl CH groups directed into the strained macrocyclic cavity. In 2016, the Stępień group synthesized octulene **15**, a structural homologue to kekulene, which has hyperbolic curvature with approximately 30 kcal mol^{-1} in strain energy.[43] DFT geometries of the unsubstituted and methoxy-substituted ring showed a deep, saddle-like ring with eight aryl CH bonds pointing into the center of the large cavity (Fig. 9). The electrostatic potential (ESP) of these internal hydrogens was shown to be 23-24 kcal mol^{-1}, making these aryl CH hydrogens about half as positive as the Flood triazolophane receptor (ESP = 41-55 kcal mol^{-1}).[37] This electrostatic potential is achieved through a neutral aromatic belt that lacks electron-withdrawing groups, but interestingly, is on par with the ESP of the aryl CH hydrogen bond donor in our most

polarized, electropositive arylethynyl bis-urea receptors (ESP = 28.9 and 22.1 kcal mol^{-1} when the R group in Fig. 5 = NO_2 and Cl, respectively).[44]

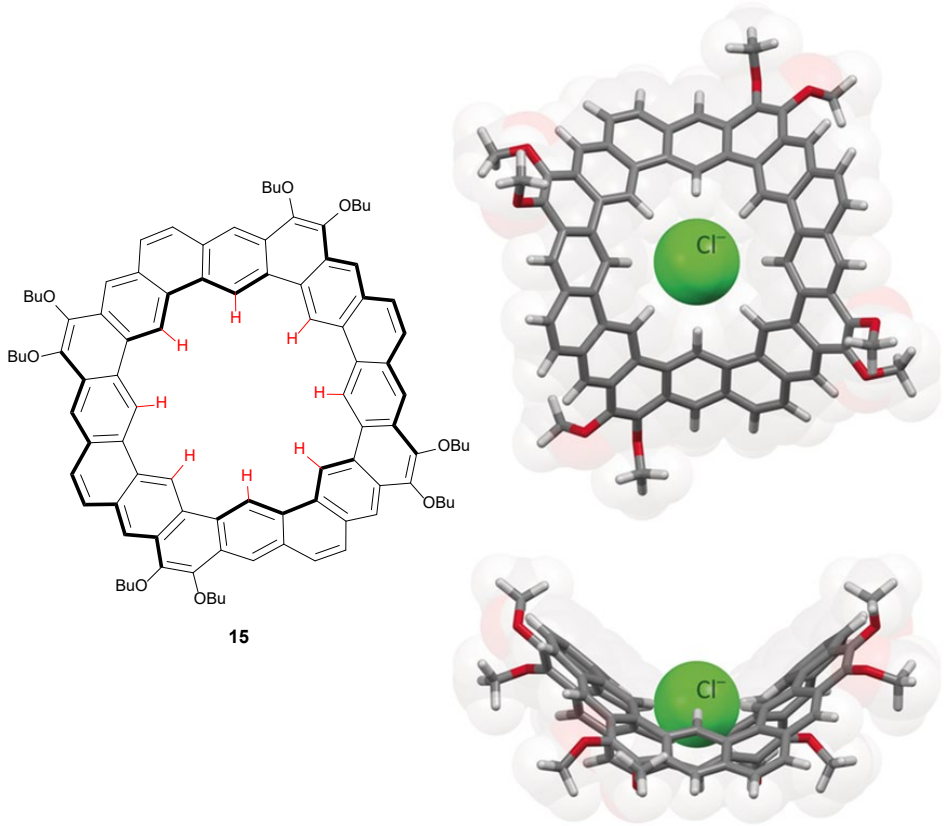

Figure 9. Chemical structure of aromatic belt octulene **15** and the gas-phase DFT geometries (level of theory: ωB97XD/6-31G(d,p)) of the chloride-adduct showing the hyperbolic host pocket with eight aryl CH hydrogen bonds. Molecular models are reproduced with permission of Wiley from ref. 43. Copyright 2016.

With eight electropositive aryl CH hydrogen bond donors and a rigid, pre-organized binding cavity around the same size as that shown in triazolophane,[35] Stępień and coworkers were able to bind Cl^- with an association constant (K_a) of 2.2 x 10^4.[43] This K_a, measured in 1% CD_2Cl_2 in C_6D_6, is particularly strong for a receptor that binds Cl^- through only moderately-activated aryl CH hydrogen bonds. In comparison, the Flood triazolophanes, which feature many more electropositive aryl CH hydrogen bond donors, show a K_a of 1.3 x 10^5 in CH_2Cl_2.[35] The strong association of octulene with Cl^- shows the

combined strength of these "weak" aryl CH hydrogen bond and may suggest that incorporating strain into a macrocylic host may be another strategy to increase the acidity and hydrogen bond donor strength of aryl CH hydrogen bonds.[43]

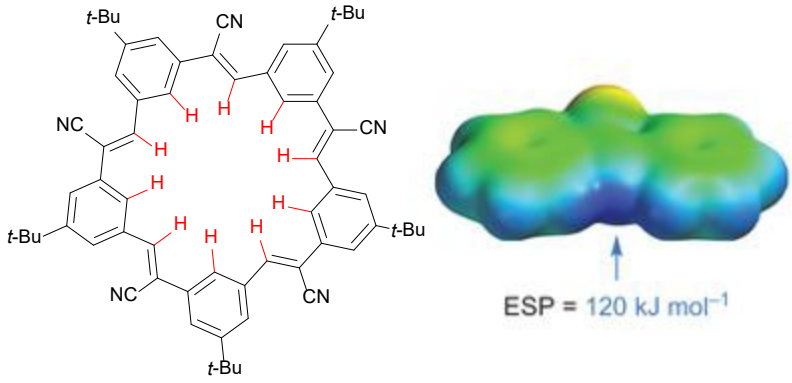

16

Figure 10. Cyanostilbene-based macrocycle "cyanostar" **16** obtained through the Knoevenagel condensation binds anions through 10 aryl CH HBs per host and a strongly electropositive binding pocket. Electrostatic potential surface map reproduced with permission of Springer Nature from ref. 45. Copyright 2013.

An even larger shape-persistent macrocyclic host was reported by Lee, Flood, and coworkers, again featuring all aryl CH hydrogen bonds oriented into the host cavity for anion recognition.[45] This C_5-symmetric penta-*t*-butyl-pentacyanopentabenzo[25]annulene macrocycle, aptly named "cyanostar", was obtained through a one-pot Knoevenagel self-condensation (Fig. 10). It strongly binds large, weakly coordinating anions through polarized cyanostilbene aryl and olefinic CH hydrogen bonds. It is important to note that the cooperative π-stacking behavior of the cyanostars with large anions plays a role in creating a 2-to-1 host-to-guest "sandwich" complex.[45] This electropositive binding pocket, combined with a total of 20 CH hydrogen bonds, resulted in an overall binding affinity of log $\beta_{12} > 11$ for weakly coordinating anions PF_6^-, ClO_4^-, and BF_4^- in 40% CD_3OD in CD_2Cl_2. Since that initial report on cyanostars, the Flood group has continued

to investigate the anion binding properties of differentially-substituted cyanostar macrocycles and has contributed significantly to the field of aryl CH···X^- hydrogen bonding by investigating the nature of the contributions of the aryl CH···X^- hydrogen bond in these host-guest complexes.[46]

Physical Organic Chemistry Investigations into the Nature of the Aryl CH Hydrogen Bond

To employ aryl CH HBs as functional anion-binding motifs in supramolecular structures effectively—and perhaps still necessary in the recent past to convince skeptics that this attractive interaction rises to the level of inclusion as a hydrogen bond—detailed studies on the nature and contribution of these "non-traditional" hydrogen bond donors have been undertaken. Our lab became interested in using classical physical organic techniques to examine aryl CH HBs after receptor **10** showed moderate binding strength toward Cl^-.[32] We hypothesized that we could modulate the strength of the aryl CH HB in the binding pocket by installing various electron donating or withdrawing groups in the *para* position to the HB donor to study substituent effects. If these CH HBs were truly fundamentally related to their more traditional NH and OH counterparts, their HB binding energies should show linear free energy relationships to, e.g., traditional Hammett constants.

In 2016, Tresca and colleagues in our lab implemented a linear free energy relationship (LFER) study to probe the characteristics of these CH···X^- interactions by modulating the HB strength through these varied *para*-substituents.[44] The modular synthesis of our receptors allowed us to build a series of receptors (Fig. 11a, **17**).[44] We

reported the association constants of the series of receptors with chloride, bromide, iodide, and nitrate in water-saturated $CHCl_3$. We found that the binding energies were well described in LFER studies by using Hammett parameters, showing that the acidity of the aryl CH HB could be modulated by EWGs and EDGs in the *para* position, much like NH and OH HBs. Additionally, plotting the electrostatic potential of the aryl CH HB (calculated at the B3LYP/6-31+g(d) level of theory) against the ΔG of binding in solution revealed that the aryl CH HB was an important contributor to the overall binding energy, with the strongest aryl CH anion HB contributing up to –2.20 kcal mol^{-1}.[44] In fact, the aryl CH HB amounted to as high as 47% of the total binding energy with I^-.[44]

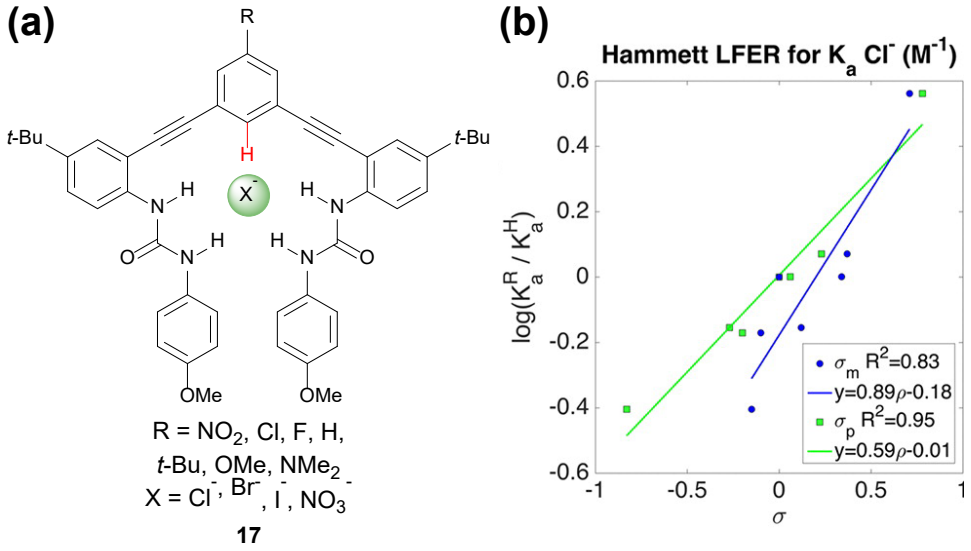

Figure 11. (a) Chemical structure of the differentially substituted phenylethynyl bis-urea receptors **17** implemented in the LFER study by Tresca et al. (b) Hammett plot of the binding constants of the various receptors with Cl^-, indicating a σ_p relationship between the binding strength and aryl CH hydrogen bond donor. Hammett plot reproduced with permission of the American Chemical Society from ref. 44. Copyright 2015.

This research also highlighted differences in binding strength between the harder anions (Cl^- and Br^-) and the softer anions (I^- and NO_3^-). Performing Hammett plots with

σ_p or σ_m parameters for the different *para* substituents revealed subtle differences between the various anions.[44] Binding energies with Cl^- fit σ_p values best (Fig. 11b), while binding energies with I^- better fit σ_m, suggesting that resonance contributions may play a more important role in binding the harder Cl^- than when binding the softer I^-. We also saw that NO_3^- fit both σ_p and σ_m equally well, perhaps due to the added geometric considerations of the larger, trigonal planar anion.[44] Using the induction (*F*) and resonance (*R*) parameters developed by Swain and Lupton enabled determination of the inductive and resonance contributions of the receptors when binding the different anions. This analysis also revealed slightly higher resonance contributions for the harder anions than for the softer anions. These findings reinforce that linear free energy relationships can be a powerful tool in deciphering subtleties in non-covalent interactions, and potentially even provide approaches to achieving selectivity for different anions.[44]

Even without resorting to comprehensive LFER investigations, many other studies have explored the effect of polarizing CH bonds with electron withdrawing and donating groups. For example, in 2014 the Hill group reported an arylpyrrole oligomer possessing pyrrole NH and aryl CH hydrogen bonds for anion binding.[47] These aryl CH hydrogen bonding motifs could be polarized through functional groups in the *ortho*-, *meta*-, and *para*-positions (Fig. 12a). When comparing five different receptors (**18a-e**) to six different anions (Cl^-, HCO_3^-, AcO^-, $H_2PO_4^-$, NO_3^-, and Br^-), the authors could not pinpoint a consistent trend across all host-guest pairs, with one exception: host **18e**.[47] This receptor, which combined a nitrogen lone pair pointing into the binding pocket with aryl CH HBs activated at the *meta*-position, bound all of the anions the weakest. This was likely due to the steric and/or electrostatic repulsion from the nitrogen lone pair pointing

into the binding pocket. For the remaining host-guest pairs, the authors concluded that steric hindrance of the anion binding pocket was just as important to consider as the polarization of the aryl CH HB in host-guest interactions.[47]

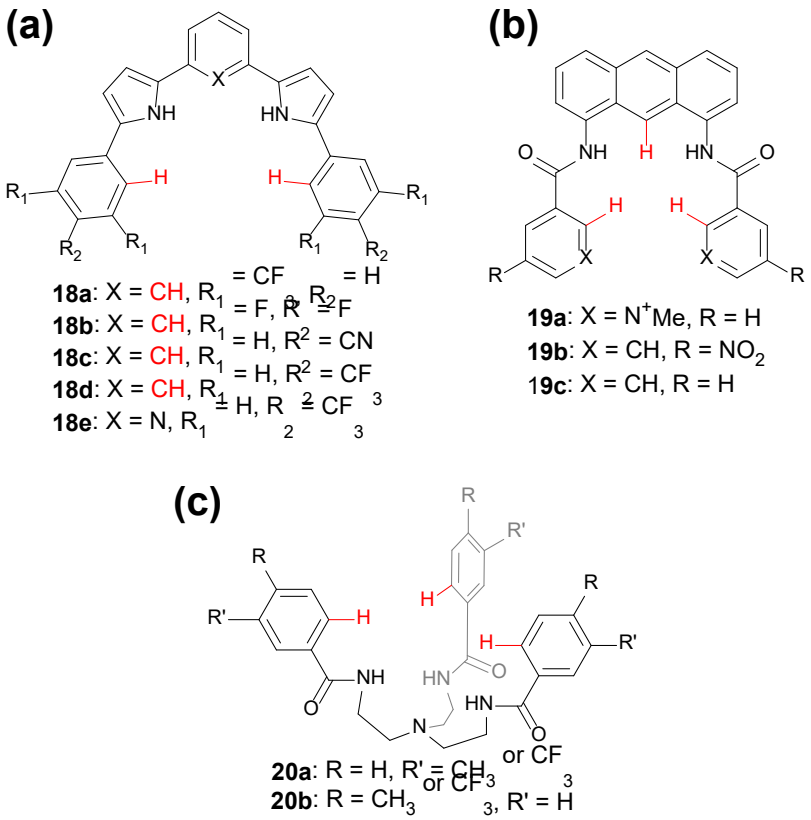

Figure 12. Chemical structures of various anion receptors used to probe the strength of the aryl CH hydrogen bond through differential substitution of (a) arylpyrrole oligomers **18**, (b) anthracene-amide based receptors **19**, and (c) TREN-based receptors **20**.

The Kang group also reported on the effect of polarization of aryl CH hydrogen bonds on anion binding.[48] Their receptors utilized an amide NH HB, a central anthracene CH HB, and an aryl CH polarized by an *ortho* pyridinium, a *para*-nitro group, or a control receptor without substituents (Fig. 12b, **19a-c**, respectively). The unsubstituted receptor **19c** showed no affinity toward a range of anions, while the slightly-more

polarized receptor **19b** only bound $H_2PO_4^-$.[48] Receptor **19a**, however, which featured the most polarized aryl CH hydrogen bond, was able to bind all four anions studied ($H_2PO_4^-$, HSO_4^-, Cl^-, and Br^-). In this case, the extent of polarization of this aryl CH HB, along with the favorable electrostatic interactions and possible N-methyl pyridinium CH HBs in **19a**, were critical in creating a favorable host-guest interaction in solution.[48]

We previously collaborated with our colleagues in the lab of Michael Pluth at the University of Oregon to show that receptors of the type in Fig. 12c could bind the highly nucleophilic hydrosulfide anion (HS^-, conjugate base of hydrogen sulfide, H_2S).[56] These studies revealed that a short CH···S contact contributed to the strong association of hydrosulfide in these complexes, and solution phase measurements supported the existence of this HB as well. In a continued attempt to determine the contribution of aryl CH hydrogen bonds in anion binding, the Pluth group published a series of tribenzamide TREN-based receptors (Fig. 12, **20**).[49] Within their series, two receptors were functionalized with CF_3 electron withdrawing groups either in the *meta* (**20a**) or *para* (**20b**) position relative to the amide functional group. In the *para* position (**20b**), the CF_3 group polarized the NH HB donor, making it more acidic, through both inductive and resonance effects. Likewise, in the *meta* position (**20a**), the CF_3 group more greatly polarized the aryl CH HB donor. Titration of **20a** and **20b** (R = CF_3) with TBASH revealed higher binding affinities than a receptor with an unfunctionalized aryl ring. Furthermore, they saw that the K_a for **20b** was three times greater than for **20a**, suggesting that the amide NH HB was more important in anion binding than the aryl CH HB.

To further explore the system, the Pluth group then installed methyl groups in both the *para* (**20b**, R = CH_3) and *meta* (**20a**, R' = CH_3) position to the amide functional group, decreasing the acidity of both NH and CH HB. Through titration of the methyl-substituted **20a** and **20b** with TBASH, the authors saw lower binding affinities than the unsubstituted receptor but did not observe a significant difference in binding strengths between the two methyl-substituted receptors.[49]

Electrostatic potential surface (EPS) maps also serve as an efficient physical organic tool to visualize binding pockets and the extent of aryl CH hydrogen bond polarization without requiring the need to synthesize and study the anion-binding properties of a series of receptors. In their initial report on cyanostar macrocycles, Flood et al. attributed the strong binding toward weakly coordinating anions both to the electropositive cavity of the cyanostar and to the large size of the binding pocket (~4.5 A).[45] To visualize this cavity, they used an electrostatic potential map of an intermediate building block to show that the nitrile group was able to polarize the vinylic and aryl CH bonds, thereby lining the inner cavity with an electropositive region (Fig. 10). Using calculations at the B3LYP/6-31G* level of theory, the authors calculated the EPS of the vinyl CH HB in the advanced intermediate at 29 kcal mol^{-1}, which represents a highly polarized CH bond and thus a strong CH HB donor.[45,50]

Another way to study the contribution of a CH hydrogen bond to the overall anion binding in a receptor is through the use of deuterium equilibrium isotope effects (DEIEs); such studies are quite challenging to perform on traditional NH and OH donors due to proton exchange. We are fortunate to have a scaffold that presents a CH donor that is quite easy to label with deuterium (Fig. 13), and thus we embarked on a study with

collaborator Paul Cheong's lab to investigate EIEs in an aryl CH HB an anion receptor.[51] In this investigation, receptors **21a$_H$** and **21a$_D$** were titrated with chloride in d_6-DMSO and monitored through ^{13}C NMR titrations. We reported a normal DEIE, with K_a**21a$_H$** / K_a**21a$_D$** = 1.019 +/- 0.010.[51] We also reported the computed DEIEs of fragments of the receptors (Fig. 13).[51] Interestingly, we saw that various fragments of the receptor showed an inverse DEIE. These results were surprising because they showed that the DEIE of the fragments would not be additive, as the inverse DEIEs would not sum to a positive DEIE, as was determined experimentally. Further analysis suggested that the origin of the different, normal DEIE of **21a$_H$** and **21a$_D$** was an emergent phenomenon resulting from combination of functional groups and binding geometries present in the host.[51]

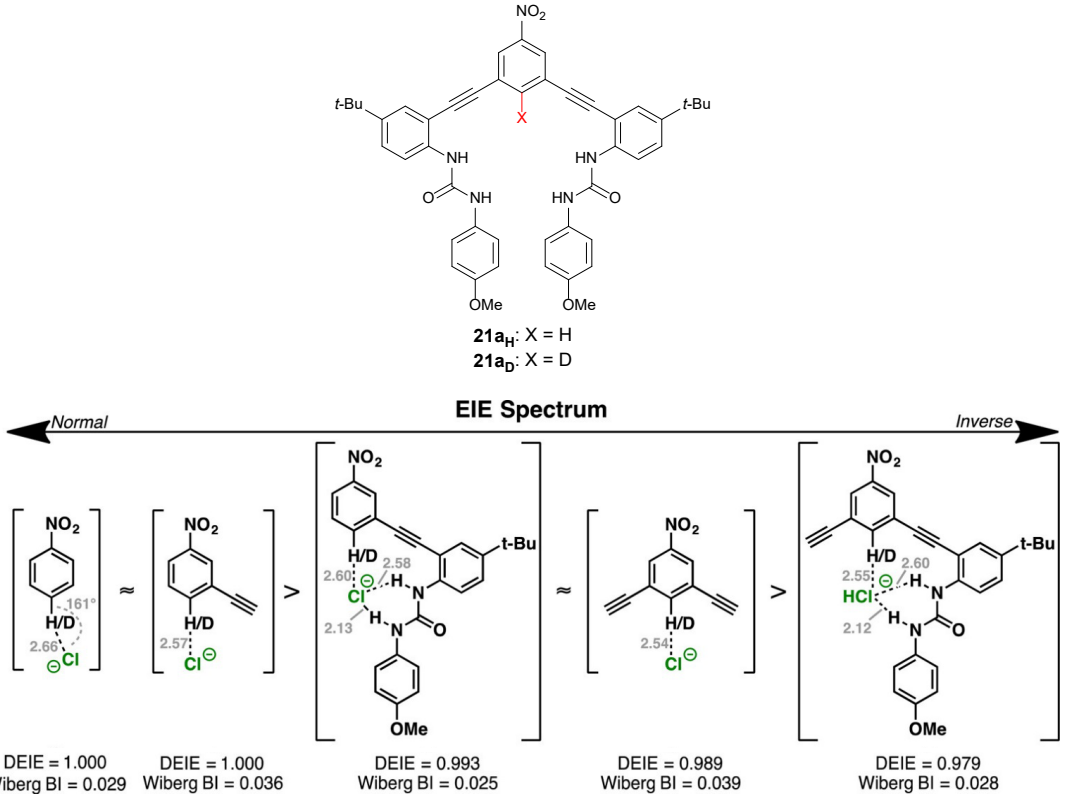

Figure 13. Deuterium labeled anion receptor **21** and subsequent computed EIE values involving the chloride complexes with fragments of receptor 20H/D. EIE spectrum reproduced with permission of the American Chemical Society from ref 51. Copyright 2017.

Probing Solvent Effects in the Aryl CH···X⁻ Interaction

We would be remiss if we did not emphasize that—especially with weak interactions—the binding forces alone do not always dominate binding structure, selectivity, strength, etc.; rather, solvent effects and entropy (through enthalpy-entropy compensation, preorganization, and cooperativity, among other factors) play their own critical, oftentimes ambiguous roles.[50,51] Unfortunately, our understanding of solvent effects in general in synthetic host-guest complexes remains incomplete, and efforts to understand these effects in anion recognition are in their infancy. This is therefore a roadblock in understanding and predicting how receptors with any variety of binding motifs will interact with and select various anions in solution, particularly in water.[51]

Until recently, most of our understanding of solvent effects come from empirical reports of receptors examined in a few solvents. In 2017, the Flood group published a comprehensive study to untangle the forces that drive anion binding in macrocylic receptors, including electrostatics and solvent effects (Fig. 14).[52] Experimental ^{1}H NMR titrations with triazolophane receptor **22b** and tetrabuylammonium chloride were conducted in solvents with a range in dieletric constant from $\varepsilon_r = 4.7$ ($CHCl_3$) to $\varepsilon_r = 56.2$ (10% v/v H_2O in DMSO).[52] Additionally, DFT calculations were performed on receptor **22a** to provide further insight into the binding events. From their experimental and computational results, the authors discovered a $1/\varepsilon_r$ dependence on anion affinity in aprotic solvents (Fig. 14). As the dielectric constant of the solvent decreased, the electrostatic forces of the receptor on the anion dominated the anion binding event and binding behavior became more and more similar to gas-phase calculations. As the

dielectric constant increased, electrostatics gave way to other inter- and intramolecular forces, such as dispersion, induction, and exchange forces. With the switch from aprotic solvents to a mixture of DMSO and water, Flood et al. found a deviation from the $1/\varepsilon_r$ dependency: instead of plateauing, binding affinities began to decrease linearly in a fashion that was not predicted by computational binding models (Fig. 14).[52]

This unexpected trend in solvent influence on the strength of anion binding highlights how many forces are truly at play in these host-anion systems. While the strength of aryl CH hydrogen bonds can improve the overall association strength in a host-guest system, protect from proton transfer reactions, and even aid in anion binding selectivity, the role of dynamic electrostatic and solvent forces clearly warrants further scrutiny.[53-55]

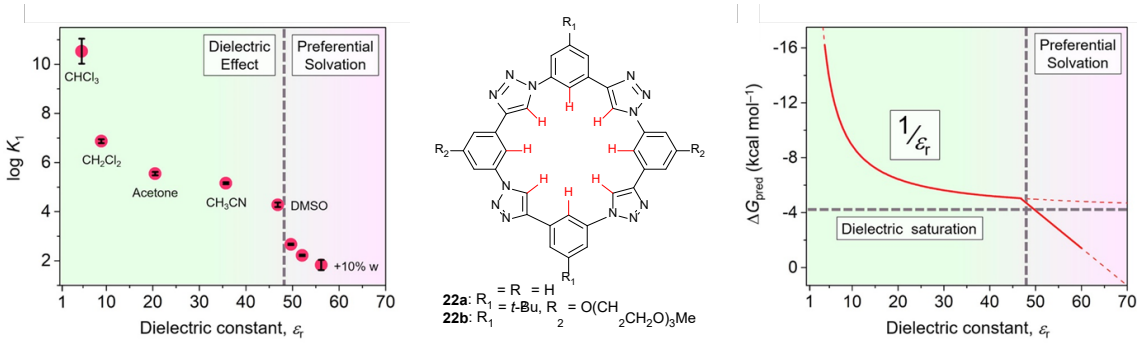

Figure 14. Understanding solvent effects on aryl CH···anion receptors is the next frontier in understanding the nature of this unique bond. Triazolophane macrocycles **22a** and **22b** showed a predictable $1/\varepsilon_r$ dependency in aprotic solvents but an unexpected linear decrease in anion association strength in protic solvents. Graphs reproduced with permission of Elsevier from ref. 52. Copyright 2017.

Our Future in the Field of Aryl CH···Anion Hydrogen Bonding

Flood's comprehensive approach to teasing apart solvent effects on anion binding is a notable contribution to the understanding of CH-anion recognition, and they make sure to highlight how much work remains in generalizing our understanding of solvent

effects and moving theoretical models to shift from the gas phase into the more relevant solvent phase.[52] We are inspired to continue thinking "beyond the electrostatic regime" in order to explain the deviation from the dielectric dependency upon moving into protic solvents, water-DMSO mixtures, and even neat water; to investigate solvent effects on our more flexible anion receptors; to explore the fundamental CH HB interactions and its role in driving anion binding selectivity; and to study the impact of solvent on hosts with binding geometries not perfectly designed for the guest.

The use of aryl CH hydrogen bonds and other anion binding approaches in the development of molecular probes and sensors for anions of biological relevance is another area that requires continued exploration. In one case, these pursuits led us to report the first examples of supramolecular receptors for the reversible binding of biologically-critical yet highly-reactive hydrosulfide (HS^-) anion.[56] Subsequent to these studies, new receptors targeting these types of biologically relevant anions through the use of aryl CH HBs have appeared.[49,57] We are now further exploring the use of aryl CH hydrogen bonds to bind other reactive, yet biologically-relevant (hydro)chalcogenide anions, including hydroselenide.[58]

We also note that the studies on CH-anion HBs have focused on organic solvent mixtures predominantly, so there is still plenty of opportunity to study CH HBs in water to parallel other studies on anion recognition in water.[53,55] We foresee combining the utility and tunability of the aryl $CH\cdots X^-$ interaction with halogen bonding interactions to achieve strong and selective anion detection in water. These types of interaction motifs are now starting to appear in the design of organocatalysts and as bioisosteres in drug discovery. Finally, new generations of chemists continue to inspire us with the

development of new binding motifs to consider for anion recognition, with a recent report showing the RCF_2H group can serve as a HB donor that may mimic the function of ROH HB donors.[59]

Bridge to Chapter II

This chapter provided a general introduction and history of hydrogen bonding, with a particular focus on the aryl CH···anion hydrogen bond as a secondary binding motif. Chapter II will present two cases where urea hydrogen bonds are used as anchors in arylethynyl mono-urea anion receptors. One scaffold utilizes the aryl CH···anion interaction as a supporting binding motif, while the other scaffold is designed to promote an anion-pi interaction. The work in Chapter II will show that each of these secondary binding motifs influences the mechanism of binding in a 2-to-1 host-guest system.

CHAPTER II

DO CH-ANION AND ANION-Π INTERACTIONS ALTER THE MECHANISM OF 2:1 HOST-GUEST COMPLEXATION IN ARYLETHYNYL MONOUREA ANION RECEPTORS?

From L. M. Eytel, A. K. Gilbert, P. Görner, D. W. Johnson, M. M. Haley, "Do CH–Anion and Anion–π Interactions Alter the Mechanism of 2:1 Host–Guest Complexation in Arylethynyl Monourea Anion Receptors?" *Chem. Eur. J.* **2017**, *23*, 4051-4054. The experimental work was performed by me or A. K. Gilbert or P. Görner under my guidance. The X-ray diffraction data was collected and solved by Dr. L. N. Zakharov. The writing is entirely my own with editorial assistance provided by Dr. L. N. Zakharov, Prof. D. W. Johnson and Prof. M. M. Haley.

Introduction

For the past few decades, the field of anion sensing has been dominated by supramolecular receptors.[1] Supramolecular hosts have been shown to bind anionic guests through a variety of host-guest interactions, including anion-π interactions, hydrogen bonds, and weak-σ interactions.[1–3] Disregarding the larger molecular structure or type of guest, supramolecular hosts are currently designed to include some degree of preorganization and an attractive binding pocket.[1,2,4] Ideally, such probes can be easily tuned for analyte specificity and optoelectronic responses.[1–5]

Arylethynyl urea scaffolds make up the foundation of the supramolecular anion sensing scaffolds in our studies. A preorganized binding cavity is formed by a rigid alkyne linkage between arene rings and urea-based hydrogen bond (HB) donors.[6,7] The easily-functionalized core and pendant arenes are strategic designs, as they can be modified with electron-donating or electron-withdrawing substituents to modulate the acidity of the HB donors.[7b] Our previously reported arylethynyl bis-urea (e.g., **1**) and tris-urea receptors (**2**) have exhibited a variety of binding motifs for anions.[6–9] The majority of the bipodal hosts bind anions via aryl CH or pyridinium hydrogen bond donors at the core of the host, with the urea groups forming a U-shaped pocket that dominates the binding event, as shown in Figure 1.[7,8] This binding pattern is altered in trifluorophenyl tripodal receptor **2**, however, where anion-π interactions influence selectivity in favour of binding nitrate over chloride.[9] Furthermore, the crystal structure of the tris-urea host indicated that only two of the three available urea "arms" were interacting with an anionic guest.[9] This suggested that the number of urea donors may influence anion binding as much as the type of binding motif utilized in the host-guest interaction. Anion-π interactions have been observed in a myriad of receptors, and the ability to tune arenes to increase their selectivity for anion-π binding has been shown in other arene-based hosts.[1,9,10]

To elucidate both the degree of tunability of the anion binding motifs and the number of arylethynyl urea recognition elements necessary to bind an anion, we designed mono-urea host scaffolds **3** and **4** (Figure 1). The single "arm" permits more aggressive tuning of the arene core than what is synthetically accessible on the bis-arylethynyl scaffold, and the increased rotational freedom around the single ethynyl unit permits the

core arene to rotate to facilitate the preferred binding motif (i.e. anion-π, aryl CH H-bond, or weak-σ interactions). Berryman et al. utilized dinitro-substituted arenes in a tris-arene scaffold to host anions.[11] It was calculated that the 3,5-dinitro groups sterically block the aryl CH, preventing an H-bond interaction between the phenyl core and an anionic guest.[11] With the additional rotational freedom of scaffold **3**, we hypothesized that the 3,5-dinitrobenzene substitution pattern would promote anion-π or weak-σ interactions between the host scaffold and an anionic guest. Similarly, the pentafluoroarene scaffold **4** was inspired by the trifluorophenyl tripodal receptor **2**.[9] We hypothesized that the combination of an electron deficient aromatic ring and the removal of aryl H-bond donors would result in a scaffold that hosts anionic guests exclusively via an anion-π interaction in combination with the urea HB donors.

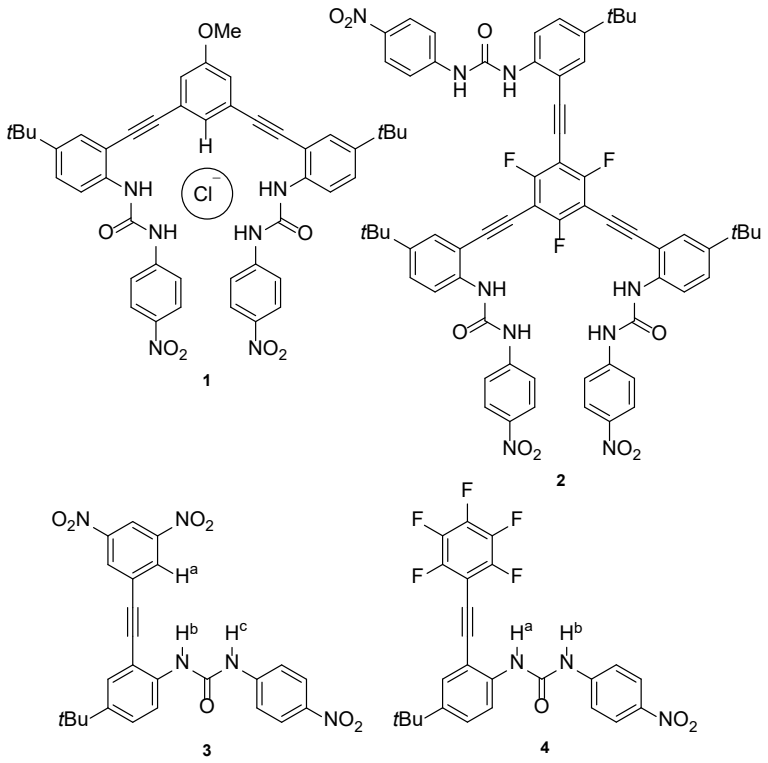

Figure 1. Previously reported bipodal bis-urea (**1**) and tripodal tris-urea (**2**) receptors along with the new monopodal arylethynyl mono-urea scaffolds (**3**, **4**).

Results and Discussion

Monopodal hosts **3** and **4** were synthesized as shown in Scheme 1. Desilylation of known ethynylaniline **5**[8b,f] and subsequent Sonogashira cross-coupling with 1-iodo-3,5-dinitrobenzene or iodopentafluorobenzene furnished cores **6** and **7** in 87% and 73% yield, respectively. Reaction of **6** or **7** with *p*-nitrophenyl isocyanate provided receptors **3** and **4** in 73% and 71% yield, respectively. The final compounds were fully characterized by ^{1}H, ^{13}C, and ^{19}F NMR spectroscopies, and 2D ^{1}H-^{13}C HSQC NMR spectroscopy was used to assign the aryl and urea proton resonances of **3**.

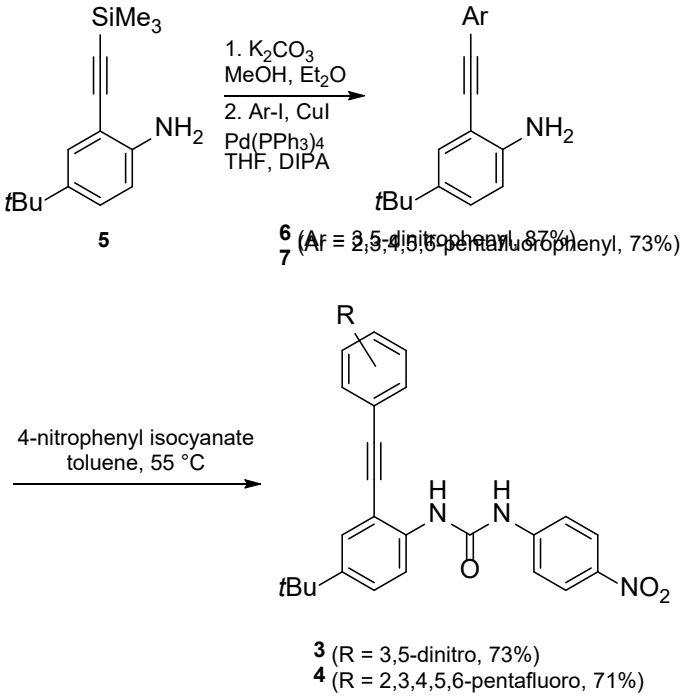

Scheme 1. Synthesis of arylethynyl mono-urea receptors **3** and **4**.

The anion binding characteristics of **3** and **4** were investigated with tetrabutylammonium (TBA) halide salts in 10% DMSO/$CHCl_3$ or the perdeutero equivalent. Titration experiments were performed at 1.0 mM concentration of chosen

host (Figure 2).[12] Association constants (K_a) for **3** and **4** with halides Cl^-, Br^-, and I^- were calculated using non-linear regression, non-cooperative fitting models in MatLab by simultaneously fitting the downfield shifting of the urea protons (H^b, H^c for **3**; H^a, H^b for **4**).[13] The internal aryl proton (H^a) resonance shifts were also included in the fitting of **3**.

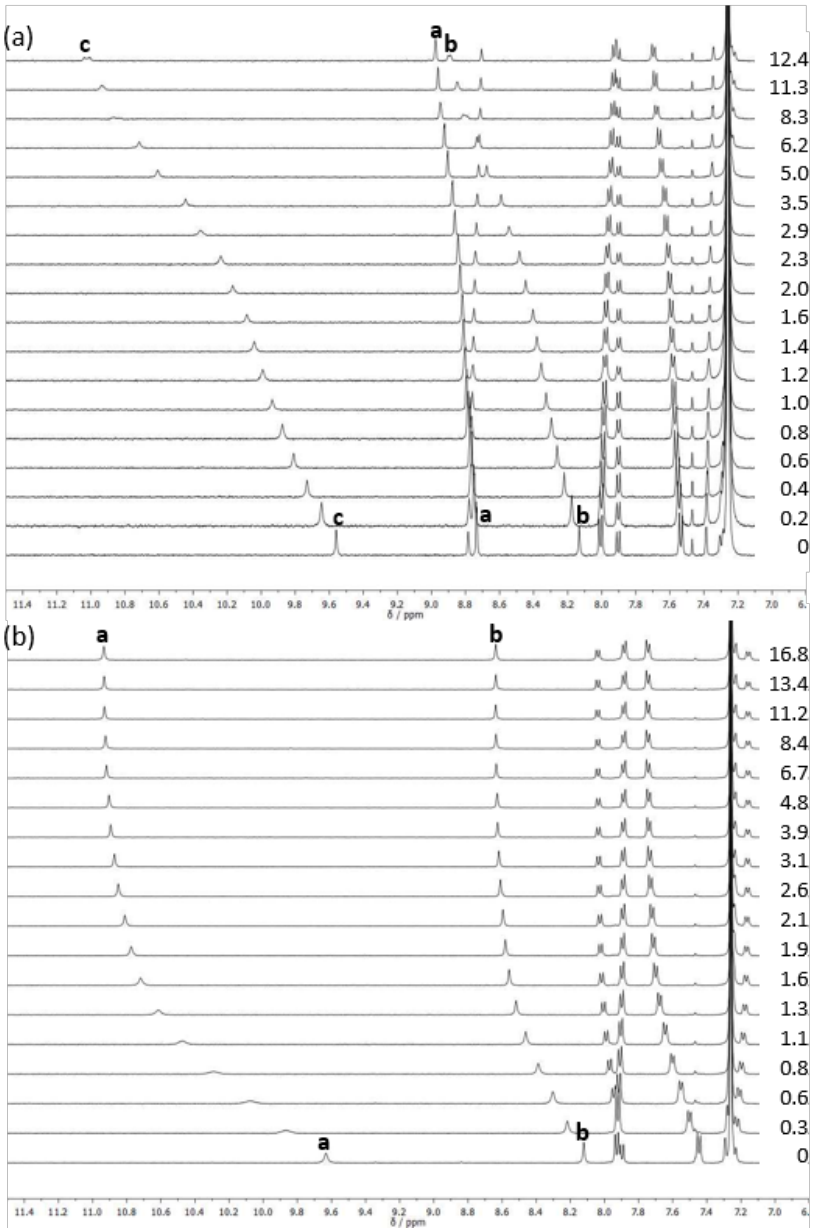

Figure 2. (a) ^{1}H NMR titration of **3** with TBA^+Cl^- at 298K; [**3**] = 0.4 mM in 10% water-saturated d_6-DMSO/$CDCl_3$. (b) ^{1}H NMR titration of **4** with TBA^+Br^- at 298K; [**4**] = 1.0 mM in 10% water-saturated d_6-DMSO/$CDCl_3$. Peak assignments refer to labelled hydrogen atoms in Figure 1.

Titrations were initially fit to a 1:1 host-guest model, but residual errors were large, indicating a poor fit. In addition, the serpentine-like shift of urea proton H^c in the titrations of **3** hinted at the possibility of higher-order binding stoichiometry (Figure 2a).[14–16] Job's plot analysis revealed a 2:1 host-guest model might be more appropriate for the binding stoichiometry (See ESI). Indeed, titrations fit to a 2:1 host-guest model provided minimalized residual errors.[15] The previous arylethynyl urea probes studied by our lab included at least two-urea recognition motifs to host a guest anion, and the fit of the mono-arylethynyl urea probes **3** and **4** to a 2:1 host-guest system further signifies the necessity of including multiple urea recognition motifs in a scaffold's design.

Table 1. Anion association constants (K_a) for receptors **3** and **4** obtained by fitting titration data to a step-wise 2:1 host-guest model in MatLab.[a]

Host	Cl^-/M^{-1}[a]		Br^-/M^{-1}[a]		I^-/M^{-1}[a]	
	K_a1	K_a2	K_a1	K_a2	K_a1	K_a2
3	300	740	320	1040	360	6570
4	118000[b]	10200	930	2500	130	750

[a] Anions added as tetrabutylammonium salts in 10% water-saturated d_6-DMSO/$CDCl_3$. Values represent an average of three ^{1}H NMR titrations. Error is *ca.* ±15%. [b] Reference 17.

The stepwise K_a1 and K_a2 values for both **3** and **4** with the various halides were determined across three titrations with less than a 15% error (Table 1). The K_a1 values for **3** are within error of each other, but the K_a2 values increase by an order of magnitude with increasing guest size. The trend could be related to the ability of the recognition scaffolds to donate increasingly linear hydrogen bonds in the assembled binding pocket. Interestingly, there is a clear statistically significant difference in the K_a1 values for **4** with the halides, and the overall trend of association constants appears to be opposite in **4**

versus **3**; that is, in **3** there is a slight reverse Hofmeister trend in anion binding of $I^- > Br^- > Cl^-$ and in **4** the opposite is true: $Cl^- > Br^- > I^-$. The change in anion preference could be due to the formation of an anion-π interaction in **4**·X^-, and the smaller anions are capable of a closer interaction with the π-systems.[2] The preference for larger halides in **3** could be the result of both aryl CH hydrogen bonds becoming more linear, increasing the strength of the interactions.

The order in which the anion binds the two hosts could shed additional light on the nature of the interactions of these hosts with anions. There are two likely mechanisms in which a 2:1 host-guest complex can form: two hosts associate, then an anion binds in the dimer pocket (Figure 3a), or one host binds the anion, followed by a second host binding the 1:1 complex (Figure 3b).[13,14] If a complex initially dimerizes/aggregates, the K_a1 value would likely be independent of the nature of anion present; this rings true for scaffold **3**. Additionally, these K_a1 values are on the same order of magnitude as the dimerization constant for **3** in the absence of an anion/salt, suggesting that K_a1**[3]** might resemble a receptor dimerization event.[18] It is also possible the supporting "weak' interaction in **3** (e.g., CH-anion from the dinitrophenyl ring) creates a competing trend in anion binding that prefers the softer iodide over chloride/bromide, and thus mechanism (b) is still at play but this competing selectivity cancels the anion binding dependence in K_a1.

The 2:1 assembly situation is much more clear for the anion complexes of **4**. Both K_a1 and K_a2 values of **4** change across the anion series, as predicted by relative anion basicity, supporting the 2:1 complex forming via a step-wise mechanism dominated by

traditional hydrogen bonding interactions with the ureas and possible supporting anion-π interactions with the pendant pentafluorphenyl rings (Figure 3b).

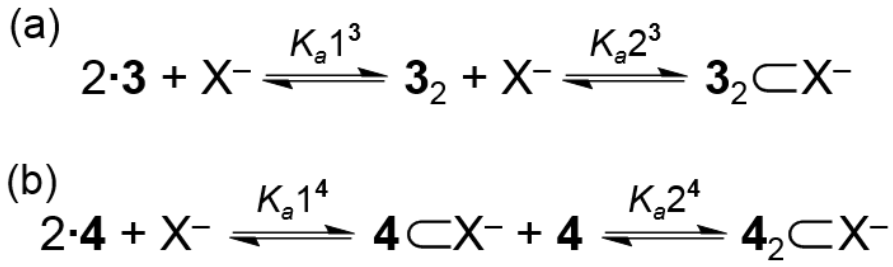

Figure 3. Simplified equilibrium equations illustrating the two possible modes for formation of a 2:1 host-guest complex: (a) initially a dimer forms, followed by the anion addition to form the 2:1 complex, or (b) a 1:1 host-guest complex forms and a second host binds to form a 2:1 complex.

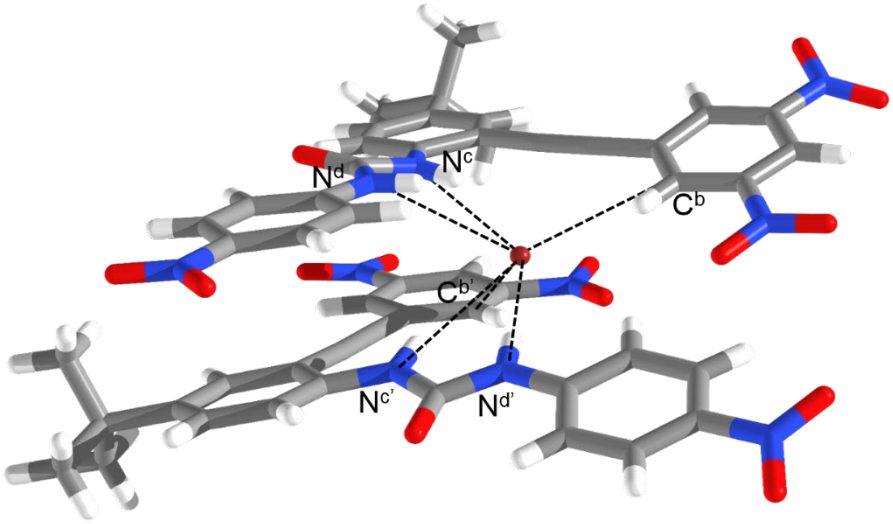

Figure 4. X-ray crystal structure of **3₂·Br⁻**. Hydrogen bond interactions shown as dotted line. TBA^+ counter cation and solvent molecules have been omitted for clarity.

The 2:1 host-guest stoichiometry was further confirmed in the solid-state via X-ray crystallography. Single crystals of **3** grown in the presence of TBA^+Br^- were obtained via slow evaporation from $CHCl_3$/DMSO.[19] Two receptors asymmetrically encapsulate the Br^- atom through a total of six weak hydrogen bond contacts (Figure 4). Each

receptor donates two hydrogen-bonds through the urea moiety and another weak CH hydrogen- bond through the dinitrophenyl core with distances N^{d}–Br 3.27(1) Å, N^{c}–Br 3.63(2) Å, C^{b}–Br 3.62(2) Å, $N^{d'}$–Br 3.29(2) Å, $N^{c'}$–Br 3.64(2) Å, $C^{b'}$–Br 3.69(2) Å and angles N^{d}–H^{d}•••Br 141.3(4)°, N^{c}–H^{c}•••Br 146.3(2)°, C^{b}–H^{b}•••Br 161.8(6)°, $N^{d'}$–$H^{d'}$•••Br 172.6(4)°, $N^{c'}$–$H^{c'}$•••Br 151.2(9)°, $C^{b'}$–$H^{b'}$•••Br 133.3(1)°.

Although previous calculations predicted the aryl CH HBs would be inaccessible due to the steric hindrance of the nitro substituents,[11] the importance of aryl CH HBs is not lost in the crystal structure of scaffold **3**. The ability for two equivalents of **3** to encapsulate an anionic guest via six weak hydrogen bonds also contributes to the large association constants seen in the solution state studies. Though solid state data has yet to be obtained, it is reasonable to hypothesize that **4** shows a similar binding interaction as **3**, with the CH HBs replaced by anion-pi interactions since **4** lacks CH HB donors. A color change was not seen upon the addition of anion, indicating that a weak-σ interaction/charge-transfer complex is not involved. This lends further credence to our speculation that anion-π is the most probable supporting interaction in the host-guest complex of **4**, whereas CH-anion interactions are present in **3**. An anionic guest can interact with **4** through two anion-π interactions, along with the four urea HB donors.

In summary, the solid state data in combination with the solution phase K_a values provide a convincing argument for the necessity of at least two urea recognition motifs in a strong arylethynyl receptor scaffold. The inclusion of a phenyl core with the ability to host an anionic guest via an aryl CH HB or an anion-π interaction also appears to influence the order of the halide binding within the self-assembled binding pocket.

Further research on the effect of cooperativity of these monopodal arylethynyl-urea scaffolds is currently in progress.

Experimental

General methods

^{1}H, ^{13}C, and ^{19}F NMR spectra were obtained on a Varian Mercury 300 MHz (^{1}H: 300.09 MHz), Inova 500 MHz (^{1}H: 500.10 MHz, ^{13}C 125.75 MHz, ^{19}F: 470.56 MHz), or Bruker Avance III HD 600 MHz NMR spectrometer with Prodigy multinuclear broadband BBO CryoProbe (^{1}H: 600.02 MHz, ^{13}C: 150.89 MHz). Chemical shifts (δ) are expressed in ppm downfield from tetramethylsilane (TMS) using non-deutrated solvent present in the bulk deutrated solvent ($CDCl_3$, ^{1}H 7.26 ppm, ^{13}C 77.16 ppm; *d*$_6$-DMSO: ^{1}H 2.50 ppm, ^{13}C 39.52 ppm; *d*$_6$-acetone ^{1}H 2.05 ppom, ^{13}C 206.7 ppm, 29.9 ppm). Mixed solvent systems were referenced to the most abundant solvent. All NMR spectra were processed using MestReNova NMR processing software. Unless otherwise specified, all materials were obtained from TCI-America, Sigma-Aldrich, or Acros and used as received. Tetrabutylammonium salts were dried at 50 °C in vacuo prior to use. Aniline **5** was synthesized and desilated following known procedures.[7]

Synthesis

3,5-Dinitrophenyl aniline 6. In a sealable flask, 1-iodo-3,5-dinitrobenzene (1.20 g, 4.08 mmol) was dissolved in DIPA (20 mL) and THF (20 mL). The mixture was purged with N_2 for 30 min, then CuI (0.076 g, 0.408 mmol) was added. The mixture was purged for an additional 30 min, followed by the addition of $Pd(PPh_3)_4$ (0.38 g, 0.327 mmol). An N_2-purged solution of 4-*tert*-butyl-2-ethynylaniline (1.05 g, 6.05 mmol) in

DIPA (10 mL) and THF (10 mL) was then transferred into the flask via cannula. The flask was sealed and the mixture was stirred overnight at 50 °C. The cooled solution was filtered through a 6 cm silica gel plug eluting with CH_2Cl_2 and the concentrated *in vacuo*. Column chromatography (2:1 EtOAc:hexanes) of the crude material afforded **6** (1.24 g, 87%) as an orange solid. ^{1}H NMR (500 MHz, $CDCl_3$) δ 8.95 (t, J = 1.8 Hz, 1H), 8.64 (d, J = 2.0 Hz, 2H), 7.41 (d, J = 2.1 Hz, 1H), 7.17 (d, J = 7.5 Hz, 1H), 6.72 (d, J = 8.4 Hz, 1H), 4.21 (s, 2H), 1.30 (s, 9H). ^{13}C NMR (126 MHz, $CDCl_3$) δ 148.94, 146.56, 141.69, 140.39, 129.54, 129.43, 127.77, 117.84, 115.17, 105.45, 93.43, 90.39, 34.40, 31.74. HRMS (TOF-MS-ES$^-$) for $C_{18}H_{16}N_3O_4$ $[M–H]^-$: calcd 338.1141, found 338.1157.

Pentafluorophenyl aniline 7. Following the procedure for the synthesis of **6**, iodopentafluorobenzene (1.25 g, 4.25 mmol) was reacted with 4-*tert*-butyl-2-ethynylaniline (1.11 g, 6.38 mmol) in the presence of THF (25 mL), DIPA (25 mL), CuI (0.040 g, 0.21 mmol), and $Pd(PPh_3)_4$ (0.393 g, 0.340 mmol). Product **7** was obtained via a silica plug (2:1 hexanes:EtOAc) as a black-brown solid and used without further purification (1.04 g, 72%). ^{1}H NMR (500 MHz, $CDCl_3$) δ 7.36 (d, J = 2.3 Hz, 1H), 7.21 (dd, J = 8.5, 2.4 Hz, 1H), 6.73 (d, J = 8.7 Hz, 1H), 4.52 (s, 2H), 1.26 (s, 9H). ^{13}C{^{19}F} NMR (126 MHz, $CDCl_3$) δ 147.25, 146.24, 141.08, 129.62, 128.91, 128.73, 128.22, 114.60, 106.01, 105.56, 80.31, 78.72, 34.08, 31.47. ^{19}F NMR (471 MHz, $CDCl_3$) δ –136.62 (dd, J = 22.1, 7.7 Hz), –153.44 (t, J = 41.0 Hz), –161.86 (m). HRMS (TOF-MS-ES$^+$) for $C_{18}H_{15}NF_5$ $[M–H]^+$: calcd 340.1125, found 340.1137.

3,5-Dinitrophenyl receptor 3. In flame dried glassware, aniline **6** (0.250 g, 0.737 mmol) and *p*-nitrophenyl isocyanate (0.212 g, 1.29 mmol) was dissolved in freshly distilled toluene (75 mL). The reaction mixture was stirred for 48 h at 50 °C. The reaction

was quenched with acetone, allowed to cool, and concentrated *in vacuo*. Product **3** was precipitated with acetone from a hexanes solution (0.271 g, 73%) as an orange solid. ^{1}H NMR (500 MHz, d_6-acetone) δ 9.18 (s, 1H), 8.91 (t, J = 2.1 Hz, 1H), 8.34 (s, 1H), 8.24 (d, J = 9.1 Hz, 2H), 8.19 (d, J = 2.6 Hz, 1H), 7.80 (d, J = 9.2 Hz, 2H), 7.72 (d, J = 2.4 Hz, 1H), 7.57 (dd, J = 8.9, 2.4 Hz, 1H), 1.36 (s, 9H). ^{13}C NMR (126 MHz, d_6-acetone) δ 152.65, 149.82, 147.10, 146.93, 143.21, 139.15, 132.21, 130.51, 129.23, 127.29, 125.98, 121.14, 119.19, 118.85, 111.74, 92.10, 91.43, 35.08, 31.63. HRMS (TOF-MS-ES$^-$) for $C_{25}H_{20}N_5O_7$ [M–H]$^-$: calcd 502.1363, found 502.1358.

Pentafluorophenyl receptor 4. In flame dried glassware, aniline **7** (0.500 g, 1.47 mmol) and *p*-nitrophenyl isocyanate (0.423 g, 2.58 mmol) was dissolved in freshly distilled toluene (150 mL). The reaction mixture was stirred for 72 h at 50 °C. The reaction was quenched with acetone, allowed to cool, and concentrated *in vacuo*. Pure product **4** was precipitated out of hot EtOAc (0.574 g, 71%) as a yellow solid. ^{1}H NMR (500 MHz, d_6-DMSO/$CDCl_3$) δ 9.52 (s, 1H), 8.04 (s, 1H), 7.86 (dd, J = 9.2, 2.1 Hz, 2H), 7.83 (d, J = 8.8 Hz, 1H), 7.37 (dd, J = 9.1, 2.3 Hz, 2H), 7.18 (d, J = 2.3 Hz, 1H), 7.16 (dd, J = 8.8, 2.4 Hz, 1H), 1.05 (s, 9H). ^{13}C{^{19}F} (125.75 MHz, d_6-DMSO/$CDCl_3$) 151.99, 145.76, 145.63, 145.57, 145.55, 138.52, 129.46, 127.91, 127.79, 124.96, 124.77, 120.10, 117.24, 110.03, 109.80, 79.91, 79.26, 39.99, 30.88. ^{19}F NMR (471 MHz, d_6-DMSO/$CDCl_3$) δ –135.24 (m), –152.00 (m), –161.49 (m). HRMS (TOF-MS-ES$^+$) for $C_{25}H_{18}F_5N_3O_7$ [M–H]$^+$: calcd 504.1347, found 504.1350.

X-Ray Crystallography

Diffraction intensities were collected at 173 K on a Bruker Apex2 CCD diffractometer using CuKα radiation, λ = 1.54178 Å. Space group was determined based

on systematic absences. Absorption correction was applied by SADABS.[20] Structure was solved by direct methods and Fourier techniques and refined on F^2 using full matrix least-squares procedures. All non-H atoms were refined with anisotropic thermal parameters. All H atoms were refined in calculated positions in a rigid group model. There are two symmetrically independent molecules in the crystal structure. One of the terminal –Me groups in the $[N(n\text{-Bu})_4]^+$ cation is disordered over two positions in the ratio 0.69/0.31. The Br^- anion forms H-bonds to the two main molecules. Crystals of the investigated compound were very small needles and even using a strong *Incoatec IμS Cu* source the diffraction data were collected only up to $2\theta_{max} = 100°$. The reflections at high angles were very weak and as a result reflection statistics at high angles is poor and value of R_{int} is high. While the found X-ray structure is not precise, it provides clear chemical information about the formed complex. All calculations were performed by the Bruker SHELXL-2013 package.[21]

Crystal structure 3_2•(*n*-Bu)$_4$NBr. $C_{68}H_{84}BrN_{11}O_{15}S$, M = 1407.43, 0.23 x 0.01 x 0.01 mm, T = 173 K, Monoclinic, space group $P2_1/c$, a = 20.6647(10) Å, b = 10.3192(5) Å, c = 35.0367(16) Å, β = 104.992(3)°, V = 7217.0(6) Å^3, Z = 4, D_c = 1.295 Mg/m^3, μ(Cu) = 1.630 mm^{-1}, F(000) = 2960, $2\theta_{max}$ = 100.0°, 25199 reflections, 7300 independent reflections [R_{int} = 0.3631], R1 = 0.1166, wR2 = 0.2657 and GOF = 0.974 for 7300 reflections (850 parameters) with I>2σ(I), R1 = 0.3173, wR2 = 0.3633 and GOF = 0.974 for all reflections, max/min residual electron density +1.343/–0.516 eÅ^3. CCDC 1507418 contains the supplementary crystallographic data for these compounds. These data can be obtained free of charge from The Cambridge Crystallographic Data Centre via www.ccdc.cam.ac.uk/data_request/cif.

Titrations

General Titration Procedures. Concentration of receptor was kept constant by preparing a stock solution of the receptor and performing a serial dilution with the receptor stock solution to dissolve the guest. Receptor concentration was maintained constant throughout the titration to avoid concentration effects on the proton chemical shifts. Tetrabutylammonium salts, purchased from TCI America or SigmaAldrich, were dried by heating to 50 °C *in vacuo* before use. Hamilton gas-tight syringes were used for all titrations. Titrations were performed in triplicate and the reported association constants represent the average fits across all titrations. Representative data are provided for each receptor and halide.

^{1}H NMR Titration Conditions. ^{1}H NMR titrations were carried out on an Inova 500 MHz NMR spectrometer (^{1}H: 500.10 MHz). Chemical shifts (δ) are expressed in ppm downfield from tetramethylsilane (TMS) using non-deutrated solvent present in the bulk deutrated solvent ($CDCl_3$, ^{1}H 7.26 ppm; d_6-DMSO: ^{1}H 2.50 ppm). Mixed solvent systems were referenced to the most abundant solvent. All NMR spectra were processed using MestReNova NMR processing software. Association constants were determined using step-wise non-linear regression fitting in MatLab.[13]

UV-Vis Titration Conditions. UV-Vis titrations were carried out on an HP 8453 UV-Vis spectrometer. Water-saturated 10% DMSO/$CHCl_3$ was prepared in the same manner as for the ^{1}H NMR titrations. Association constants were determined by non-linear regression using Open Data Fit.[13]

Bridge to Chapter III

Chapter II introduces the concept of selective anion sensing through modifying the secondary binding motifs. Chapter III follows-up with this concept through the synthesis and study of the anion-binding properties of three bis-urea anion receptor scaffolds with varied aromatic cores. Chapter III presents either a 2,6- or 3,5-pyridine or a bipyridyne-based bis-urea scaffolds that are found to bind three disparate oxoanions in equally high affinities. Surprisingly, the anion binding properties of these receptors are more dependent on solvent and entropic effects than on the supporting interactions.

CHAPTER III

CONFORMATIONALLY FLEXIBLE ARYLETHYNYL BIS-UREA RECEPTORS BIND DISPARATE OXOANIONS WITH SIMILAR, HIGH AFFINITIES

From L. M. Eytel, A. C. Brueckner, J. A. Lohrman, M. M Haley, P. H.-Y. Cheong, and D. W. Johnson, "Conformationally flexible arylethynyl bis-urea receptors bind disparate oxoanions with similar, high affinities" *Chem. Commun.* 2018, **54**, 13208-13211. I synthesized both pyridine receptors and completed the analytical work of all three receptors. A. C. Brueckner and Prof. P. H.-Y. Cheong completed the quantum mechanical analysis. Dr. J. A. Lohrman synthesized the bipyridine receptor through the crude bis-urea product. The writing is entirely my own with editorial assistance provided by A. C. Brueckner, Prof. P. H.-Y. Cheong,, Prof. M. M. Haley, and Prof. D. W. Johnson.

Introduction

Nitrogen and phosphorous species from agricultural run-off, particularly nitrate (NO_3^-) and phosphates (e.g., HPO_4^{2-}), are attributed to the hypoxic zone that appears in the Gulf of Mexico and other bodies of water each spring.[1,2] Sulfate (SO_4^{2-}) and perchlorate (ClO_4^-) are also problematic environmental pollutants originating from sources such as nuclear waste and jet fuels, respectively.[3,4] Recognition and dynamic monitoring of these weakly basic and charge-diffuse anions relies heavily on supramolecular receptors.[5]

Binding sensitivity toward protic and aprotic oxoanions in supramolecular host-guest systems, however, poses challenges. Many studies have reported designer supramolecular receptors for the purpose of binding these diffuse anionic systems by utilizing cages, flexible alkyl linkages, and charged binding units.[6-8] Additional fundamental understanding of the factors influencing the binding of these anions will help advance receptor design for specific anions utilizing neutral, conformationally flexible receptors.

Generally, larger, pre-organized binding pockets enhance the ability of a synthetic receptor to bind oxoanions.[5,6,8] For instance, tetracarboxamide-based macrocycles and shape-persistent cyanostar macrocycles have been shown to bind oxoanions via higher-order binding stoichiometries.[8] Herein, we investigate a class of receptors featuring conformational flexibility that apparently allows guests of varying sizes to be accommodated in what we previously considered as relatively small binding pockets. Additionally, we explore the impact of supporting attractive interactions (e.g., aryl C–H hydrogen bond donors and pyridine lone pair hydrogen bond acceptors) on the binding affinities of protic and aprotic oxoanions.

While we have reported a number of examples of recognition of spherical anions by pyridyl bis-urea receptors,[9] only a few of these receptors have shown affinities for oxoanions.[9e,10,11] One reason for this is the apparent size of the binding pocket: at first glance it does not intuitively appear large enough to bind oxoanions. However, an extended bipyridyl bis-urea host in this receptor class showed binding selectivity to dihydrogen phosphate ($H_2PO_4^-$) by rotating along the bipyridyl and/or alkynyl bonds,

suggesting other binding pockets might be accessible through conformational changes within this receptor class (Fig. 1).[10,12]

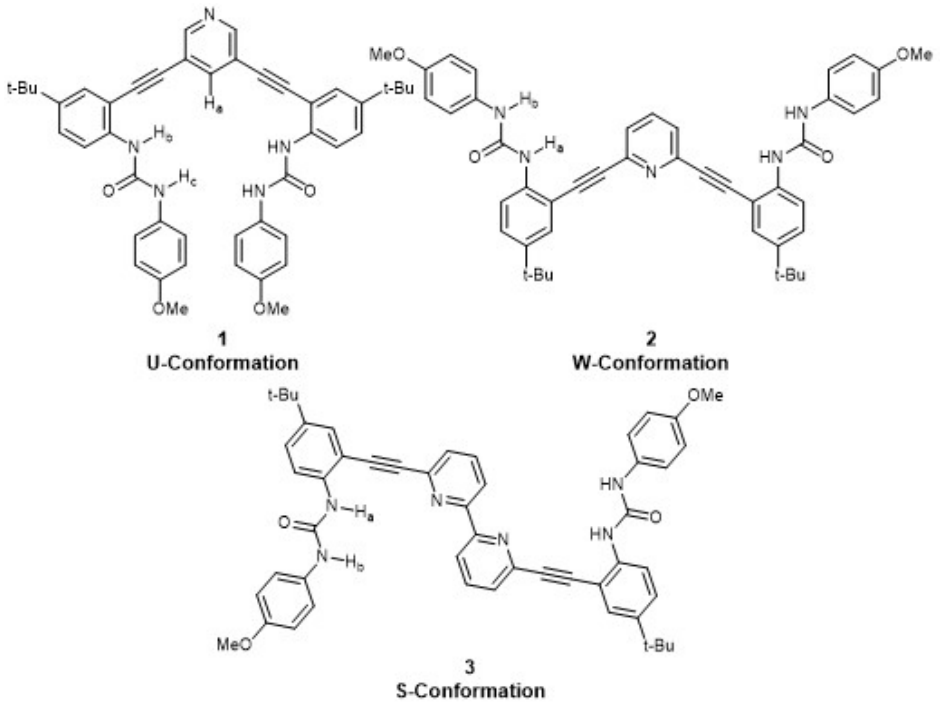

Figure 1. Pyridine core bis-urea receptors utilized in this study. New receptor with 3,5-pyridine core (**1**) shown in the "U"-conformation, along with the previously reported Chemdraw representation of 2,6-pyridine receptor (**2**) in the "W"-conformation and the modified bipyridine receptor (**3**) shown in the "S"-conformation.[9a,10]

An extension of these studies revealed that a pyridine-based mono-urea receptor served as a model for the "W" conformation and bound oxoanions at a similar magnitude as a bipyridyl bis-urea, supporting the potential affinity of this alternate binding pocket to oxoanions.[11] Subsequent studies of aryl mono-urea receptors indicated two urea binding units were preferred when binding anions (to the extent that even 2:1 host:guest complexes were favourable in this mono-urea host), indicating the next logical step was to investigate the affinity of pyridyl bis-urea receptors toward oxoanions.[12] Herein we

report the solution-state association constants and computed binding geometries of three pyridine-based bis-urea receptors (Fig. 1) in the presence of three disparate tetrahedral oxoanions and find that they are all excellent hosts for these anions.

To investigate the differences in oxoanion affinity between different binding interactions, we compared two similar pyridine-based receptors (3,5- and 2,6-bis(2-anilinoethynyl)pyridine bis(4-methoxyphenyl)urea; Fig. 1, **1** and **2**, respectively) as well as a bipyridyl-based bis-urea (Fig. 1, **3**). In all interactions between hosts **1**, **2**, and **3** and the respective oxoanions, there are three major factors at play: the H-bond accepting or donating ability of the aromatic core of the receptor, the inherent properties of the anion (i.e., number of protons, pK_a of corresponding acid, and ionic radii), and the size/shape of the binding pocket within each receptor.

These pyridine receptors directly probe the preference of aryl H-bond acceptors or donors in protic and aprotic oxoanions. All receptors have the ability to bind anions in several conformations, including the U, W, and S conformation (Fig. 1, **1**, **2**, and **3**, respectively).[9b] Newly designed host **1** allows for a weak aryl C–H hydrogen bond to anions; the presence of five hydrogen bond donors (one C–H and four N–H bonds) in the W-shaped pocket suggested **1** should preferentially bind more basic and/or aprotic oxoanions and halides.[9]

We compared this to known host **2**, which features our traditional 2,6-pyridyl core. We hypothesized **2** would prefer monoprotic oxoanions, as the nitrogen lone pair in the pocket acts as an H-bond acceptor. When investigating the 1-to-1 host-guest interaction, the homologous bipyridine receptor **3** was expected to have the greatest binding preference toward oxoanions, particularly diprotic oxoanions, due to the large

binding pocket and its ability to accept multiple H-bonds from the (di)protic oxoanions in the bipyridyl core.[11]

Results and Discussion

The syntheses of **1** and modified host **3** are based on previously reported strategies for related aryl acetylene bis-urea systems (Scheme 1, see appendix for detailed procedures).[9a,10] The anion-binding characteristics of **1**-**3** were probed by spectroscopic titrations in 10% DMSO/90% water-saturated $CHCl_3$ solutions, the perdeutero equivalent, or acetonitrile, with anions introduced as tetrabutylammonium (TBA) salts. ^{1}H NMR titrations were performed at 1.0 mM concentration of host, while UV-Vis titrations were performed at a host concentration of 25 μM. Association constants (K_a) for **1**-**3** with dihydrogen phosphate ($H_2PO_4^-$), hydrogen sulfate (HSO_4^-), and perchlorate (ClO_4^-) were obtained using non-linear regression fitting models in Bindfit by simultaneously fitting the change in absorbance for each host–guest complex at the attributed λ_{max} (Fig. 2).[13,14] K_a's for receptors **1**-**3** with bromide (Br^-) were either previously reported or obtained using non-linear regression fitting models in MatLab by simultaneously fitting the downfield shifting of the urea protons (H_b, H_c for **1**; H_a, H_b for **2** and **3**).[13] The shifts of the internal aromatic proton (H_a) were also used in the fitting of **1**.

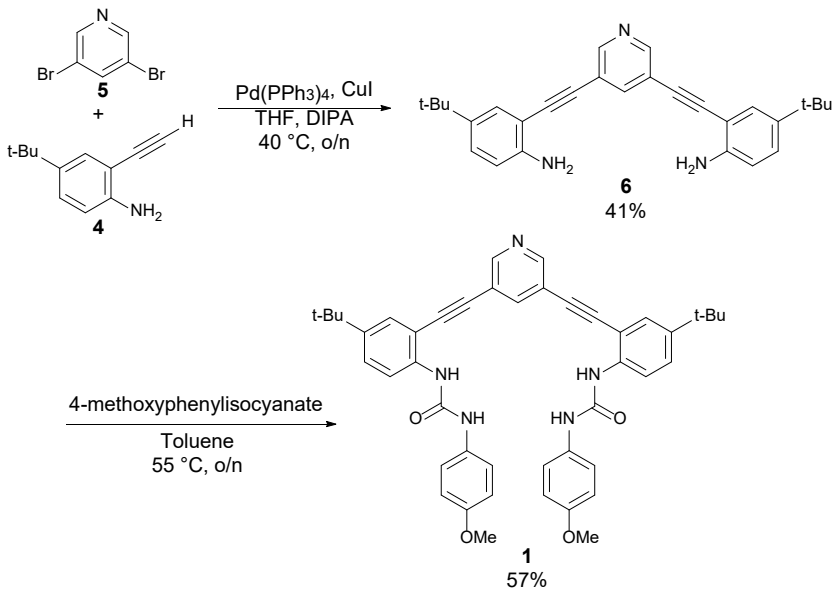

Scheme 1. Synthesis of 3,5-pyridine bis-urea receptor **1**.

Initial ^{1}H NMR titration experiments were performed on **1** with bromide, a spherical anion with relatively well-characterized binding behavior.[9] Consistent with other aryl CH hydrogen bonding phenylacetylene bis-urea receptors, the association constant for **1** with Br^- was relatively low (Table 1). Nonetheless, ^{1}H NMR titrations were used in an attempt to characterize the affinity of **1** with dihydrogen phosphate (Fig. 2a). Fitting the downfield shifts of the selected protons resulted in a K_a value nearing the detection limits of ^{1}H NMR spectroscopy. Furthermore, the serpentine-like shifts of multiple aromatic resonances and the appearance of peak-splitting, particularly in the presence of excess guest, indicated higher-order binding stoichiometries were likely occurring.[8,12,13] To support this conclusion, fitting the titration data to a 2:1 host–guest binding model resulted in better fitting (as indicated by the shape of the residual asymptotic errors) than the 1:1 host–guest binding model (see appedix for detailed titration data).[13]

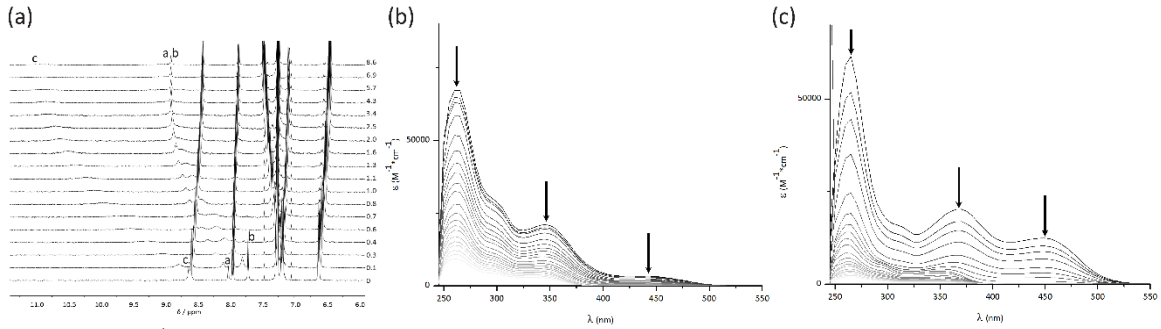

Figure 2. (a) ^{1}H NMR titration of **1** with $TBA^{+}H_2PO_4^{-}$ at 298K; [**1**] = 1.0 mM in 10% d_6-DMSO / 90% H_2O-saturated $CDCl_3$. Equivalents of guest labelled at the right of spectra. Peak assignments refer to labelled hydrogens in Fig. 1. (b) UV-Vis titration of **2** with up to 36.7 equiv. of $TBA^{+}H_2PO_4^{-}$ at 298K; [**2**] = 25 μM in 10% DMSO / 90% H_2O-saturated $CHCl_3$. Arrows represent the change in ε at the wavelengths of HG as guest is added. (c) UV-Vis titration of **3** with up to 7.4 equiv. of $TBA^{+}H_2PO_4^{-}$ at 298K; [**3**] = 25 μM in in 10% DMSO / 90% H_2O-saturated $CHCl_3$. Arrows represent the change in ε at the wavelengths of HG as guest is added.

UV-Vis titration experiments were implemented to further investigate the surprising interaction strength between receptors **1**-**3** and the selected series of oxoanions. At the more dilute 25 μM host concentration (dissolved in 10% DMSO/90% H_2O-saturated $CHCl_3$), a 1-to-1 host–guest interaction dominates the binding and 1:1 fitting models proved a better fit than higher binding stoichiometry models (i.e., 2:1 or 1:2 host:guest).[12,13] Job's method of continuous variation further confirms this 1:1 binding stoichiometry (see appendix).

To our surprise, all three receptors exhibited similar affinities toward all three oxoanions, with observed free-energies of binding (ΔG) ranging from –6.56 to –6.32 kcal mol^{-1}. In an attempt to understand the lack of trends in binding between the receptors with different supporting binding interactions and the disparate anions, we turned to quantum mechanical (QM) computations. Interestingly, the trend in computed free energies of binding (ΔG_{QM}) closely follows the trend in aqueous conjugate acid pK_a (2, –3, and –10 for H_3PO_4, H_2SO_4, and $HClO_4$, respectively; Table 1).[15]

Table 1. Association constants (K_a) and free energies of binding (ΔG, kcal mol^{-1}) reported for receptors **1**-**3**. Observed free energies obtained by fitting titration data to a step-wise 1:1 host-guest model in Bindfit.[a,13,14] Quantum mechanical free energies computed at PBE/6-31G(d) in PCM(DMSO).[17]

			1				2			3		
Anion	pK_a[15]	logK_a	ΔG$_{obs}$	ΔG$_{QM}$	logK_a[b]	ΔG$_{obs}$[b]	logK_a	ΔG$_{obs}$	ΔG$_{QM}$	logK_a	ΔG$_{obs}$	ΔG$_{QM}$
Br$^-$	–9.0	2.07[c]	–2.80[c]	–	–	–	2.00[d]	–2.72[d]	–	1.78	–2.42	–
$H_2PO_4^-$	2.1	4.74	–6.44	–4.6	5.02	–6.83	4.77	–6.48	–9.7	4.83	–6.56	–12.8
HSO_4^-	–3.0	4.68	–6.37	1.3	3.21	–4.36	4.78	–6.49	–3.5	4.76	–6.47	–4.8
ClO_4^-	–10.0	4.66	–6.33	6.2	*N.D.*[e]	~0[e]	4.65	–6.32	7.3	4.71	–6.39	2.4

[a]Anions added as TBA^+ salts in 10% DMSO/90% water-saturated $CHCl_3$ or the perdeutero equivalent (unless noted). Values represent an average of three UV-Vis titrations at 25 μM host concentration. Error is *ca.* ±15%. [b]Measured in acetonitrile. [c]Value obtained using ^{1}H NMR titrations at 1 mM host concentration. [d]Value previously reported.[9] [e]Value not detectible.

The conformational freedom within these receptors appears to allow for the formation of binding pockets of appropriate size to host these oxoanions. In fact, DFT structures reveal all three receptors prefer the U-shaped binding conformation, with each binding pocket spanning roughly 5.9 Å between the proximal urea hydrogens (H_b for **1** and H_a for **2** and **3**, see appendix). The ionic radii of each oxoanion is also similar (~2.4 Å),[16] and space-filling models show that $H_2PO_4^-$ is able to fit neatly into each of the receptors in their lowest-energy U-conformations (Fig. 3). Curiously, however, the secondary interactions with the varying pyridyl cores (CH donor versus pyridyl/bipyridyl H-bond acceptors) appear significant in the computed structures but did not contribute to dramatic changes in observed binding energies in the low-polarity mixed solvent system studied (10% DMSO/90% H_2O-saturated $CHCl_3$). Considering the accuracies of the experimental measurements and the wide range of computational methods tested,[17] it appears that the discrepancies between the experimental and computational values are not simply in error. In the absence of other effects, we hypothesized that entropic and/or solvation effects in this solvent mixture contribute to these differences.

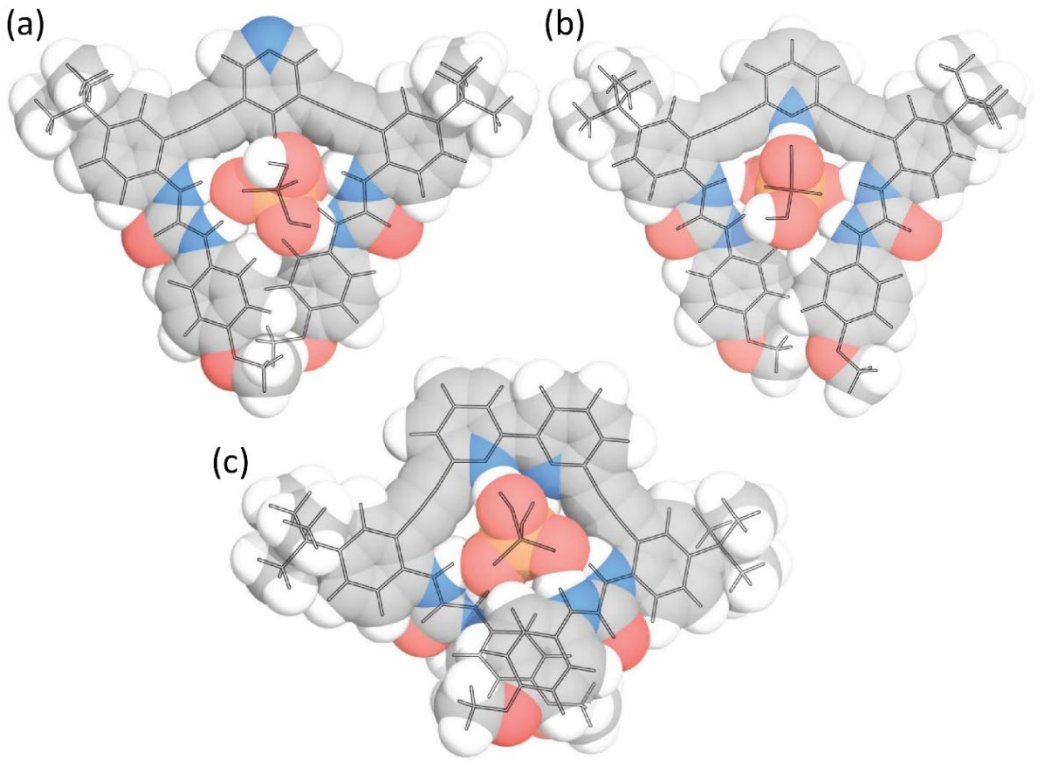

Figure 3. Space-filling models of receptors (a) **1**, (b) **2**, and (c) **3** binding $H_2PO_4^-$. Complexes computed at PBE/6-31G(d) in PCM(DMSO).

To further investigate the presence of solvation effects, titrations were performed in neat acetonitrile, a more competitive, polar solvent ($\varepsilon = 36.6$ for CH_3CN versus effective ε ~8.1–8.5 for 10% DMSO/90% water-saturated $CHCl_3$ mixture).[18] Due to solubility restrictions with **2** and **3** in pure CH_3CN, titrations were only performed with receptor **1** and the array of oxoanions. In this more polar solvent, the observed binding energies follow the expected basicity trend, with **1** showing no detectible affinity toward the least basic ClO_4^- anion. Additionally, the higher K_a value of **1** with $H_2PO_4^-$ in acetonitrile versus that determined in the less polar, mixed solvent system indicates that this receptor has a particularly high selectivity toward this relatively large anion, even in competitive solvents. The stark contrasts between the binding energies in the less polar

solvent mixture and more polar solvent lends to the hypothesis that entropy/solvation plays a significant role in the binding events at play between these receptors and the tetrahedral oxoanions. To further understand the influence of the solvent and entropic effects on binding energies within this class of arylethynyl bis-urea receptors, we are currently pursuing the synthesis of receptors soluble in solvents with a range of polarities (i.e., soluble in solvents ranging from neat $CHCl_3$ through DMSO).

In conclusion, while the flexibility around the alkyl linkages in this class of receptors leads to a sizable binding pocket perfectly suited for tetrahedral oxoanions, we suspect that entropy and dynamic solvation effects are major contributors to the free energies of binding in these systems. Thus, we are currently pursuing studies to tease-out the enthalpic and entropic contributions involved in these host-guest systems. While intuitively one might first look to pK_b / conjugate acid pK_a trends in predicting affinity of protic and aprotic oxoanions toward hydrogen bonding hosts, these studies serve as a reminder that—especially in conformationally flexible hosts—this might not always be the dominant factor influencing the binding of oxoanions.

Experimental

General methods

^{1}H, ^{13}C, and ^{19}F NMR spectra were obtained on a Varian Mercury 300 MHz (^{1}H: 300.09 MHz), Inova 500 MHz (^{1}H: 500.10 MHz, ^{13}C 125.75 MHz, ^{19}F: 470.56 MHz), or Bruker Avance III HD 600 MHz NMR spectrometer with Prodigy multinuclear broadband BBO CryoProbe (^{1}H: 600.02 MHz, ^{13}C: 150.89 MHz). Chemical shifts (δ) are expressed in ppm downfield from tetramethylsilane (TMS) using non-deutrated solvent

present in the bulk deutrated solvent ($CDCl_3$: ^1H 7.26 ppm, ^{13}C 77.16 ppm; d_6-DMSO: ^1H 2.50 ppm, ^{13}C 39.52 ppm; d_6-acetone: ^1H 2.05 ppom, ^{13}C 206.7 and 29.9 ppm). Mixed solvent systems were referenced to the most abundant solvent. All NMR spectra were processed using MestReNova NMR processing software. All oxygen-sensitive reactions were performed under an inert atmosphere of nitrogen using Schlenk techniques. Unless otherwise specified, all materials were obtained from TCI-America, Sigma-Aldrich, or Acros and used as received. Tetrabutylammonium salts were dried at 60 °C in vacuo prior to use. Aniline **4** was synthesized and desilated following known procedures.[1] 2,6-Pyridine receptor **2** was synthesized via known procedures.[9a] 2,2'-Bipyridyl-6,6'-bis-ethynylaniline was synthesized following published procedures.[10]

Synthesis

Dianiline 6. To a sealable flask, 3,5-dibromopyridine (0.505 g, 2.13 mmol), CuI (0.099 g, 0.524 mmol), and $Pd(PPh_3)_4$ (0.212 g, 0.184 mmol) was added under nitrogen. A mixture of degassed DIPA (30 mL) and THF (30 mL) was added to the flask via cannula. The solution was continuously purged with N_2 for an additional 30 min. An N_2-purged solution of 4-*tert*-butyl-2-ethynylaniline (1.11 g, 6.41 mmol) in degassed DIPA (15 mL) and THF (15 mL) was then transferred into the flask via cannula. The mixture was stirred overnight at 55 °C under an inert atmosphere. The cooled solution was filtered through a 10 cm silica gel plug eluting with CH_2Cl_2 and then concentrated *in vacuo*. Column chromatography (2:1 hexanes:Et_2O) of the crude material afforded **6** (0.368 g, 41%) as an brown-orange solid. ^1H NMR (600 MHz, $CDCl_3$) δ 8.67 (s, 2H), 7.94 (s, 1H), 7.39 (d, J = 2.2 Hz, 2H), 7.23 (dd, J = 8.5, 2.2 Hz, 2H), 6.70 (d, J = 8.5 Hz, 2H), 4.18 (s, 4H), 1.30 (s, 18H). ^{13}C NMR (151 MHz, $CDCl_3$) δ 150.48, 145.82, 141.17,

140.24, 128.99, 128.08, 120.47, 114.64, 106.53, 90.83, 90.15, 34.09, 31.51. HRMS (TOF-MS-ES$^+$) for $C_{29}H_{31}N_3$ $[M+H]^+$: calcd 422.2596, found 422.2587.

3,5-Pyridine receptor 1. In flame dried glassware under inert N_2 atmosphere, aniline **6** (0.240 g, 0.568 mmol) was dissolved in freshly distilled toluene (75 mL) and *p*-methoxyphenyl isocyanate (0.2 mL, 2.02 mmol) was added via syringe. The reaction mixture was stirred for 24 h at 55 °C. The reaction was cooled and the precipitate was isolated via vacuum filtration. The precipitate was washed with hexanes and dried to give **1** (0.209 g, 51%) as a yellow-white solid. ^{1}H NMR (500 MHz, d_6-acetone) δ 8.75 (s, 2H), 8.48 (s, 1H), 8.25 (d, J = 8.4 Hz, 2H), 8.18 (s, 1H), 7.91 (s, 1H), 7.57 (d, J = 2.5 Hz, 2H), 7.49 (dd, J = 8.9, 2.5 Hz, 2H), 7.43 (d, J = 8.4 Hz, 4H), 6.84 (d, J = 8.5 Hz, 4H), 3.74 (s, 6H), 1.34 (s, 18H). ^{13}C NMR (151 MHz, d_6-acetone/DMSO) δ 155.70, 153.23, 151.65, 144.99, 141.36, 139.59, 139.57, 133.66, 127.96, 120.90, 120.53, 120.24, 114.57, 110.89, 91.41, 90.57, 55.48, 34.52, 31.36. HRMS (TOF-MS-ES$^+$) for $C_{45}H_{45}N_5O_4$ $[M+H]^+$: calcd 720.3566, found 720.3559.

Bipyridine receptor 3. In flame dried glassware under inert N_2 atmosphere, 2,2'-bipyridyl-6,6'-bis-ethynylaniline (0.124 g, 0.248 mmol) was dissolved in freshly distilled toluene (50 mL) and *p*-methoxyphenyl isocyanate (0.150 mL, 1.52 mmol) was added via syringe. The reaction mixture was stirred at room temperature for 16 h. Hexanes was used to precipitate the crude product, which was then filtered and further washed with hexanes. A minimal amount of ethanol was then added to the crude product in a vial. The vial was sonicated and five drops of deionized water was added to re-precipitate the product. Receptor **3** was then isolated via vacuum filtration (0.104 g, 53%) as a cream-colored powder. ^{1}H NMR (500 MHz, d_6-acetone/DMSO) δ 9.28 (s, 2H), 8.55 (d, J = 7.9

Hz, 2H), 8.23 (s, 2H), 8.20 (d, J = 8.8 Hz, 2H), 8.07 (t, J = 7.8 Hz, 2H), 7.90 (d, J = 7.6 Hz, 2H), 7.60 (d, J = 2.4 Hz, 2H), 7.52–7.44 (m, 6H), 6.88 (d, J = 8.5 Hz, 4H), 3.75 (s, 6H), 1.35 (s, 18H). ^{13}C NMR (151 MHz, d_6-acetone/DMSO) δ 155.73, 155.26, 152.93, 144.77, 142.94, 139.33, 138.22, 133.31, 129.30, 128.72, 127.74, 120.88, 120.48, 120.09, 114.31, 110.55, 94.55, 85.76, 55.27, 34.25, 31.12. HRMS (TOF-MS-ES$^+$) for $C_{50}H_{48}N_6O_4$ $[M+H]^+$: calcd 797.3815, found 797.3799.

Titrations

General Titration Procedures. Concentration of receptor was kept constant by preparing a stock solution of the receptor and performing a serial dilution with the receptor stock solution to dissolve the guest. Receptor concentration was maintained constant throughout the titration. Tetrabutylammonium salts, purchased from TCI America or SigmaAldrich, were dried by heating to 60 °C *in vacuo* before use. Hamilton gas-tight syringes were used for all titrations. Titrations were performed in triplicate and the reported association constants represent the average fits across all titrations. Representative data are provided for each receptor and anion.

UV-Vis Titration Conditions. UV-Vis titrations were carried out on an Agilent Technologies Cary 60 UV-Vis spectrometer. Water-saturated 10% DMSO/90% $CHCl_3$ v/v% was prepared using HPLC-grade solvents purchased from SigmaAldrich or Fisher Scientific. Association constants were determined by non-linear regression models using Open Data Fit.[13c] All host solutions in 10% DMSO/90% $CHCl_3$ started as deep, marigold-yellow solutions and transitioned to colorless over the course of the titrations. All host solutions in CHCN started as colorless and remained so over the course the

titrations. The 10% DMSO/90% $CHCl_3$ spectra is more easily trackable when displayed as ε instead of absorbance. All data fit with change in absorbance values.

^{1}H NMR Titration Conditions. ^{1}H NMR titrations were carried out on an Inova 500 MHz NMR spectrometer (^{1}H: 500.10 MHz). Chemical shifts (δ) are expressed in ppm downfield from tetramethylsilane (TMS) using non-deutrated solvent present in the bulk deutrated solvent ($CDCl_3$, ^{1}H 7.26 ppm; *d_6*-DMSO: ^{1}H 2.50 ppm). Mixed solvent systems were referenced to the most abundant solvent. All NMR spectra were processed using MestReNova NMR processing software. Association constants were determined using step-wise non-linear regression fitting in MatLab.[13a]

Computations

Complete Authorship of Gaussian 09. Gaussian 09, Revision **D.01**, M. J. Frisch, G. W. Trucks, H. B. Schlegel, G. E. Scuseria, M. A. Robb, J. R. Cheeseman, G. Scalmani, V. Barone, G. A. Petersson, H. Nakatsuji, X. Li, M. Caricato, A. Marenich, J. Bloino, B. G. Janesko, R. Gomperts, B. Mennucci, H. P. Hratchian, J. V. Ortiz, A. F. Izmaylov, J. L. Sonnenberg, D. Williams-Young, F. Ding, F. Lipparini, F. Egidi, J. Goings, B. Peng, A. Petrone, T. Henderson, D. Ranasinghe, V. G. Zakrzewski, J. Gao, N. Rega, G. Zheng, W. Liang, M. Hada, M. Ehara, K. Toyota, R. Fukuda, J. Hasegawa, M. Ishida, T. Nakajima, Y. Honda, O. Kitao, H. Nakai, T. Vreven, K. Throssell, J. A. Montgomery, Jr., J. E. Peralta, F. Ogliaro, M. Bearpark, J. J. Heyd, E. Brothers, K. N. Kudin, V. N. Staroverov, T. Keith, R. Kobayashi, J. Normand, K. Raghavachari, A. Rendell, J. C. Burant, S. S. Iyengar, J. Tomasi, M. Cossi, J. M. Millam, M. Klene, C. Adamo, R. Cammi, J. W. Ochterski, R. L. Martin, K. Morokuma, O. Farkas, J. B. Foresman, and D. J. Fox, Gaussian, Inc., Wallingford CT, 2016.[19]

General Computational Procedure. Manual, exhaustive conformation searches were performed to locate all relevant structures. All conformers were optimized using the Gaussian 09 computational package (see above reference) using PBE[19] with the 6-31G(d)[6] basis set for all atoms. Minima were confirmed with vibrational frequency computations, with all structures having zero imaginary vibrational frequencies. Frequencies were computed at 1 atm and 298.15 K (25 ºC) in order to match experimental reaction conditions as close as possible. All images were generated with PyMOL[20] with distances in Ångströms (Å).

Bridge to Chapter IV

Chapter III presents three bis-urea anion receptors with the ability to strongly bind oxoanions. Each of the receptors presented herein are capable of binding anions through different secondary binding motifs and were designed in an attempt to create selective sensors for diprotic, monoprotic, and aprotic oxoanions. Solvent and entropic effects contributed a bigger role in the overall binding energies than previously expected, though, and differential responses could not be achieved between the three receptors and the oxoanions studied. Chapter IV explores the concept of developing an array with a variety of bis-urea receptors to overcome the limitations of the lock-and-key method for anion sensing.

CHAPTER IV

DEVELOPMENT OF A QUICK-SCREEN ARRAY FOR ANION SENSING

This chapter is compiled from unpublished, co-authored work. I performed the analytical experimental work. Prof. Blakely W. Tresca synthesized the receptors or supervised undergraduates Leif Winstead and Anne-Lise Emig who assisted with the synthesis of the receptors. H. Camille Richardson performed the principal component analysis and linear discriminant analysis with supervision from Prof. P. H.-Y. Cheong. The writing is entirely mine with editorial assistance from Profs. M. M. Haley and D. W. Johnson.

Introduction

The ideal small molecule anion sensor exhibits a selective and highly sensitive detectible response toward an anion of interest.[1] This idealized single receptor approach is referred to as the lock-and-key model, where one host receptor is designed to bind a specific anion over others.[1, 2] In efforts to screen a variety of combinations of affinity, selectivity, and response, dozens of arylethynyl urea receptors have been synthesized and studied in our lab.[3] Each receptor has varying electron-withdrawing and electron-donating groups on the central arene core and the urea pendant phenyls in order to promote a change in selectivity toward different anionic guests by changing the strength of the hydrogen bond donors and acceptors. While we still seek the perfect lock-and-key

receptor for many anions of interest, the library of receptors provides a foundation for a quick-screen sensing array.[2]

A sensing array utilizes a composite response of multiple receptors, rather than a single molecule, to detect specific anions.[2] This approach utilizes pattern recognition algorithms to identify an unknown analyte based on the differential data collected from all receptors, similar to taste receptors on a tongue. Sensing arrays and pattern recognition algorithms, such as principle component analysis (PCA), can also elucidate design rules for the lock-and-key model of anion sensors.[2] This provides a quick screen of what substituents promote a spectroscopic response and any unexpected responses toward a certain anion from previously unscreened receptors.

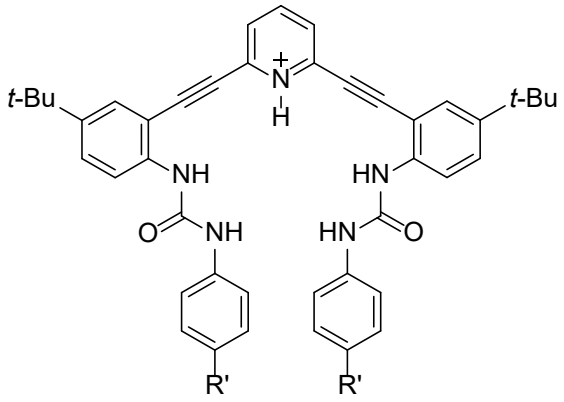

1

R' = OMe or NO_2

Figure 1. Previously reported pyridinium receptor **1** showed on-to-off or off-to-on fluorescence with electron donating (R' = OMe) or electron withdrawing (R' = NO_2) groups, respectively, in the *para*-position of the pendant phenyl with the presence of Cl^-.[4]

Previously reported studies on the 2,6-bis(anilinoethynyl)pyridinium scaffold (Figure 1) showed that substitution of the pendant phenyls (R') with an electron withdrawing group (EWG) promoted a selective off-to-on fluorescence response in the presence of chloride (Cl^-), while an electron donating group (EDG) promoted an on-to-

off response.[4] Therefore, we hypothesized that in general, substitution of EWG's at the R' positon results in a turn-off fluorescence response for anions and EDG's promote a turn-on fluorescence response.

A series of phenyl derived bis-urea receptors were designed to test the generality of this design principle original proposed for the pyridine receptors (Figure 2). The R' position of these phenyl receptors can be easily tuned with similar electron withdrawing or electron donating groups. Additionally, the strength of the hydrogen-bond donor of the core phenyl ring can be tuned more easily with *para*-substituents in comparison to its charged pyridinium counterpart.[3f] Herein, we report the optoelectronic properties resulting from a change in the R and R' substituents on the core arene and pendant phenyls. Sixteen receptors were screened against five anions of biological and environmental interest with a multi-well plate reader. Principal component analysis was utilized to help identify how substituents influence fluorescence behavior and binding selectivity.

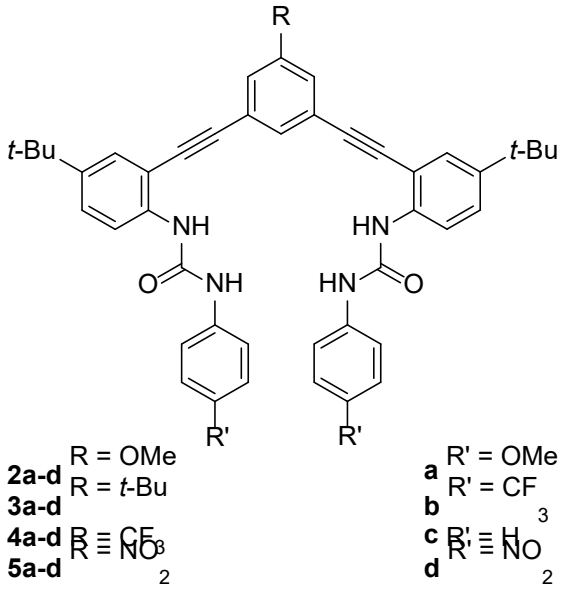

Figure 2. Library of phenyl-based bis-urea anion receptors analyzed for fluorescence response.

Results and Discussion

The library of host compounds were previously synthesized.[3f, 5] The absorbance and emission properties of the bis-urea receptors were measured in water-saturated chloroform ($CHCl_3$). A method to quickly determine the fluorescence intensity change in the presence of chloride (Cl^-), bromide (Br^-), iodide (I^-), nitrate (NO_3^-), and perchlorate (ClO_4^-) was developed. A stock solution of receptor ([H] = 0.10 mM) was prepared in water-saturated $CHCl_3$ and 200 μL was distributed into six wells of a black quartz 96-well plate. To each well, 50 μL of one salt solution ([X^-] = 6.0-7.0 mM) was added, giving a total well volume of 250 μL and ~20 equivalents of anion. The sixth well served as a blank host control, to which 50 μL of the chloroform was added to give a final host concentration equal to that of the other wells ([H] = ~80 μM).

Figure 3 shows the emission spectra for each fluorescent host and host-guest solutions. Unlike the previously reported turn-on fluorescence for pyrdinium receptor **1** where R' = NO_2, all of the phenyl-based receptors studied herein with nitro substituents (**2d**, **3d**, **4d**, and **5a-d**) were not fluorescent. This is likely due to the well-known quenching behavior of nitro groups.

While the nitro-substituted receptors were not fluorescent, the receptors with the other electron-withdrawing group, trifluoromethyl (CF_3), were quite fluorescent. Interestingly, the push-pull system **2b** and the pull-push system **4a** are the only receptors that quench in the presence of all five anions. In these two systems, the anion with the strongest association constant (Cl^-) also results in the most quenching. Typically, iodide acts as a fluorescence quencher due to the heavy atom effect. This poses a question for

future computational study and subsequent synthetic design: what orbital interactions or change in binding conformations in these push-pull or pull-push systems might lead to the largest quench in fluorescence in the presence of a strongly bound anion?

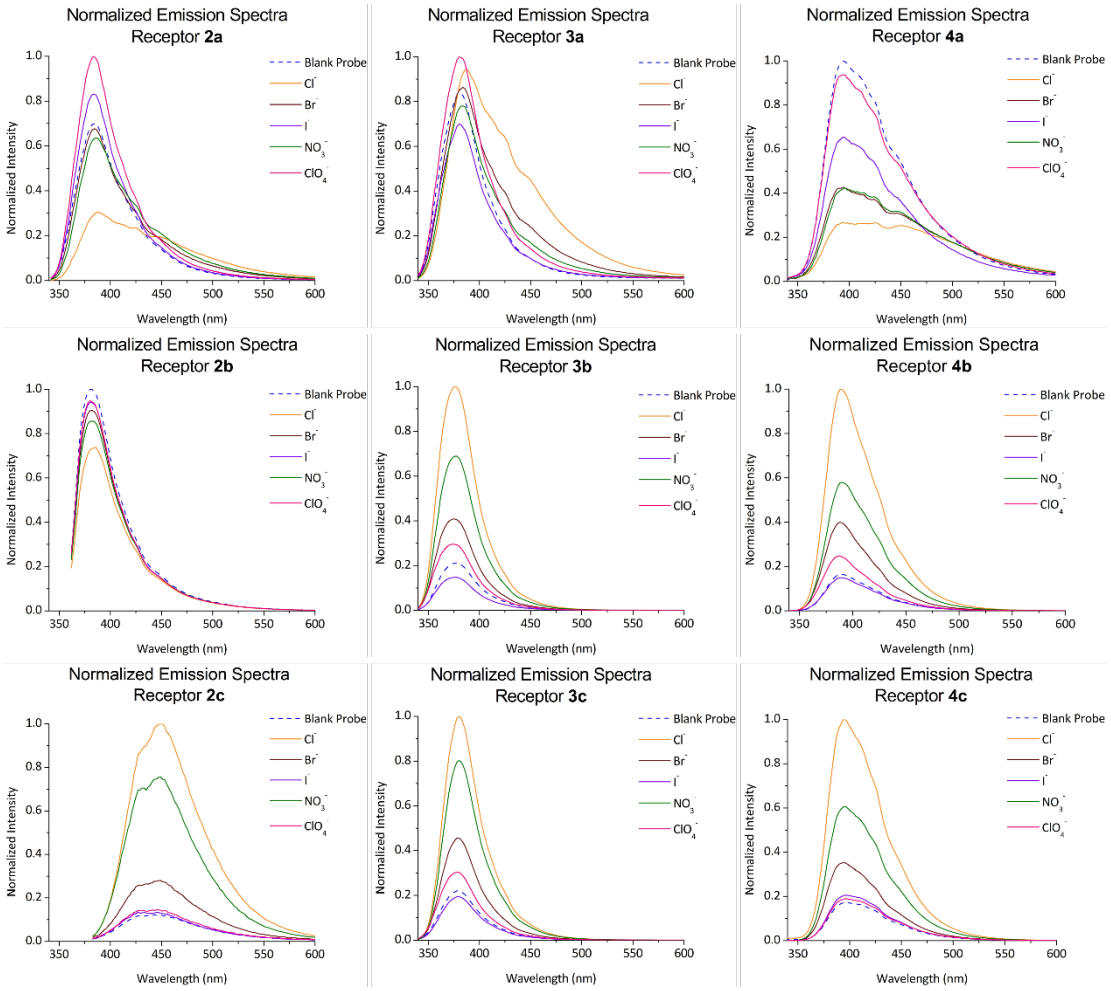

Figure 3. Fluorescence emission spectra of blank receptors **2a-c**, **3a-c**, and **4a-c** in H_2O-sat. $CHCl_3$ and upon binding Cl^-, Br^-, I^-, NO_3^-, and ClO_4^-. Each group of spectra is individually normalized with respect to each receptor. Spectra represent an average of four experiments.

Looking at the change in fluorescence of the receptors with unsubstituted phenyl bis-ureas (**2c**, **3c**, and **4c**), we see a significant increase in fluorescence in the presence of chloride and nitrate. This series of receptors is the only series to show predictable

behavior across all three receptors with all five anions, with fluorescence intensity increasing in the presence of most anions, with $Cl^- > NO_3^- > Br^-$. Receptors **2c** and **4c** show an indiscriminate change in fluorescence in the presence of ClO_4^- and I^-, but receptor **3c** shows a slight increase in fluorescence for ClO_4^- and an indiscriminate change for I^-. Receptors **3b** and **4b** showed similar trends as their unsubstituted counterparts, but the methoxy-substituted bis-urea receptors **2a**, **3a**, and **4a** do not appear to have any trending patterns in their fluorescence response to anions.

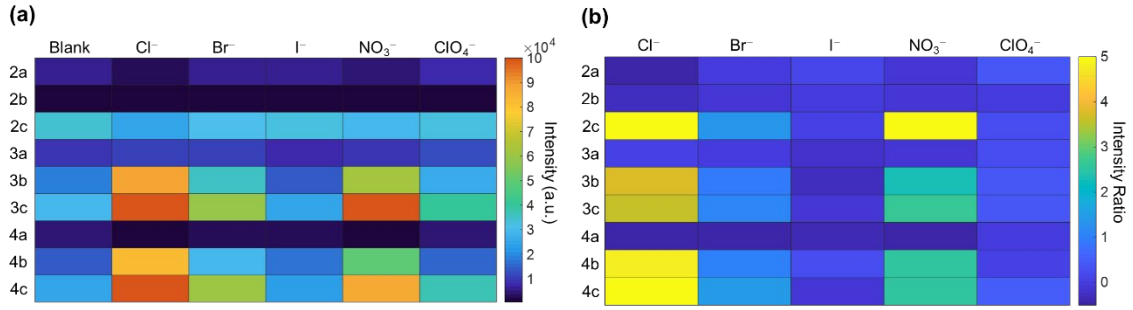

Figure 4. (a) Heat map of the maximum fluorescence at the optimal λ_{exc} for free receptors **2a-c**, **3a-c**, and **4a-c** in H_2O-sat. $CHCl_3$ and upon binding Cl^-, Br^-, I^-, NO_3^-, and ClO_4^-. Color corresponds to emission intensity in absorbance units (Table 1). **(b)** Heat map of the anion response for receptors **2a-c**, **3a-c**, and **4a-c** with anions. Color corresponds to intensity ratio, change in emission intensity with 20 equiv. TBA^+ salt, calculated by $IR = I - I_0 / I_0$. Maximum cut-off at 5.0 to highlight small changes. Values represent an average of four experiments.

It is important to note that the spectra in figure 3 are individually normalized with respect to each receptor set. Thus, the aggregate data has been visualized as two additional heat-maps for comparisons between the difference receptors: 1) based on the maximum fluorescence intensity at the optimal wavelength for maximum emission of the blank receptors, and 2) as intensity ratios, which represent the overall change in fluorescence with respect to the blank receptor (Figure 4, Table 1). When looking at the raw maximum fluorescence intensity for each receptor, the spectra for **2c** do not exhibit fluorescence in comparison to **3c** and **4c** (Figure 4a). In fact, with the exception of **2c**, all

Receptor	$\lambda_{exc.}$ (nm)	$\lambda_{em.}$ (nm)	Emission Intensity (a.u.)						Intensity Ratio[b]				
			Blank	Cl^-	Br^-	I^-	NO_3^-	ClO_4^-	Cl^-	Br^-	I^-	NO_3^-	ClO_4^-
2a	322	386	5320	2290	5130	6290	4820	7520	-0.57	-0.04	0.18	-0.09	0.41
2b	342	382	170	1440	400	180	1090	200	-0.27	-0.09	-0.06	-0.14	-0.06
2c	363	449	34500	25300	31200	32400	29500	32500	7.42	1.35	0.07	5.37	0.19
3a	296	380	9680	9980	9800	8050	8860	11600	0.03	0.01	-0.17	-0.09	0.19
3b	314	378	18800	88800	36100	13100	61300	26000	3.72	0.92	-0.30	2.26	0.38
3c	296	380	28700	130000	59300	25100	105000	39400	3.54	1.07	-0.12	2.65	0.38
4a	298	394	4680	1210	1970	3050	1930	4390	-0.74	-0.58	-0.35	-0.59	-0.06
4b	298	388	14100	81800	28700	16900	49700	15500	4.79	1.04	0.19	2.52	0.10
4c	298	396	24500	149000	59700	22300	86100	36900	5.08	1.44	-0.09	2.51	0.51

Table 1. Emission properties of receptors **2a-c**, **3a-c**, and **4a-c** in H_2O-sat. $CHCl_3$ and the responses to 20 equiv anions.[a] [a]Anions added as tetrabutylammonium salts in H_2O-sat. $CHCl_3$. Values represent an average of four experiments. Error is *ca.* ±20%. [b]Intensity ratio represents the change in intensity upon addition of anion. Calculated as $IR = I - I_0 / I_0$

receptors with methoxy substituents are essentially not fluorescent compared to the receptors with weakly-donating or electron-withdrawing substituents. This leads to a second design rule to fall out of these studies: phenylethynyl bis-urea receptors with methoxy substituents are only weakly fluorescent, even in the presence of strongly bound anionic guests.

Statistical analysis techniques, like pattern recognition algorithms, like principal component analysis (PCA) or linear discriminant analysis (LDA), can be used to process large data sets for differential sensing. These analytical methods produce score plots in two- or three-dimensional space and ultimately reveal a coordinate system where the analytes are best discriminated, or clustered, from one another.[2] Once a matrix with a high level of discrimination (accuracy) is determined, unknown analytes can be quickly sorted and identified based on where they land on the matrix. Our brains utilize a similar method of discriminating flavor in foods via the taste receptors on our tongues: we can determine how a food tastes (i.e. sweet, salty, bitter, sour, etc.) by sorting the responses of the taste buds and relating them to a known category of flavor. In this sense, we can think of pattern recognition algorithms as a sort of electronic tongues.

We applied principal component analysis (PCA) in an attempt to elicit other design rules regarding receptor substituents and anion response.[2] The raw fluorescence data did not result in any significant clustering. However, upon taking the difference in fluorescence between the host-guest combination and the empty host, we were able to see some clustering emerge (Figure 5). At first, it appeared the major problem with the clustering was the significant overlap of the fluorescence data for iodide and perchlorate.

After excluding the data for perchlorate, there were still outliers in the clustering. Upon analyzing these outliers, we noted that they were all data points for receptors with methoxy substituents. Thus, we then excluded the data for receptors **2a-c**, **3a**, and **4a** but replaced the data for perchlorate sensing and achieved our best results for PCA. This supports the design principle outlined above: methoxy substituents on phenylethynyl bis-urea receptors result in unpredictable and weak fluorescence responses, so these functional groups should be avoided in this system in array-based sensor platforms or in the development of possible turn-on fluorescence molecular probes.

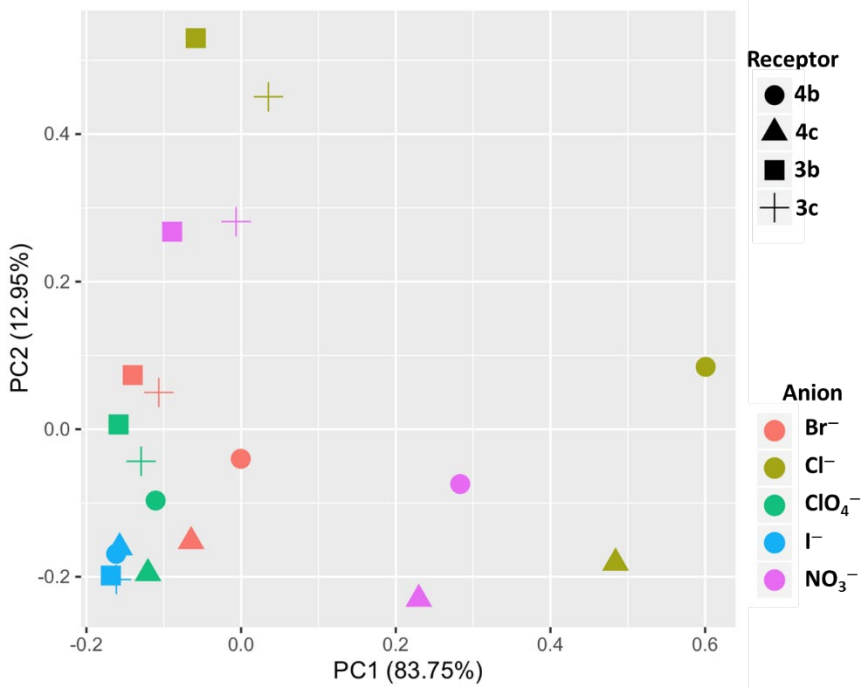

Figure 5. Principal component analysis matrix of receptors **3b**, **3c**, **4b**, and **4c** with the Cl^-, Br^-, I^-, NO_3^-, and ClO_4^-. LDA accuracy = 0.791667 at a 95% confidence level.

Linear discriminant analysis (LDA) was determined to be the best clustering method for the aggregate data, with an accuracy value of 0.792. While this value is not within an applicable range, it does indicate that we can use a pattern recognition

algorithm to better understand the design of our receptors and potentially achieve an anion sensing array in the future. Future array studies should include pyridine- and pyrdinium-based receptors, along with receptors modified with different binding motifs, like halogen-bonding receptors (see ref. 3k). Ideally, the different binding motifs will result in differential fluorescence sensing, which will increase the clustering in PCA. Once a combination of receptors with a high accuracy of clustering (greater than 0.9) is found, an unknown analyte can be sorted and deteceed based on the array clustering.[1, 2]

In conclusion, this work presents the photophysical data for a collection of phenylethynyl bis-urea anion receptors and points to essential design elements for this class of anion sensors. If we want to design a phenyl-based anion receptor with high fluorescence intensity, we should not include a nitro or methoxy substitutent on the core or pendant arenes. Additional research is needed to better understand the relationship between the strength of the binding interaction and the fluorescent behavior, and, with that understanding, we can begin to build an anion sensing array with the receptor scaffolds studied in our lab. Furthermore, computational studies can help provide insight on the quenching behavior of the push-pull and pull-push systems presented herein.

Experimental

General methods

^{1}H spectra were obtained on a Varian Mercury 300 MHz (^{1}H: 300.09 MHz), Inova 500 MHz (^{1}H: 500.10 MHz, ^{13}C 125.75 MHz, ^{19}F: 470.56 MHz), or Bruker Avance III HD 600 MHz NMR spectrometer with Prodigy multinuclear broadband BBO CryoProbe (^{1}H: 600.02 MHz, ^{13}C: 150.89 MHz). Chemical shifts (δ) are expressed in

ppm downfield from tetramethylsilane (TMS) using non-deutrated solvent present in the bulk deutrated solvent ($CDCl_3$: ^1H 7.26 ppm, ^{13}C 77.16 ppm; d_6-DMSO: ^1H 2.50 ppm, ^{13}C 39.52 ppm; d_6-acetone: ^1H 2.05 ppom, ^{13}C 206.7 and 29.9 ppm). Mixed solvent systems were referenced to the most abundant solvent. All NMR spectra were processed using MestReNova NMR processing software. UV-Vis and fluorescence spectra were obtained using a Tecan Spark 20M Multimode Microplate reader equipped with a monochromator. A Hellma-Analytics quartz black glass 96-well plate topped with a UV-clear plastic cover was used for the microplate studies. Unless otherwise specified, all materials were obtained from TCI-America, Sigma-Aldrich, or Acros and used as received. Tetrabutylammonium salts were dried at 60 °C in vacuo prior to use.

Synthesis

Receptors **2b**, **2c**, **5b**, **5c**, and **5d** were synthesized via similar procedures as those reported in reference 5.

Receptor 2c. ^1H NMR (500 MHz, $CDCl_3$) δ 8.41 (s, 2H), 7.97 (d, J = 9.1 Hz, 2H), 7.72 (s, 2H), 7.66 (t, J = 7.8 Hz, 1H), 7.51 (d, J = 7.8 Hz, 2H), 7.36 (d, J = 8.0 Hz, 4H), 7.15 (t, J = 7.7 Hz, 4H), 6.96 (d, J = 3.0 Hz, 2H), 6.91 – 6.85 (m, 4H), 3.70 (s, 4H), 1.89 (s, 18H).

Receptor 5b. ^1H NMR (300 MHz, d_6-DMSO) δ 10.30 (s, 2H), 8.54 (s, 2H), 8.08 (d, J = 7.8 Hz, 4H), 7.90 (d, J = 9.0 Hz, 2H), 7.72 (d, J = 8.8 Hz, 5H), 7.65 (s, 2H), 7.52 (s, 2H), 7.41 (d, J = 8.8 Hz, 2H), 1.30 (s, 18H).

Receptor 5c. ^1H NMR (600 MHz, d_6-DMSO) δ 9.42 (s, 2H), 8.28 (s, 1H), 8.26 (s, 2H), 8.11 (s, 2H), 8.03 (d, J = 8.8 Hz, 2H), 7.57 (d, J = 2.4 Hz, 2H), 7.49 – 7.46 (m, 6H), 7.28 (t, J = 7.9 Hz, 4H), 6.98 (t, J = 7.3 Hz, 2H), 1.30 (s, 18H).

Receptor 5d. ^{1}H NMR (300 MHz, d_6-DMSO) δ 10.13 (s, 2H), 8.55 (d, J = 7.3 Hz, 4H), 8.42 (s, 1H), 8.19 (d, J = 8.9 Hz, 4H), 8.04 (d, J = 8.9 Hz, 2H), 7.73 (d, J = 8.8 Hz, 4H), 7.65 (s, 2H), 7.53 (d, J = 9.0 Hz, 2H), 1.33 (s, 18H).

Array Screening

General Array Procedures. Concentrated solutions of receptors **2**-**5** (2.18-3.64 mg, [H] ≈ 0.400 mM) in 10.0 mL of water-saturated $CHCl_3$ were prepared. A serial dilution was then performed with 2200-3500 µL of ~0.400 mM solution of receptors **2**-**5** was then diluted to 10.0 mL to yield the stock solution of receptors **2**-**5** ([H] ≈ 0.100 mM). Concentrated solutions of tetrabutylammonium salts TBA·Cl, TBA·Br, TBA·I, TBA·NO_3, TBA·ClO_4 were prepared in 3.0 mL of water-saturated $CHCl_3$ (6.4-7.8 mg, [X^-] ≈ 7.0 mM). Each run consisted of 35 wells in a 5-by-7 matrix, with each well filled to a total volume of 250 µL. The wells in the top column and the first row of the plate contained only salt or receptor in order to act as the blank controls. For the blank host wells (vertical rows), this included 200 µL of receptor stock solution ([H] ≈ 0.100 mM) and 50 µL of chloroform to give a total [H] ≈ 80 µM. The blank anion wells (horizontal columns) included 50 µL of salt solution ([X^-] ≈ 7.0 mM) and 200 µL of chloroform. The first well contained only water-saturated chloroform to act as a solvent control. All other wells contained 200 µL of receptor stock solution ([H] ≈ 0.100 mM) and 50 µL of one salt solution ([X^-] ≈ 7.0 mM), giving a total well volume of 250 µL and ~20 equivalents of anion for each host (final [H] ≈ 80 µM).

The UV-Vis absorbance spectra were first collected by scanning wells A1-E6 (inclusive) from 200-1000 nm with 2 nm step-size excitation and a 50 ms settle time. The maximum emission wavelength was determined for the blank receptors. This wavelength

was then used as the excitation wavelength for the subsequent fluorescence scans. The fluorescence intensity scans were collected as a bottom reading with the monochromator. The excitation bandwidth was set at 5 nm, with collection beginning at λ_{em}+20 nm and ending at 750 nm. The Z-position was determined from well B1 (blank receptor) for each scan.

Bridge to Chapter V

Chapters I-IV introduce complex research topics in the field of physical organic chemistry. Chapter V introduces a project-based learning approach to teaching physical organic chemistry topics to first-year graduate students. This case-study and intervention lays out a general method to approach science communication in an upper division chemistry course through a write-to-learn Wikipedia project.

CHAPTER V

UNDERSTANDING THE UPPER-LEVEL CHEMISTRY STUDENTS' PERSPECTIVE ON SCIENCE COMMUNICATION THROUGH WIKIPEDIA PROJECT-BASED LEARNING: A CASE-STUDY AND INTERVENTION

This chapter is comprised of unpublished, co-authored work. I conceived and designed the course project. Prof. Eleanor V. H. Vandegrift provided guidance and insight in creating the survey. The writing is entirely my own with editorial assistance from Prof. Eleanor V. H. Vandegrift.

Introduction

Research says that students who graduate with an advanced degree in science should be able to communicate science effectively "to a range of audiences, for a range of purposes, and using a variety of modes" (Jones, et al. 2010). Despite the clarity for a need for learning goals for science communication, there is on-going debate about the best approach to implement broad-audience focused science communication curriculum into an upper division science course (Brownell, et al. 2013; Mercer-Mapstone & Kuchel 2015). While there is reason to believe science students gain the skills necessary to communicate with a broad audience through their general education coursework, research is needed to clarify connections on how these skills translate into their ability to communicate complex science topics for a general audience.

The standards for bachelor's degrees in a variety of science disciplines focus on students' ability to effectively communicate scientific results to scientists and to diverse audiences (AAAS, 2011; AAMC-HHMI, 2009). Despite the multiple degrees graduate students and professors hold, many have never received formal training on communicating science to diverse audience (Blanchard 2017; Mercer-Mapstone & Kuchel 2015; Baram-Tsarabi & Lewenstein 2017; Baram-Tsarabi & Osborne 2015). At what point do we draw the line between education focused on communicating science to a broad audience versus communicating to a specific scientific audience? How we approach engaging these two audiences should, in fact, be quite different (Brownell, et al. 2013). However, the education system currently focuses on learning to communicate to a science audience, incorporating the perfect jargon and motivation-to-data ratio (Baram-Tsarabi & Lewenstein 2017; Gardner, et al. 2017). Granted, this is a vital component of the science education process, but it leaves out a main motivation behind scientific research: to advance society through understanding the minutiae of life and nature (Higgins, et al., 2006, NSB, 2000). In educational settings, we neglect to stress the importance of communicating a specific chemistry topic to a broad audience, yet we, as researchers and society as a whole, rely on policymakers and media sources to correctly interpret results and understand the significances of the basic-science research (Brownell, et al., 2013; Mercer-Mapstone & Kuchel, 2015, Nadkarni & Stasch, 2013).

Learning to explain complex scientific concepts to a general audience is often seen as a skill honed through years in a graduate program, general education courses, or even just in passing. To address this gap in formal science education, we designed an

end-of-term science communication project for a combined undergraduate/graduate-level chemistry course: Physical Organic Chemistry I.

Aim of study

In this case study, we explored how graduate-level chemistry students define and rank the importance of science communication before and after a project-based intervention. All students in the course answered survey questions about how they interact with science research on the web, their own perceived ability to communicate complex chemistry topics, their science educational background, and ways they think the general population interacts with science on the web. Additionally, the graduate students wrote and published a Wikipedia article on a topic related to physical organic chemistry. Students presented their published page to their peers and instructors through a two-minute elevator pitch. This project-based intervention aimed to broaden the students' perceptions of science communication and provide an opportunity for students to write about a complex scientific topic for a general audience.

The following questions guided this study:

1. How do graduate-level chemistry students define science communication and its impact on society?
2. How do the students' perspectives of their own abilities to communicate science change after writing a Wikipedia article on a complex chemistry topic aimed at a general audience?

Method

Participants

A Wikipedia writing project was introduced into a mixed undergraduate and graduate-level course on physical organic chemistry. The students in the course ranged from third-year undergraduate students to second-year graduate students ($N = 21$; 19 enrolled, 2 audited, 5 undergraduate students, 16 graduate students) in the Department of Chemistry & Biochemistry at a mid-sized public research university in the Pacific Northwest of the United States. One year of organic chemistry is a prerequisite for the course. The course met twice a week for 80 minutes each and a third day for 50 minutes.

By the end of the term, students should be able to meet the following learning goals and objectives:

1. demonstrate a firm foundation in the conceptual and quantitative thinking that underlies the theories and models that form the basis for reasoning about physical organic chemistry,
2. demonstrate excellent critical thinking and problem solving abilities,
3. integrate chemical concepts and ideas learned in lecture courses with skills learned in the laboratories,
4. understand how scientific information is shared between peers in modern science,
5. and demonstrate an awareness of the benefits and impacts of chemistry related to the environment, society, and other disciplines in the scientific community.

The course provided an opportunity for students to increase proficiency in rationally estimating the solution to organic chemistry problems and properly analyzing the result for correctness. To this end, students ideally leave the course prepared to contribute solutions to society's challenges at the intersection of science and society.

This physical organic chemistry course is the first in a two-course sequence that expands on the concepts taught in organic chemistry. It is taught through *Modern Physical Organic Chemistry* (Anslyn & Doughtery, 2006), alongside primary research experience from the instructor of record. To distinguish the graduate-level curriculum from the undergraduate-level curriculum, graduate students are assigned six reviews of primary literature, submitted with their solutions to problem sets, and an end-of-term project. The primary literature reviews required students to first search a non-peer reviewed journalism outlet (i.e. *Science Daily*, *New York Times*, etc.) for a recent press release on a chemistry related topic. Students then compared the press release to the original peer-reviewed journal article to analyze accuracy of the journalist's interpretation of the research article. This recurring assignment was designed to engage students in ways the general public convey and consume science news.

In an attempt to meet the goal of students contributing scientific solutions to society's challenges, we realized the need for students to formally practice communicating a complex scientific topic to a general audience. Furthermore, the fact that students rely on Wikipedia as an information source means that the most up-to-date and accurate information needs to be on the webpage (Lladós-Masllorens, et al., 2017). It is often the first "hit" in a Google for most topics and most students (some professors!) regularly choose to use it as a reference point to refresh their memory on a subject or find resources for further reading. Inspiration for this particular project came from a *Journal of Chemistry Education* article titled "Glaring Chemical Errors Persist for Years on Wikipedia" (Mandler, 2017). The article, which is a response to another using Wikipedia editing as an assignment (Martineau & Boisvert, 2011), describes multiple chemistry-

related Wikipedia pages with obvious errors and calls on educators to help remedy the pages to prevent future mistakes from occurring. This call to fix errors and create accurate chemistry-related articles resulted in the formation of the final project for graduate students: the task of publishing a Wikipedia article on a subject of their choice from physical organic chemistry.

Procedures and materials

Students were provided guidelines for the project during the fifth week of the ten-week term (Figure 1, see appendix for complete details). Intermediate deadlines were provided to encourage students to work on the project over the course of the remaining five weeks. To encourage guided inquiry and self-learning in the graduate students, feedback was provided only on the scope of the topic (i.e. broadness, specificity, repetition, etc.) and accuracy/grammar of the finalized page. The first author offered two optional workshops on editing, compiling, and publishing Wikipedia pages, including how to add images to the page. All graduate students chose to attend at least one of two workshops. Additional help on organizing and publishing the pages was provided during office-hours or on a drop-in basis throughout the term. Graduate students were graded on the general scope and detail of their final page, and how engaging they were in presenting a two-minute elevator pitch to encourage people to read their article. No undergraduates chose to complete the project for extra-credit.

All students were surveyed at the beginning and end of the course. Survey questions were distributed through Qualtrics. For the pre-survey, the students wrote their definition of science communication, their level of agreement with a range of statements related to the importance of science communication and perceptions of their own abilities

to communicate science, and their history related to their use of Wikipedia and other search engines for research. In the post-survey, students ranked the importance of a variety of features in a Wikipedia article that appeared as emergent codes in the initial survey's short-response answers. Of the 21 students in the course, 21 completed the pre-course survey and 18 completed the post-course survey (85.7%).

Results and Discussion

Defining science communication and how science can impact society

Students were asked to define science communication during both pre- and post-surveys. Responses were coded qualitatively and sorted into one of three emergent codes: explaining science to others to the point of understanding, presenting research findings from scientists, or presenting science to others (with no intent for audience to understand). Within each of these definitions, the intended audience was coded as non-science background/general public or other scientists. Additionally, the original definitions were sorted into the AEIOU vowel analogy categories from the Burns et al. definition of science communication: Awareness, Enjoyment, Interest, Opinion-forming, and Understanding (Burns, et al. 2003).

Overall, the students' definitions for science communication in the pre-survey leaned toward presenting science to the general public, without mention of audience understanding (52%, with N total = 21). In the post-course survey, the definitions were more split between presenting science to others to the point of understanding and simply presenting science to others (41% each, with N total = 17). When analyzing the same definitions with the AEIOU code described by Burns et al., there was not a discernable

difference between the pre- and post-survey. The majority of students (86% pre- and 76% post-) defined science communication as a way to promote awareness of scientific concepts in their intended audience. Some students also explicitly promoted the verb "understand" in their definitions (23% pre and 41% post). The other verb definition from this sorting system was "opinion". Burns et al. defines this as "the forming, reforming, or confirming of science-related attitudes." This falls in with the ability to recognize how science can impact policy. Only 14% and 24% of students in the pre- and post-survey, respectively, defined science communication as a method to incite opinions.

Table 1. Graduate student responses (N = 14) to the pre- and post- survey questions regarding their opinions on science communication, their abilities to communicate science, and the impact they can have on the public's opinions of science.

Survey question	***N* = 14**	**Strongly Disagree**	**Disagree**	**Agree**	**Strongly Agree**
Communicating science to the general public is important	Pre-course	-	-	2	12
	Post-course	-	-	5	9
I have the ability to impact the public with science	Pre-course	-	-	5	9
	Post-course	-	1	9	4
The public is well-educated on science	Pre-course	5	9	-	-
	Post-course	6	7	1	-
I am able to effectively communicate the importance of a topic of science to the general public (i.e. organic chemistry)	Pre-course	-	2	10	2
	Post-course	-	1	12	1
I am able to effectively communicate the importance of a sub-topic of science to the general public (i.e. kinetics)	Pre-course	-	7	7	-
	Post-course	-	3	11	-
My education has prepared me to defend science funding to the general public	Pre-course	-	3	10	1
	Post-course	-	3	10	1

Of the graduate students who completed the survey (N=14), 100% disagreed or strongly disagreed to the statement "The public is well-educated on science" in the pre-survey and 92% disagreed or strongly disagreed with the statement in the post-statement (Table 1). Furthermore, 100% of the students said that they agreed or strongly agreed that communicating science with the public is important, but compellingly only 50% of the students in the pre-survey agreed that they were able to effectively communicate the importance of a sub-topic of science to the general public (i.e. kinetics, hydrogen bonding, proteins, CRISPR, etc.). The intervention described herein was designed to provide an experiential learning opportunity for graduate-level chemistry students to communicate a complex chemistry topic to a general audience through Wikipedia and build that lacking skill.

Graduate students' perspectives of their own abilities to communicate science to a broad audience

Wikipedia was chosen for this project-based intervention because it is the most consulted source on the web, reaching billions of readers monthly (Anderson, et al. 2016). It also provides an easy-to-use platform for students to edit and quickly publish an article from a broad range of chemistry-related topics (Martineau & Boisvert, 2011). In recent years, multiple educators have touted the benefits of students editing Wikipedia articles as an assignment, including collaborative learning, writing skills, and literature review skills (Martineau & Boisvert, 2011; Lladós-Masllorens, et al., 2017; Grange & Retief, 2018; Sternberger & Wyatt, 2018).

Students chose their own topic with the guidelines that it must fit within the broad subject of physical organic chemistry and could not already have a completed article on

Wikipedia. Students selected topics ranging from basic science topics (e.g. field effect) to synthetic methods (e.g. co-solvent) to materials science topics (e.g. impregnation resins and electronic skin).[1] Figure 1 shows the requirements students were provided to guide their article creations.

Your Wikipedia article must be well-written so a member of the public with general organic chemistry knowledge can understand it. It must include:

- *An introduction and at least three, well-written sub-sections;*
- *A description of the chemical importance/applications of the subject matter;*
- *A minimum of three high-quality images that help explain the topic;*
- *A proper Wikipedia-style bibliography with at least eight citations provided for the general reader to find more information (you will likely find that you will need to use many more than eight citations to cover your topic properly).*

Figure 1. The minimum requirements of the Wikipedia article assignment, as provided to the students.

A note in these guidelines is the audience: these graduate students, who are aiming to be experts in their selected fields of chemistry, are communicating with sophomore-level undergraduate students with a basic background in organic chemistry. In this sense, the students are not communicating to a broad audience, as is described in their pre- and post-survey, but the audience is still far less knowledgeable in the field than the typical audience of a graduate student: professors, lifelong chemistry researchers, and other graduate students. Although some topics, particularly materials or application-based topics, resulted in Wikipedia articles that are accessible to a broader audience (e.g. electronic skin).

[1] Screenshots of Wikipedia pages submitted by students can be viewed in the appendix.

After the course, student responses to the post-survey question about their own abilities to communicate a sub-topic of science to a broad audience changed favorably; 79% of the students now agreed that they had the ability to communicate a sub-topic of science to a broad audience (Table 1).

However, an open response question posed to students regarding any other pertinent information related to the Wikipedia project resulted in surprising revelations about the students' own perceived abilities. One student wrote "I was a little nervous writing the page because I didn't really feel like an expert on the subject, and [sic.] did not want to present bad information as a fact." This statement alone shows a lack of confidence in their abilities to research and write a Wikipedia article, even after earning a bachelor's of science in chemistry and as a student in a PhD program. This lack of confidence could be due to the imposter syndrome, a well-studied feeling present in many graduate students, or something else entirely (Parkman, 2016). Another student sums this up perfectly by saying "It is very hard to write a good review article. It is not surprising that many scientists are bad at communicating science to general public."

Conclusion

A third student noted that "We need more accurate science discussions in society," and we could not agree more! This presents a question: How can we, as educators, continue to provide opportunities for students (who are training to be experts in their fields) to research and write about their subjects for a broad audience more often? Journal articles and conference presentations do not cut it – we need to broaden our training grounds to reach more members of the public. The Wikipedia project described

here is one possible method of reaching this goal: the articles on Wikipedia reach broad audiences, require intensive literature reviews, and place accurate chemistry information in an easily-accessible location on the web. While such a method does not directly engage the public in a discussion, it does ensure the knowledge is available for public consumption, ideally increasing the public understanding of science.

Bridge to Chapter VI

The research presented in Chapter V offers an approach to implement science communication practice in an upper division chemistry course. By assigning students to write a Wikipedia page on a complex physical organic chemistry topic, the students practice communicating a science topic for a broader audience and ensure the dissemination of accessible, science information to the public. The final Chapter VI in this dissertation offers opportunities for future research for the arylethynyl anion receptors described herein.

CHAPTER VI

CONCLUSION AND FUTURE DIRECTIONS

Conclusion

The aim of this dissertation was to explore the impact of weak, intramolecular binding interactions on the anion binding selectivity of arylethynyl urea receptors. In doing so, we have furthered our understanding of tunable properties of arylethynyl urea receptors in an effort to design selective, sensitive, and responsive fluorescent sensors. Our initial study investigated the impact of secondary binding motifs, like aryl CH hydrogen bonds and anion-pi interactions, on anion selectivity. This study also influenced the design of our anion receptors by indicating the need for at least two urea recognition motifs in arylethynyl receptor scaffolds. The arylethynyl mono-urea receptors studied herein also elucidated the impact secondary interactions may have on the self-assembly properties of 2-to-1 host-to-guest systems with halides.

To further probe the influence of secondary binding motifs on anion selectivity, we designed three pyridine-based receptors. These receptors were designed to preferentially bind diprotic, monoprotic, and aprotic oxoanions based on the hydrogen bond donating or accepting ability of the pyridine cores. Additionally, computational studies indicated the size of each binding pocket was a near-perfect fit for the range of oxoanions. However, the inherent conformational flexibility of the arylethynyl bis-urea scaffolds lead to a surprising lack of binding preference across the three anions studied. Additional binding experiments in a more polar solvent showed binding energies that

followed the expected trend of anion basicity. This study suggests the contribution of solvent and entropic effects contribute to a larger role in overall binding energies and needs to be investigated more thoroughly when looking for the perfect lock-and-key host-guest pair.

In an attempt to overcome the elusive lock-and-key method for anion sensing, we also laid-out an array sensing platform with sixteen phenylethynyl bis-urea receptors. The fluorescence response of each receptor was analyzed against five anions of biological and environmental interest. Interestingly, phenyl-based receptors with nitro-substituents were not fluorescent, unlike the pyridine-based counterparts that inspired this study. This study provided additional insights into the fluorescence response of receptors with methoxy-substituents: the overall emission intensity is weak compared to other functional groups studied. Despite this property, when analyzing the intensity ratios, the methoxy receptor with unsubstituted phenyl ureas offers the most promising turn-on fluorescence response for chloride and nitrate. Additionally, principal component analysis (PCA) showed promise as a method to begin to discern sensing patterns based on the receptor-anion combination. Thus, we have laid-out future directions for work in the area of anion sensing arrays with the receptor scaffolds studied in our lab.

Not only did the research presented herein provide insights into the binding behavior of supramolecular anion receptors, but it also offered an intervention method for approaching the teaching of physical organic chemistry topics to first-year graduate students. A write-to-learn Wikipedia article project was implemented in a physical organic chemistry course to aid in concept learning and promote science communication skills to the next generation of chemists. This case-study and intervention allowed us to

teach and share complex chemical concepts, like those presented in this dissertation, to upper division chemistry students who then learned to communicate these topics to a general audience, allowing access to the broader community.

Future Directions

The research presented in this dissertation provides a foundation for studying the effects of secondary binding motifs in arylethynyl anion receptors on binding selectivity. The work presented in Chapter III establishes the need to study the relationship of flexible anion receptors in solvents of varying polarity. Such a study could tease out complex solvent and entropic effects related to polarity, anion size, binding pocket size, conformational changes, and secondary binding interactions. An anion-sensing array combined with PCA, as described in Chapter IV, could be applied to such a study to quickly screen the impacts of the different components of the receptors on the binding responses. To accomplish this, it is necessary to first isolate receptors soluble in solvents with a range of dielectric constants, like those presented in Scheme 1. The synthesis of receptors **1** and **2** is already underway.

In order to achieve the ideal array sensing platform for detection of unknown analytes, a larger variety of anion receptors should be studied. Analyzing receptors with a high intensity ratio response toward a wider range of anions would allow for differential sensing via PCA clustering by anions. Since different binding motifs and different sized binding pockets show varied responses toward the range of anions, arylethynyl bis-urea receptors with pyridinium and pyridine N-oxide cores, along with halogen-bonding receptors, could be applied in the array to promote a differential sensing response.

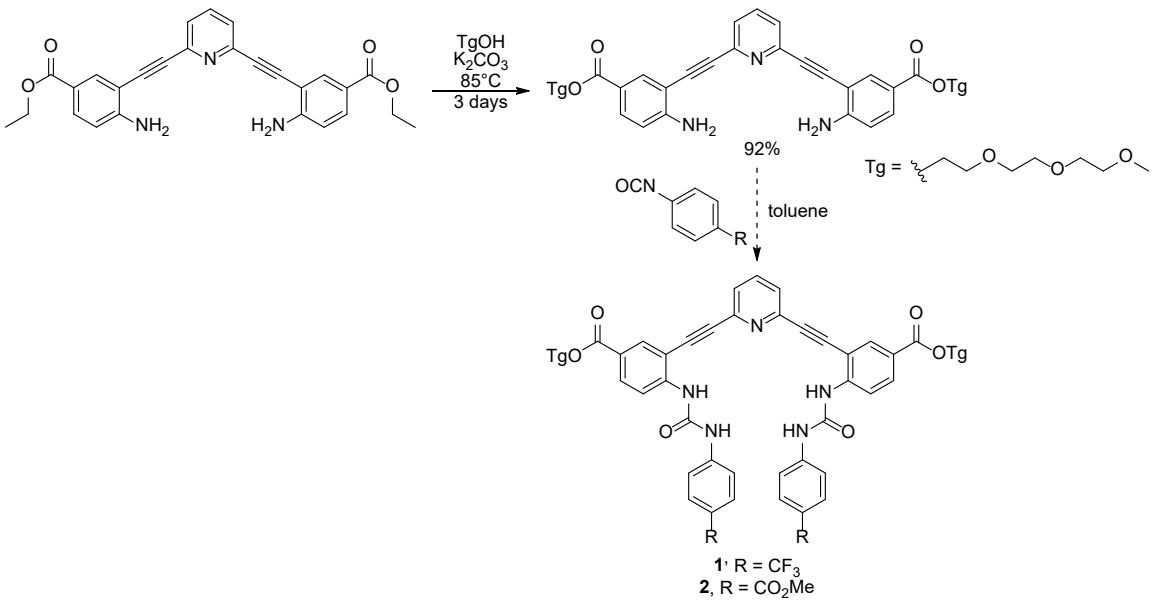

Scheme 1. Proposed synthetic approach to isolate two arylethynyl bis-urea receptors predicted to be soluble in polar and non-polar solvents.

Additional computational studies are also needed to better understand the selectivity preferences of push-pull phenylethynyl systems described in Chapter IV.

Furthermore, the solution-state fluorescence studies could be correlated to a solid-state resistivity response by incorporating the receptors into a chemically sensitive field effect transistor (ChemFET). One would first need to determine the fluorescent response to a variety of anions in solution. The ideal receptor would have a large change in fluorescence in the presence of one or two anions. Once the appropriate receptor is selected, the fluorescent receptor and polymer matrix used in the ChemFET can be drop-cast onto a glass slide. The fluorescence can be observed by the naked eye under a UV lamp. If the solution-state behavior is maintained in the polymer matrix, the fluorescent response should change in the presence of the selected anion(s). If there is a correlation between the change in fluorescence in the solid-state and a current response in the ChemFET devices, this approach could lead to a quick screen method to discover viable

chemical receptors for ChemFETs. Initial solid-state studies of the receptors studied in Chapter IV mixed with a polymer membrane are already underway (Figure 1).

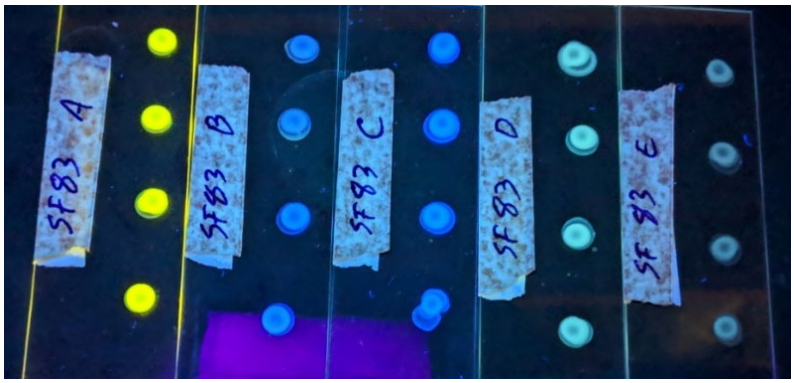

Figure 1. Photograph of the dropcasts of four receptors studied in Chapter IV in a polymer matrix used in ChemFET devices. The polymer matrix is pictured on the right as a control.

APPENDIX A

SUPPLEMENTARY INFORMATION FOR CHAPTER II

Titrations

^{1}H NMR titrations

Tetrabutylamamonium chloride with 3. A concentrated solution of **3** (2.45 mg, [R]=4.87 mM) in 10% d_6-DMSO/$CDCl_3$ (1.00 mL) was prepared. A serial dilution was then performed with 250 µL of 4.87 mM solution of **3** diluted to 3 mL to yield the stock solution of **3** ([R]=0.406 mM). This solution was used in the dilution of TBACl guest solution (6.53 mg, [G]= 9.98 mM). The remaining stock solution (0.600 mL) was used as the starting volume in the NMR tube.

Table 1. Representative titration data for Cl^- with **3**.

	Guest (µL)	[**1**] (M)	[Cl^-] (M)	Equiv.	H^c δ (ppm)	H^a δ (ppm)	H^b δ (ppm)
1	0	4.06E-04	0.00E+00	0.00	9.553	8.725	8.126
2	5	4.06E-04	8.25E-05	0.20	9.634	8.737	8.167
3	10	4.06E-04	1.64E-04	0.40	9.713	8.751	8.208
4	15	4.06E-04	2.43E-04	0.60	9.783	8.759	8.244
5	20	4.06E-04	3.22E-04	0.79	9.844	8.771	8.276
6	25	4.06E-04	3.99E-04	0.98	9.901	8.779	8.304
7	30	4.06E-04	4.75E-04	1.17	9.950	8.785	8.329
8	35	4.06E-04	5.50E-04	1.36	9.998	8.794	8.354
9	40	4.06E-04	6.24E-04	1.54	10.039	8.800	8.375
10	50	4.06E-04	7.67E-04	1.89	10.114	8.813	8.417
11	60	4.06E-04	9.07E-04	2.24	10.186	8.824	8.452
12	80	4.06E-04	1.17E-03	2.89	10.295	8.842	8.508
13	100	4.06E-04	1.43E-03	3.51	10.385	8.857	8.556
14	150	4.06E-04	2.00E-03	4.92	10.550	8.885	8.641
15	200	4.06E-04	2.49E-03	6.15	10.661	8.903	8.709
16	300	4.06E-04	3.33E-03	8.20	10.789	8.929	8.770
17	400	4.06E-04	3.99E-03	9.84	10.873	8.939	8.810
18	600	4.06E-04	4.99E-03	12.30	10.926	8.952	8.840

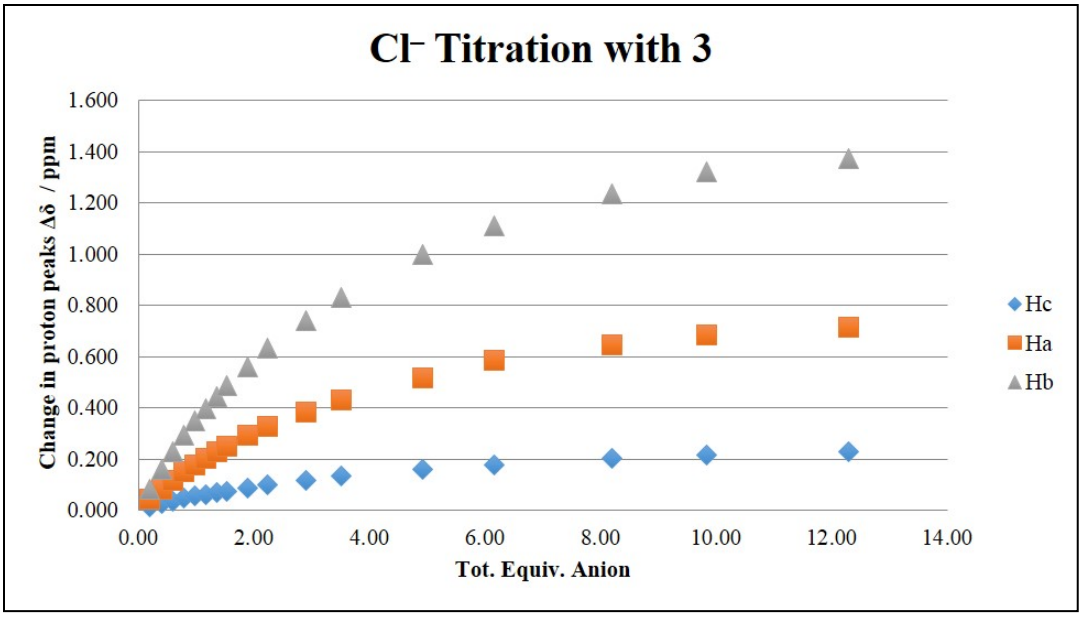

Figure 1. Binding isotherm for Cl^- titration with **3** in 10% d_6-DMSO/$CDCl_3$ by ^1H NMR.

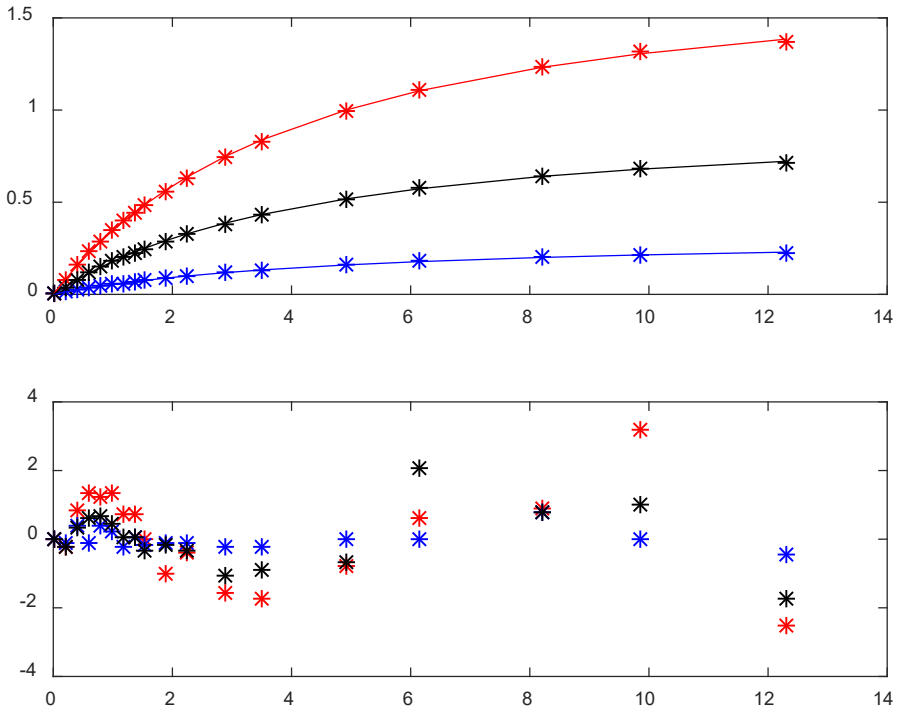

Figure 2. MatLab fit of binding isotherm for Cl^- titration with **3**.

Tetrabutylamamonium bromide with 3. A concentrated solution of **3** (5.16 mg, [R]=5.12 mM) in 10% d_6-DMSO/$CDCl_3$ (2.00 mL) was prepared. A serial dilution was then performed with 590 µL of 5.12 mM solution of **3** diluted to 3 mL to yield the stock solution of **3** ([R]=1.01 mM). This solution was used in the dilution of TBABr guest solution (45.03 mg, [G]=6.00 mM). The remaining stock solution (0.600 mL) was used as the starting volume in the NMR tube.

Table 2. Representative titration data for Br^- with **3**.

	Guest (µL)	[**1**] (M)	[Br^-] (M)	Equiv.	H^c δ (ppm)	H^a δ (ppm)	H^b δ (ppm)
1	0	1.01E-03	0.00E+00	0.00	9.590	8.730	8.144
2	5	1.01E-03	4.95E-04	0.49	9.743	8.759	8.225
3	10	1.01E-03	9.83E-04	0.98	9.828	8.770	8.270
4	15	1.01E-03	1.46E-03	1.45	9.900	8.784	8.310
5	20	1.01E-03	1.93E-03	1.92	9.943	8.793	8.333
6	25	1.01E-03	2.40E-03	2.38	9.984	8.799	8.356
7	30	1.01E-03	2.85E-03	2.83	10.024	8.805	8.377
8	35	1.01E-03	3.30E-03	3.28	10.058	8.810	8.395
9	40	1.01E-03	3.75E-03	3.72	10.089	8.816	8.412
10	50	1.01E-03	4.61E-03	4.58	10.139	8.825	8.440
11	60	1.01E-03	5.45E-03	5.41	10.194	8.834	8.470
12	80	1.01E-03	7.05E-03	7.00	10.258	8.846	8.506
13	100	1.01E-03	8.56E-03	8.50	10.312	8.855	8.534
14	150	1.01E-03	1.20E-02	11.90	10.415	8.873	8.592
15	200	1.01E-03	1.50E-02	14.87	10.458	8.885	8.616
16	300	1.01E-03	2.00E-02	19.83	10.544	8.896	8.662
17	400	1.01E-03	2.40E-02	23.79	10.581	8.904	8.682
18	600	1.01E-03	3.00E-02	29.74	10.589	8.904	8.693

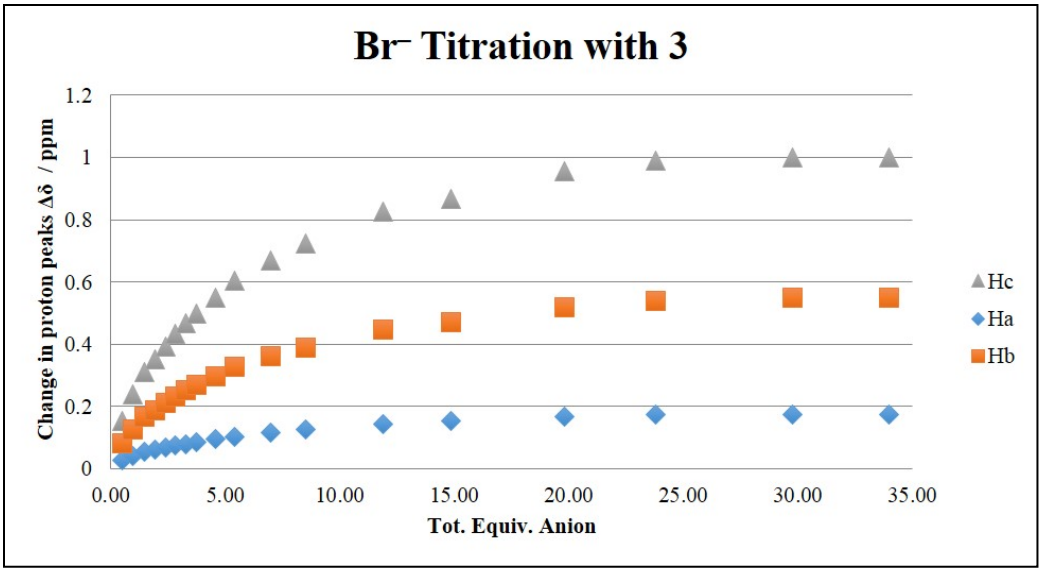

Figure 3. Binding isotherm for Br^- titration with **3** in 10% d_6-DMSO/$CDCl_3$ by ^1H NMR.

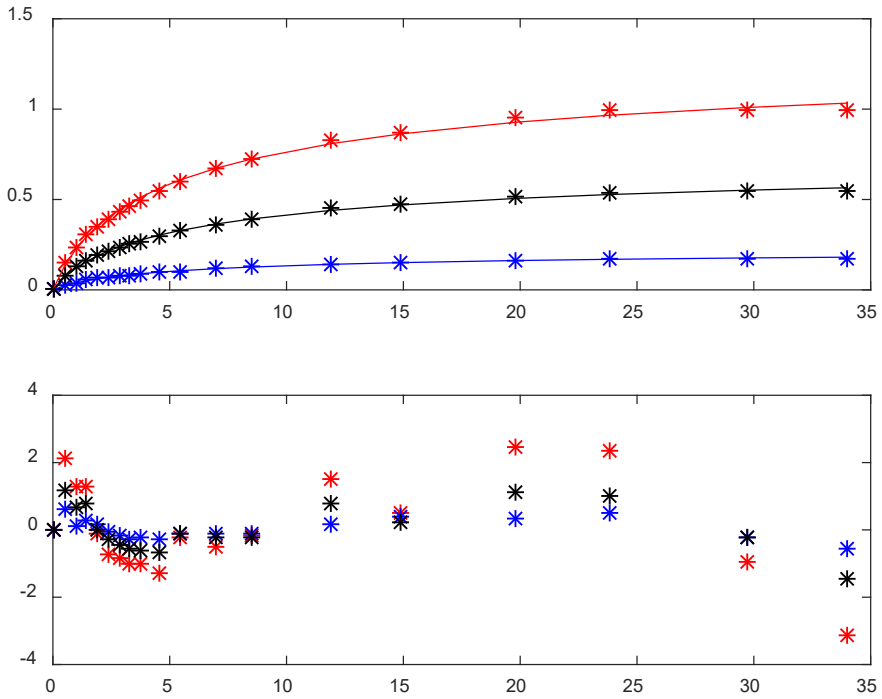

Figure 4. MatLab fit of binding isotherm for Br^- titration with **3**.

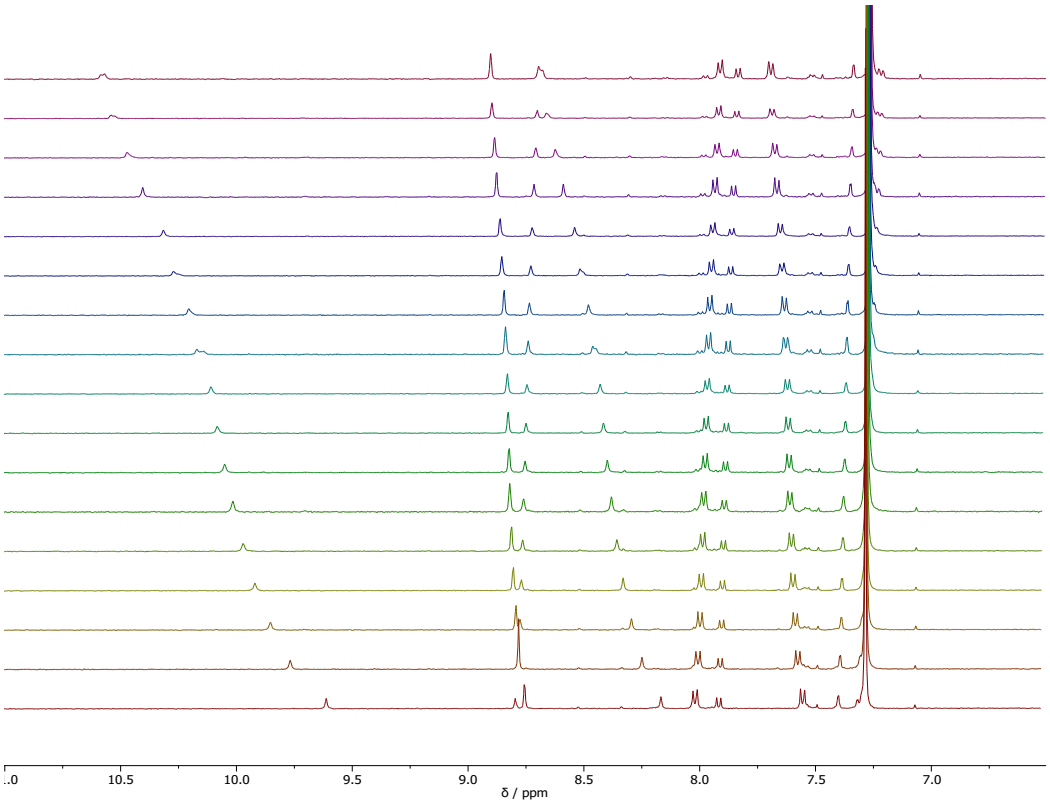

Figure 5. ^{1}H NMR spectra of Br^{-} titration with **3**.

Tetrabutylamamonium iodide with 3. A concentrated solution of **3** (5.22 mg, [R]=5.18 mM) in 10% d_6-DMSO/$CDCl_3$ (2.00 mL) was prepared. A serial dilution was then performed with 590 μL of 5.18 mM solution of **3** diluted to 3 mL to yield the stock solution of **3** ([R]=1.02 mM). This solution was used in the dilution of TBAI guest solution (51.76 mg, [G]=5.94 mM). The remaining stock solution (0.600 mL) was used as the starting volume in the NMR tube.

Table 3. Representative titration data for I^- with **3**.

	Guest (μL)	[**1**] (M)	[I^-] (M)	Equiv.	H^c δ (ppm)	H^a δ (ppm)	H^b δ (ppm)
1	0	1.01E-03	0.00E+00	0.00	9.590	8.730	8.144
2	5	1.01E-03	4.95E-04	0.49	9.743	8.759	8.225
3	10	1.01E-03	9.83E-04	0.98	9.828	8.770	8.270
4	15	1.01E-03	1.46E-03	1.45	9.900	8.784	8.310
5	20	1.01E-03	1.93E-03	1.92	9.943	8.793	8.333
6	25	1.01E-03	2.40E-03	2.38	9.984	8.799	8.356
7	30	1.01E-03	2.85E-03	2.83	10.024	8.805	8.377
8	35	1.01E-03	3.30E-03	3.28	10.058	8.810	8.395
9	40	1.01E-03	3.75E-03	3.72	10.089	8.816	8.412
10	50	1.01E-03	4.61E-03	4.58	10.139	8.825	8.440
11	60	1.01E-03	5.45E-03	5.41	10.194	8.834	8.470
12	80	1.01E-03	7.05E-03	7.00	10.258	8.846	8.506
13	100	1.01E-03	8.56E-03	8.50	10.312	8.855	8.534
14	150	1.01E-03	1.20E-02	11.90	10.415	8.873	8.592
15	200	1.01E-03	1.50E-02	14.87	10.458	8.885	8.616
16	300	1.01E-03	2.00E-02	19.83	10.544	8.896	8.662
17	400	1.01E-03	2.40E-02	23.79	10.581	8.904	8.682
18	600	1.01E-03	3.00E-02	29.74	10.589	8.904	8.693

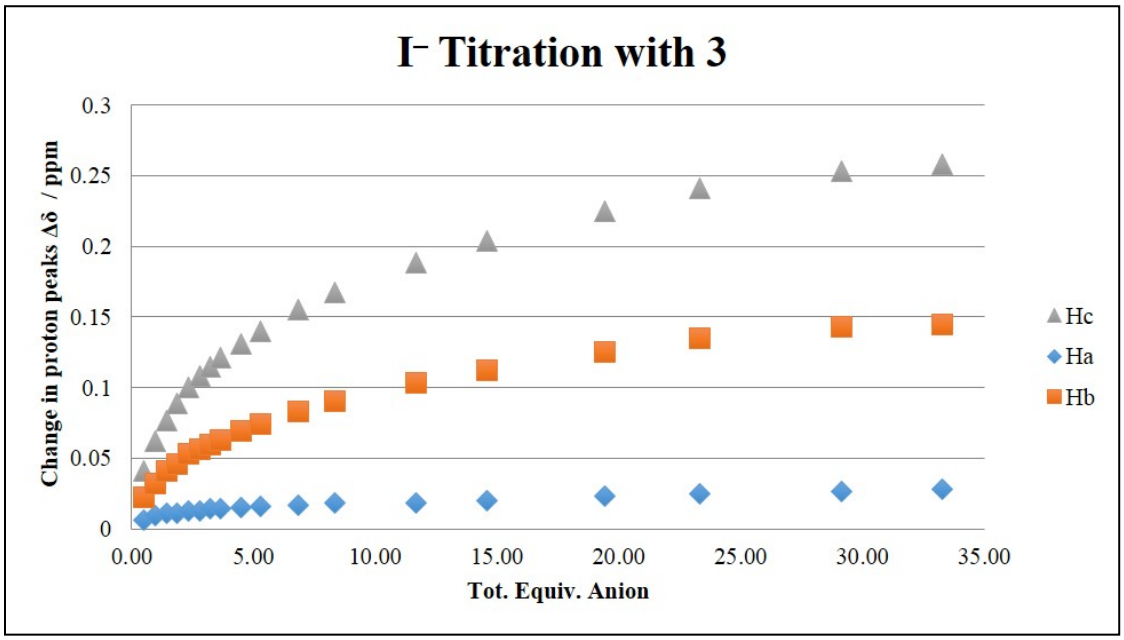

Figure 6. Binding isotherm for I^- titration with **3** in 10% d_6-DMSO/$CDCl_3$ by ^1H NMR.

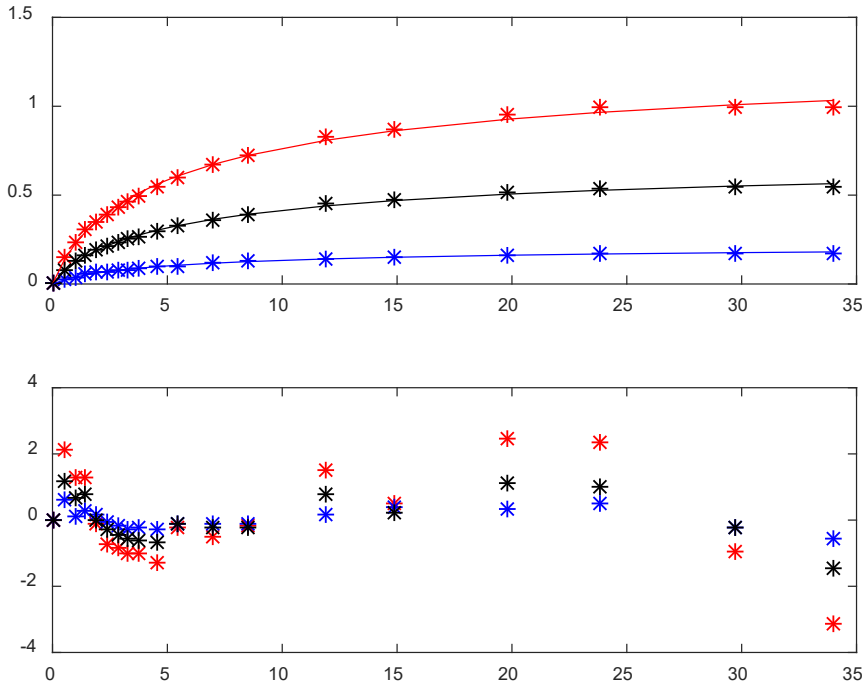

Figure 7. MatLab fit of binding isotherm for I^- titration with **3**.

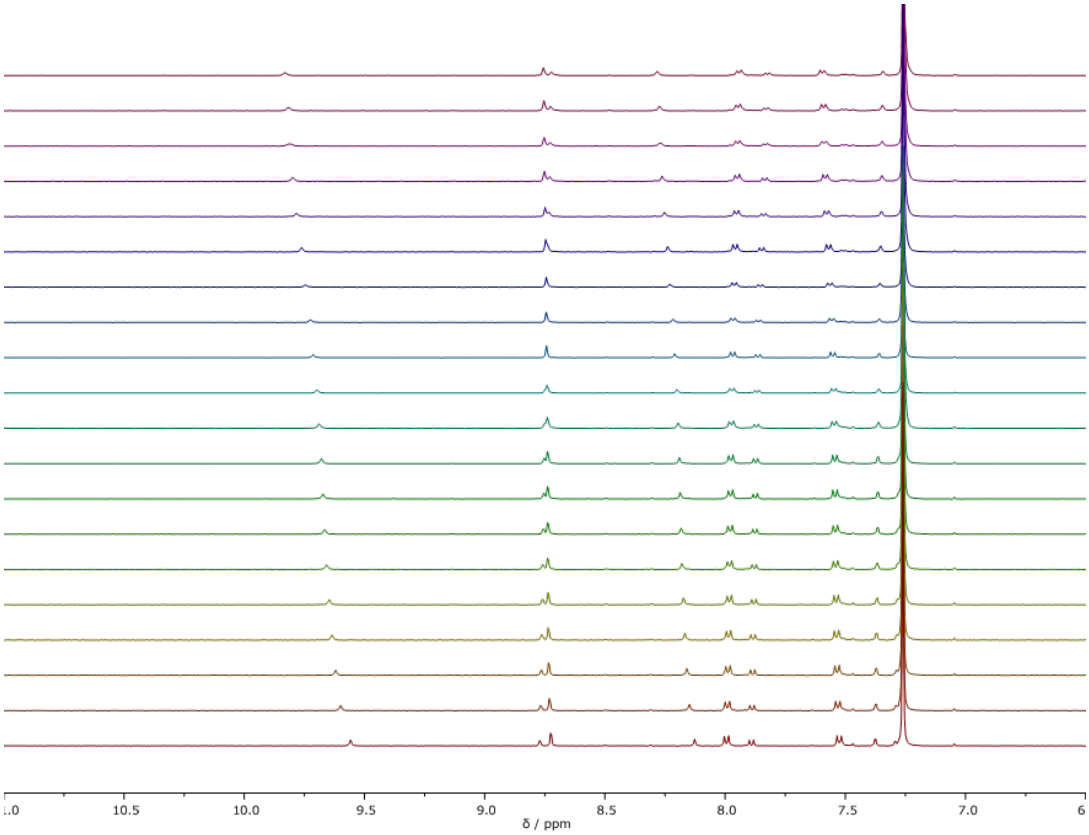

Figure 8. ^{1}H NMR spectra of I^- titration with **3**.

Tetrabutylamamonium chloride with 4. A concentrated solution of **4** (2.96mg, [R]=5.88 mM) in 10% d_6-DMSO/$CDCl_3$ (1.00 mL) was prepared. A serial dilution was then performed with 511 μL of 5.88 mM solution of **4** diluted to 3 mL to yield the stock solution of **4** ([R]=1.00 mM). This solution was used in the dilution of TBACl guest solution (9.56 mg, [G]=14.9 mM). The remaining stock solution (0.600 mL) was used as the starting volume in the NMR tube. The calculated association constants for the titration of TBACl with **4** were at the limits of ^{1}H NMR titrations, although errors were less than 15% across three titrations. The μM concentrations needed to obtain UV-Vis spectroscopy titration data dilute out the expected 2:1 host-guest model, however, leading to titrations only appropriately fit to a 1:1 host-guest model.

Table 4. Representative titration data for Cl^- with **4**.

	Guest (μL)	[**2**] (M)	[Cl^-] (M)	Equiv.	H^a δ (ppm)	H^b δ (ppm)
1	0	1.00E-03	0.00E+00	0.00	9.617	8.119
2	5	1.00E-03	1.23E-04	0.12	9.888	8.230
3	10	1.00E-03	2.44E-04	0.24	10.145	8.335
4	15	1.00E-03	3.62E-04	0.36	10.379	8.428
5	20	1.00E-03	4.79E-04	0.48	10.562	8.502
6	25	1.00E-03	5.94E-04	0.59	10.695	8.555
7	30	1.00E-03	7.08E-04	0.71	10.775	8.587
8	35	1.00E-03	8.19E-04	0.82	10.819	8.604
9	40	1.00E-03	9.29E-04	0.93	10.847	8.615
10	50	1.00E-03	1.14E-03	1.14	10.877	8.626
11	60	1.00E-03	1.35E-03	1.35	10.892	8.631
12	80	1.00E-03	1.75E-03	1.75	10.910	8.637
13	100	1.00E-03	2.12E-03	2.12	10.919	8.640
14	150	1.00E-03	2.97E-03	2.97	10.929	8.643
15	200	1.00E-03	3.71E-03	3.71	10.933	8.643
16	300	1.00E-03	4.95E-03	4.95	10.939	8.645
17	400	1.00E-03	5.94E-03	5.93	10.941	8.645
18	600	1.00E-03	7.43E-03	7.42	10.944	8.646

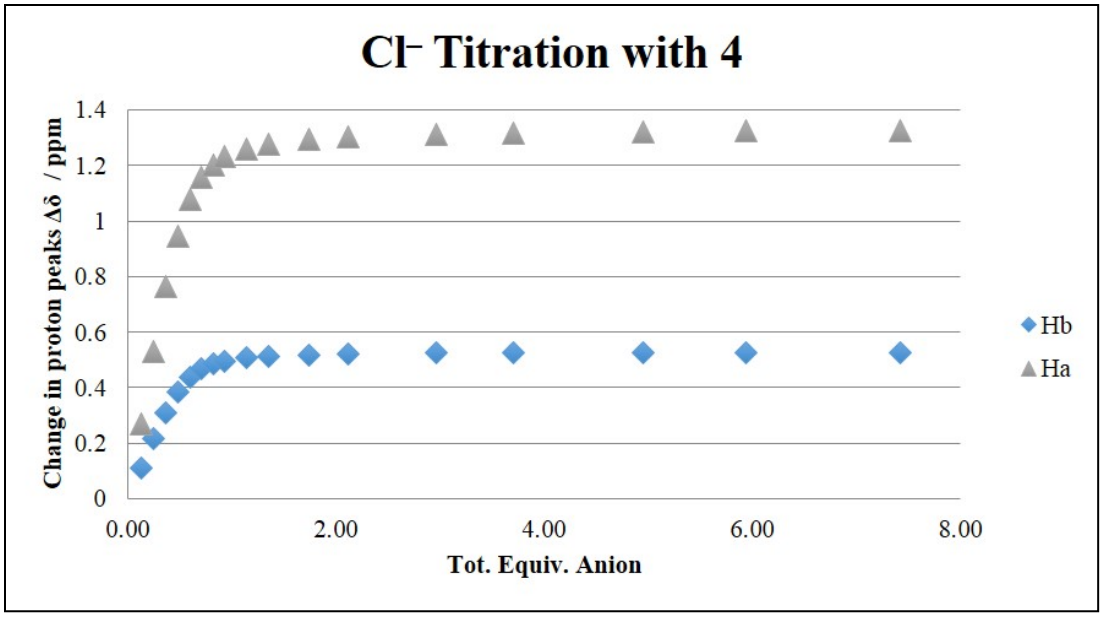

Figure 9. Binding isotherm for Cl^- titration with **4** in 10% d_6-DMSO/$CDCl_3$ by ^1H NMR.

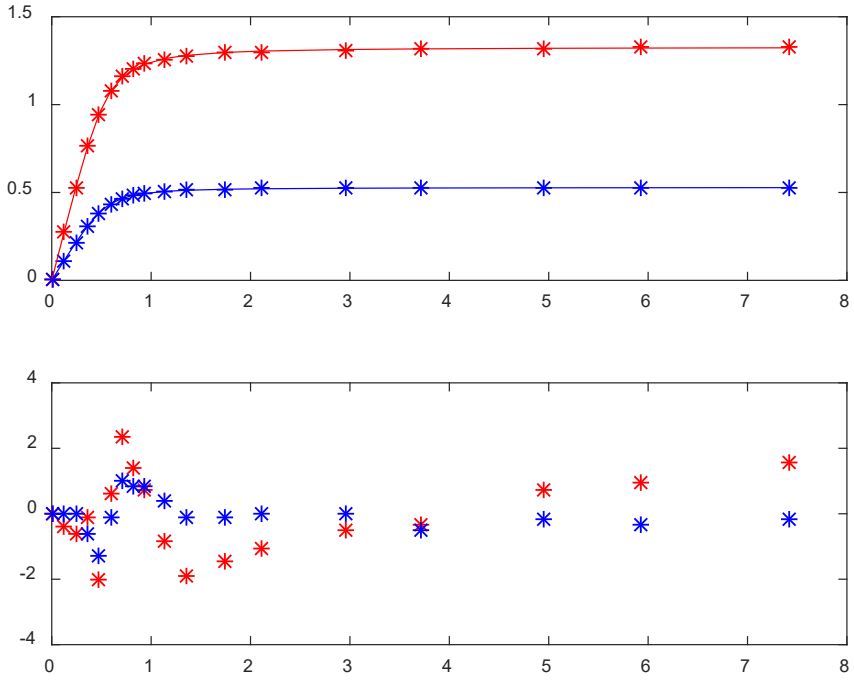

Figure 10. MatLab fit of binding isotherm for Cl^- titration with **4**.

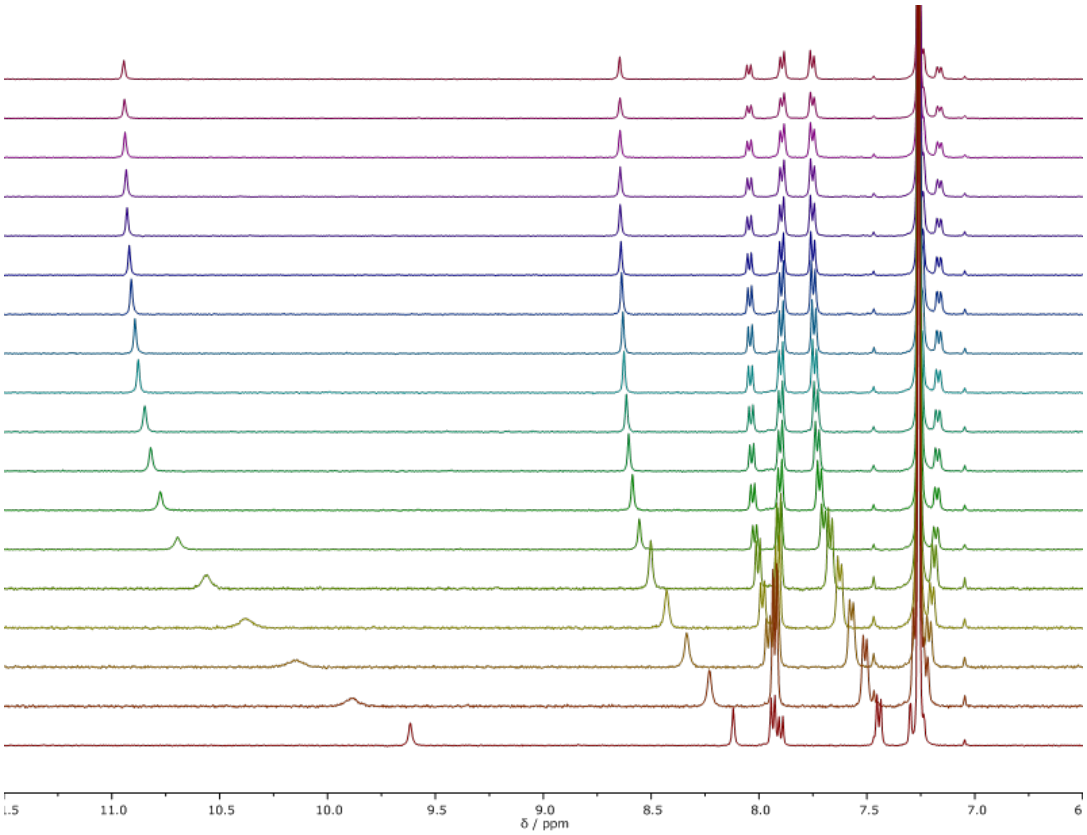

Figure 11. ^{1}H NMR spectra of Cl^{-} titration with **4**.

Tetrabutylamamonium bromide with 4. A concentrated solution of **4** (5.21 mg, [R]=5.17 mM) in 10% d_6-DMSO/$CDCl_3$ (2.00 mL) was prepared. A serial dilution was then performed with 590 µL of 5.17 mM solution of **4** diluted to 3 mL to yield the stock solution of **4** ([R]=1.02 mM). This solution was used in the dilution of TBABr guest solution (23.01 mg, [G]=31.0 mM). The remaining stock solution (0.600 mL) was used as the starting volume in the NMR tube.

Table 5. Representative titration data for Br^- with **2**.

	Guest (μL)	[**2**] (M)	[Br^-] (M)	Equiv.	H^a δ (ppm)	H^b δ (ppm)
1	0	1.02E-03	0.00E+00	0.25	9.754	8.178
2	5	1.02E-03	2.56E-04	0.50	9.975	8.285
3	10	1.02E-03	5.08E-04	0.74	10.101	8.345
4	15	1.02E-03	7.55E-04	0.98	10.181	8.382
5	20	1.02E-03	9.99E-04	1.22	10.233	8.407
6	25	1.02E-03	1.24E-03	1.45	10.266	8.422
7	30	1.02E-03	1.47E-03	1.68	10.290	8.434
8	35	1.02E-03	1.71E-03	1.90	10.307	8.441
9	40	1.02E-03	1.94E-03	2.34	10.322	8.447
10	50	1.02E-03	2.38E-03	2.77	10.341	8.456
11	60	1.02E-03	2.82E-03	3.58	10.356	8.463
12	80	1.02E-03	3.64E-03	4.35	10.369	8.468
13	100	1.02E-03	4.42E-03	6.09	10.377	8.472
14	150	1.02E-03	6.19E-03	7.61	10.388	8.477
15	200	1.02E-03	7.74E-03	10.14	10.391	8.478
16	300	1.02E-03	1.03E-02	12.17	10.394	8.478
17	400	1.02E-03	1.24E-02	15.21	10.398	8.480
18	600	1.02E-03	1.55E-02	0.25	10.398	8.480

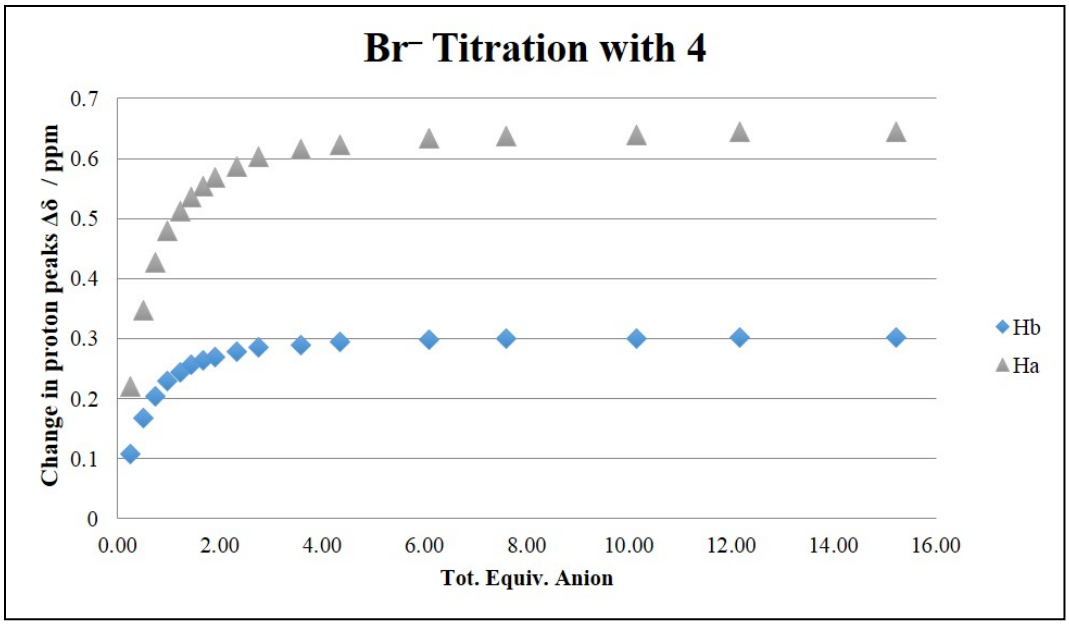

Figure 12. Binding isotherm for Br^- titration with **4** in 10% d_6-DMSO/$CDCl_3$ by ^1H NMR.

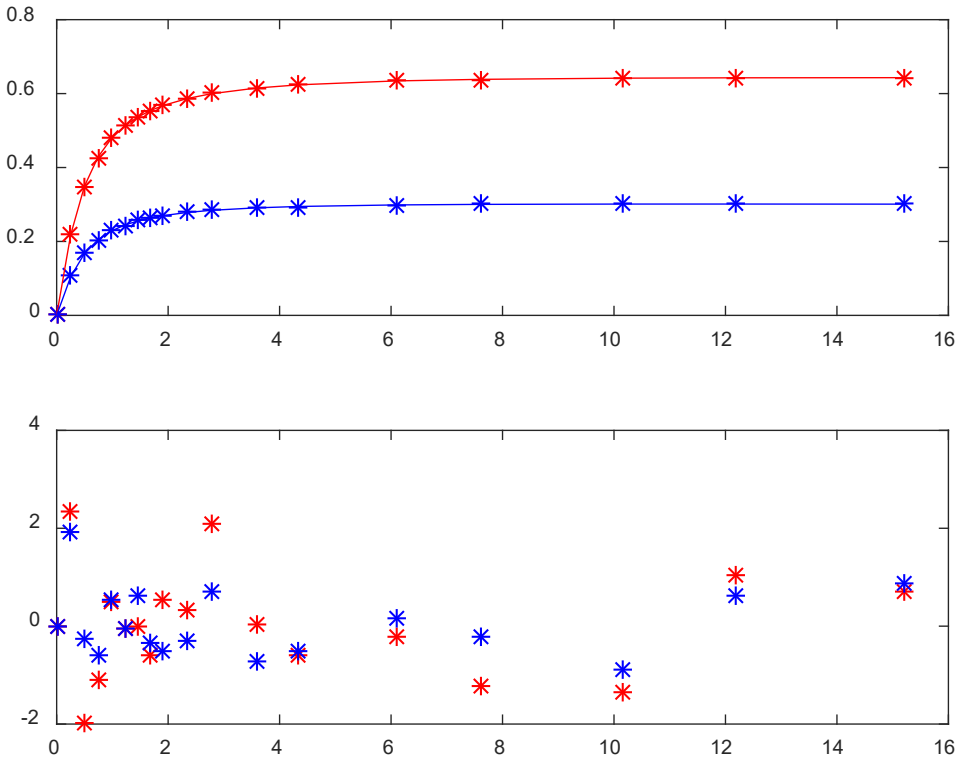

Figure 13. MatLab fit of binding isotherm for Br^- titration with **4**.

Tetrabutylamamonium iodide with 4. A concentrated solution of **4** (5.21 mg, [R]=5.17 mM) in 10% d_6-DMSO/$CDCl_3$ (2.00 mL) was prepared. A serial dilution was then performed with 576 µL of 5.17 mM solution of **4** diluted to 3 mL to yield the stock solution of **4** ([R]=0.994 mM). This solution was used in the dilution of TBAI guest solution (26.11mg, [G]=31.21 mM). The remaining stock solution (0.600 mL) was used as the starting volume in the NMR tube.

Table 6. Representative titration data for I^- with **4**.

	Guest (μL)	[**2**] (M)	[I^-] (M)	Equiv.	H^a δ (ppm)	H^b δ (ppm)
1	0	9.94E-04	0.00E+00	0.26	9.644	8.131
2	5	9.94E-04	2.58E-04	0.51	9.651	8.135
3	10	9.94E-04	5.12E-04	0.77	9.661	8.141
4	15	9.94E-04	7.61E-04	1.01	9.668	8.146
5	20	9.94E-04	1.01E-03	1.26	9.675	8.151
6	25	9.94E-04	1.25E-03	1.50	9.681	8.154
7	30	9.94E-04	1.49E-03	1.73	9.685	8.156
8	35	9.94E-04	1.72E-03	1.96	9.689	8.160
9	40	9.94E-04	1.95E-03	2.42	9.691	8.161
10	50	9.94E-04	2.40E-03	2.86	9.698	8.166
11	60	9.94E-04	2.84E-03	3.70	9.708	8.170
12	80	9.94E-04	3.67E-03	4.49	9.718	8.177
13	100	9.94E-04	4.46E-03	6.28	9.726	8.183
14	150	9.94E-04	6.24E-03	7.85	9.750	8.197
15	200	9.94E-04	7.80E-03	10.47	9.767	8.206
16	300	9.94E-04	1.04E-02	12.57	9.778	8.214
17	400	9.94E-04	1.25E-02	15.71	9.788	8.223
18	600	9.94E-04	1.56E-02	0.26	9.803	8.230

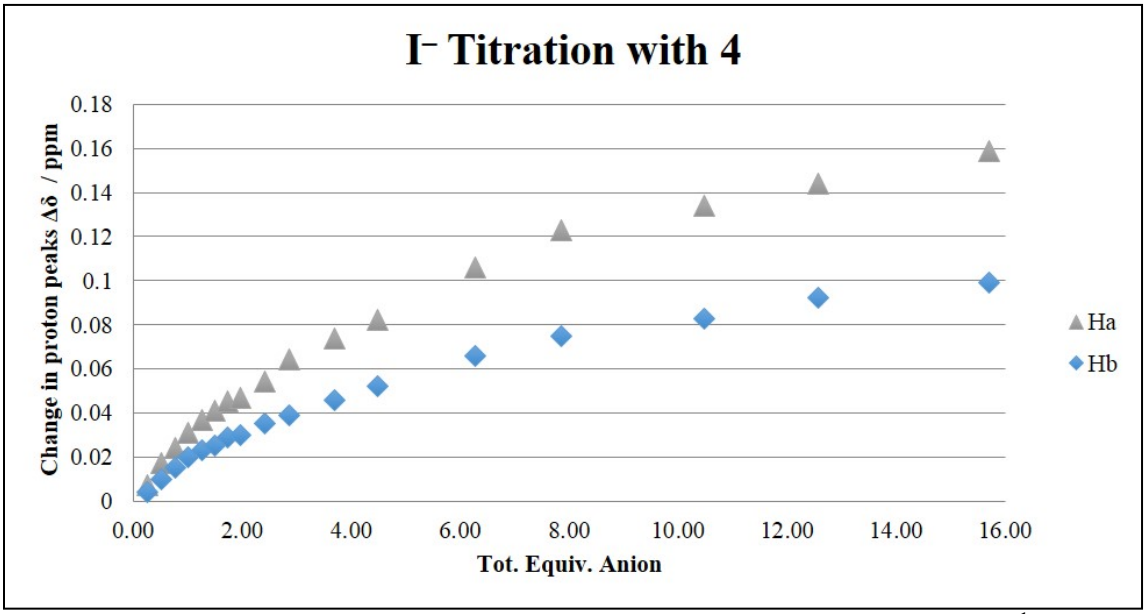

Figure 14. Binding isotherm for I^- titration with **4** in 10% d_6-DMSO/$CDCl_3$ by ^1H NMR.

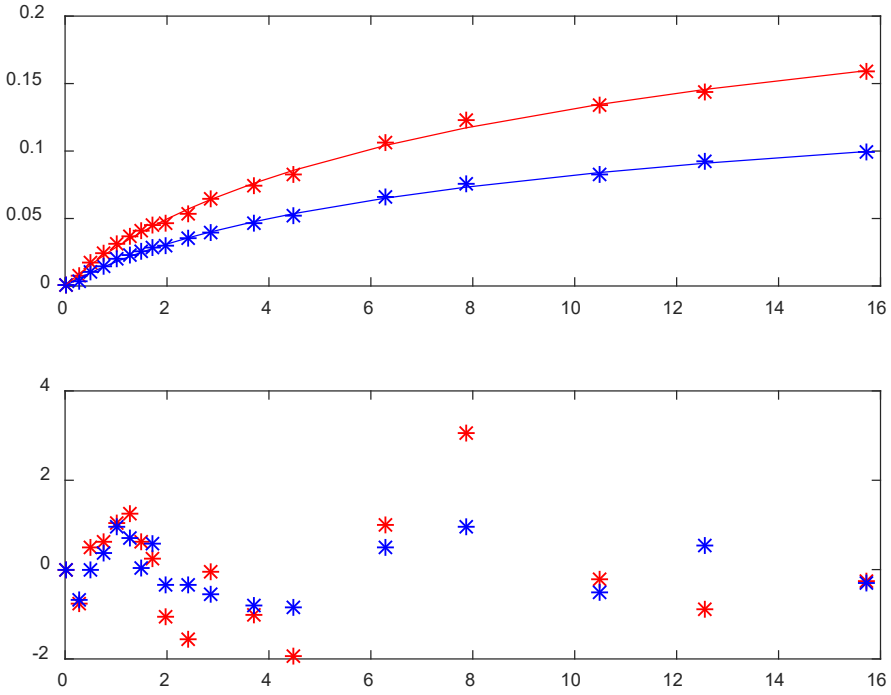

Figure 15. MatLab fit of binding isotherm for I^- titration with **4**.

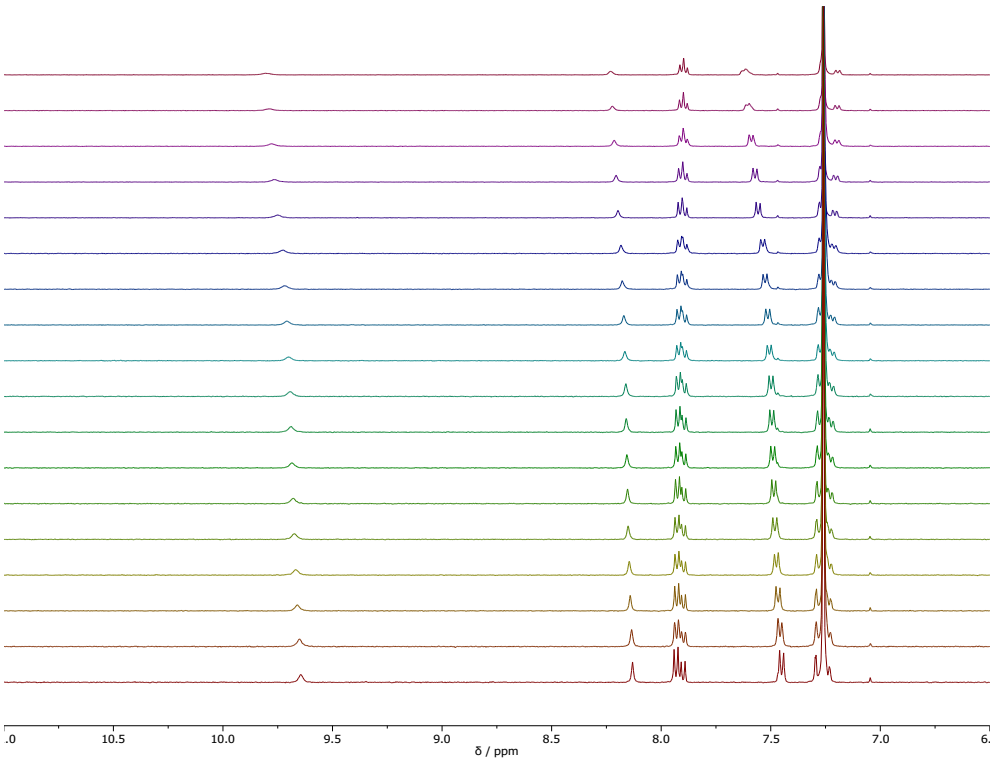

Figure 16. ^{1}H NMR spectra of I^- titration with **4**.

UV-Vis titrations

Tetrabutylammonium chloride with 4. A concentrated solution of **4** (2.00 mg, [R]=0.199 mM) in 10% DMSO/$CHCl_3$ (20.00 mL) was prepared. A serial dilution was then performed with 50 μL of 0.199 mM solution of **4** diluted to 5 mL to yield the stock solution of **4** ([R]= 1.99 μM). A 2 mL solution of TBACl (2.53 mg, [G]=0.984 mM) was prepared by serial dilution with the stock solution of **4**. The starting volume in the cuvette was 2.0 mL.

Table 7. Representative titration data for Cl^- with **4**.

	Guest (μL)	[**2**] (M)	[Cl^-] (M)	Equiv.
1	0	1.99E-06	0.00E+00	0.00
2	5	1.99E-06	2.45E-06	1.23
3	10	1.99E-06	4.89E-06	2.46
4	15	1.99E-06	9.74E-06	4.90
5	20	1.99E-06	1.93E-05	9.71
6	25	1.99E-06	2.87E-05	14.42
7	30	1.99E-06	3.78E-05	19.05
8	40	1.99E-06	4.68E-05	23.58
9	50	1.99E-06	5.79E-05	29.13
10	60	1.99E-06	6.86E-05	34.55
11	70	1.99E-06	8.94E-05	45.02
12	80	1.99E-06	1.09E-04	55.03
13	100	1.99E-06	1.28E-04	64.60
14	120	1.99E-06	1.47E-04	73.76
15	140	1.99E-06	1.64E-04	82.54
16	180	1.99E-06	1.97E-04	99.05
17	220	1.99E-06	2.27E-04	114.28
18	300	1.99E-06	2.55E-04	128.39
19	400	1.99E-06	3.05E-04	153.69
20	600	1.99E-06	3.49E-04	175.73
21	800	1.99E-06	4.22E-04	212.24

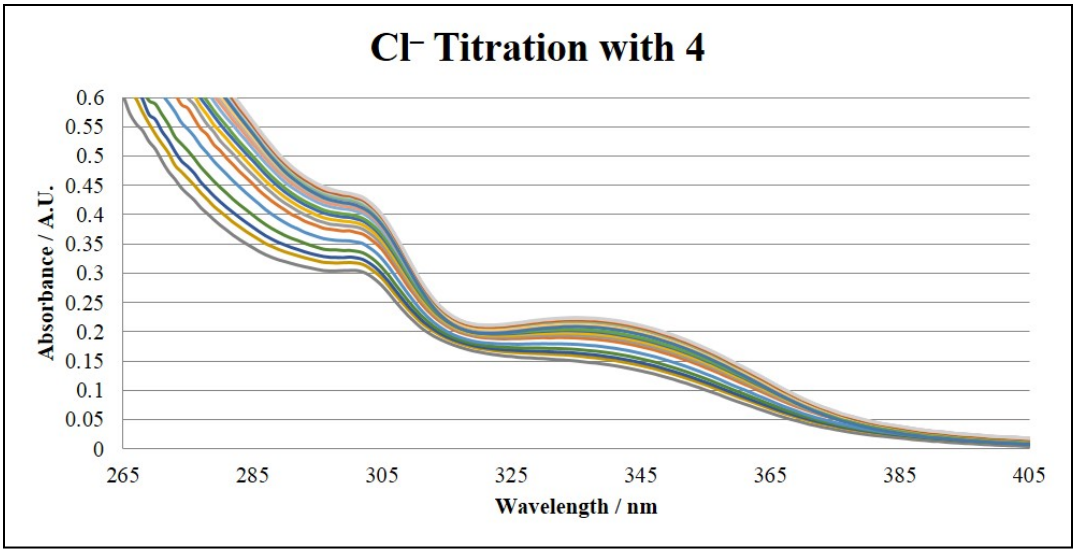

Figure 17. UV-Vis spectra of **4** titrated with Cl^- in 10% -DMSO/$CHCl_3$.

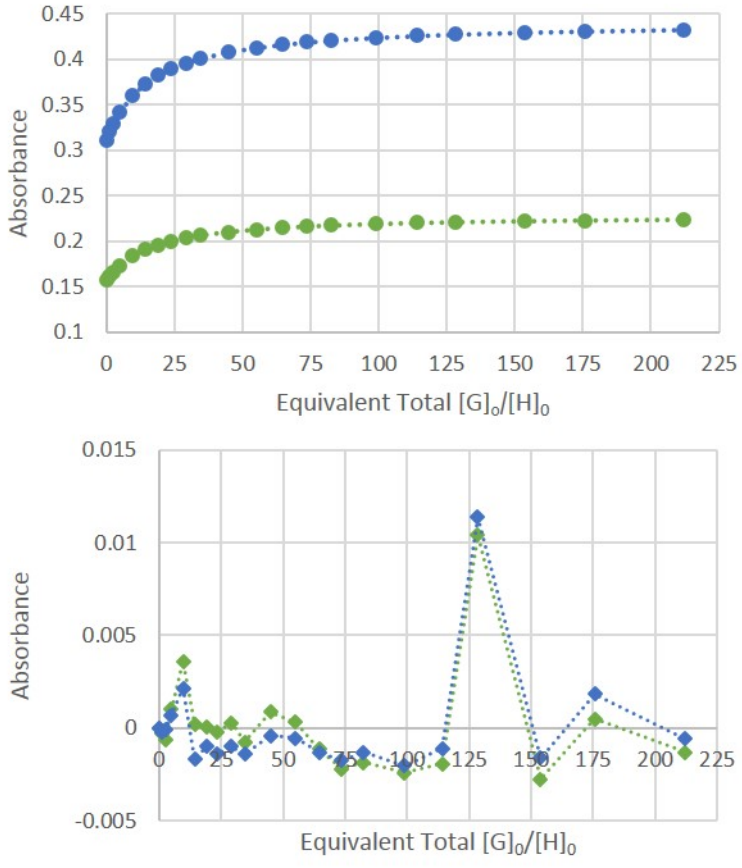

Figure 18. Open Data Fit fit of binding isotherm for Cl^- titration with **4**.

Job's Plot Analysis

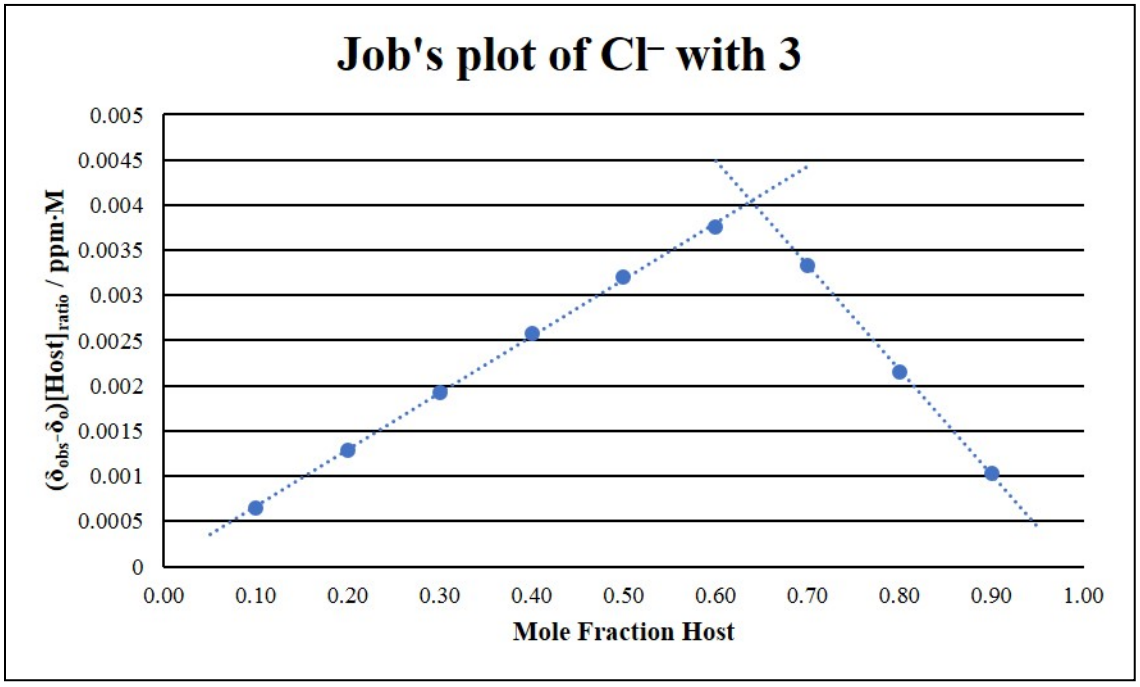

Figure 18. Job's plot analysis for Cl^- titration with **3** in 10% d_6-DMSO/$CDCl_3$ by ^1H NMR.

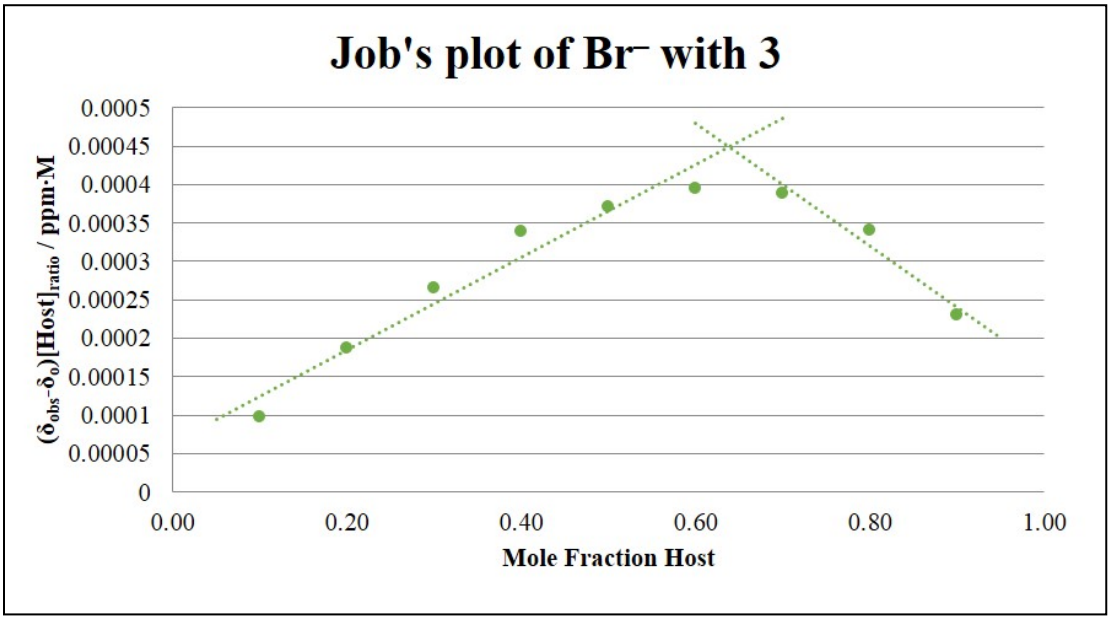

Figure 19. Job's plot analysis for Br^- titration with **3** in 10% d_6-DMSO/$CDCl_3$ by ^1H NMR.

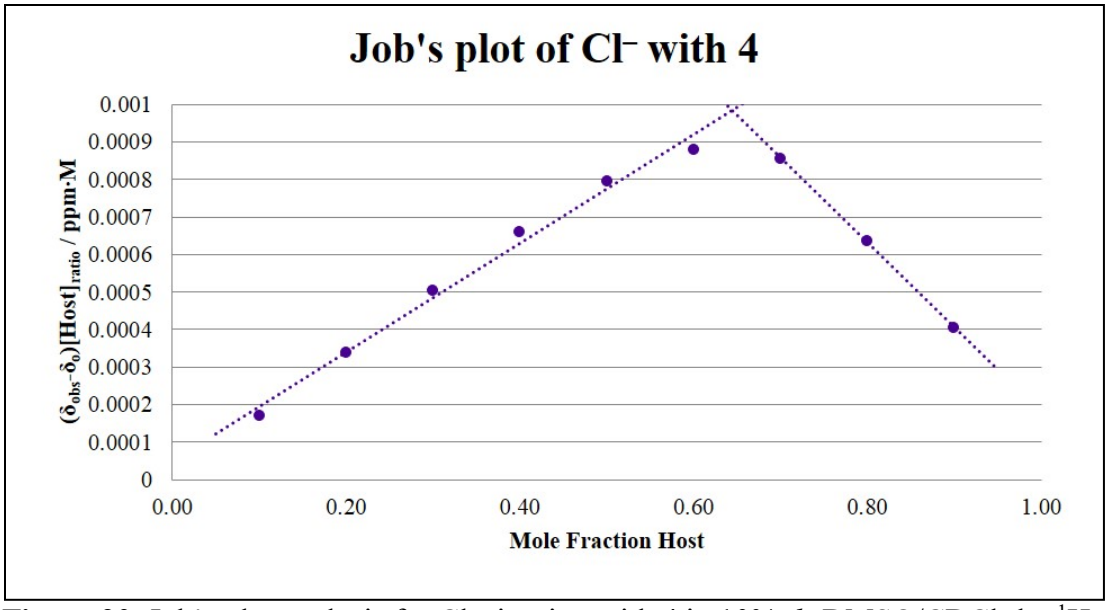

Figure 20. Job's plot analysis for Cl^- titration with **4** in 10% d_6-DMSO/$CDCl_3$ by ^1H NMR.

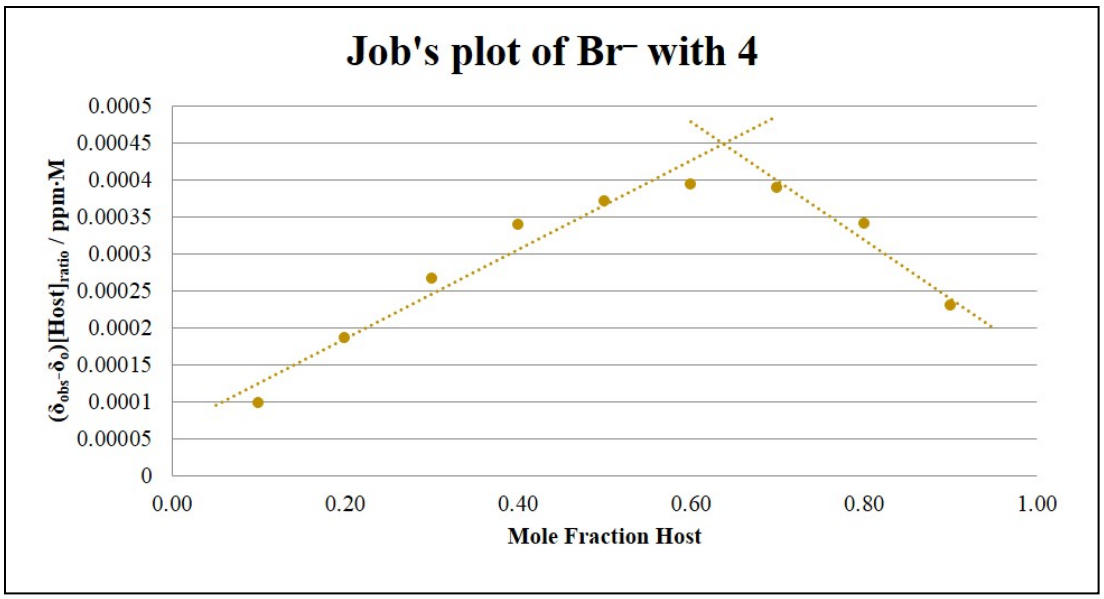

Figure 21. Job's plot analysis for Br^- titration with **4** in 10% d_6-DMSO/$CDCl_3$ by ^1H NMR.

NMR Spectra

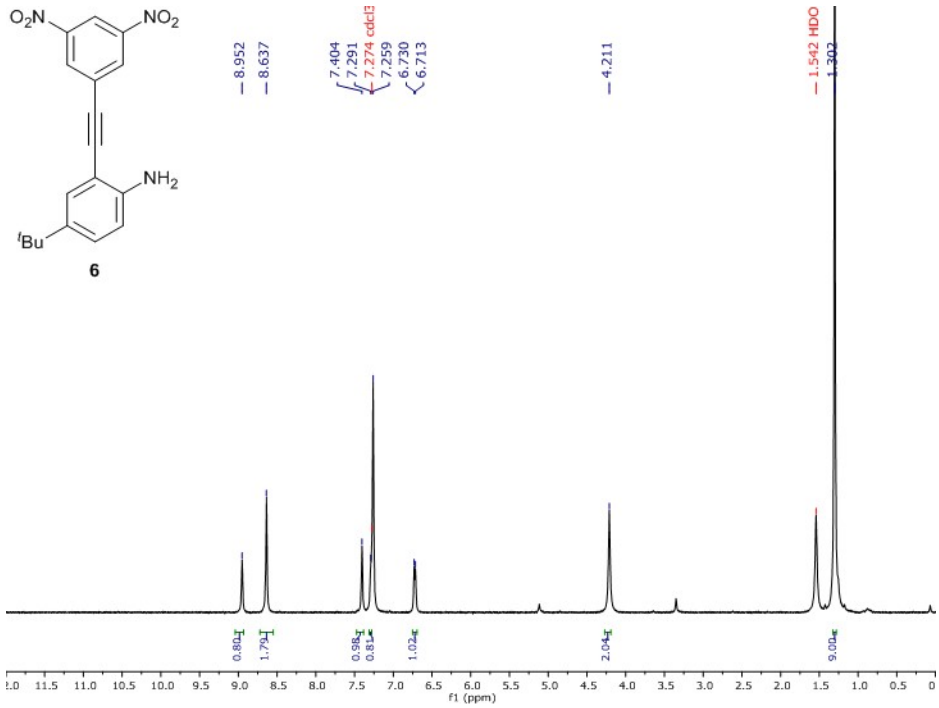

Figure 22. ^{1}H NMR spectra of **6** in $CDCl_3$.

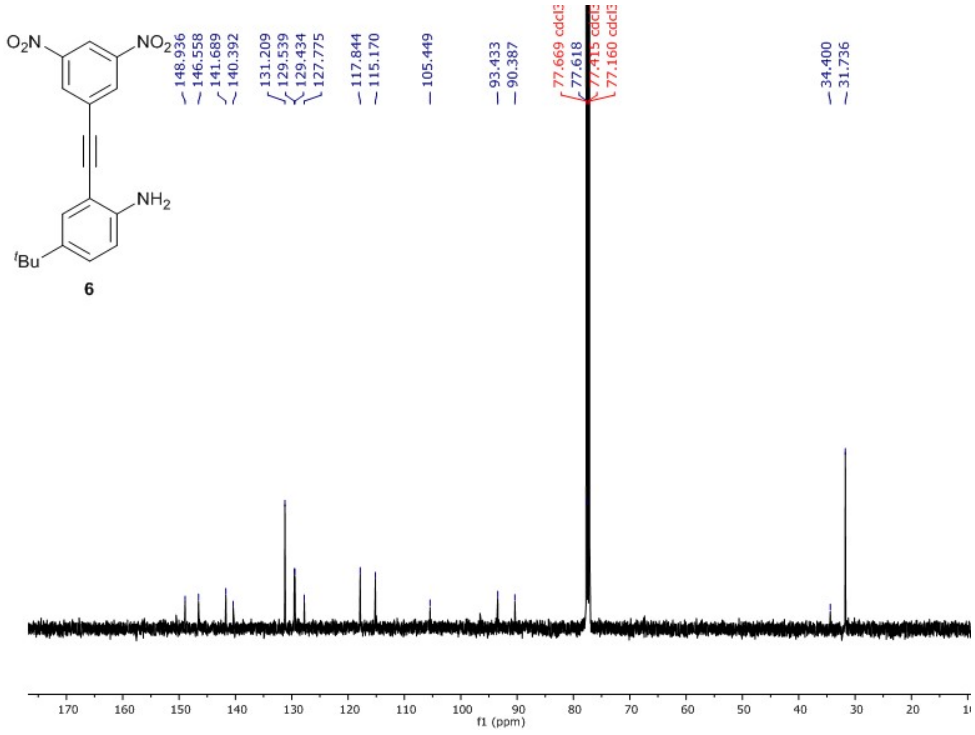

Figure 23. ^{13}C NMR spectra of **6** in $CDCl_3$.

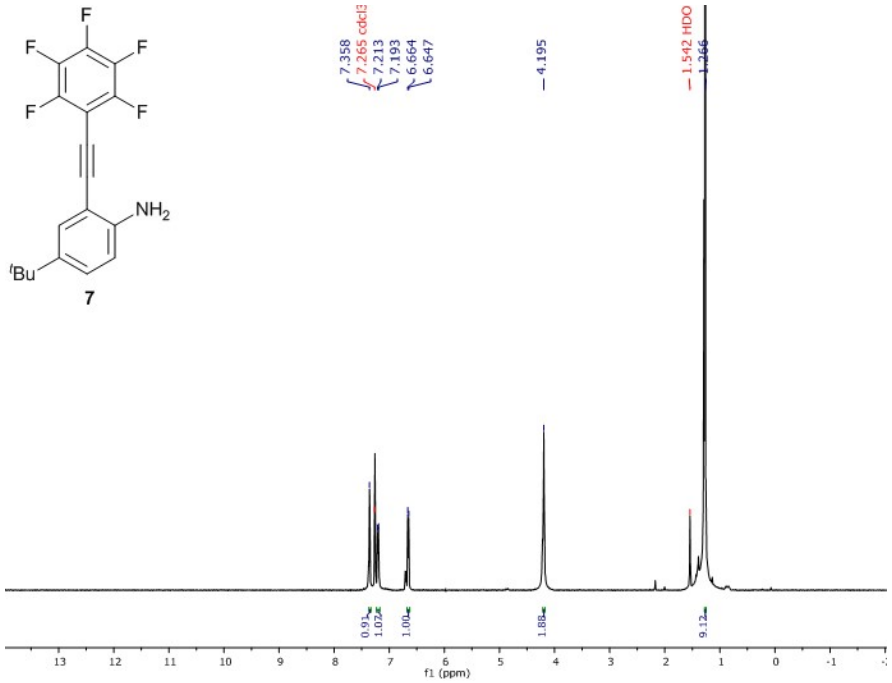

Figure 24. ^{1}H NMR spectra of **7** in $CDCl_3$.

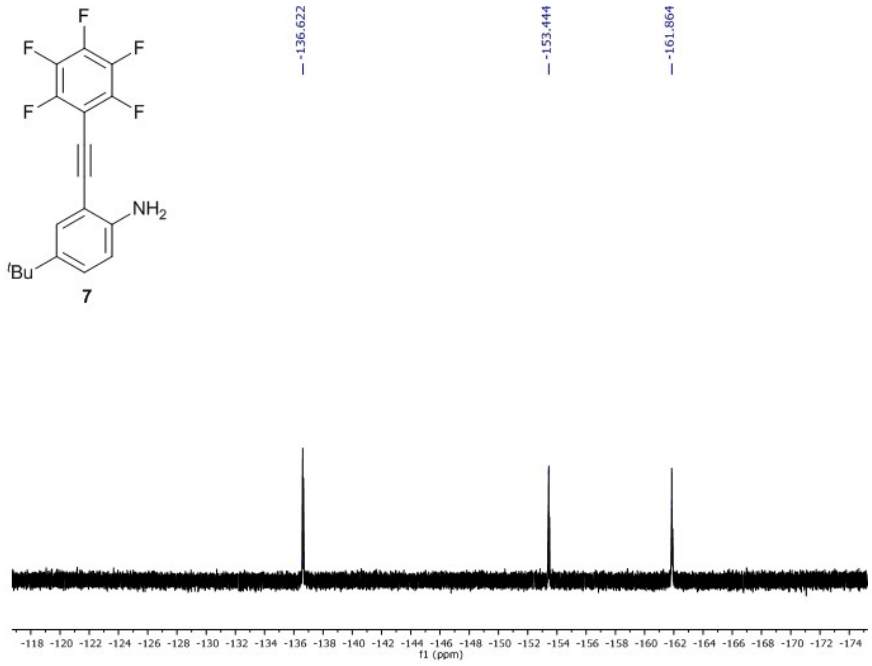

Figure 25. ^{19}F NMR spectra of **7** in $CDCl_3$.

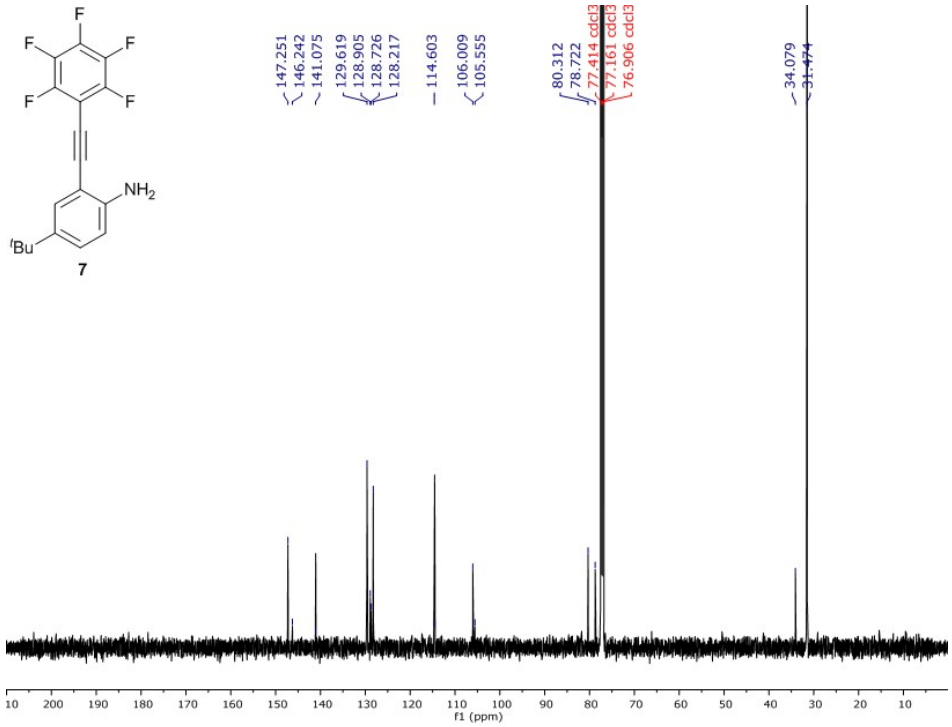

Figure 26. ^{13}C NMR spectra of **7** in $CDCl_3$.

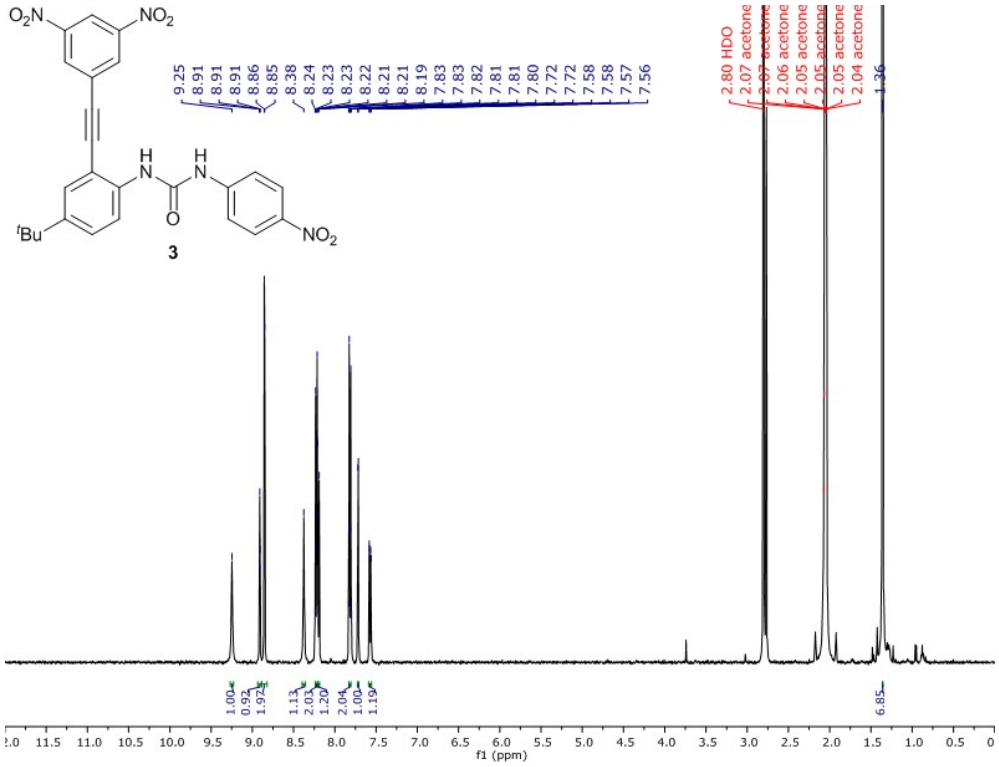

Figure 27. ^{1}H NMR spectra of **3** in acetone-d_6.

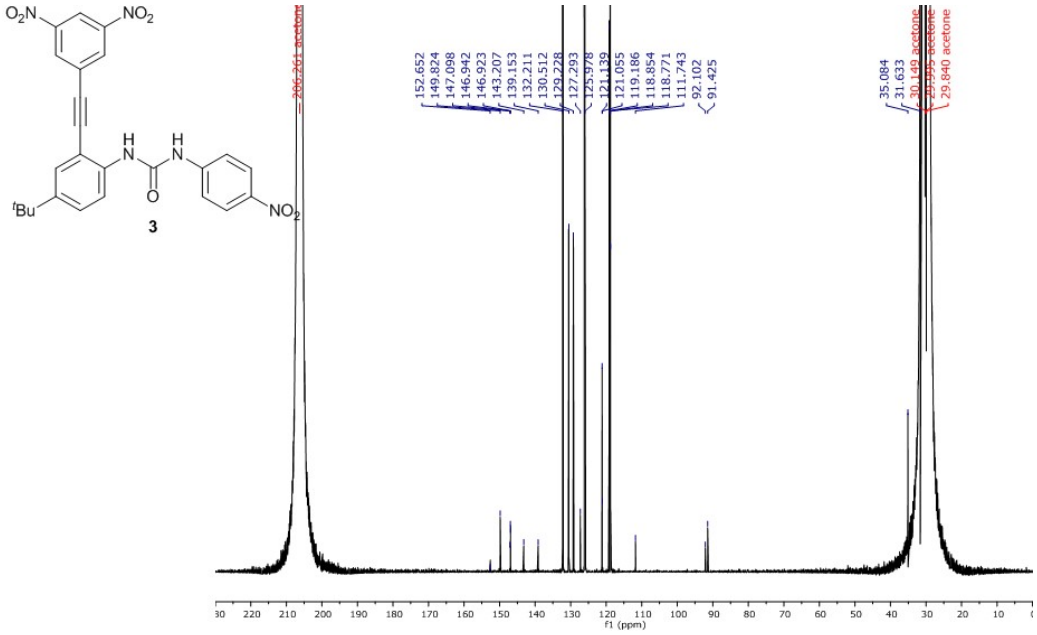

Figure 28. ^{13}C NMR spectra of **3** in acetone-d_6.

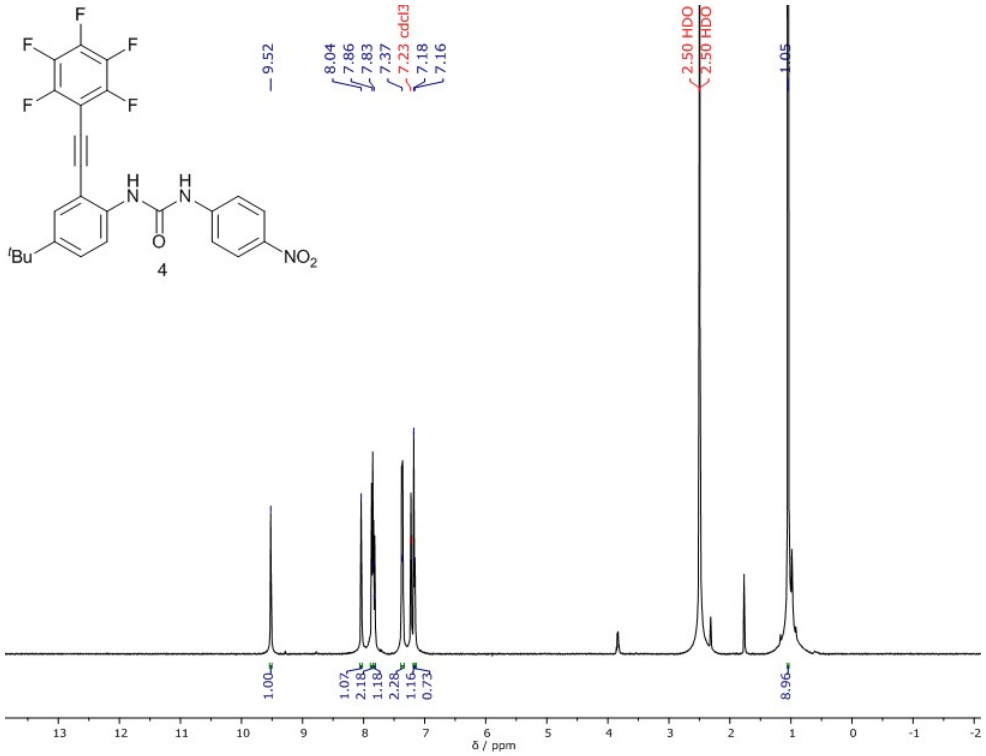

Figure 29. ^{1}H NMR spectra of **4** in $CDCl_3$.

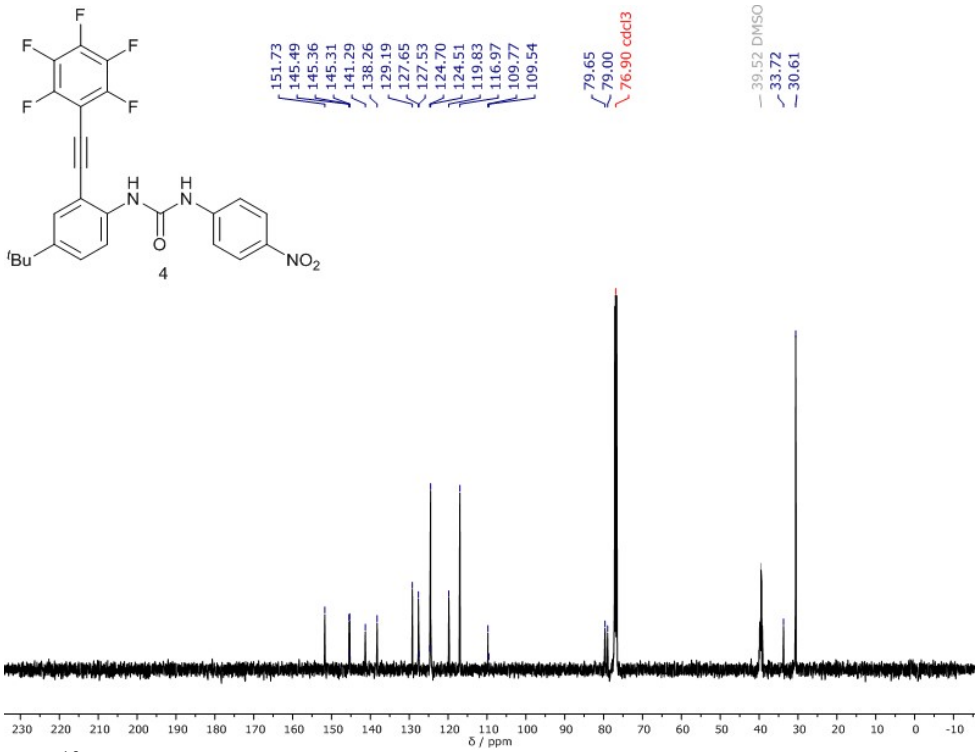

Figure 30. ^{13}C NMR spectra of **4** in $CDCl_3$/DMSO-d_6.

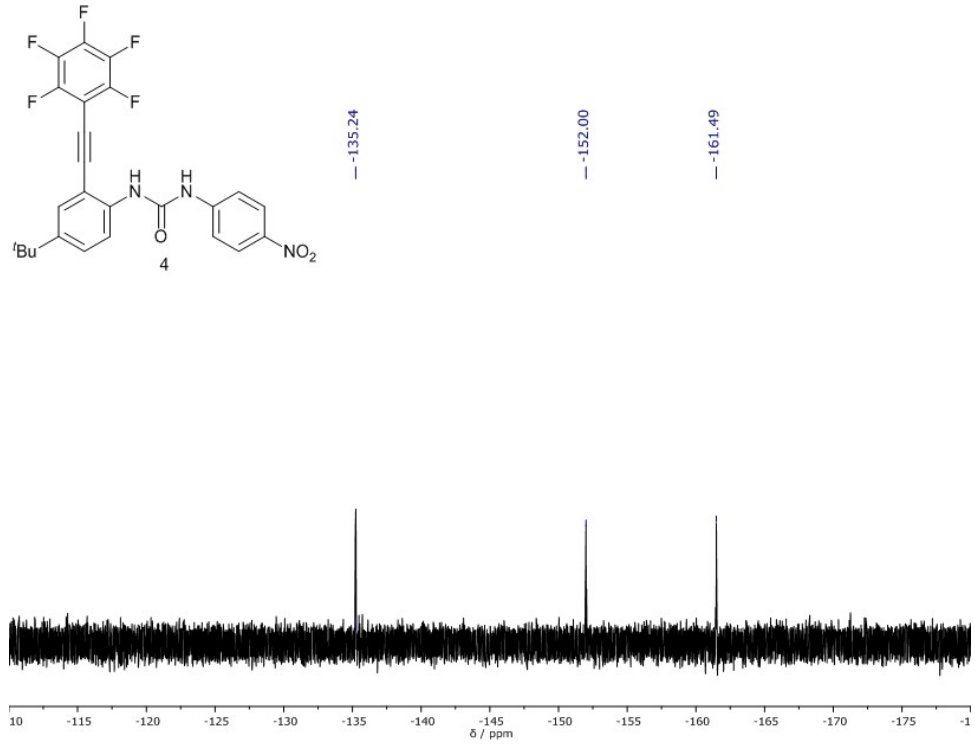

Figure 31. ^{19}F NMR spectra of **4** in $CDCl_3$/DMSO-d_6.

APPENDIX B

SUPPLEMENTARY INFORMATION FOR CHAPTER III

Titrations

UV-Vis titrations

Tetrabutylammonium dihydrogenphosphate with 1. A concentrated solution of 1 (2.25 mg, [R] = 0.313 mM) in 10% DMSO/$CHCl_3$ (10.00 mL) was prepared. A serial dilution was then performed with 800 µL of 0.313 mM solution of 1 diluted to 10.00 mL to yield the stock solution of 1 ([R] = 25.0 µM). A 3.00 mL solution of $TBAH_2PO_4$ (2.14 mg, [G] = 2.10 mM) was prepared by solvation with the stock solution of 1. A serial dilution was then performed with 1200 µL of the 2.10 mM solution of $TBAH_2PO_4$ diluted to 3.00 mL with the stock solution of 1 to yield guest solution ([G] = 8.41 mM). The starting volume in the cuvette was 2.0 mL.

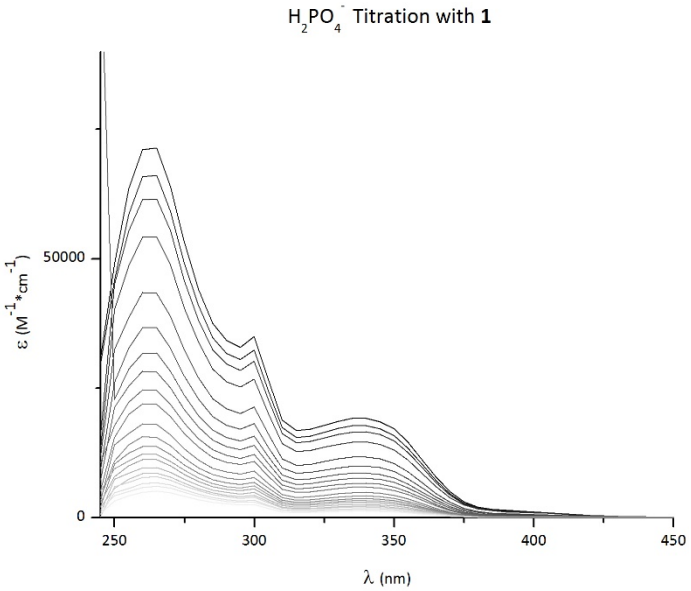

Figure 1. UV-Vis spectra of **1** titrated with $H_2PO_4^-$ in 10% DMSO/$CHCl_3$.

Table 1. Representative titration data for $H_2PO_4^-$ with **1**.

	Guest (μL)	[**1**] (M)	[$H_2PO_4^-$] (M)	Equiv.
1	0	2.50E-05	0.00E+00	0.00
2	5	2.50E-05	2.39E-06	0.10
3	10	2.50E-05	4.78E-06	0.19
4	20	2.50E-05	9.50E-06	0.38
5	40	2.50E-05	1.88E-05	0.75
6	60	2.50E-05	2.79E-05	1.11
7	80	2.50E-05	3.67E-05	1.47
8	100	2.50E-05	4.54E-05	1.82
9	125	2.50E-05	5.60E-05	2.24
10	150	2.50E-05	6.64E-05	2.65
11	200	2.50E-05	8.62E-05	3.45
12	250	2.50E-05	1.05E-04	4.20
13	300	2.50E-05	1.23E-04	4.92
14	350	2.50E-05	1.40E-04	5.60
15	400	2.50E-05	1.56E-04	6.25
16	500	2.50E-05	1.87E-04	7.47
17	600	2.50E-05	2.15E-04	8.58
18	700	2.50E-05	2.40E-04	9.61
19	900	2.50E-05	2.85E-04	11.42
20	1100	2.50E-05	3.24E-04	12.98
21	1500	2.50E-05	3.88E-04	15.52

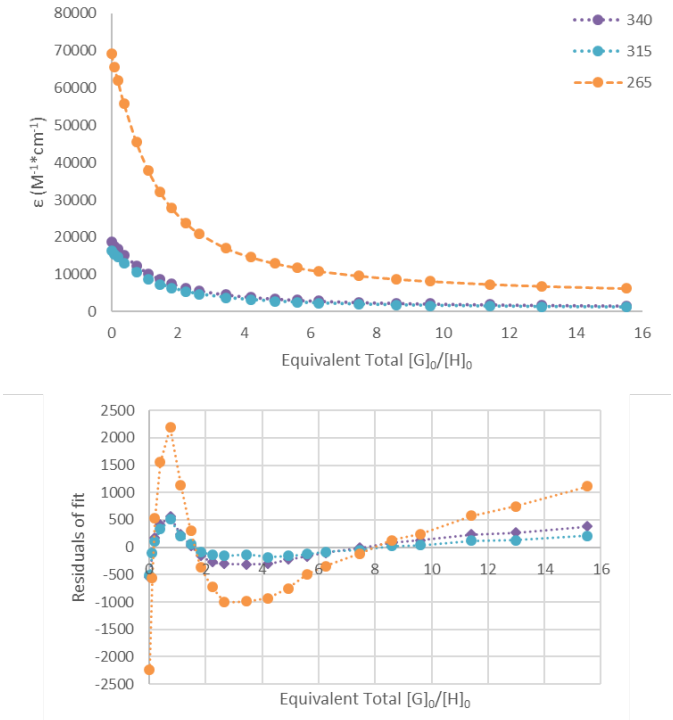

Figure 2. Binding isotherm and Bindfit output for $H_2PO_4^-$ titration with **1**.

Tetrabutylammonium hydrogensulfate with 1. A concentrated solution of **1** (2.25 mg, [R] = 0.313 mM) in 10% DMSO/$CHCl_3$ (10.00 mL) was prepared. A serial dilution was then performed with 800 μL of 0.313 mM solution of **1** diluted to 10.00 mL to yield the stock solution of **1** ([R] = 25.0 μM). A 3.00 mL solution of $TBAHSO_4$ (3.23 mg, [G] = 3.17 mM) was prepared by solvation with the stock solution of **1**. A serial dilution was then performed with 1200 μL of the 3.23 mM solution of $TBAHSO_4$ diluted to 3.00 mL with the stock solution of **1** to yield guest solution ([G] = 12.7 mM). The starting volume in the cuvette was 2.0 mL.

Table 2. Representative titration data for HSO_4^- with **1**.

	Guest (μL)	[**1**] (M)	[HSO_4^-] (M)	Equiv.
1	0	2.50E-05	0.00E+00	0.00
2	5	2.50E-05	3.61E-06	0.14
3	10	2.50E-05	7.21E-06	0.29
4	20	2.50E-05	1.43E-05	0.57
5	40	2.50E-05	2.84E-05	1.13
6	60	2.50E-05	4.21E-05	1.68
7	80	2.50E-05	5.55E-05	2.22
8	100	2.50E-05	6.86E-05	2.74
9	125	2.50E-05	8.46E-05	3.38
10	150	2.50E-05	1.00E-04	4.01
11	200	2.50E-05	1.30E-04	5.20
12	250	2.50E-05	1.59E-04	6.34
13	300	2.50E-05	1.86E-04	7.43
14	350	2.50E-05	2.11E-04	8.46
15	400	2.50E-05	2.36E-04	9.44
16	500	2.50E-05	2.82E-04	11.28
17	600	2.50E-05	3.24E-04	12.96
18	700	2.50E-05	3.62E-04	14.50
19	900	2.50E-05	4.31E-04	17.23
20	1100	2.50E-05	4.90E-04	19.58
21	1500	2.50E-05	5.86E-04	23.42

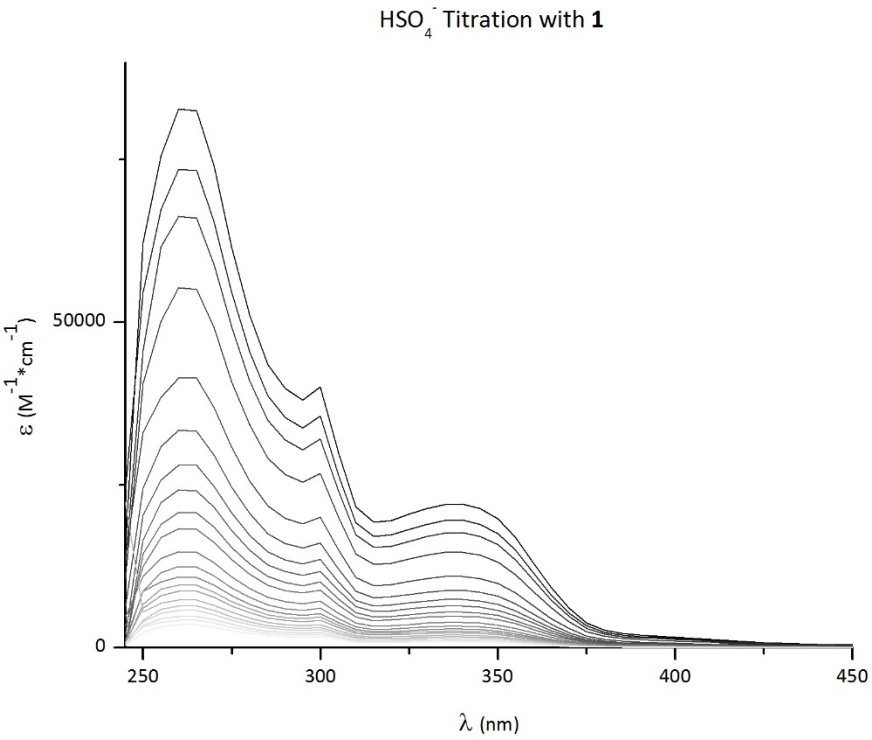

Figure 3. UV-Vis spectra of **1** titrated with HSO_4^- in 10% DMSO/$CHCl_3$.

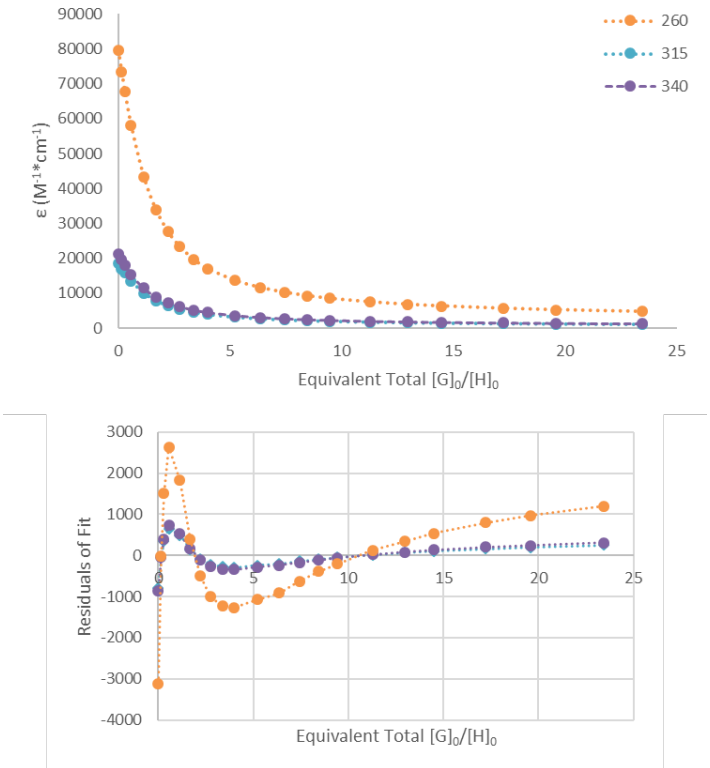

Figure 4. Binding isotherm and Bindfit output for HSO_4^- titration with **1**.

Tetrabutylammonium perchlorate with 1. A concentrated solution of **1** (2.27 mg, [R] = 0.285 mM) in 10% DMSO/$CHCl_3$ (10.00 mL) was prepared. A serial dilution was then performed with 900 μL of 0.285 mM solution of **1** diluted to 10.00 mL to yield the stock solution of **1** ([R] = 25.6 μM). A 3.00 mL solution of $TBAClO_4$ (3.53 mg, [G] = 3.44 mM) was prepared by solvation with the stock solution of **1**. A serial dilution was then performed with 1000 μL of the 3.53 mM solution of $TBAClO_4$ diluted to 3.00 mL with the stock solution of **1** to yield guest solution ([G] = 11.5 mM). The starting volume in the cuvette was 2.0 mL.

Table 3. Representative titration data for ClO_4^- with **1**.

	Guest (μL)	[**1**] (M)	[ClO_4^-] (M)	Equiv.
1	0	2.56E-05	0.00E+00	0.00
2	5	2.56E-05	3.27E-06	0.13
3	10	2.56E-05	6.52E-06	0.25
4	20	2.56E-05	1.30E-05	0.51
5	40	2.56E-05	2.56E-05	1.00
6	60	2.56E-05	3.80E-05	1.48
7	80	2.56E-05	5.01E-05	1.96
8	105	2.56E-05	6.49E-05	2.53
9	125	2.56E-05	7.65E-05	2.98
10	150	2.56E-05	9.06E-05	3.53
11	200	2.56E-05	1.18E-04	4.59
12	250	2.56E-05	1.43E-04	5.59
13	300	2.56E-05	1.68E-04	6.55
14	350	2.56E-05	1.91E-04	7.46
15	400	2.56E-05	2.13E-04	8.33
16	500	2.56E-05	2.55E-04	9.94
17	600	2.56E-05	2.93E-04	11.43
18	700	2.56E-05	3.28E-04	12.79
19	900	2.56E-05	3.90E-04	15.20
20	1100	2.56E-05	4.43E-04	17.27
21	1500	2.56E-05	5.29E-04	20.65

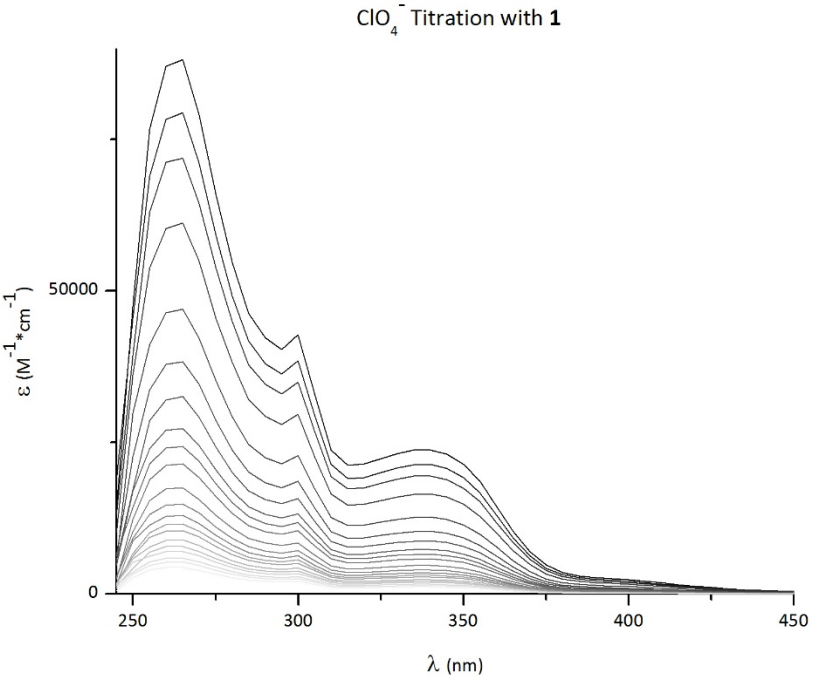

Figure 5. UV-Vis spectra of **1** titrated with ClO_4^- in 10% DMSO/$CHCl_3$.

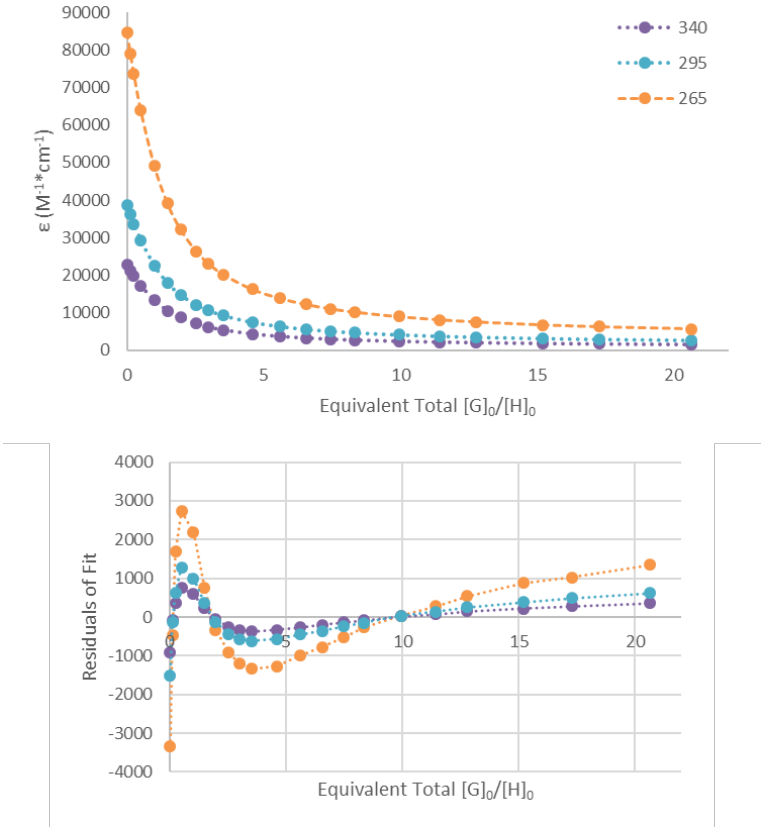

Figure 6. Binding isotherm and Bindfit output for ClO_4^- titration with **1**.

Tetrabutylammonium dihydrogenphosphate with 2. A concentrated solution of **2** (2.23 mg, [R] = 0.310 mM) in 10% DMSO/$CHCl_3$ (10.00 mL) was prepared. A serial dilution was then performed with 800 μL of 0.310 mM solution of **2** diluted to 10.00 mL to yield the stock solution of **2** ([R] = 24.7 μM). A 3.00 mL solution of $TBAH_2PO_4$ (2.02 mg, [G] = 1.97 mM) was prepared by solvation with the stock solution of **2** to prepare guest solution. The starting volume in the cuvette was 2.0 mL.

Table 4. Representative titration data for $H_2PO_4^-$ with **2**.

	Guest (μL)	[**2**] (M)	[$H_2PO_4^-$] (M)	Equiv.
1	0	2.48E-05	0.00E+00	0.00
2	5	2.48E-05	5.61E-06	0.23
3	10	2.48E-05	1.12E-05	0.45
4	20	2.48E-05	2.23E-05	0.90
5	40	2.48E-05	4.40E-05	1.78
6	60	2.48E-05	6.53E-05	2.64
7	80	2.48E-05	8.62E-05	3.48
8	100	2.48E-05	1.07E-04	4.30
9	125	2.48E-05	1.31E-04	5.30
10	150	2.48E-05	1.56E-04	6.28
11	200	2.48E-05	2.02E-04	8.16
12	250	2.48E-05	2.46E-04	9.94
13	300	2.48E-05	2.88E-04	11.64
14	350	2.48E-05	3.28E-04	13.25
15	400	2.48E-05	3.67E-04	14.80
16	500	2.48E-05	4.38E-04	17.67
17	600	2.48E-05	5.03E-04	20.30
18	700	2.48E-05	5.63E-04	22.72
19	900	2.48E-05	6.69E-04	27.01
20	1100	2.48E-05	7.61E-04	30.69
21	1500	2.48E-05	9.10E-04	36.70

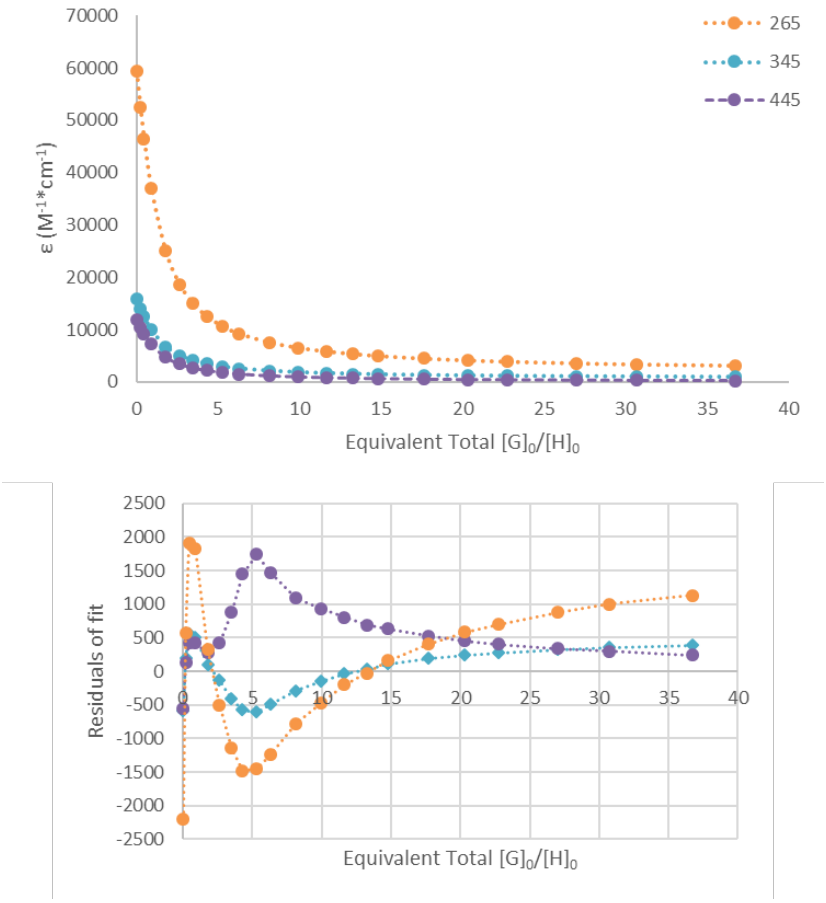

Figure 7. Binding isotherm and Bindfit output for $H_2PO_4^-$ titration with **2**.

Tetrabutylammonium hydrogensulfate with 2. A concentrated solution of **2** (2.58 mg, [R] = 0.358 mM) in 10% DMSO/$CHCl_3$ (10.00 mL) was prepared. A serial dilution was then performed with 700 µL of 0.358 mM solution of **2** diluted to 10.00 mL to yield the stock solution of **2** ([R] = 25.1 µM). A 3.00 mL solution of $TBAHSO_4$ (2.27 mg, [G] = 1.34 mM) was prepared by solvation with the stock solution of **2** to yield the guest solution. The starting volume in the cuvette was 2.0 mL.

Table 5. Representative titration data for HSO_4^- with **2**.

	Guest (μL)	[**2**] (M)	[HSO_4^-] (M)	Equiv.
1	0	2.51E-05	0.00E+00	0.00
2	5	2.51E-05	3.81E-06	0.15
3	10	2.51E-05	7.60E-06	0.30
4	15	2.51E-05	1.14E-05	0.45
5	35	2.51E-05	2.62E-05	1.05
6	55	2.51E-05	4.07E-05	1.62
7	75	2.51E-05	5.50E-05	2.19
8	95	2.51E-05	6.89E-05	2.74
9	115	2.51E-05	8.25E-05	3.29
10	140	2.51E-05	9.90E-05	3.95
11	165	2.51E-05	1.15E-04	4.59
12	215	2.51E-05	1.46E-04	5.83
13	265	2.51E-05	1.76E-04	7.01
14	315	2.51E-05	2.04E-04	8.13
15	365	2.51E-05	2.31E-04	9.20
16	415	2.51E-05	2.56E-04	10.22
17	515	2.51E-05	3.04E-04	12.12
18	615	2.51E-05	3.48E-04	13.86
19	715	2.51E-05	3.88E-04	15.46
20	915	2.51E-05	4.59E-04	18.30
21	1115	2.51E-05	5.20E-04	20.74

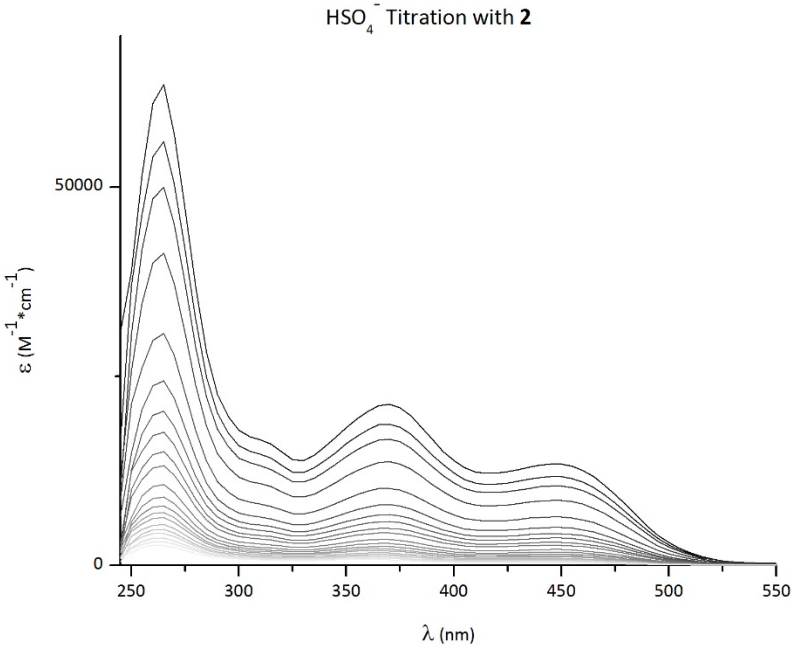

Figure 8. UV-Vis spectra of **2** titrated with HSO_4^- in 10% DMSO/$CHCl_3$.

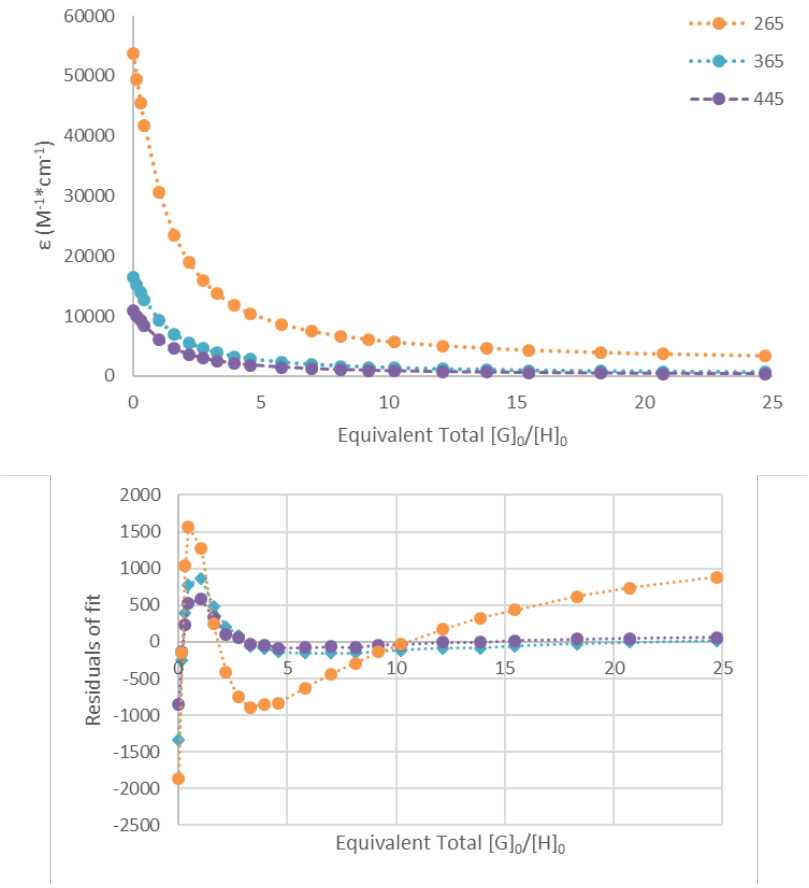

Figure 9. Binding isotherm and Bindfit output for HSO_4^- titration with **2**.

Tetrabutylammonium perchlorate with 2. A concentrated solution of **2** (2.58 mg, [R] = 0.358 mM) in 10% DMSO/$CHCl_3$ (10.00 mL) was prepared. A serial dilution was then performed with 6500 µL of 0.358 mM solution of **2** diluted to 10.00 mL to yield the stock solution of **2** ([R] = 23.3 µM). A 3.00 mL solution of $TBAClO_4$ (2.79 mg, [G] = 1.63 mM) was prepared by solvation with the stock solution of **2** to yield the guest solution. The starting volume in the cuvette was 2.0 mL.

Table 6. Representative titration data for ClO_4^- with **2**.

	Guest (μL)	[**2**] (M)	[ClO_4^-] (M)	Equiv.
1	0	2.33E-05	0.00E+00	0.00
2	5	2.33E-05	4.65E-06	0.20
3	10	2.33E-05	9.27E-06	0.40
4	20	2.33E-05	1.84E-05	0.79
5	40	2.33E-05	3.65E-05	1.57
6	60	2.33E-05	5.41E-05	2.32
7	85	2.33E-05	7.56E-05	3.25
8	100	2.33E-05	8.82E-05	3.79
9	125	2.33E-05	1.09E-04	4.67
10	150	2.33E-05	1.29E-04	5.53
11	200	2.33E-05	1.67E-04	7.19
12	250	2.33E-05	2.04E-04	8.76
13	300	2.33E-05	2.39E-04	10.25
14	350	2.33E-05	2.72E-04	11.68
15	450	2.33E-05	3.34E-04	14.33
16	550	2.33E-05	3.90E-04	16.75
17	700	2.33E-05	4.66E-04	20.02
18	900	2.33E-05	5.54E-04	23.79
19	1100	2.33E-05	6.30E-04	27.04
20	1400	2.33E-05	7.25E-04	31.14
21	1800	2.33E-05	8.27E-04	35.52

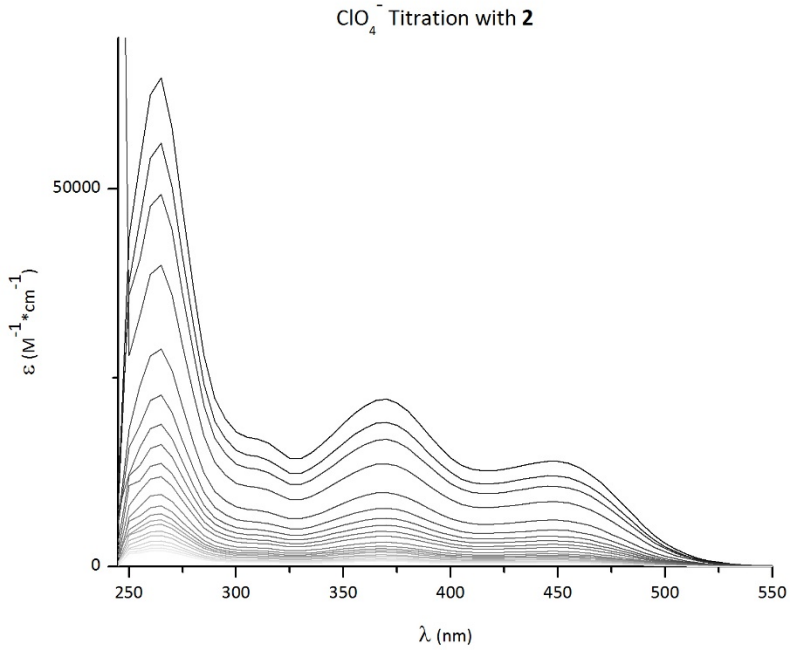

Figure 10. UV-Vis spectra of **2** titrated with ClO_4^- in 10% DMSO/$CHCl_3$.

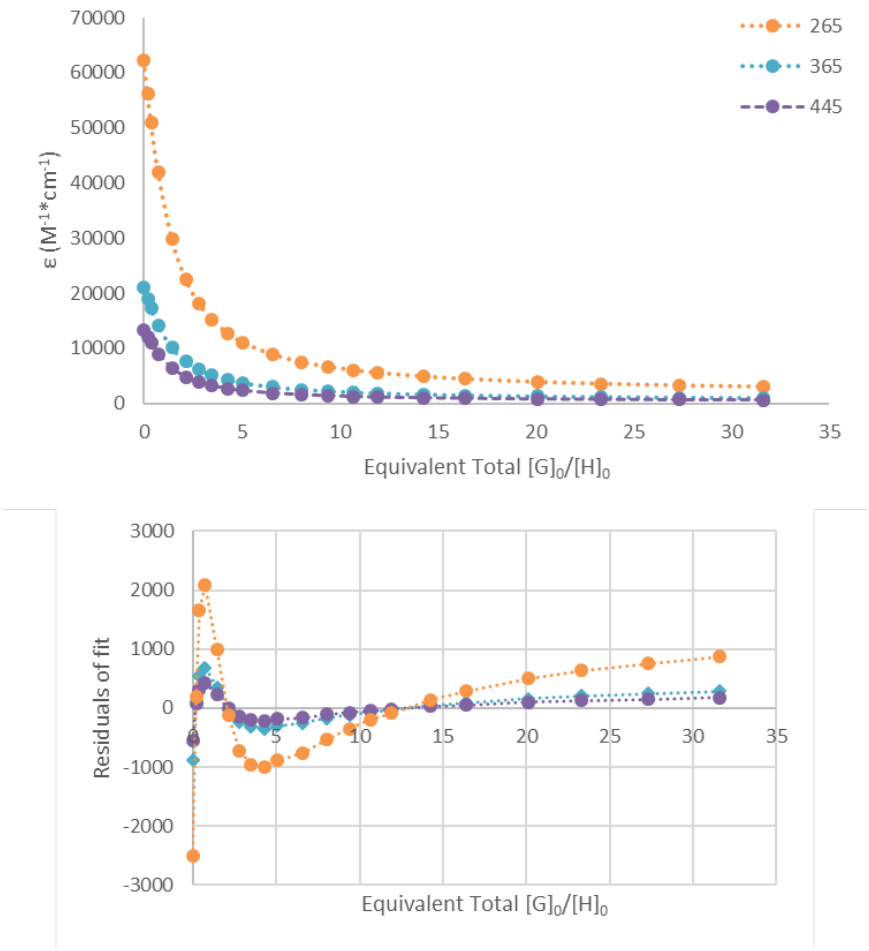

Figure 11. Binding isotherm and Bindfit output for ClO_4^- titration with **2**.

Tetrabutylammonium dihydrogenphosphate with 3. A concentrated solution of **3** (2.05 mg, [R] = 0.257 mM) in 10% DMSO/$CHCl_3$ (10.00 mL) was prepared. A serial dilution was then performed with 975 µL of 0.257 mM solution of **3** diluted to 10.00 mL to yield the stock solution of **3** ([R] = 25.1 µM). A 3.00 mL solution of $TBAH_2PO_4$ (2.46 mg, [G] = 2.42 mM) was prepared by solvation with the stock solution of **3**. A serial dilution was then performed with 500 µL of the 2.42 mM solution of $TBAH_2PO_4$ diluted to 3.00 mL with the stock solution of **3** to yield guest solution ([G] = 4.03 mM). The starting volume in the cuvette was 2.0 mL.

Table 7. Representative titration data for $H_2PO_4^-$ with **3**.

	Guest (µL)	[**3**] (M)	[$H_2PO_4^-$] (M)	Equiv.
1	0	2.51E-05	0.00E+00	0.00
2	5	2.51E-05	1.15E-06	0.05
3	10	2.51E-05	2.29E-06	0.09
4	20	2.51E-05	4.55E-06	0.18
5	40	2.51E-05	9.00E-06	0.36
6	60	2.51E-05	1.33E-05	0.53
7	80	2.51E-05	1.76E-05	0.70
8	100	2.51E-05	2.18E-05	0.87
9	125	2.51E-05	2.68E-05	1.07
10	150	2.51E-05	3.18E-05	1.27
11	200	2.51E-05	4.13E-05	1.65
12	250	2.51E-05	5.03E-05	2.01
13	300	2.51E-05	5.89E-05	2.35
14	350	2.51E-05	6.71E-05	2.68
15	400	2.51E-05	7.49E-05	2.99
16	500	2.51E-05	8.95E-05	3.57
17	600	2.51E-05	1.03E-04	4.10
18	700	2.51E-05	1.15E-04	4.59
19	900	2.51E-05	1.37E-04	5.45
20	1100	2.51E-05	1.55E-04	6.20
21	1500	2.51E-05	1.86E-04	7.41

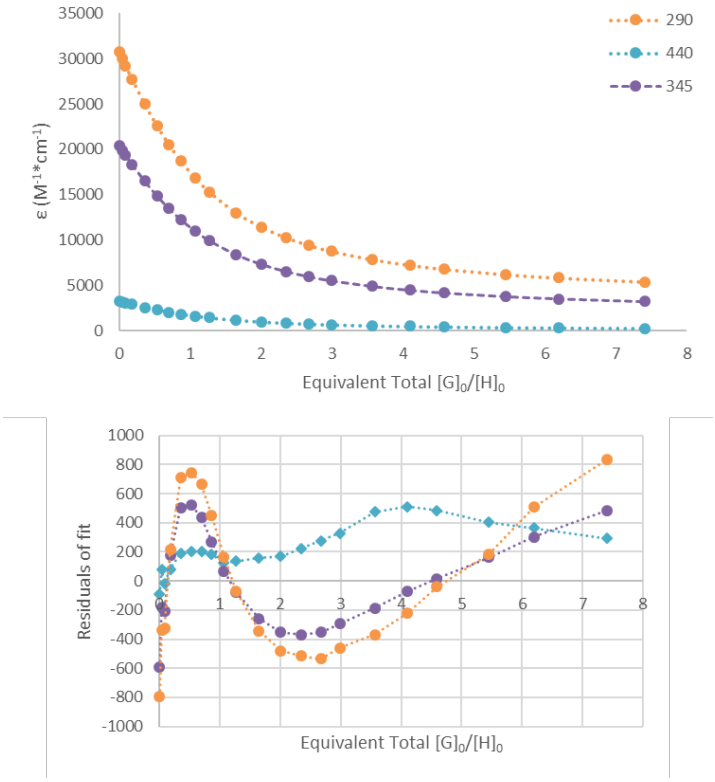

Figure 12. Binding isotherm and Bindfit output for $H_2PO_4^-$ titration with **3**.

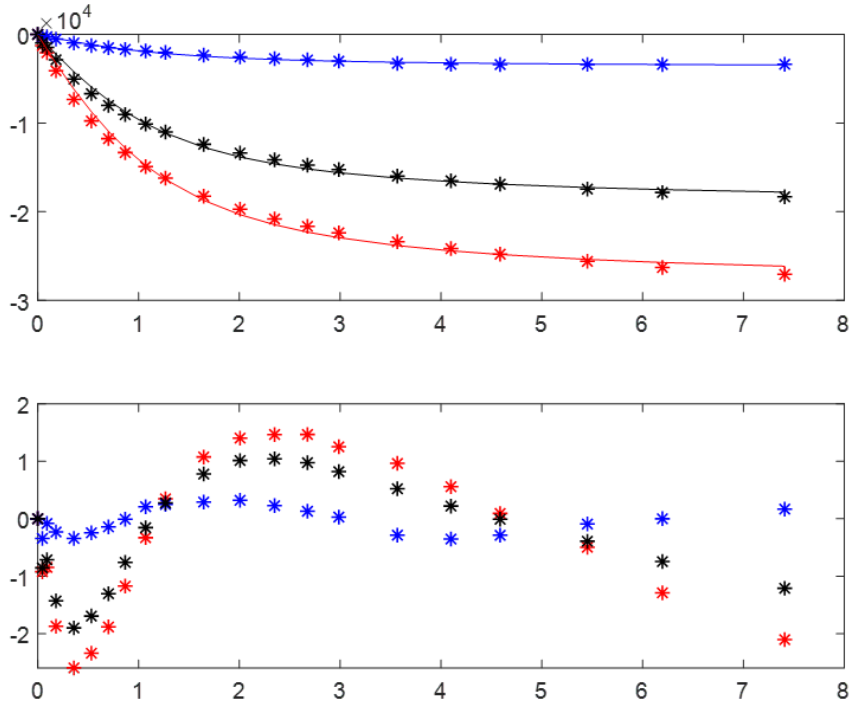

Figure 13. MatLab fit of binding isotherm for $H_2PO_4^-$ titration with **3**.

Tetrabutylammonium hydrogensulfate with 3. A concentrated solution of **3** (2.27 mg, [R] = 0.285 mM) in 10% DMSO/$CHCl_3$ (10.00 mL) was prepared. A serial dilution was then performed with 800 µL of 0.285 mM solution of **3** diluted to 10.00 mL to yield the stock solution of **3** ([R] = 22.8 µM). A 3.00 mL solution of $TBAHSO_4$ (2.87 mg, [G] = 2.82 mM) was prepared by solvation with the stock solution of **3**. A serial dilution was then performed with 1000 µL of the 2.82 mM solution of $TBAHSO_4$ diluted to 3.00 mL with the stock solution of **3** to yield guest solution ([G] = 9.39 mM). The starting volume in the cuvette was 2.0 mL.

Table 8. Representative titration data for HSO_4^- with **3**.

	Guest (μL)	[**3**] (M)	[HSO_4^-] (M)	Equiv.
1	0	2.28E-05	0.00E+00	0.00
2	5	2.28E-05	2.68E-06	0.12
3	10	2.28E-05	5.34E-06	0.23
4	20	2.28E-05	1.06E-05	0.47
5	40	2.28E-05	2.10E-05	0.92
6	60	2.28E-05	3.11E-05	1.37
7	80	2.28E-05	4.11E-05	1.80
8	105	2.28E-05	5.32E-05	2.33
9	125	2.28E-05	6.26E-05	2.75
10	150	2.28E-05	7.41E-05	3.25
11	200	2.28E-05	9.63E-05	4.23
12	250	2.28E-05	1.17E-04	5.15
13	300	2.28E-05	1.37E-04	6.03
14	350	2.28E-05	1.57E-04	6.87
15	400	2.28E-05	1.75E-04	7.67
16	500	2.28E-05	2.09E-04	9.16
17	600	2.28E-05	2.40E-04	10.52
18	700	2.28E-05	2.68E-04	11.78
19	900	2.28E-05	3.19E-04	14.00
20	1100	2.28E-05	3.63E-04	15.91
21	1500	2.28E-05	4.33E-04	19.02

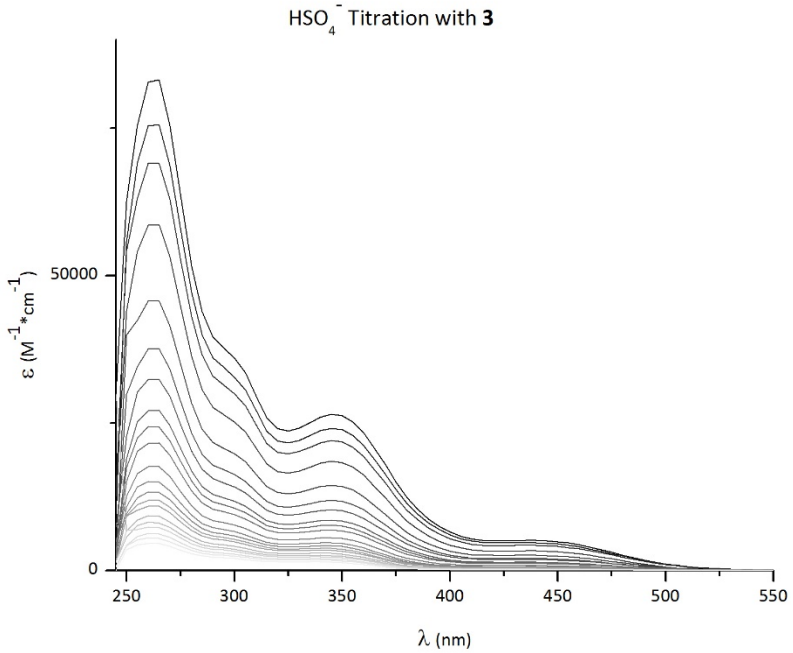

Figure 14. UV-Vis spectra of **3** titrated with HSO_4^- in 10% DMSO/$CHCl_3$.

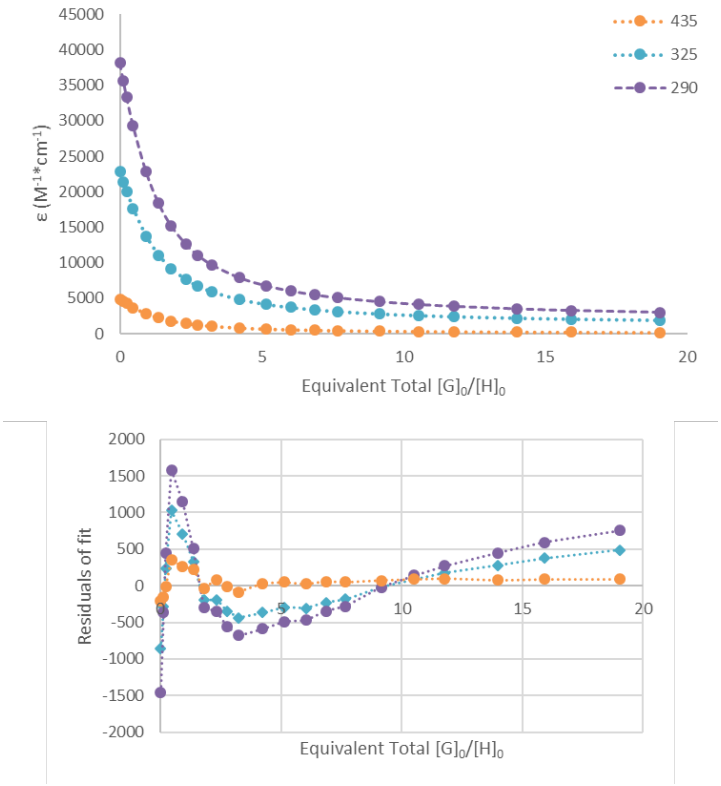

Figure 15. Binding isotherm and Bindfit output for HSO_4^- titration with **3**.

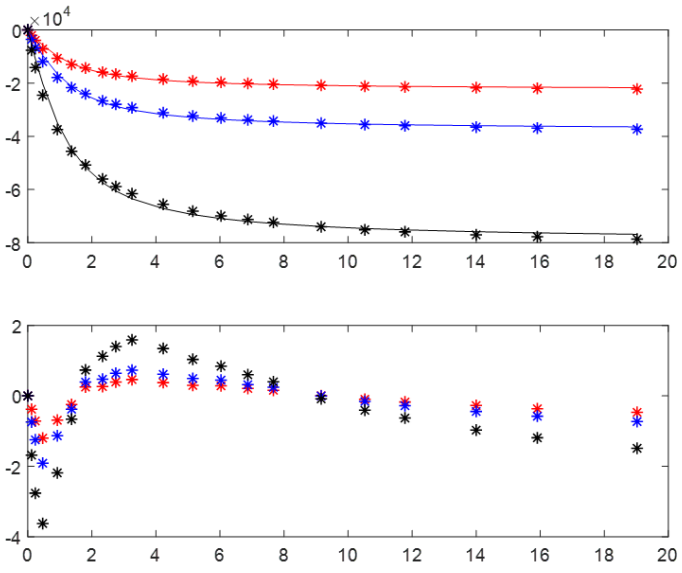

Figure 16. MatLab fit of binding isotherm for HSO_4^- titration with **3**.

Tetrabutylammonium perchlorate with 3. A concentrated solution of **3** (2.27 mg, [R] = 0.285 mM) in 10% DMSO/$CHCl_3$ (10.00 mL) was prepared. A serial dilution was then performed with 900 μL of 0.285 mM solution of **3** diluted to 10.00 mL to yield the stock solution of **3** ([R] = 25.6 μM). A 2.00 mL solution of $TBAClO_4$ (3.50 mg, [G] = 5.12 mM) was prepared by solvation with the stock solution of **3**. A serial dilution was then performed with 700 μL of the 5.12 mM solution of $TBAClO_4$ diluted to 3.00 mL with the stock solution of **3** to yield guest solution ([G] = 11.9 mM). The starting volume in the cuvette was 2.0 mL.

Table 9. Representative titration data for ClO_4^- with **3**.

	Guest (μL)	[**3**] (M)	[ClO_4^-] (M)	Equiv.
1	0	2.56E-05	0.00E+00	0.00
2	5	2.56E-05	3.40E-06	0.13
3	10	2.56E-05	6.79E-06	0.26
4	20	2.56E-05	1.35E-05	0.53
5	40	2.56E-05	2.67E-05	1.04
6	60	2.56E-05	3.96E-05	1.54
7	80	2.56E-05	5.22E-05	2.04
8	105	2.56E-05	6.76E-05	2.64
9	125	2.56E-05	7.96E-05	3.11
10	150	2.56E-05	9.43E-05	3.68
11	200	2.56E-05	1.22E-04	4.78
12	250	2.56E-05	1.49E-04	5.82
13	300	2.56E-05	1.75E-04	6.82
14	350	2.56E-05	1.99E-04	7.76
15	400	2.56E-05	2.22E-04	8.67
16	500	2.56E-05	2.65E-04	10.35
17	600	2.56E-05	3.05E-04	11.89
18	700	2.56E-05	3.41E-04	13.31
19	900	2.56E-05	4.06E-04	15.82
20	1100	2.56E-05	4.61E-04	17.98
21	1500	2.56E-05	5.51E-04	21.50

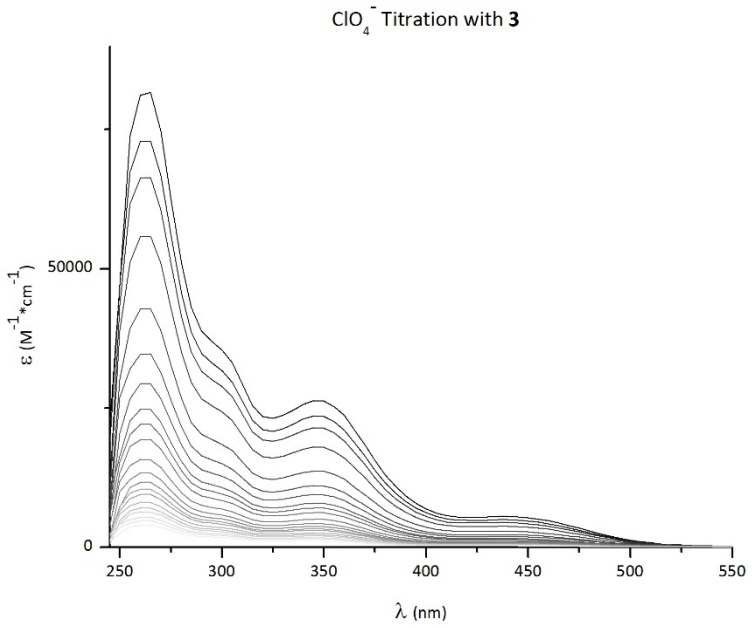

Figure 17. UV-Vis spectra of **3** titrated with ClO_4^- in 10% DMSO/$CHCl_3$.

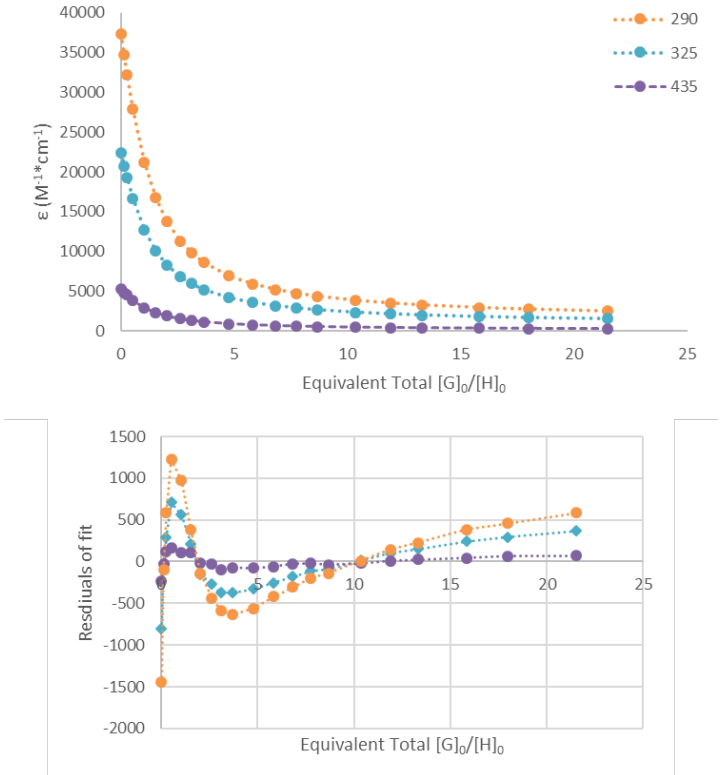

Figure 18. Binding isotherm and Bindfit output for ClO_4^- titration with **3**.

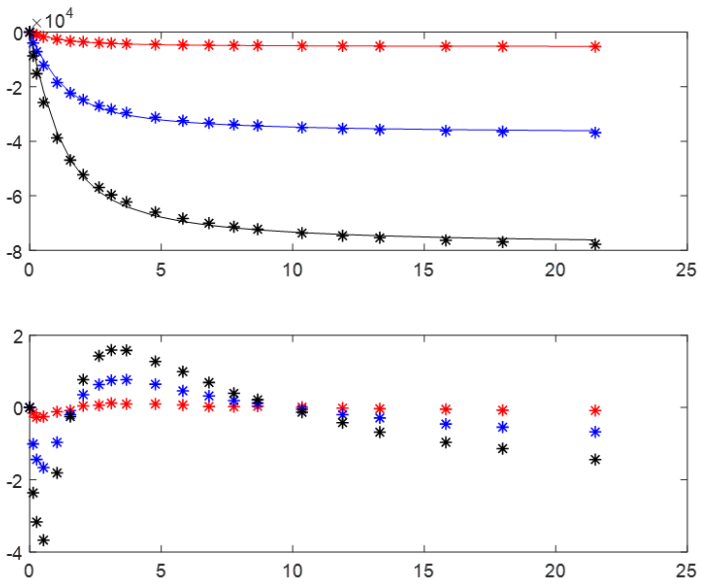

Figure 19. MatLab fit of binding isotherm for ClO_4^- titration with **3**.

Acetonitrile titrations

Tetrabutylammonium dihydrogenphosphate with 1. A concentrated solution of **1** (2.43 mg, [R] = 0.338 mM) in CH_3CN (10.00 mL) was prepared. A serial dilution was then performed with 600 µL of 0.338 mM solution of **1** diluted to 10.00 mL to yield the stock solution of **1** ([R] = 20.3 µM). A 3.00 mL solution of $TBAH_2PO_4$ (2.80 mg, [G] = 2.75 mM) was prepared by solvation with the stock solution of **1**. A serial dilution was then performed with 350 µL of the 2.75 mM solution of $TBAH_2PO_4$ diluted to 2.00 mL with the stock solution of **1** to yield guest solution ([G] = 0.481 mM). The starting volume in the cuvette was 2.0 mL.

Table 10. Representative titration data for $H_2PO_4^-$ with **1**.

	Guest (μL)	[**1**] (M)	[$H_2PO_4^-$] (M)	Equiv.
1	0	2.03E-05	0.00E+00	0.00
2	5	2.03E-05	1.37E-06	0.07
3	10	2.03E-05	2.73E-06	0.13
4	20	2.03E-05	5.44E-06	0.27
5	40	2.03E-05	1.08E-05	0.53
6	60	2.03E-05	1.60E-05	0.79
7	80	2.03E-05	2.10E-05	1.04
8	100	2.03E-05	2.60E-05	1.28
9	125	2.03E-05	3.21E-05	1.58
10	150	2.03E-05	3.80E-05	1.88
11	200	2.03E-05	4.94E-05	2.44
12	250	2.03E-05	6.01E-05	2.97
13	300	2.03E-05	7.04E-05	3.48
14	350	2.03E-05	8.02E-05	3.96
15	400	2.03E-05	8.95E-05	4.42
16	500	2.03E-05	1.07E-04	5.28
17	600	2.03E-05	1.23E-04	6.07
18	700	2.03E-05	1.37E-04	6.79
19	900	2.03E-05	1.63E-04	8.07
20	1100	2.03E-05	1.86E-04	9.17
21	1500	2.03E-05	2.22E-04	10.97

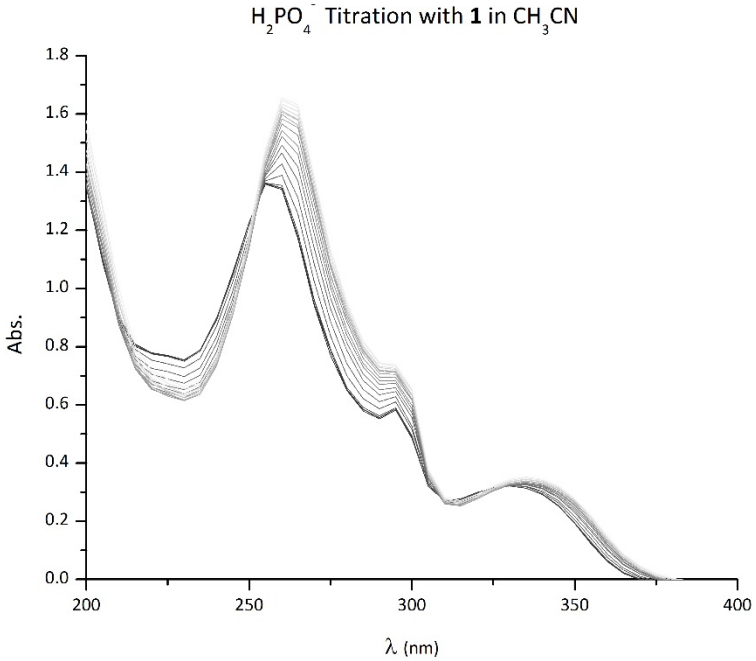

Figure 20. UV-Vis spectra of **1** titrated with $H_2PO_4^-$ in CH_3CN.

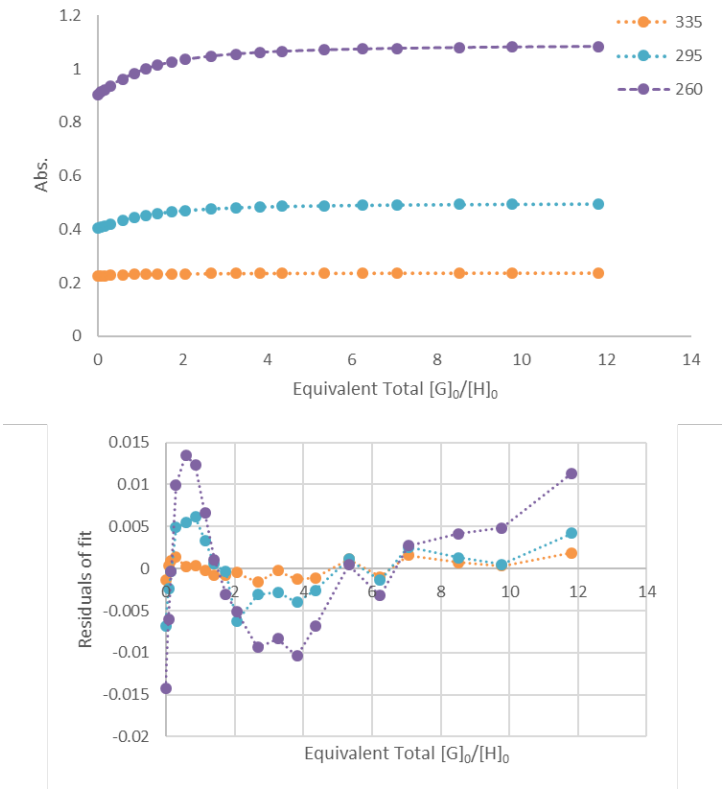

Figure 21. Binding isotherm and Bindfit output for $H_2PO_4^-$ titration with **1**.

Tetrabutylammonium hydrogensulfate with 1. A concentrated solution of **1** (2.43 mg, [R] = 0.338 mM) in CH_3CN (10.00 mL) was prepared. A serial dilution was then performed with 500 µL of 0.338 mM solution of **1** diluted to 10.00 mL to yield the stock solution of **1** ([R] = 16.9 µM). A 2.015 mL solution of $TBAHSO_4$ (6.54 mg, [G] = 9.56 mM) was prepared by solvation with the stock solution of **1**. A serial dilution was then performed with 1400 µL of the 9.56 mM solution of $TBAHSO_4$ diluted to 3.046 mL with the stock solution of **1** to yield guest solution ([G] = 4.39 mM). The starting volume in the cuvette was 2.0 mL.

Table 11. Representative titration data for HSO_4^- with **1**.

	Guest (μL)	[**1**] (M)	[HSO_4^-] (M)	Equiv.
1	0	1.69E-05	0.00E+00	0.00
2	5	1.69E-05	1.25E-05	0.74
3	10	1.69E-05	2.50E-05	1.48
4	20	1.69E-05	4.97E-05	2.94
5	40	1.69E-05	9.82E-05	5.82
6	60	1.69E-05	1.46E-04	8.63
7	80	1.69E-05	1.92E-04	11.38
8	100	1.69E-05	2.38E-04	14.07
9	125	1.69E-05	2.93E-04	17.36
10	150	1.69E-05	3.47E-04	20.56
11	200	1.69E-05	4.51E-04	26.71
12	250	1.69E-05	5.49E-04	32.55
13	300	1.69E-05	6.43E-04	38.11
14	350	1.69E-05	7.32E-04	43.40
15	400	1.69E-05	8.18E-04	48.44
16	500	1.69E-05	9.77E-04	57.86
17	600	1.69E-05	1.12E-03	66.48
18	700	1.69E-05	1.26E-03	74.40
19	900	1.69E-05	1.49E-03	88.43
20	1100	1.69E-05	1.70E-03	100.50
21	1500	1.69E-05	2.03E-03	120.18
22	1900	1.69E-05	2.29E-03	135.54
23	2300	1.69E-05	2.50E-03	147.87

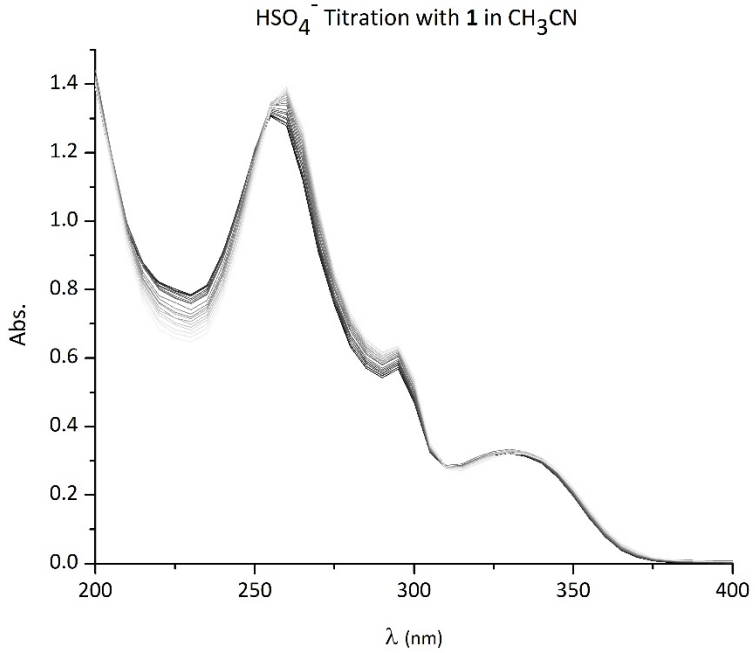

Figure 22. UV-Vis spectra of **1** titrated with HSO_4^- in CH_3CN.

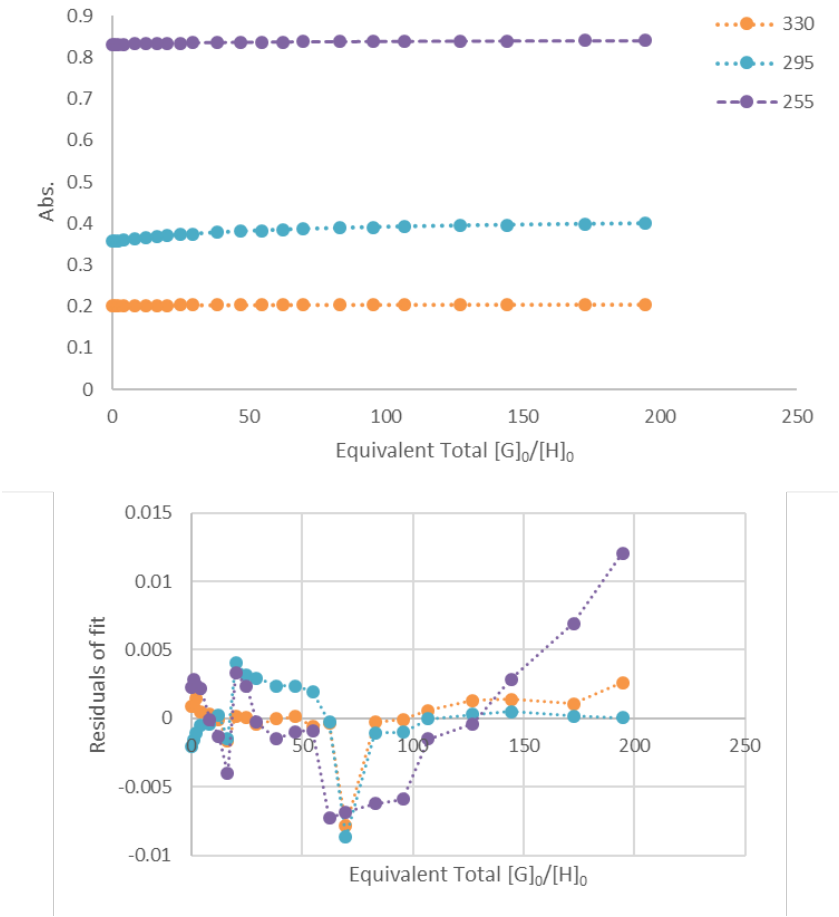

Figure 23. Binding isotherm and Bindfit output for HSO_4^- titration with **1**.

Tetrabutylammonium perchlorate with 1. A concentrated solution of **1** (2.43 mg, [R] = 0.338 mM) in CH_3CN (10.00 mL) was prepared. A serial dilution was then performed with 300 µL of 0.338 mM solution of **1** diluted to 10.00 mL to yield the stock solution of **1** ([R] = 10.1 µM). A 2.00 mL solution of $TBAClO_4$ (6.53 mg, [G] = 9.55 mM) was prepared by solvation with the stock solution of **1**. A serial dilution was then performed with 1300 µL of the 9.55 mM solution of $TBAClO_4$ diluted to 3.00 mL with the stock solution of **1** to yield guest solution ([G] = 4.14 mM). The starting volume in the cuvette was 2.0 mL.

Table 12. Representative titration data for ClO_4^- with **1**.

	Guest (μL)	[**1**] (M)	[ClO_4^-] (M)	Equiv.
1	0	1.01E-05	0.00E+00	0.00
2	5	1.01E-05	1.18E-05	1.16
3	10	1.01E-05	2.35E-05	2.32
4	20	1.01E-05	4.68E-05	4.62
5	40	1.01E-05	9.25E-05	9.13
6	60	1.01E-05	1.37E-04	13.55
7	80	1.01E-05	1.81E-04	17.86
8	100	1.01E-05	2.24E-04	22.09
9	125	1.01E-05	2.76E-04	27.24
10	150	1.01E-05	3.27E-04	32.26
11	200	1.01E-05	4.24E-04	41.91
12	250	1.01E-05	5.17E-04	51.08
13	300	1.01E-05	6.06E-04	59.80
14	350	1.01E-05	6.90E-04	68.11
15	400	1.01E-05	7.70E-04	76.02
16	500	1.01E-05	9.20E-04	90.81
17	600	1.01E-05	1.06E-03	104.33
18	700	1.01E-05	1.18E-03	116.75
19	900	1.01E-05	1.41E-03	138.78
20	1100	1.01E-05	1.60E-03	157.72
21	1500	1.01E-05	1.91E-03	188.60

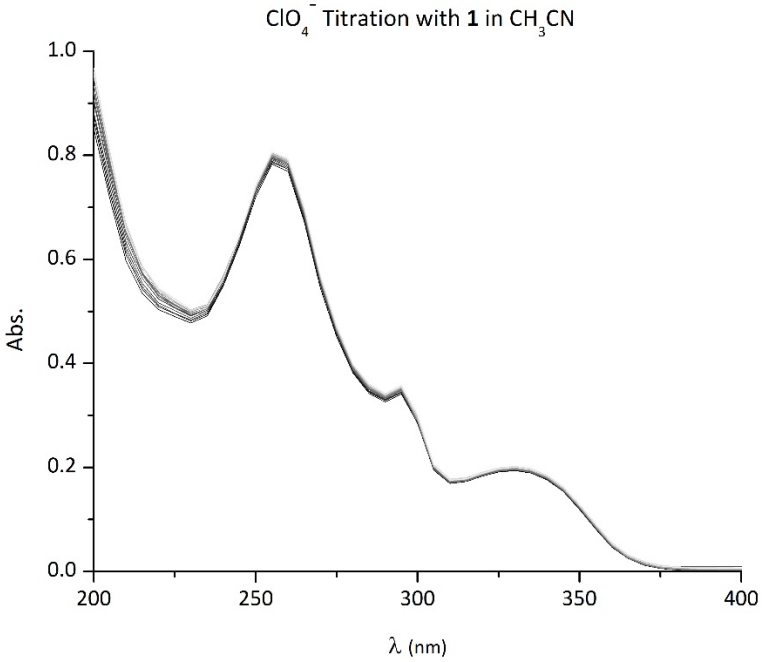

Figure 24. UV-Vis spectra of **1** titrated with ClO_4^- in CH_3CN.

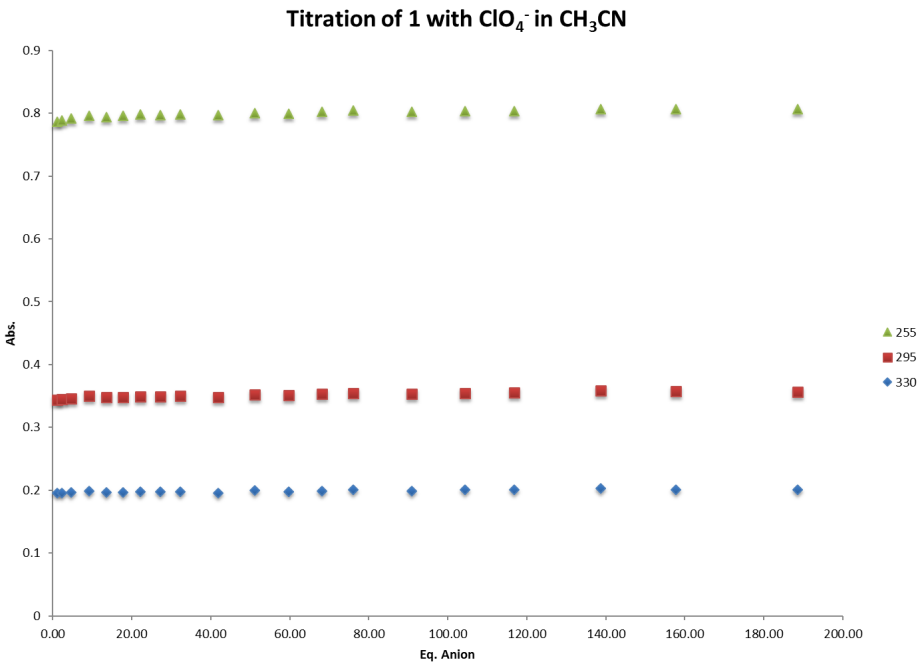

Figure 25. Binding isotherm ClO_4^- titration with **1**. The change in absorbance is negligible. Fitting the data across a series of titrations with ClO_4^- in CH_3CN resulted in an error for K_a value.

^{1}H NMR titrations

Tetrabutylammonium dihydrogenphosphate with 1. A concentrated solution of 1 (2.09 mg, [R] = 0.968 mM) in 10% d_6-DMSO/$CDCl_3$ (3.00 mL) was prepared to yield the stock solution of **1**. This solution (2.34 mL) was used in the dilution of $TBAH_2PO_4$ guest solution (12.84 mg, [G] = 16.2 mM). The remaining stock solution (0.600 mL) was used as the starting volume in the NMR tube.

Table 13. Representative titration data for $H_2PO_4^-$ with **1**.

	Guest (μL)	[**1**] (M)	[$H_2PO_4^-$] (M)	Equiv.	H^c δ (ppm)	H^d δ (ppm)	H^a δ (ppm)	H^b δ (ppm)
1	0	9.68E-04	0.00E+00	0.00	8.635	8.592	8.024	7.714
2	5	9.68E-04	1.34E-04	0.14	8.829	8.575	8.125	7.819
3	10	9.68E-04	2.65E-04	0.27	9.140	8.551	8.274	7.993
4	15	9.68E-04	3.94E-04	0.41	9.444	8.529	8.409	8.152
5	20	9.68E-04	5.21E-04	0.54	9.705	8.510	8.484	8.307
6	25	9.68E-04	6.47E-04	0.67	9.927	8.496	8.626	8.419
7	30	9.68E-04	7.70E-04	0.80	10.099	8.483	8.693	8.517
8	35	9.68E-04	8.91E-04	0.92	10.215	8.472	8.733	8.581
9	40	9.68E-04	1.01E-03	1.04	10.317	8.464	8.773	8.642
10	50	9.68E-04	1.24E-03	1.28	10.455	8.453	8.824	8.708
11	60	9.68E-04	1.47E-03	1.52	10.558	8.446	8.851	8.774
12	80	9.68E-04	1.90E-03	1.97	10.639	8.436	8.877	8.811
13	100	9.68E-04	2.31E-03	2.39	10.688	8.430	8.890	8.838
14	150	9.68E-04	3.23E-03	3.34	10.801	8.442	8.902	8.902
15	200	9.68E-04	4.04E-03	4.18	10.847	8.418	8.905	8.905
16	300	9.68E-04	5.39E-03	5.57	10.831	8.415	8.904	8.904
17	400	9.68E-04	6.47E-03	6.68	10.852	8.412	8.904	8.904
18	600	9.68E-04	8.08E-03	8.35	10.925	8.411	8.906	8.906

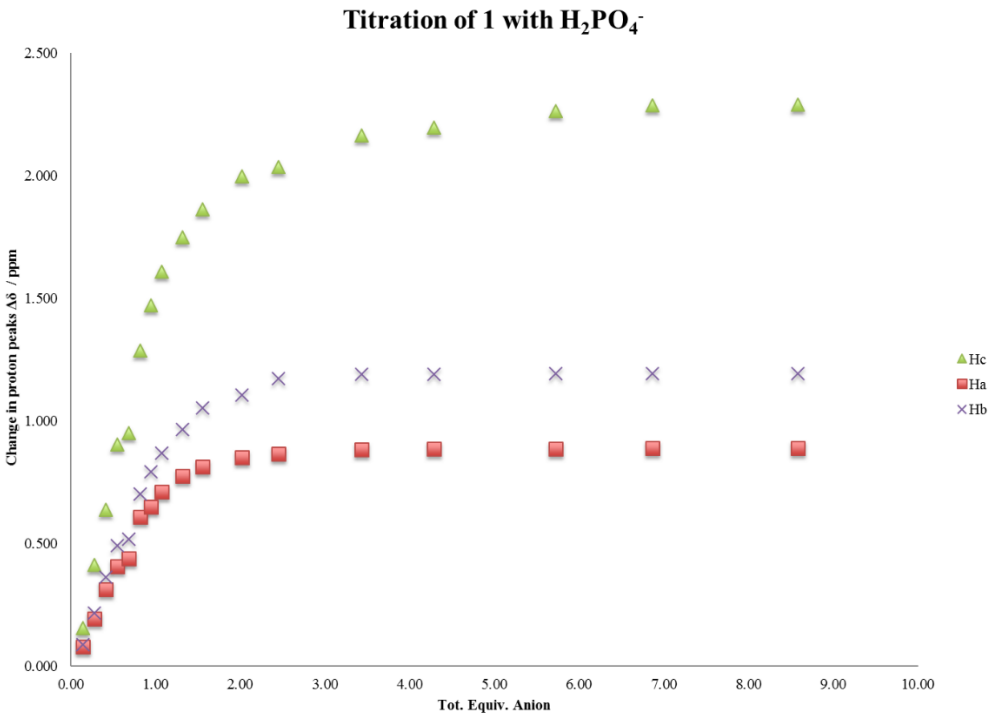

Figure 26. Binding isotherm for $H_2PO_4^-$ titration with **1** in 10% d_6-DMSO/$CDCl_3$ by ^1H NMR.

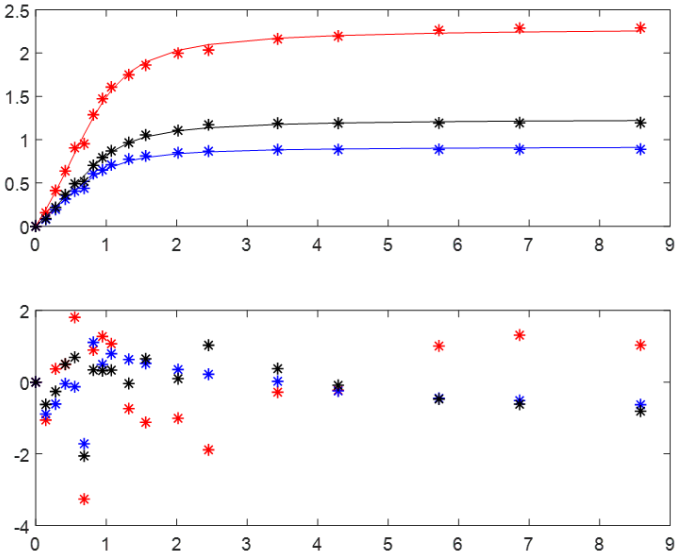

Figure 27. MatLab fit to a 2:1 model of the binding isotherm for $H_2PO_4^-$ titration with **1**.

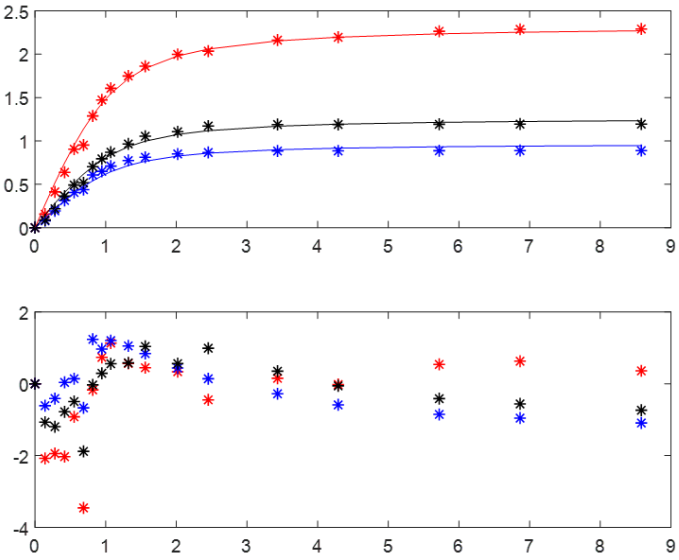

Figure 28. MatLab fit to a 1:1 model of the binding isotherm for $H_2PO_4^-$ titration with **1**. Improper fitting model due to lack of randomness of residuals.

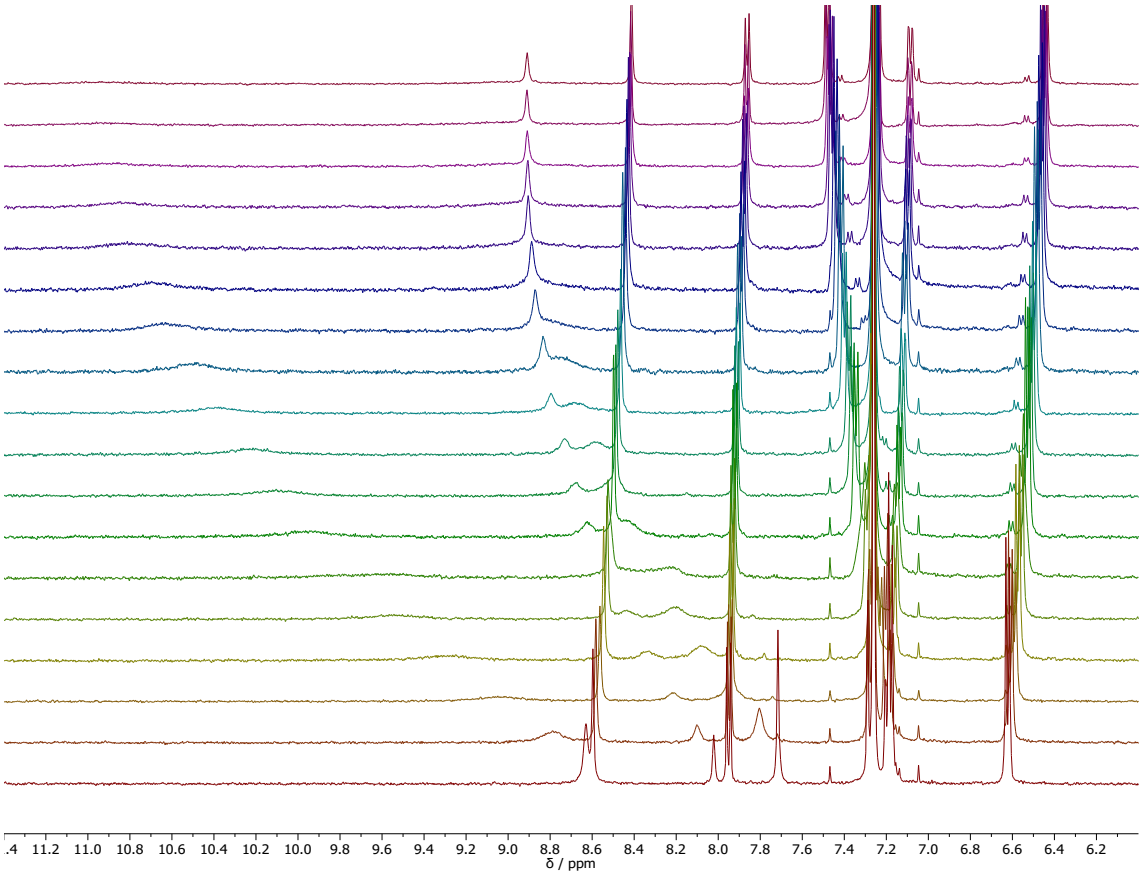

Figure 29. ^{1}H NMR spectra of $H_2PO_4^-$ titration with **1**.

Tetrabutylamamonium bromide with 1. A stock solution of **1** (2.19 mg, [R] = 1.01 mM) in 10% *d*$_6$-DMSO/$CDCl_3$ (3.00 mL) was prepared. This solution (2.34 mL) was used in the dilution of TBABr guest solution (28.1 mg, [G] = 37.3 mM). The remaining stock solution (0.600 mL) was used as the starting volume in the NMR tube.

Table 14. Representative titration data for Br^- with **1**.

	Guest (μL)	[**1**] (M)	[Br^-] (M)	Equiv.	H^c δ (ppm)	H^d δ (ppm)	H^b δ (ppm)	H^a δ (ppm)
1	0	1.01E-03	0.00E+00	0.00	8.628	8.596	8.018	7.714
2	5	1.01E-03	3.08E-04	0.30	8.657	8.592	8.056	7.717
3	10	1.01E-03	6.12E-04	0.60	8.681	8.589	8.089	7.717
4	15	1.01E-03	9.10E-04	0.90	8.701	8.584	8.116	7.718
5	20	1.01E-03	1.20E-03	1.19	8.723	8.583	8.145	7.719
6	25	1.01E-03	1.49E-03	1.47	8.744	8.580	8.174	7.720
7	30	1.01E-03	1.78E-03	1.75	8.763	8.578	8.198	7.721
8	35	1.01E-03	2.06E-03	2.03	8.780	8.575	8.220	7.722
9	40	1.01E-03	2.33E-03	2.30	8.795	8.573	8.240	7.223
10	50	1.01E-03	2.87E-03	2.83	8.821	8.569	8.276	7.726
11	60	1.01E-03	3.39E-03	3.34	8.845	8.566	8.308	7.728
12	80	1.01E-03	4.39E-03	4.33	8.885	8.561	8.363	7.731
13	100	1.01E-03	5.33E-03	5.26	8.920	8.559	8.411	7.733
14	150	1.01E-03	7.46E-03	7.36	8.985	8.550	8.506	7.739
15	200	1.01E-03	9.33E-03	9.20	9.031	8.546	8.565	7.743
16	300	1.01E-03	1.24E-02	12.26	9.094	8.538	8.655	7.747
17	400	1.01E-03	1.49E-02	14.71	9.123	8.535	8.682	7.751
18	600	1.01E-03	1.87E-02	18.39	9.160	8.532	8.722	7.756

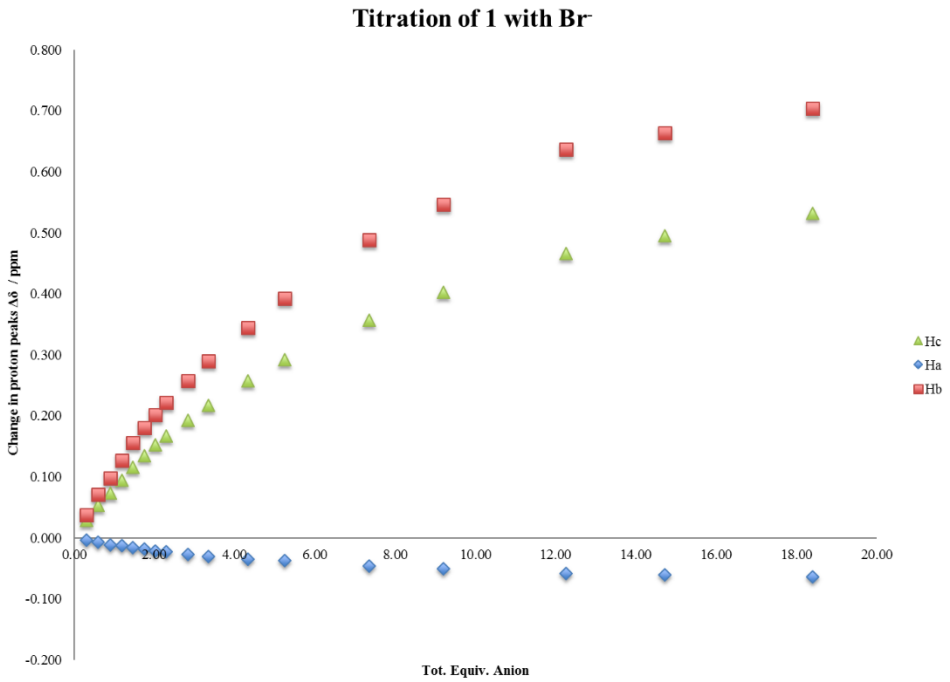

Figure 30. Binding isotherm for Br^- titration with **1** in 10% d_6-DMSO/$CDCl_3$ by ^1H NMR.

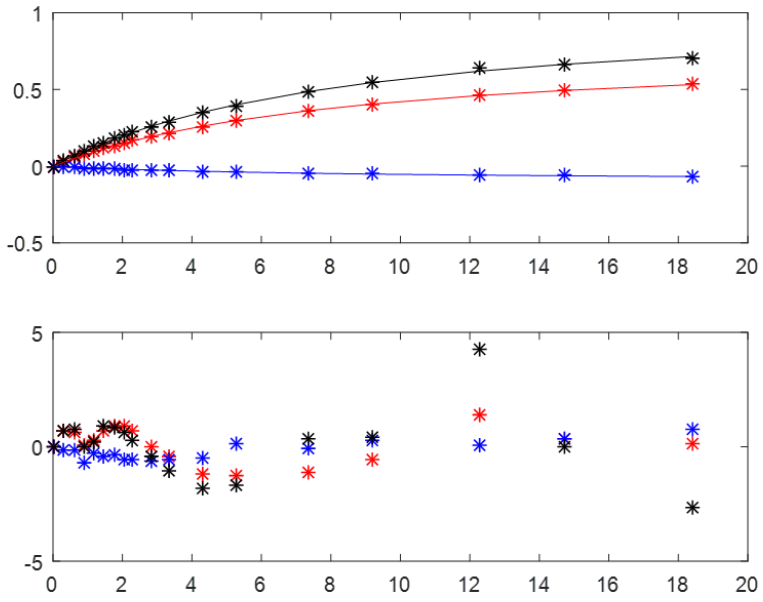

Figure 31. MatLab fit of binding isotherm for Br^- titration with **1**.

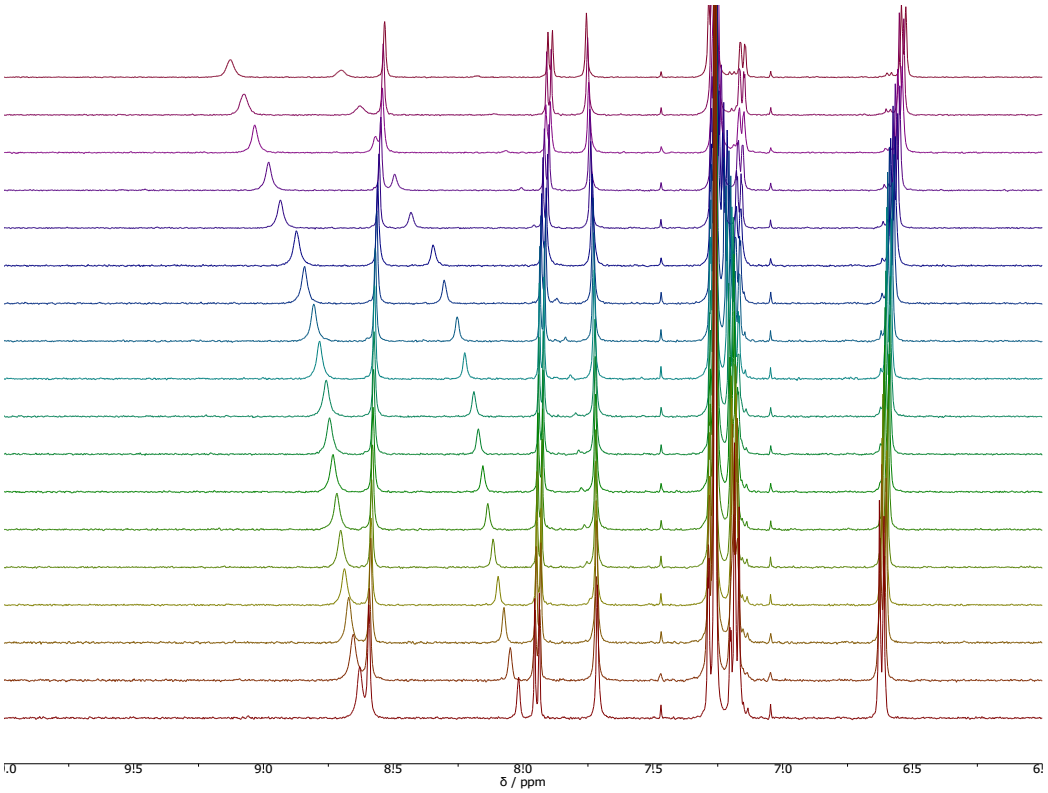

Figure 32. ^1H NMR spectra of Br^- titration with **1**.

Job's Plot Analysis

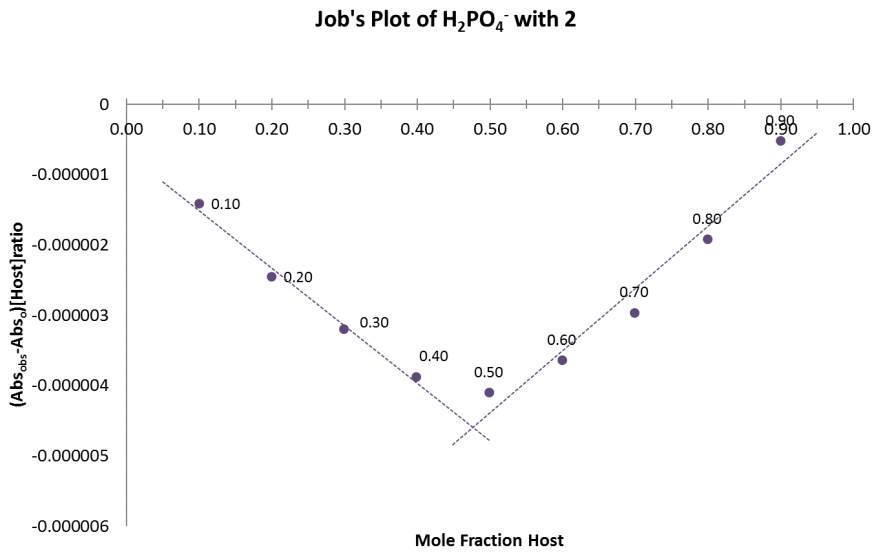

Figure 33. Binding isotherm for $H_2PO_4^-$ titration with **2** in 10% DMSO/$CHCl_3$ by UV-Vis.

Figure 34. Binding isotherm for ClO_4^- titration with **2** in 10% DMSO/$CHCl_3$ by UV-Vis.

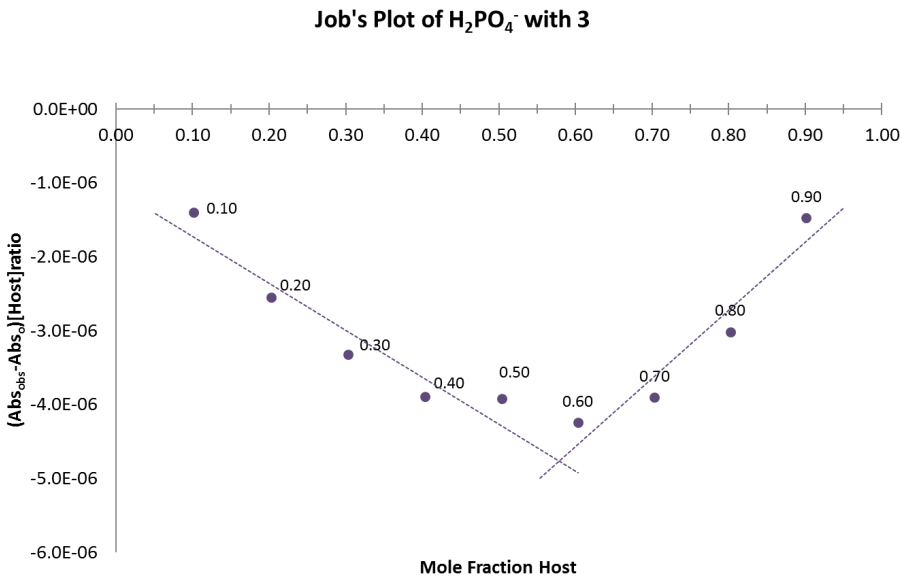

Figure 35. Binding isotherm for $H_2PO_4^-$ titration with **3** in 10% DMSO/$CHCl_3$ by UV-Vis.

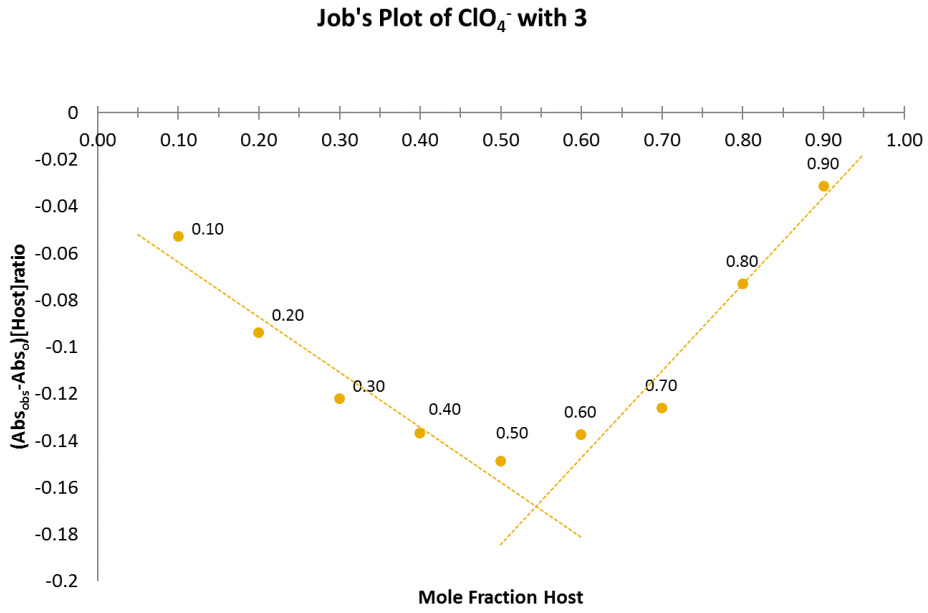

Figure 36. Binding isotherm for ClO_4^- titration with **3** in 10% DMSO/$CHCl_3$ by UV-Vis.

Computations

Computed Geometries

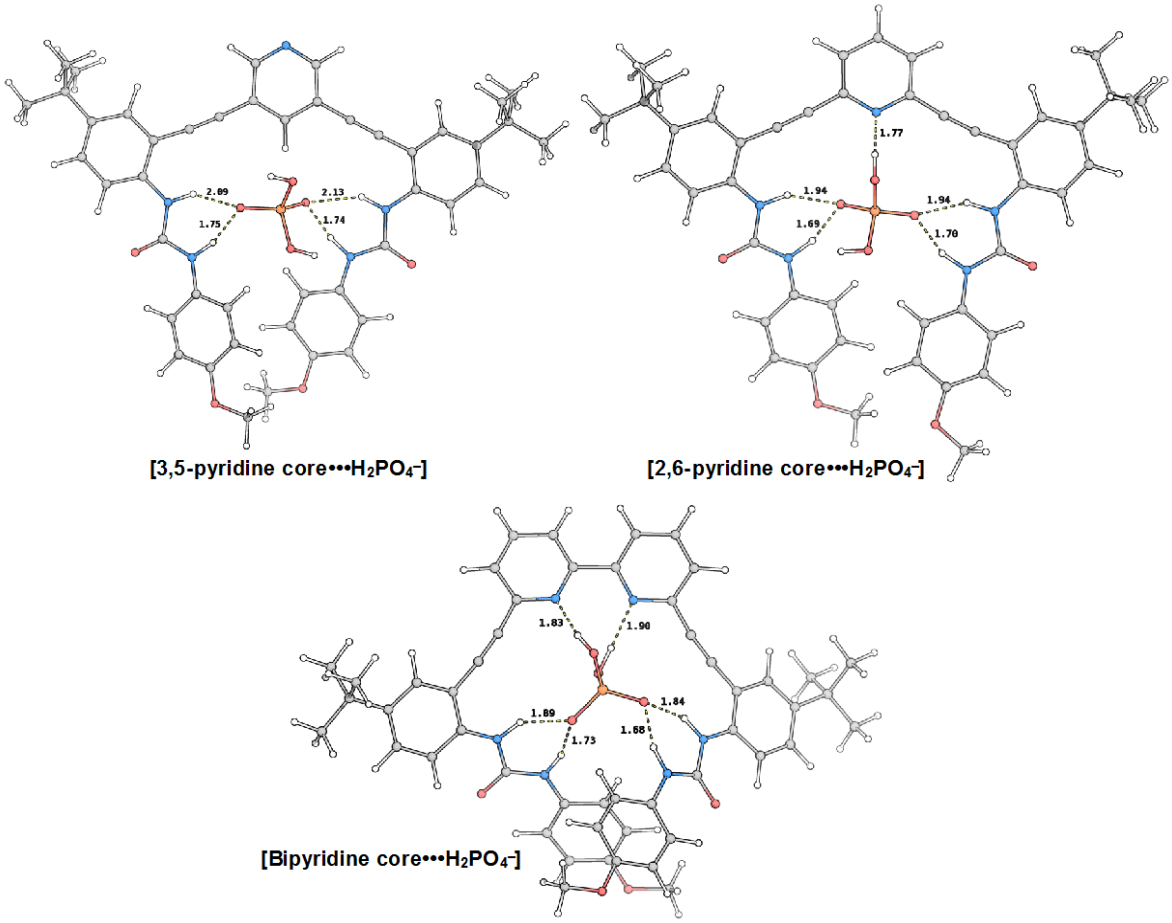

Figure 37. Optimized hosts with $H_2PO_4^-$.

Atomic Coordinates

[3,5-pyridine core•••$H_2PO_4^-$]

Using Gaussian 09: AM64L-G09RevD.01 24-Apr-2013

==========

pbepbe/6-31G*/auto gfprint gfinput scf=(direct,tight,maxcycle=300,xqc) opt=(maxcycle=250) freq=noraman iop(1/8=18) Temperature=298.15

#N Geom=AllCheck Guess=TCheck SCRF=Check Test GenChk RPBEPBE/6-31G(d)/Auto

Freq

Pointgroup= C1 Stoichiometry= C45H47N5O8P(1-) C1[X(C45H47N5O8P)]
#Atoms= 106
Charge = -1 Multiplicity = 1

SCF Energy= -2956.88311529 Predicted Change= -4.813685D-08
==========
Optimization completed. {Found 1 times}

Item	Max Val.	Criteria	Pass?	RMS Val.	Criteria	Pass?
Force	0.00001	0.00045	[YES]	0.00000	0.00030	[YES]
Displ	0.00349	0.00180	[NO]	0.00349	0.00180	[YES]

Atomic Type	Coordinates (Angstroms) X	Y	Z
C	-1.612533	-5.410922	-0.181670
H	-2.566112	-5.953815	-0.156234
N	-0.495643	-6.155740	-0.151178
C	0.679849	-5.508856	-0.162129
H	1.583435	-6.130829	-0.122005
C	0.811234	-4.093871	-0.218566
C	2.101653	-3.501664	-0.195091
C	3.247164	-3.052594	-0.149496
C	4.613580	-2.665090	-0.137395
C	-0.372017	-3.328524	-0.276966
H	-0.345049	-2.236162	-0.342888
C	-1.617575	-3.992137	-0.240195
C	-2.840331	-3.271509	-0.233372
C	-3.911540	-2.667467	-0.191991
C	-5.161960	-1.999071	-0.133954
C	5.581468	-3.676327	-0.353223
H	5.200721	-4.692832	-0.501453
C	6.959311	-3.421847	-0.393729
C	7.954187	-4.572629	-0.644049
C	7.795025	-5.646808	0.460433
H	6.770240	-6.054429	0.487184
H	8.012555	-5.221717	1.455813
H	8.489873	-6.489346	0.284975
C	9.418936	-4.089212	-0.635589
H	10.094067	-4.944633	-0.816442
H	9.696482	-3.642240	0.335231
H	9.607640	-3.340722	-1.425101
C	7.665382	-5.214344	-2.023913
H	7.791326	-4.475576	-2.834496
H	6.634580	-5.602855	-2.082765

H	8.356952	-6.056615	-2.212813
C	7.350908	-2.081027	-0.203003
H	8.411377	-1.811036	-0.222155
C	6.430314	-1.054093	0.021939
H	6.767281	-0.027212	0.157155
C	5.040889	-1.310476	0.067438
N	4.089439	-0.325649	0.323405
H	3.122021	-0.635460	0.503318
C	4.328251	1.065486	0.354210
N	3.209284	1.765494	0.755166
H	2.370678	1.201718	1.015061
C	3.077214	3.162124	0.853741
C	-5.256548	-0.567917	-0.193065
N	-4.081113	0.177091	-0.286527
H	-3.190826	-0.339052	-0.193582
C	-3.988065	1.558060	-0.538910
N	-2.665086	1.970625	-0.601011
H	-1.941831	1.219079	-0.531238
C	-2.193266	3.251561	-0.957589
C	-6.545576	0.004948	-0.144063
H	-6.629625	1.089652	-0.200926
C	-7.686851	-0.796020	-0.033343
H	-8.655690	-0.288509	0.002876
C	-7.623073	-2.202238	0.037613
C	-8.866921	-3.102935	0.172165
C	-8.766520	-3.930796	1.477611
H	-8.723484	-3.269164	2.360199
H	-7.862705	-4.563227	1.489323
H	-9.645215	-4.593951	1.584934
C	-8.942273	-4.067634	-1.037454
H	-9.031461	-3.505175	-1.983170
H	-9.819828	-4.735032	-0.948145
H	-8.042243	-4.701692	-1.108452
C	-10.175057	-2.287059	0.219546
H	-11.037179	-2.970227	0.319721
H	-10.321823	-1.695071	-0.700922
H	-10.193818	-1.594967	1.079716
C	-6.341758	-2.770583	-0.017648
H	-6.213701	-3.857568	0.027232
O	-4.966428	2.306249	-0.675603
O	5.417098	1.578982	0.053375
C	4.066887	4.089733	0.446980
H	5.013085	3.715907	0.055615
C	3.824478	5.461775	0.546657
H	4.585194	6.182134	0.227374
C	2.604204	5.950412	1.048324

O	2.464983	7.328458	1.069793
C	1.206608	7.834239	1.501135
H	0.380591	7.501192	0.842324
H	1.290484	8.931187	1.450547
H	0.977629	7.537048	2.543995
C	1.624559	5.035873	1.469671
H	0.659049	5.373703	1.854023
C	1.863215	3.659203	1.373345
H	1.081142	2.959259	1.689764
C	-0.814493	3.376467	-1.223864
H	-0.173225	2.490023	-1.168022
C	-0.242975	4.613335	-1.545863
H	0.835345	4.666618	-1.712263
C	-1.052527	5.760244	-1.609754
O	-0.598061	7.033082	-1.899730
C	0.765705	7.151049	-2.298795
H	0.904602	8.207225	-2.578000
H	0.989311	6.509375	-3.173607
H	1.464601	6.899345	-1.478794
C	-2.431247	5.641297	-1.354290
H	-3.052950	6.540768	-1.413887
C	-3.002680	4.409057	-1.029067
H	-4.072072	4.321373	-0.836066
P	-0.258074	-0.029645	1.314522
O	1.263926	-0.124987	1.315416
O	-0.650355	1.430063	2.006359
H	-1.504242	1.730905	1.625983
O	-0.836296	-1.153666	2.380852
H	-0.080810	-1.406154	2.950721
O	-1.082975	-0.181507	0.030400

Statistical Thermodynamic Analysis
Temperature= 298.150 Kelvin Pressure= 1.00000 Atm

==========

SCF Energy= -2956.88311529 Predicted Change= -4.813685D-08
Zero-point correction (ZPE)= -2956.0544 0.82871
Internal Energy (U)= -2955.9943 0.88874
Enthalpy (H)= -2955.9934 0.88969
Gibbs Free Energy (G)= -2956.1557 0.72740

Frequencies -- 7.1336 11.5027 14.1963

[2,6-pyridine core•••$H_2PO_4^-$]

Using Gaussian 09: AM64L-G09RevD.01 24-Apr-2013

==========

pbepbe/6-31G*/auto gfprint gfinput scf=(direct,tight,maxcycle=300,xqc) opt=(maxcycle=250) freq=noraman iop(1/8=18) Temperature=298.15

#N Geom=AllCheck Guess=TCheck SCRF=Check Test GenChk RPBEPBE/6-31G(d)/Auto

Freq

Pointgroup= C1 Stoichiometry= C45H47N5O8P(1-) C1[X(C45H47N5O8P)] #Atoms= 106

Charge = -1 Multiplicity = 1

SCF Energy= -2956.88200469 Predicted Change= -1.501878D-08

==========

Optimization completed. {Found 1 times}

Item	Max Val.	Criteria	Pass?	RMS Val.	Criteria	Pass?
Force	0.00001	0.00045	[YES]	0.00000	0.00030	[YES]
Displ	0.00273	0.00180	[NO]	0.00273	0.00180	[YES]

Atomic Type	Coordinates (Angstroms) X	Y	Z
C	-1.706461	-5.136709	1.603766
H	-2.696919	-5.511445	1.875549
C	-0.537503	-5.807289	1.974989
H	-0.594661	-6.740166	2.546644
C	0.703869	-5.270018	1.629304
H	1.640987	-5.752606	1.919850
C	0.743454	-4.059550	0.889069
C	1.998544	-3.488488	0.543268
C	3.136160	-3.066443	0.331432
C	4.495849	-2.742613	0.096918
N	-0.390374	-3.421779	0.496252
C	-1.593640	-3.932064	0.866400
C	-2.764021	-3.212812	0.492536
C	-3.816686	-2.629002	0.237634
C	-5.064612	-2.029358	-0.071292
C	5.421488	-3.820124	0.178750
H	5.000580	-4.800216	0.419251
C	6.790618	-3.665538	-0.041789
C	7.796606	-4.829113	0.027879

C	7.124415	-6.164187	0.406469
H	6.361942	-6.462160	-0.334427
H	6.638986	-6.109919	1.396775
H	7.882861	-6.966264	0.447211
C	8.879501	-4.516326	1.090760
H	9.622551	-5.334189	1.137487
H	8.426641	-4.403335	2.091147
H	9.420686	-3.582712	0.860761
C	8.475211	-5.003331	-1.353833
H	8.990204	-4.081055	-1.672483
H	7.729028	-5.254735	-2.127554
H	9.225135	-5.815698	-1.318944
C	7.225191	-2.354642	-0.352550
H	8.289367	-2.167254	-0.541565
C	6.358115	-1.269474	-0.432305
H	6.728857	-0.272188	-0.665604
C	4.963600	-1.419361	-0.206873
N	4.068753	-0.363154	-0.270241
H	3.061308	-0.556751	-0.100005
C	4.397587	0.995745	-0.502079
N	3.269302	1.782244	-0.534303
H	2.357316	1.294163	-0.354147
C	3.219410	3.175123	-0.703523
C	-5.257971	-0.604744	-0.088128
N	-4.188512	0.233806	0.193531
H	-3.246568	-0.191174	0.313249
C	-4.255118	1.636028	0.378426
N	-3.012067	2.154747	0.669259
H	-2.221204	1.463900	0.712552
C	-2.681382	3.502021	0.894448
C	-6.557569	-0.136984	-0.398981
H	-6.722384	0.939852	-0.406912
C	-7.601169	-1.021928	-0.677331
H	-8.577941	-0.587674	-0.912860
C	-7.436252	-2.423261	-0.666980
C	-8.572508	-3.416539	-0.981497
C	-9.904365	-2.699602	-1.283189
H	-9.820141	-2.034834	-2.160654
H	-10.246774	-2.094852	-0.425151
H	-10.688426	-3.446091	-1.502511
C	-8.794159	-4.355927	0.229917
H	-9.083750	-3.780174	1.126208
H	-7.880961	-4.923746	0.477288
H	-9.596865	-5.085300	0.012929
C	-8.189849	-4.264784	-2.219777
H	-7.251803	-4.821915	-2.055875

H	-8.047049	-3.622618	-3.106262
H	-8.984755	-4.999126	-2.448776
C	-6.152898	-2.890398	-0.354789
H	-5.945787	-3.965938	-0.326458
O	-5.302351	2.296041	0.284955
O	5.557724	1.410077	-0.659764
C	4.339988	4.029221	-0.647809
H	5.329381	3.594271	-0.503972
C	4.184095	5.419488	-0.775654
H	5.075120	6.051434	-0.718556
C	2.909897	5.978352	-0.962241
O	2.642118	7.335197	-1.072028
C	3.754795	8.210062	-0.985519
H	4.490267	8.025772	-1.794668
H	4.276189	8.123401	-0.010529
H	3.350270	9.229020	-1.090597
C	1.791594	5.128164	-1.045727
H	0.801013	5.563961	-1.208143
C	1.942135	3.748995	-0.918650
H	1.066019	3.095753	-1.001693
C	-3.608752	4.571234	0.881263
H	-4.660956	4.355477	0.694114
C	-3.172046	5.880130	1.097750
H	-3.885573	6.710788	1.083156
C	-1.814437	6.166501	1.331828
O	-1.499495	7.497845	1.523111
C	-0.123557	7.809797	1.709307
H	0.294678	7.309477	2.605661
H	-0.081835	8.900824	1.855201
H	0.492165	7.537117	0.829623
C	-0.888465	5.108767	1.356664
H	0.176813	5.287094	1.520752
C	-1.323214	3.795170	1.139950
H	-0.590837	2.980450	1.154389
P	-0.134276	-0.034376	-0.390360
O	-1.337900	0.024849	0.568570
O	-0.273110	1.175560	-1.523338
H	-1.211914	1.235258	-1.795239
O	-0.252913	-1.350661	-1.342679
H	-0.323174	-2.142592	-0.719852
O	1.266350	0.120867	0.207207

Statistical Thermodynamic Analysis
Temperature= 298.150 Kelvin Pressure= 1.00000 Atm

==========

SCF Energy= -2956.88200469 Predicted Change= -1.501878D-08
Zero-point correction (ZPE)= -2956.0539 0.82808
Internal Energy (U)= -2955.9944 0.88754
Enthalpy (H)= -2955.9935 0.88849
Gibbs Free Energy (G)= -2956.1544 0.72752

Frequencies -- 6.4289 9.4121 15.7228

[Bipyridine core•••$H_2PO_4^-$]

Using Gaussian 09: AM64L-G09RevD.01 24-Apr-2013
==========
pbepbe/6-31G*/auto gfprint gfinput scf=(direct,tight,maxcycle=300,xqc) opt=(maxcycle=250) freq=noraman iop(1/8=18) Temperature=298.15
#N Geom=AllCheck Guess=TCheck SCRF=Check Test GenChk RPBEPBE/6-31G(d)/Auto
Freq

Pointgroup= C1 Stoichiometry= C50H50N6O8P(1-) C1[X(C50H50N6O8P)] #Atoms= 115
Charge = -1 Multiplicity = 1

SCF Energy= -3203.67970897 Predicted Change= -7.545578D-09
==========
Optimization completed. {Found 1 times}

Item	Max Val.	Criteria	Pass?	RMS Val.	Criteria	Pass?
Force	0.00001	0.00045	[YES]	0.00000	0.00030	[YES]
Displ	0.00372	0.00180	[NO]	0.00372	0.00180	[YES]

Atomic Coordinates (Angstroms)

Type	X	Y	Z
C	-3.700700	-5.349797	0.721841
H	-4.744192	-5.268573	1.038436
C	-2.997836	-6.548607	0.813905
H	-3.484075	-7.445823	1.212061
C	-1.654051	-6.588267	0.417491
H	-1.064554	-7.503406	0.523296
C	-1.061885	-5.413176	-0.087699

N	-1.736095	-4.249319	-0.186800
C	-3.031037	-4.197984	0.229646
C	-3.717651	-2.955350	0.178060
C	-4.404765	-1.936164	0.266766
C	-5.282912	-0.833413	0.408433
C	-4.830782	0.472192	0.806147
N	-3.477458	0.731139	0.915845
H	-2.808921	0.162735	0.352972
C	-2.908785	1.799257	1.654076
N	-1.553766	1.871297	1.438580
H	-1.175895	1.219549	0.710620
C	-0.653614	2.811957	1.965552
C	-5.826691	1.446887	1.060457
H	-5.503342	2.430601	1.400576
C	-7.181334	1.163471	0.888355
H	-7.894560	1.969732	1.086884
C	-7.647279	-0.100299	0.459206
C	-9.138316	-0.425342	0.238890
C	-10.049437	0.776233	0.562876
H	-9.823051	1.645217	-0.079457
H	-9.949840	1.092320	1.616115
H	-11.105475	0.500197	0.393525
C	-9.556587	-1.605930	1.150263
H	-8.958352	-2.510267	0.945558
H	-10.620661	-1.861962	0.990081
H	-9.420030	-1.347875	2.214914
C	-9.366981	-0.819114	-1.241691
H	-10.429819	-1.069997	-1.418461
H	-8.760436	-1.695402	-1.527275
H	-9.091861	0.011262	-1.914963
C	-6.669849	-1.077150	0.237830
H	-6.956464	-2.087641	-0.074091
O	-3.569000	2.539036	2.401097
C	-0.975466	3.768789	2.956064
H	-1.990217	3.799154	3.354530
C	-0.001923	4.668860	3.397221
H	-0.244089	5.416112	4.160443
C	1.302170	4.648012	2.868970
O	2.175502	5.597154	3.369471
C	3.482104	5.604935	2.810494
H	3.463812	5.784423	1.717515
H	4.018330	4.653415	2.999113
H	4.019084	6.428495	3.307438
C	1.632352	3.694943	1.889922
H	2.624266	3.654027	1.431796
C	0.660120	2.787509	1.456027

H	0.922488	2.053276	0.688397
C	0.903378	-6.576879	-1.141413
H	0.266104	-7.443678	-1.338514
C	0.366568	-5.423250	-0.535986
N	1.097563	-4.309113	-0.317113
C	2.406357	-4.302206	-0.692249
C	3.018859	-5.435897	-1.290136
H	4.073484	-5.384792	-1.574269
C	2.252453	-6.575436	-1.518744
H	2.694954	-7.454041	-2.000449
C	3.190638	-3.138971	-0.460317
C	4.000623	-2.219487	-0.334500
C	5.006897	-1.239385	-0.137489
C	6.273448	-1.702637	0.299292
H	6.371425	-2.782623	0.456737
C	7.358914	-0.851689	0.539866
C	8.705954	-1.424853	1.024018
C	9.237894	-2.446983	-0.011203
H	9.410652	-1.962937	-0.988301
H	8.524687	-3.273861	-0.168927
H	10.193788	-2.885801	0.331348
C	8.506543	-2.135657	2.385764
H	7.765481	-2.949677	2.313265
H	8.147731	-1.424383	3.149858
H	9.458790	-2.573144	2.740161
C	9.774186	-0.327191	1.206841
H	9.469730	0.416988	1.963406
H	9.977869	0.206005	0.261697
H	10.721321	-0.782579	1.547293
C	7.129961	0.523643	0.317177
H	7.934616	1.245940	0.487252
C	5.903176	1.023151	-0.120801
H	5.759650	2.090489	-0.286955
C	4.802225	0.165885	-0.371142
N	3.579330	0.609072	-0.839988
H	2.819197	-0.090621	-0.993566
C	3.245460	1.940776	-1.188677
N	1.990281	1.998329	-1.747846
H	1.460963	1.087334	-1.777869
C	1.297880	3.152486	-2.155160
O	3.996317	2.915818	-1.005689
C	-0.099233	3.041635	-2.315575
H	-0.597248	2.097467	-2.060699
C	-0.861211	4.132184	-2.753201
H	-1.942752	4.009012	-2.853681
C	-0.236294	5.359989	-3.032184

O	-0.890612	6.500474	-3.464776
C	-2.302806	6.415623	-3.576183
H	-2.615958	5.662387	-4.327477
H	-2.642357	7.411764	-3.901425
H	-2.779472	6.165682	-2.607481
C	1.155615	5.476332	-2.866779
H	1.628743	6.440250	-3.081757
C	1.920477	4.390611	-2.435994
H	2.997875	4.487514	-2.296794
P	-0.170249	-0.988826	-0.911894
O	1.138982	-0.551726	-1.590245
O	0.099375	-1.738210	0.522391
H	0.498858	-2.636016	0.347560
O	-0.802265	-2.168706	-1.854658
H	-1.224280	-2.853254	-1.261102
O	-1.198578	0.122918	-0.632044

Statistical Thermodynamic Analysis
Temperature= 298.150 Kelvin Pressure= 1.00000 Atm

==========

SCF Energy= -3203.67970897 Predicted Change= -7.545578D-09
Zero-point correction (ZPE)= -3202.7835 0.89616
Internal Energy (U)= -3202.7200 0.95961
Enthalpy (H)= -3202.7191 0.96055
Gibbs Free Energy (G)= -3202.8889 0.79077

Frequencies -- 4.7093 10.1799 13.3351

NMR Spectra

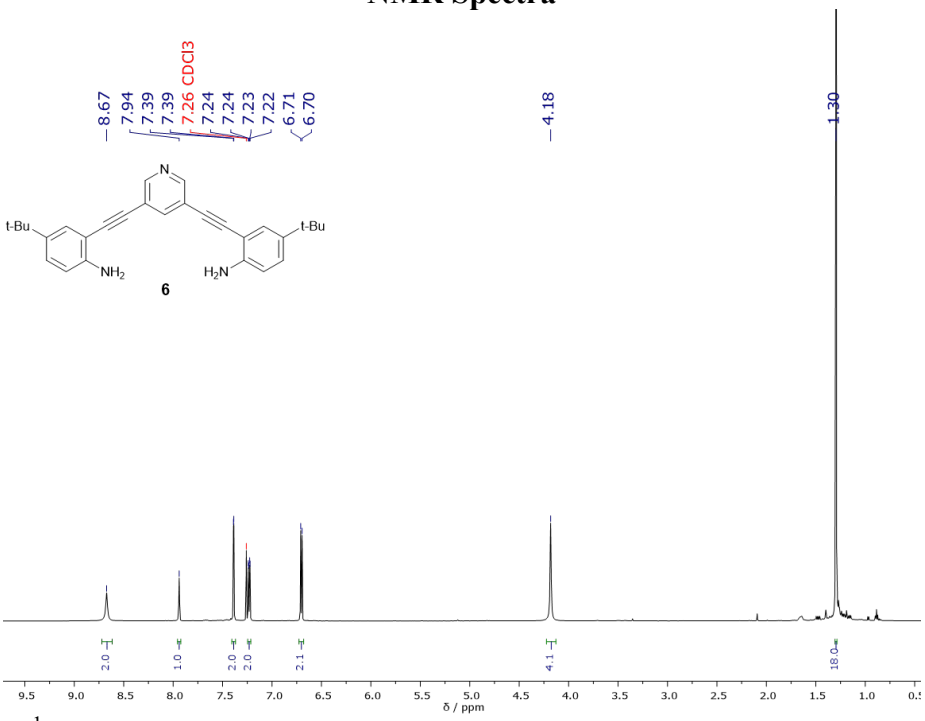

Figure 38. ^{1}H NMR spectra of **6** in $CDCl_3$.

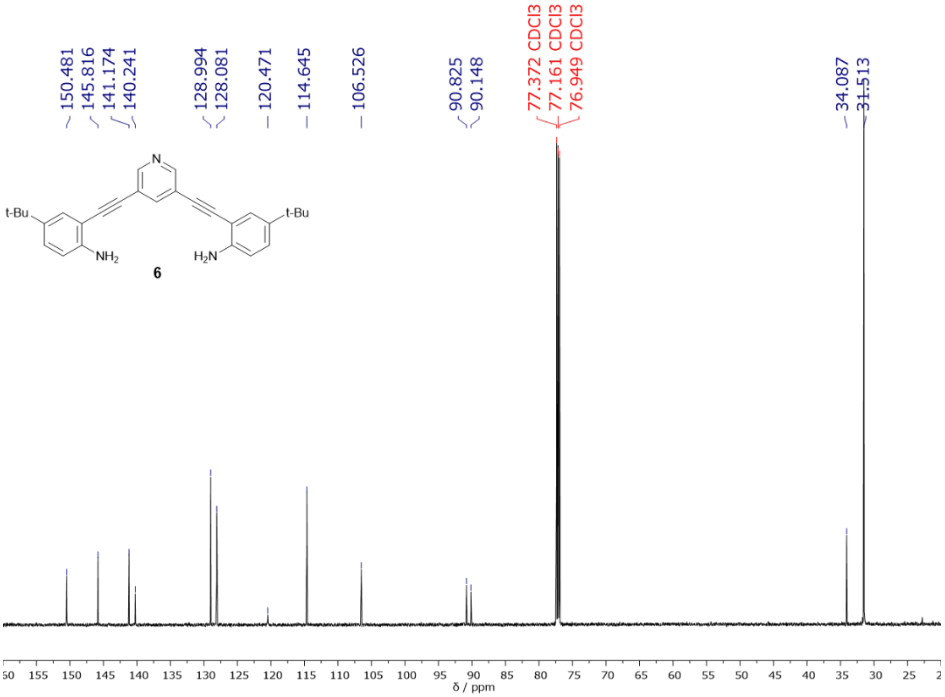

Figure 39. ^{13}C NMR spectra of **6** in $CDCl_3$.

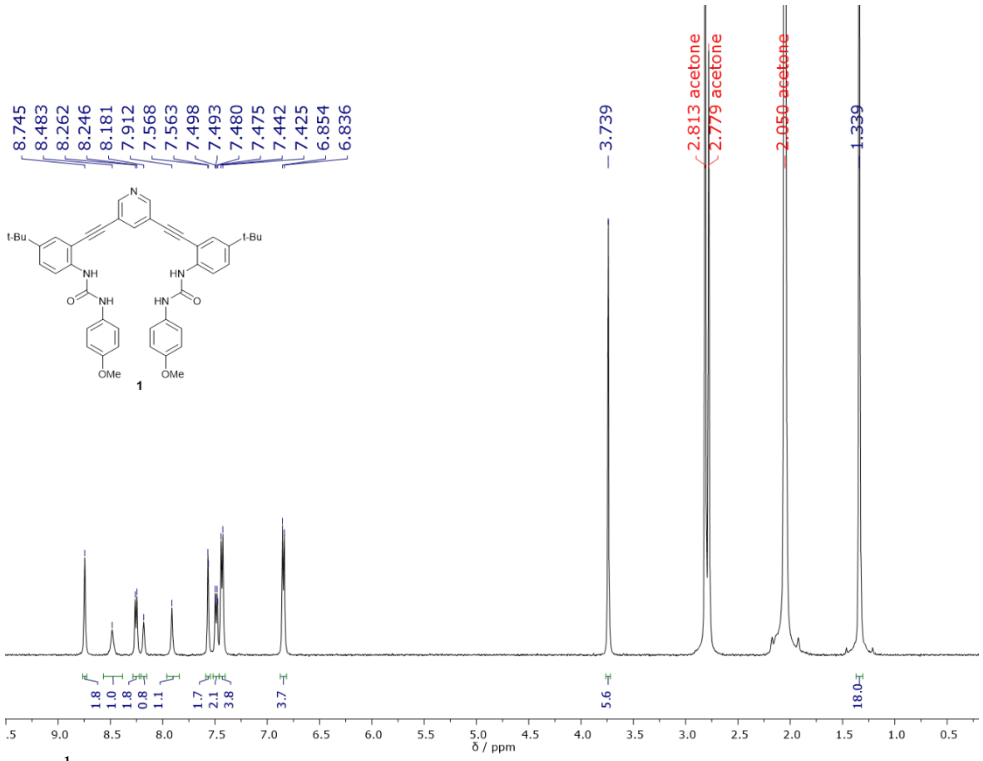

Figure 40. ^{1}H NMR spectra of **1** in acetone-d_6.

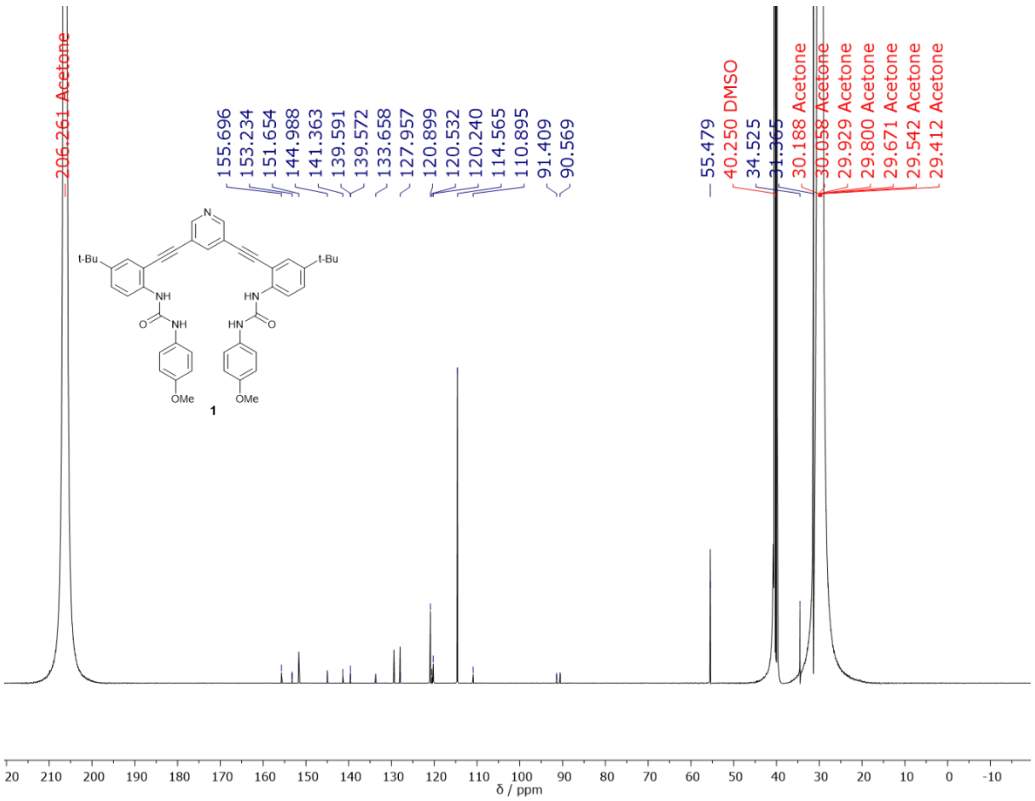

Figure 40. ^{13}C NMR spectra of **1** in acetone-d_6/DMSO-d_6.

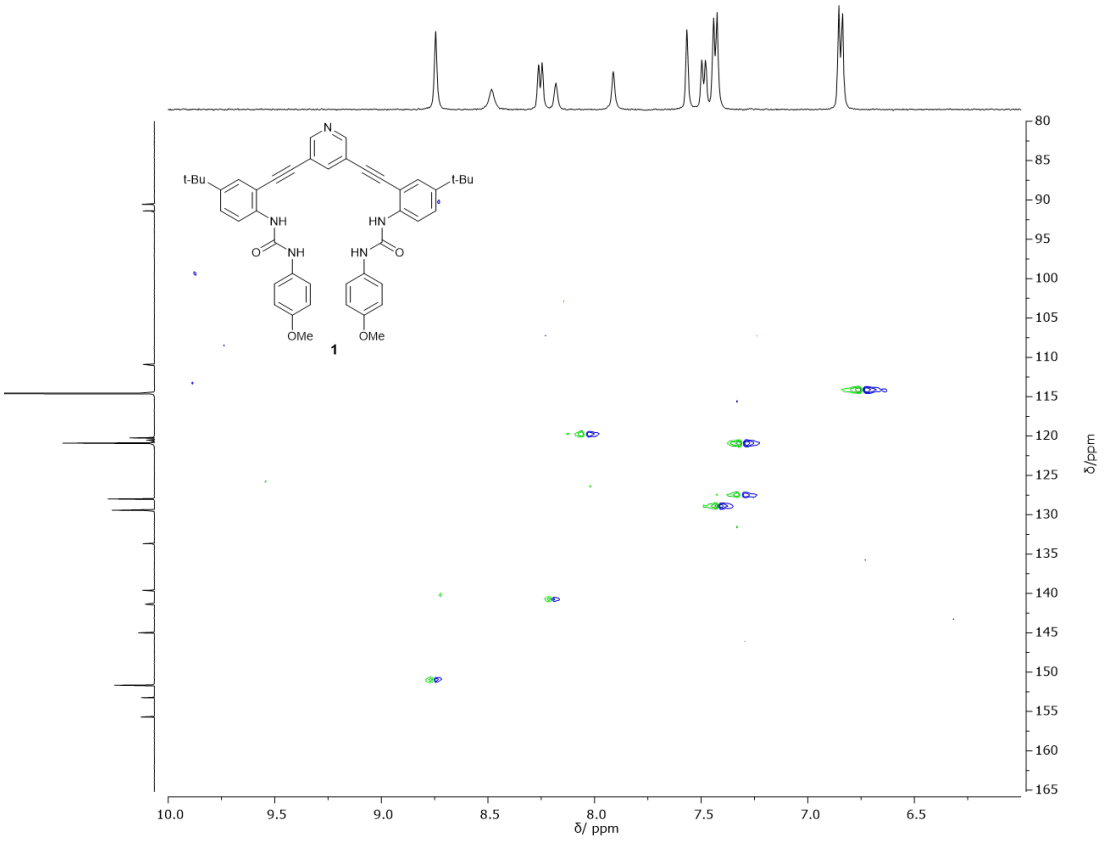

Figure 41. HSQC spectra of **1** in acetone-d_6/DMSO-d_6.

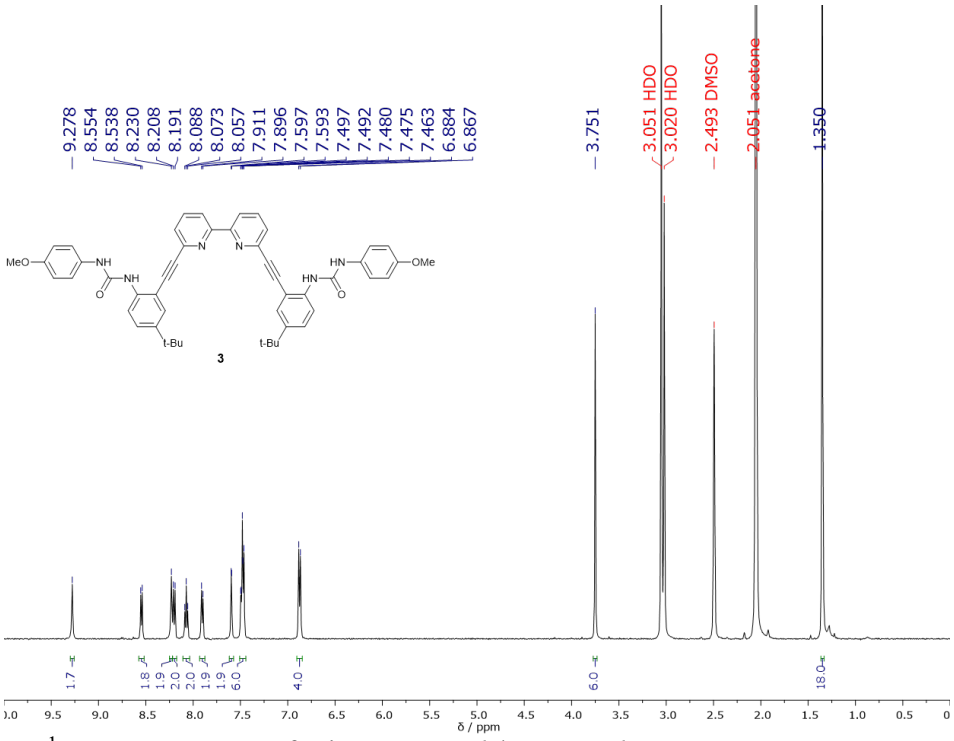

Figure 42. ^{1}H NMR spectra of **3** in acetone-d_6/DMSO-d_6.

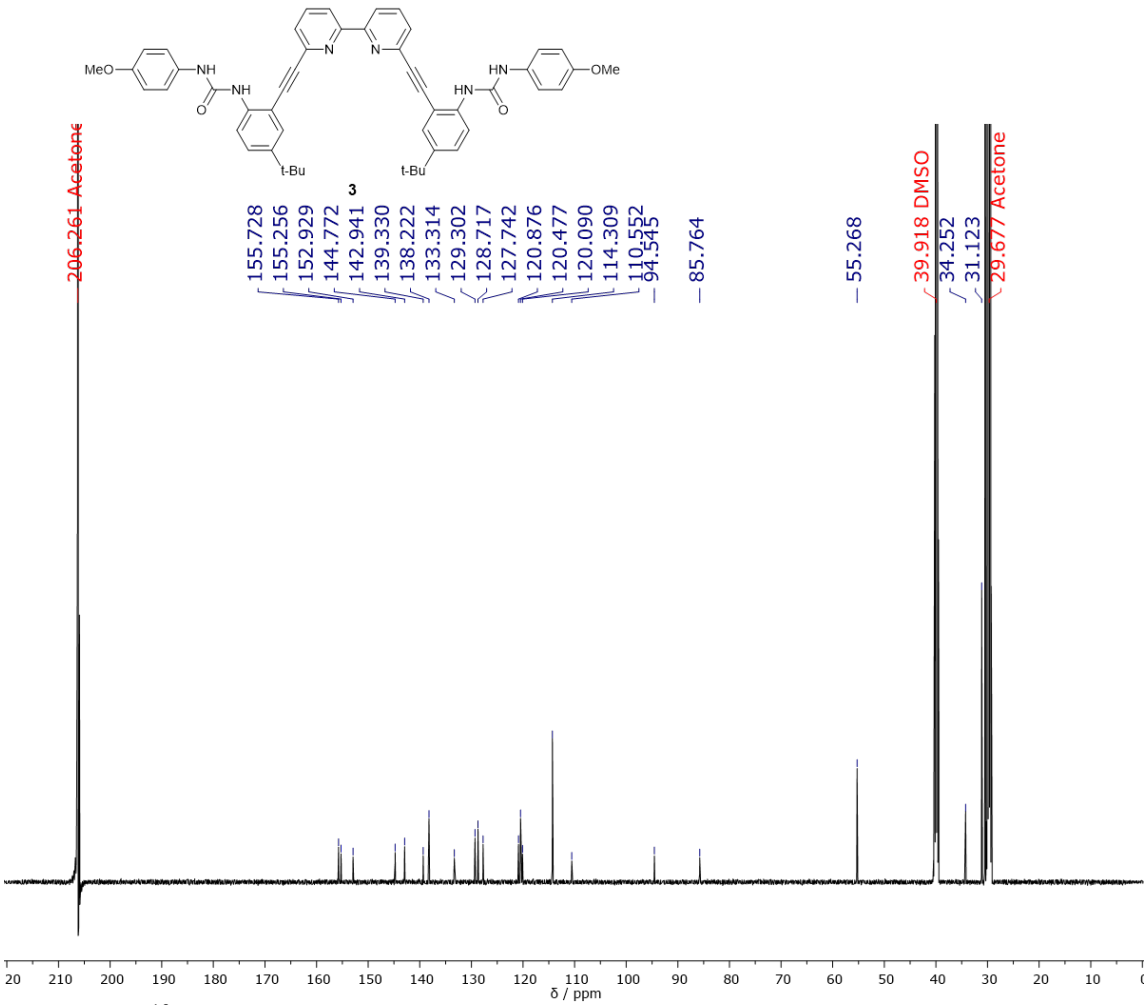

Figure 43. ^{13}C NMR spectra of **3** in acetone-d_6/DMSO-d_6.

APPENDIX B

SUPPLEMENTARY INFORMATION FOR CHAPTER IV

UV-Vis Spectra

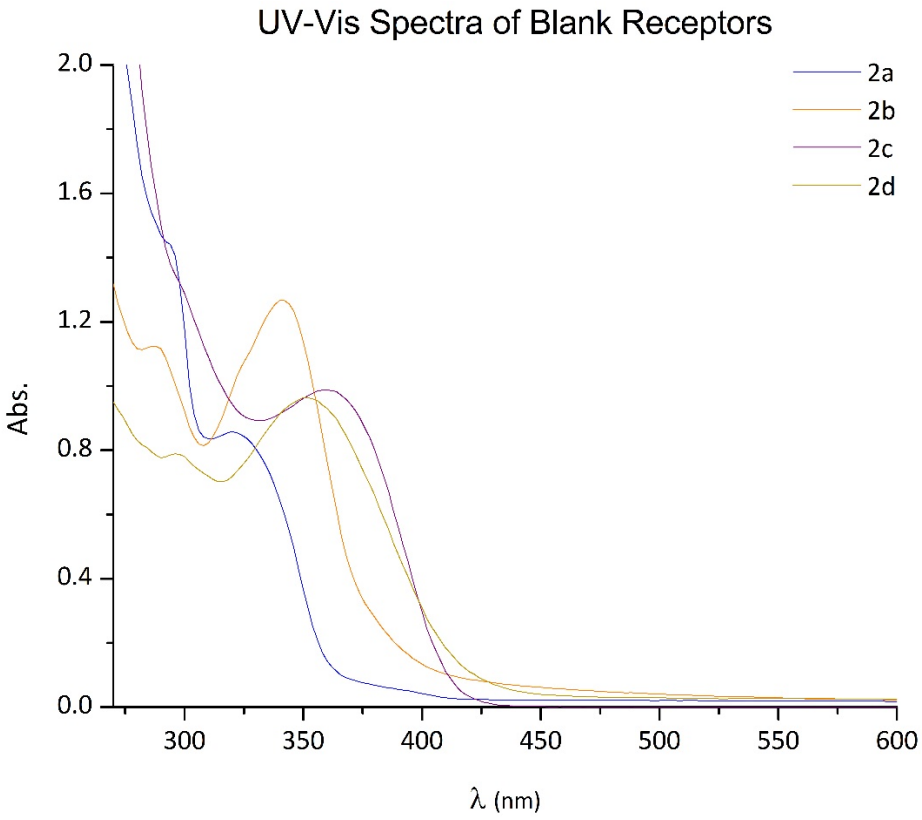

Figure 1. UV-Vis spectra of receptors **2a**-**2d** in $CHCl_3$.

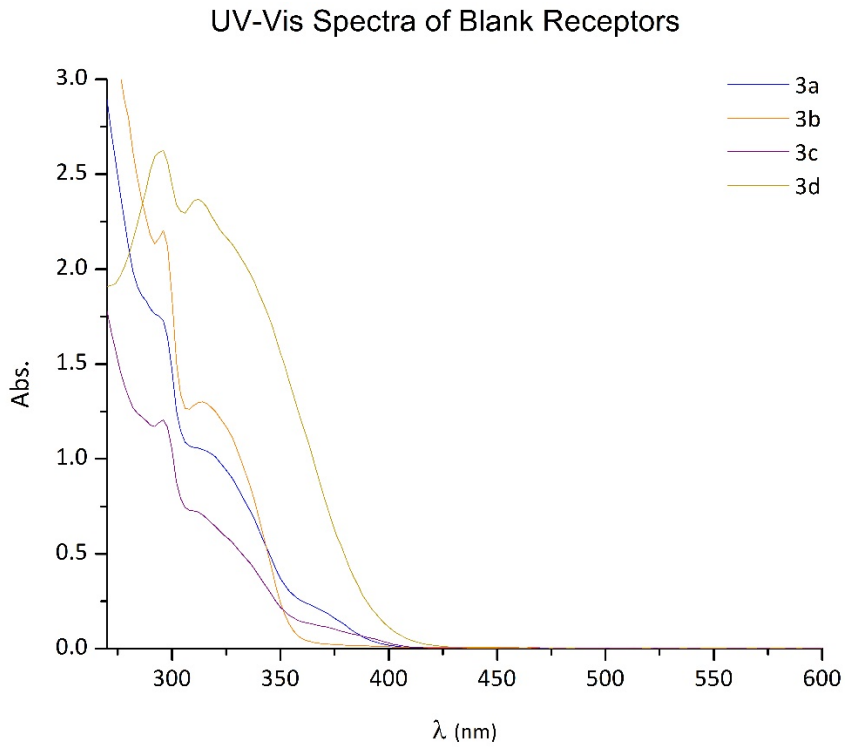

Figure 2. UV-Vis spectra of receptors **3a-3d** in $CHCl_3$.

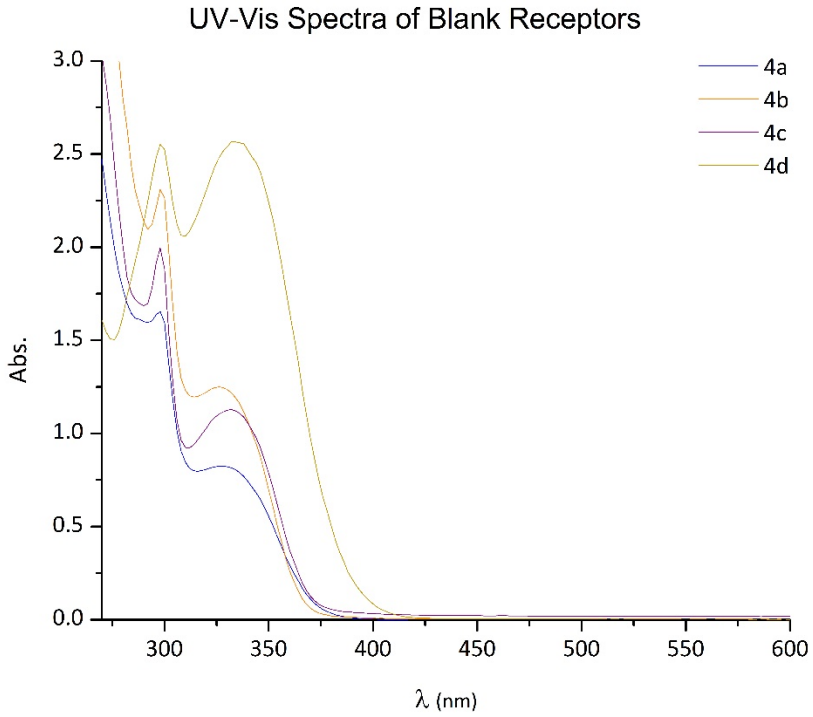

Figure 3. UV-Vis spectra of receptors **4a-4d** in $CHCl_3$.

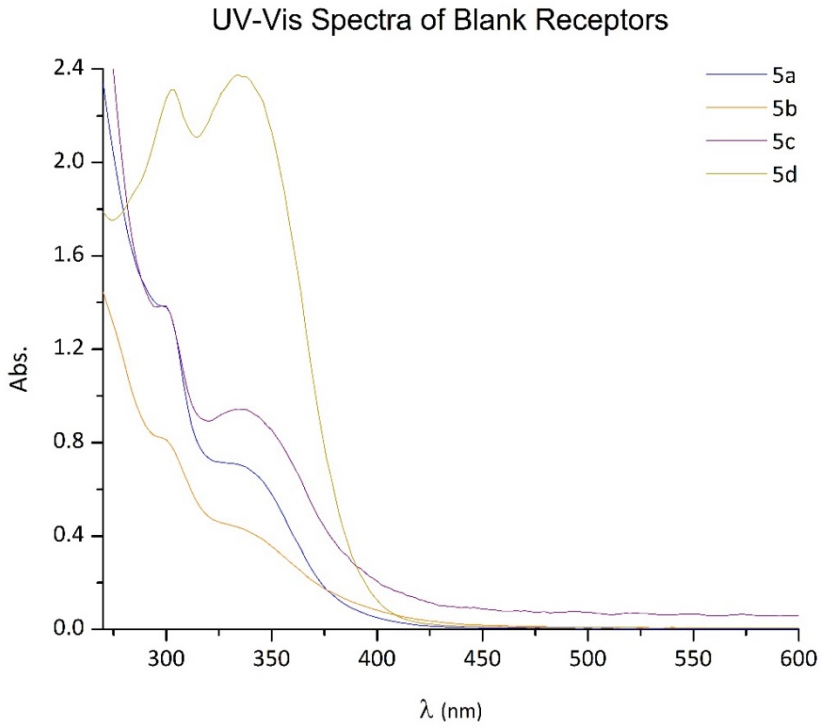

Figure 4. UV-Vis spectra of receptors **5a-5d** in $CHCl_3$.

Fluorescence Spectra

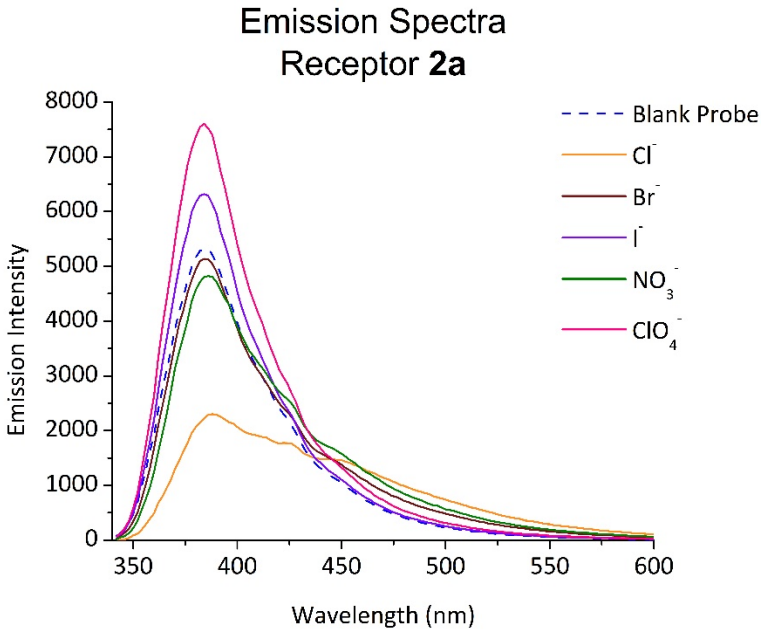

Figure 5. Fluorescence emission spectra of receptor **2a** $CHCl_3$.

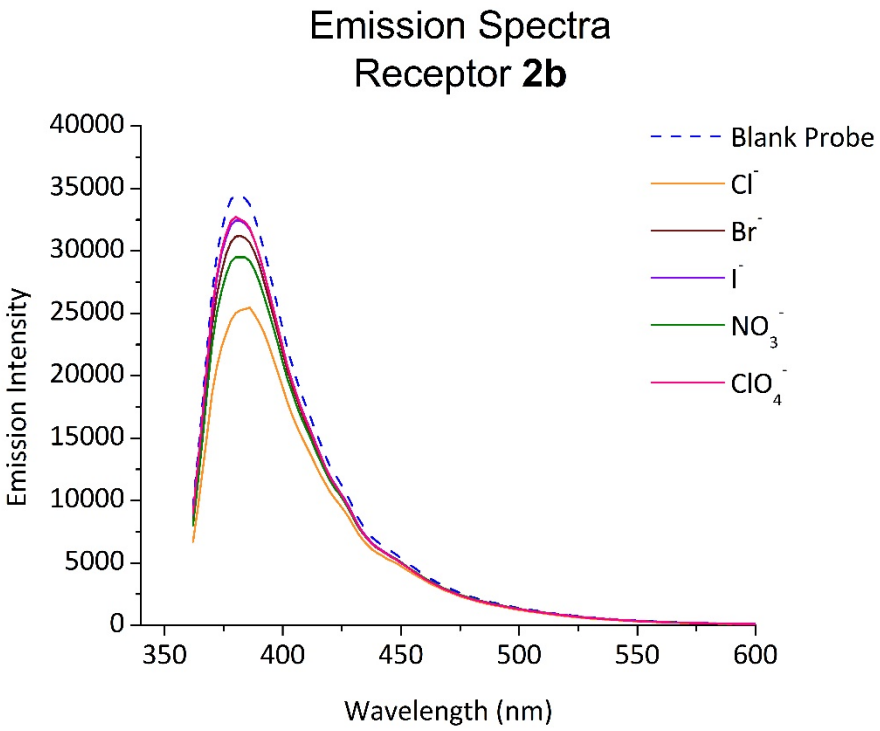

Figure 6. Fluorescence emission spectra of receptor **2b** $CHCl_3$.

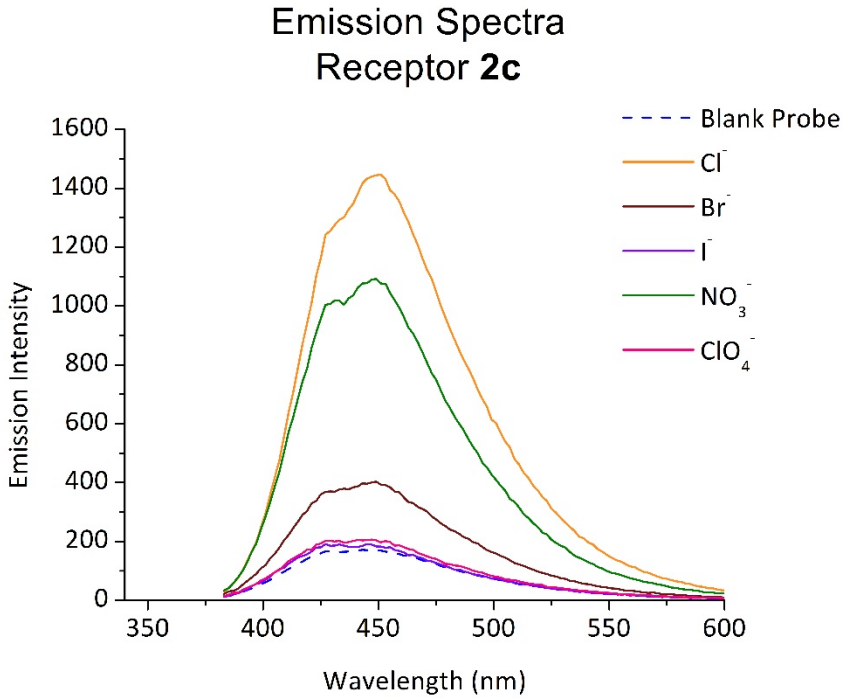

Figure 7. Fluorescence emission spectra of receptor **2c** $CHCl_3$.

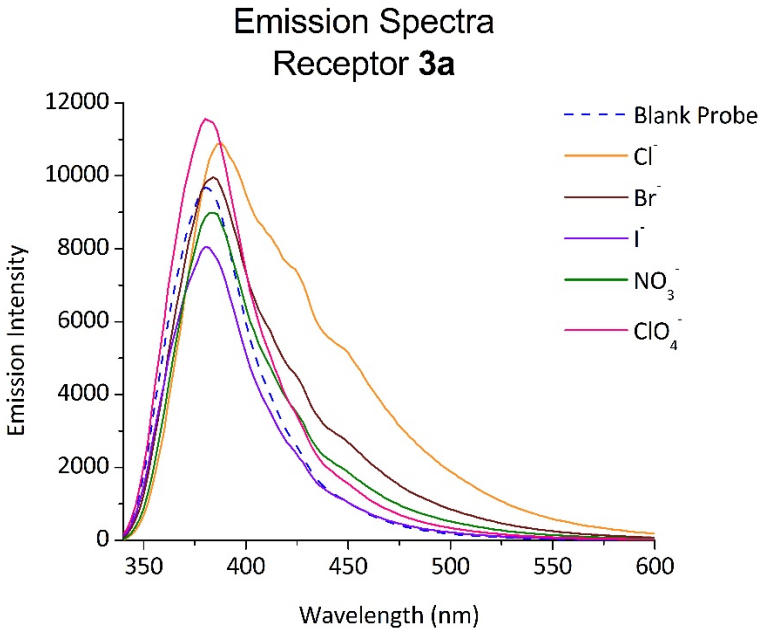

Figure 8. Fluorescence emission spectra of receptor **3a** $CHCl_3$.

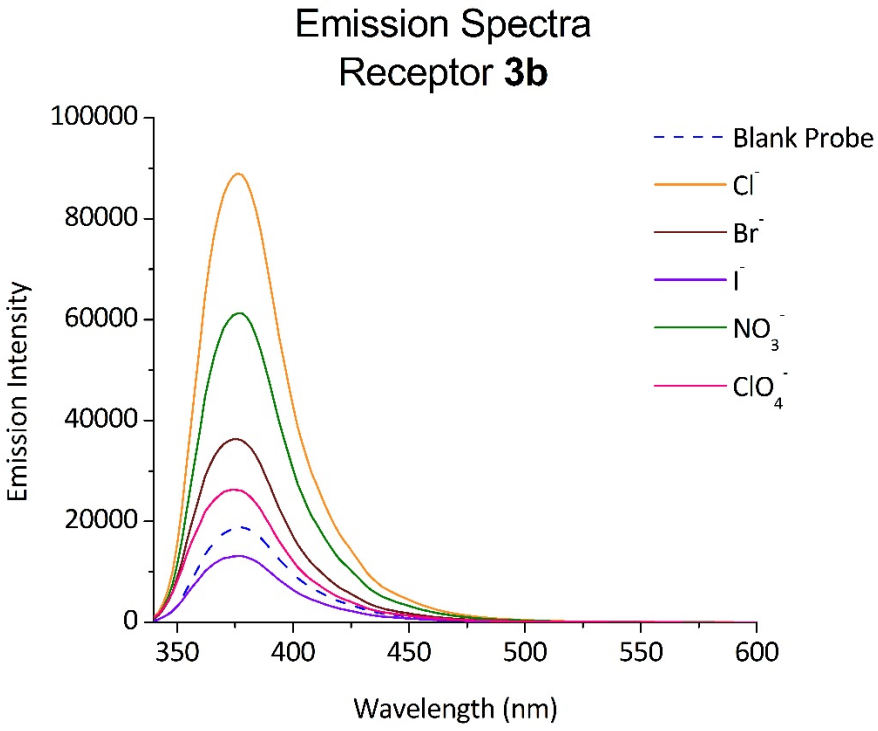

Figure 9. Fluorescence emission spectra of receptor **3b** $CHCl_3$.

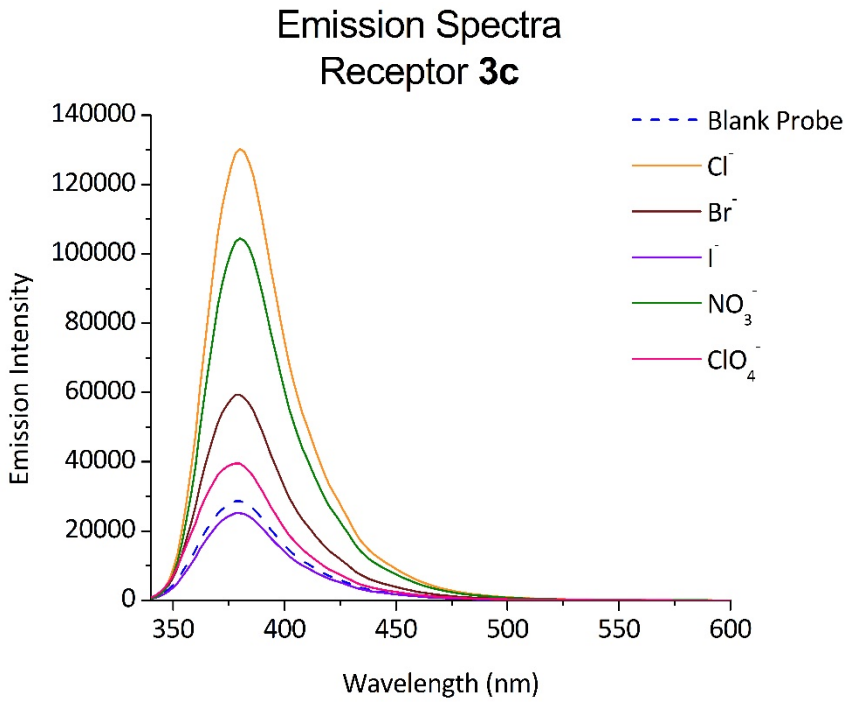

Figure 10. Fluorescence emission spectra of receptor **3c** $CHCl_3$.

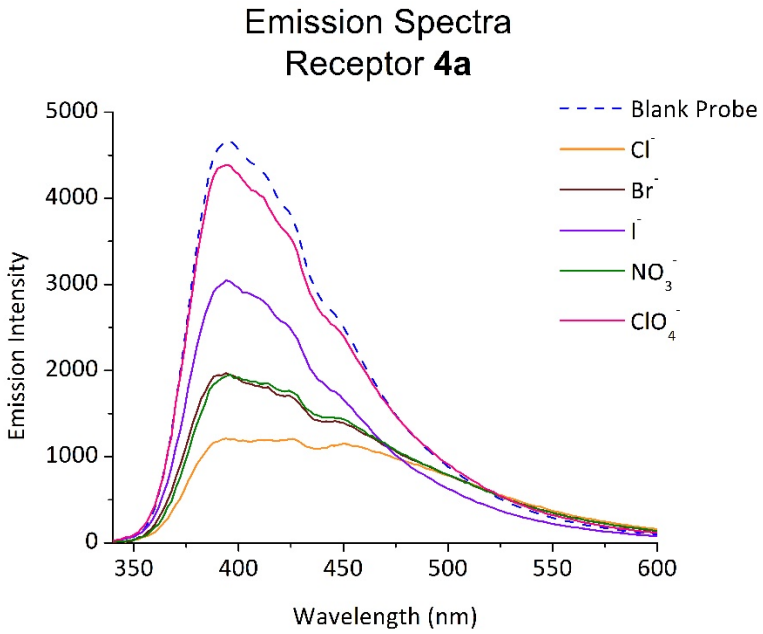

Figure 11. Fluorescence emission spectra of receptor **4a** $CHCl_3$.

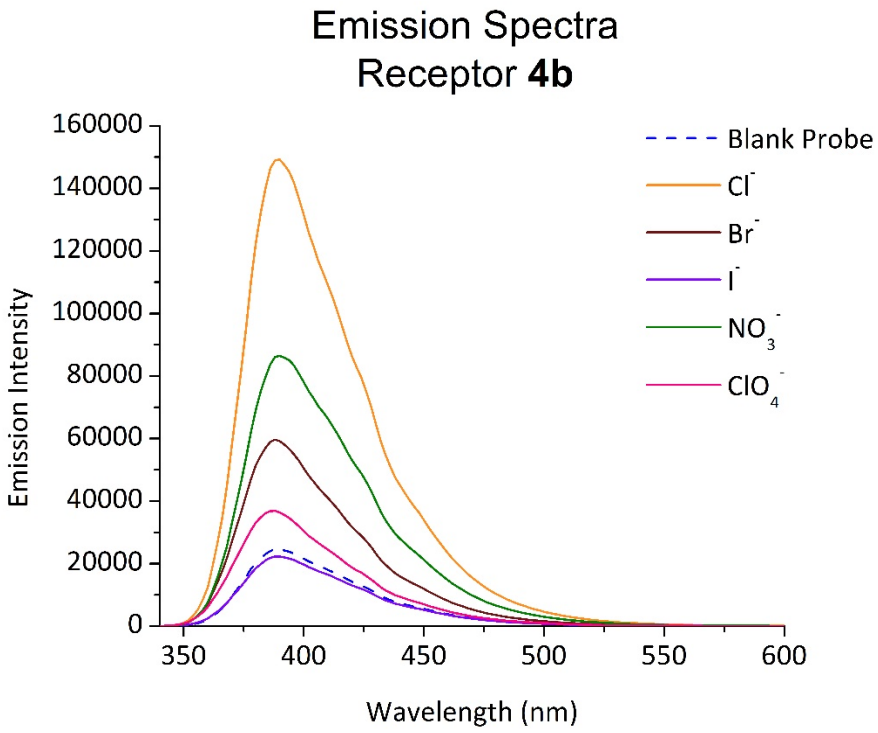

Figure 12. Fluorescence emission spectra of receptor **4b** $CHCl_3$.

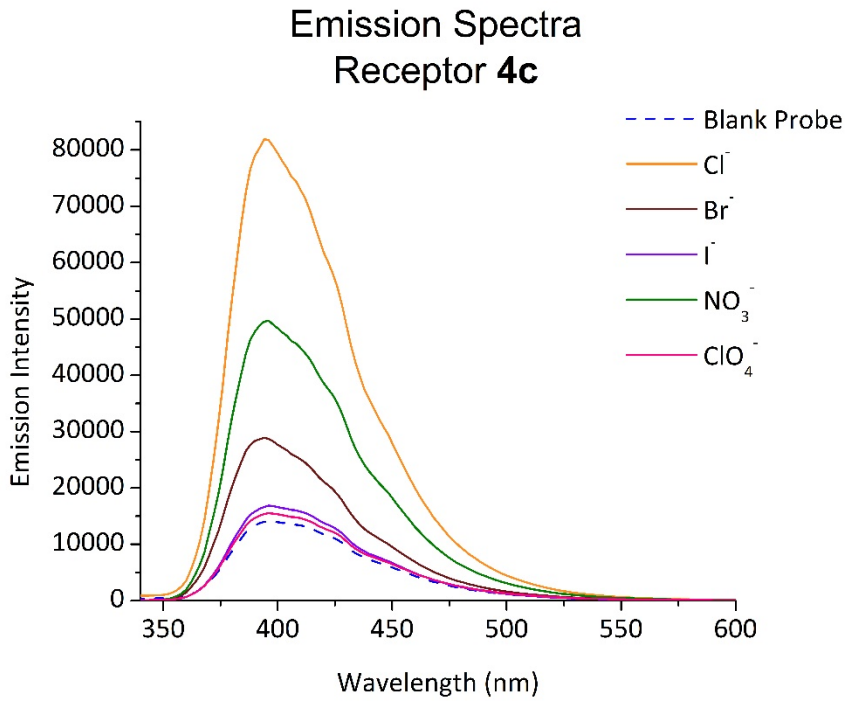

Figure 13. Fluorescence emission spectra of receptor **4c** $CHCl_3$.

NMR Spectra

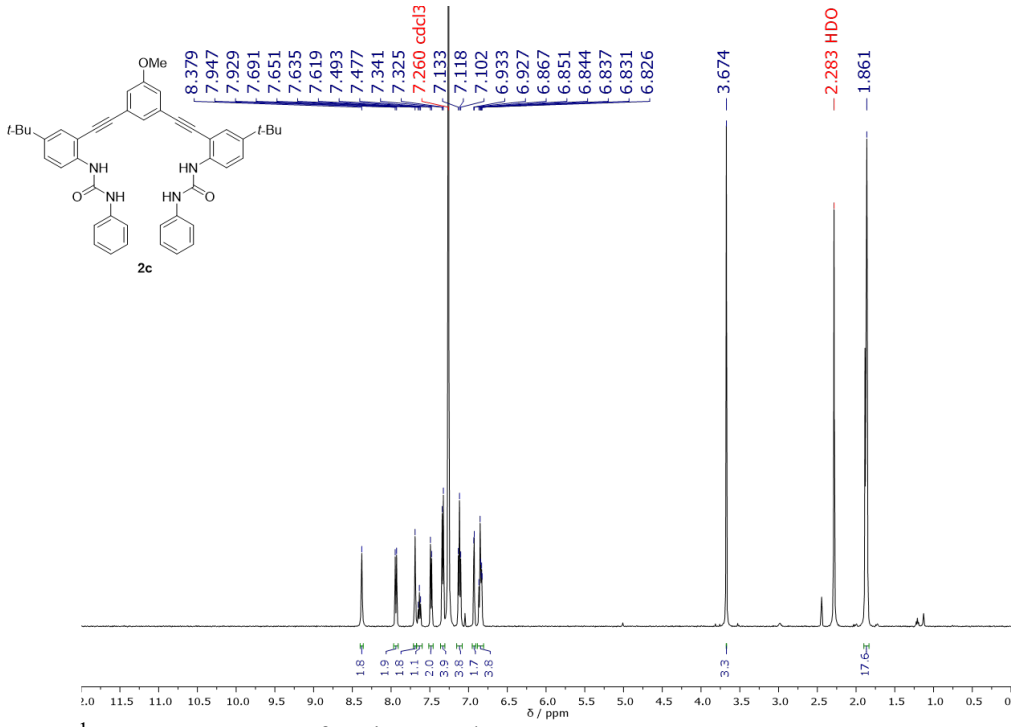

Figure 14. ^{1}H NMR spectra of **2c** in $CDCl_3$.

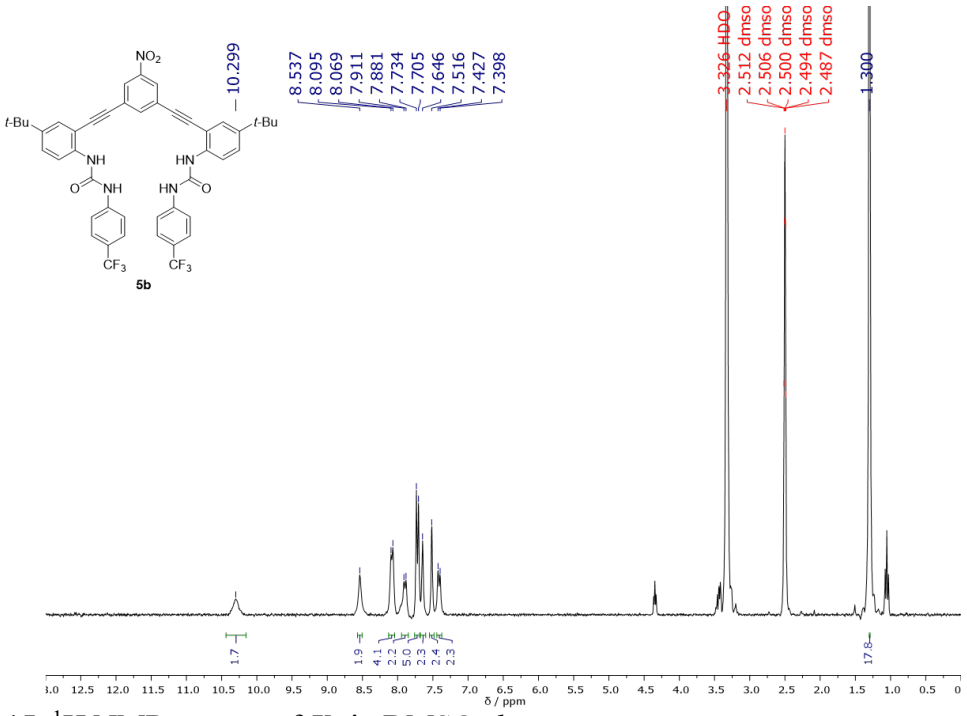

Figure 15. ^{1}H NMR spectra of **5b** in DMSO-d_6.

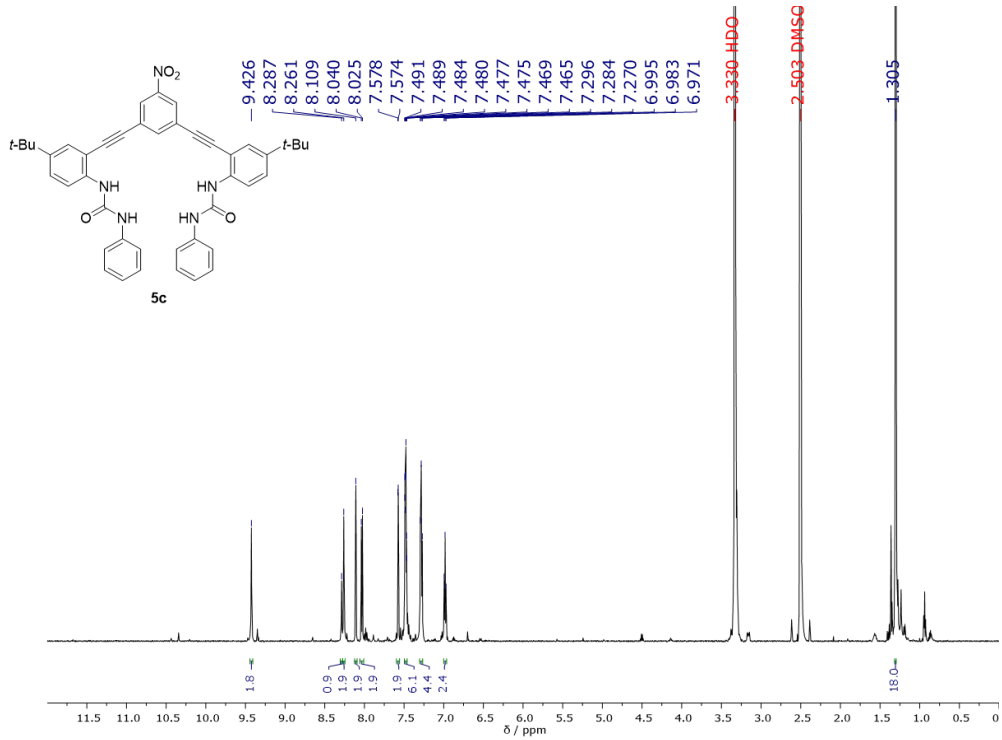

Figure 16. ^{1}H NMR spectra of **5c** in DMSO-d_6.

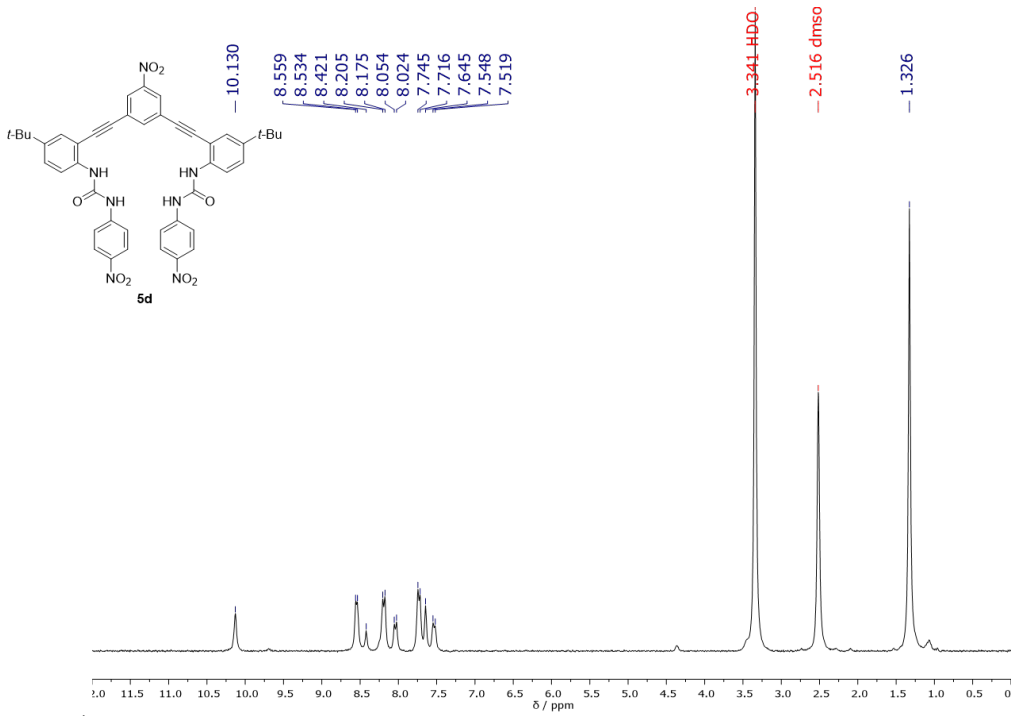

Figure 17. ^{1}H NMR spectra of **5d** in DMSO-d_6.

APPENDIX D

SUPPLEMENTARY INFORMATION FOR CHAPTER V

CH420/520 – Physical Organic Chemistry I

Wikipedia Physical Organic Chemistry Project Option
Required for CH520
Optional for CH420

Important Dates:

- **Topic approval** by Friday, February 16th
- **Intro + one sub-section, including high quality image,** due Thursday, March 1
- **"How To" Wikipedia editing sessions:** Monday, March 5 from 4-5:30pm and Wednesday, March 7, 5-6:30 pm
- **Final Presentations:** TBD Friday, March 16th
- **Final page due at time of presentation (formatted as a document and submitted to Wikipedia for publication)**

ALL SUBMISSIONS SHOULD BE MADE VIA CANVAS BY THE START OF CLASS ON DUE DATE!

Objective: Science communication, both verbal and written, is a key to being a successful scientist. Using your knowledge of physical organic chemistry, create a Wikipedia article on a subject matter in the field.

The ability for a scientist to communicate their field of study to a broad audience is vital for the advancement of science. Wikipedia is a main source of knowledge for many people around the world. When articles are written by a knowledgeable source with proper citations, Wikipedia can be a useful source but it can also be a source for extreme error and confusion if done improperly.[1] This final project allows you, a soon-to-be expert in physical organic chemistry, to write a Wikipedia page on a subject within the area of physical organic chemistry.

You are tasked with finding a page on Wikipedia written on a concept covered in physical organic chemistry that is severely lacking in information or does not exist at all. Below is a link provided on the WikiProjects Chemistry page that displays topics needing to be edited. You can pick one from this list or you can choose a different one, with the caveat that there is not already a substantive Wikipedia page about the subject.

WikiProjects Chemistry Page Requested Articles:
https://en.wikipedia.org/wiki/Wikipedia:Requested_articles/Natural_sciences/Chemistry
WikiProjects Chemistry Page Clean-Up Needed:
https://tools.wmflabs.org/bambots/cwb/bycat/Chemistry.html

Your Wikipedia article must be well-written so a member of the public with general organic chemistry knowledge can understand it. It must include:

- An introduction and at least three, well-written sub-sections;
- A description of the chemical importance/applications of the subject matter;
- A minimum of three high-quality images that help explain the topic;
- A proper Wikipedia-style bibliography with at least eight citations provided for the general reader to find more information (you will likely find that you will need to use many more than eight citations to cover your topic properly).

We will provide 2 editing sessions before the final deadline. It is highly suggested you attend these sessions and have your project completely written prior to editing the Wikipedia page itself.

This assignment is optional for CH420 students. If you are interested, talk to us and we can negotiate what appropriate "extra credit" would be for completing this.

Figure 1. Front page of the final project guidelines given to students.

CH420/520 – Physical Organic Chemistry I

At the end of the term, you will give a MAX 2-minute elevator pitch about the before/after of your Wikipedia article and the impact of the scientific information on the page. This may include one slide for assistance but a slide is not necessary. Again, you should consider your audience to be somewhat knowledgeable in the area of organic chemistry (think first-term sophomore-level organic chemistry students).

Deadline: Approve your project with us by Friday, February 16th. **Approval should be obtained by turning in to Canvas a subject decision and the sub-sections titles you plan to cover, with at least one relevant reference.**

[1]Relevant J. Chem. Ed. Article on the importance of accuracy on Wikipedia:
http://pubs.acs.org/doi/pdf/10.1021/acs.jchemed.6b00478

Example of well-done articles:
Host-guest chemistry https://en.wikipedia.org/wiki/Host%E2%80%93guest_chemistry
Energy Profile https://en.wikipedia.org/wiki/Energy_profile_(chemistry)

Info on elevator pitches:
http://idealistcareers.org/a-quick-guide-to-writing-your-elevator-pitch-with-examples/
http://www.forbes.com/sites/nextavenue/2013/02/04/the-perfect-elevator-pitch-to-land-a-job/#4afbe2877cbd
http://theinterviewguys.com/write-elevator-pitch/

Figure 2. Back page of the final project guidelines given to students.

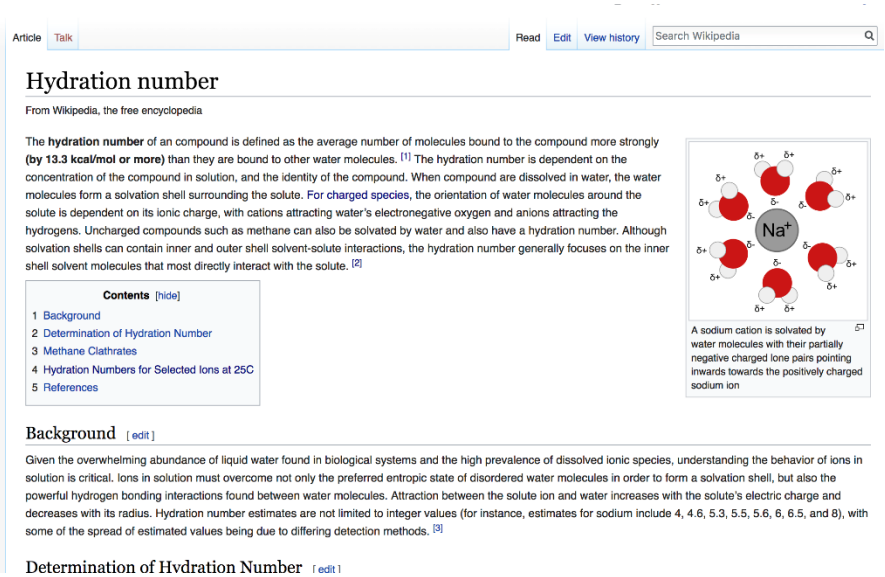

Figure 3. Screenshot of Hydration number Wikipedia page created by a student for this project. Screenshot taken March 2018.

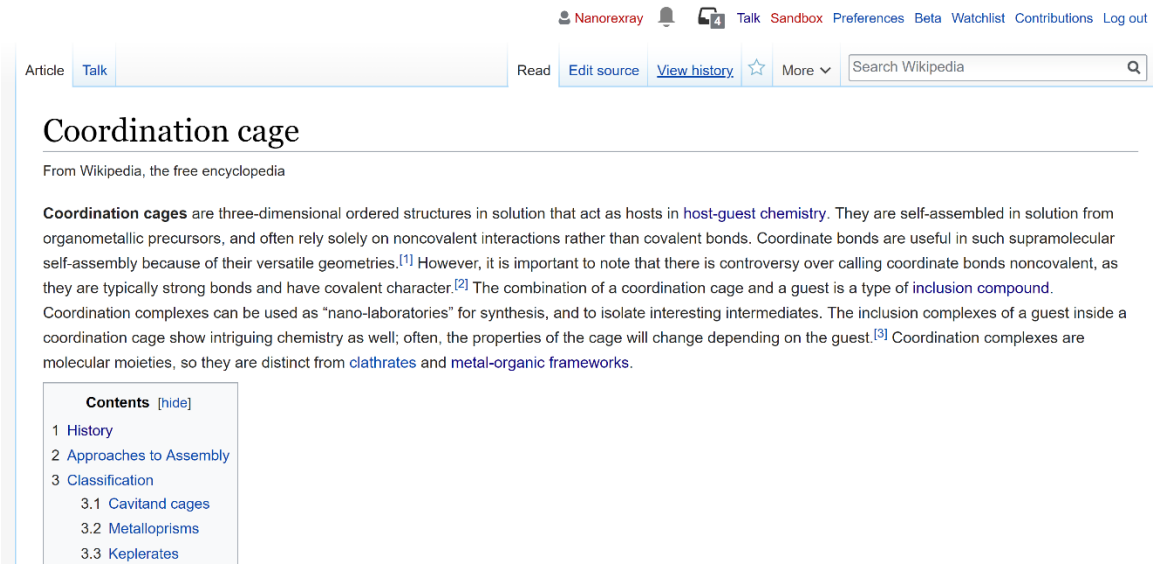

Figure 4. Screenshot of Coordination cage Wikipedia page created by a student for this project. Screenshot taken March 2018.

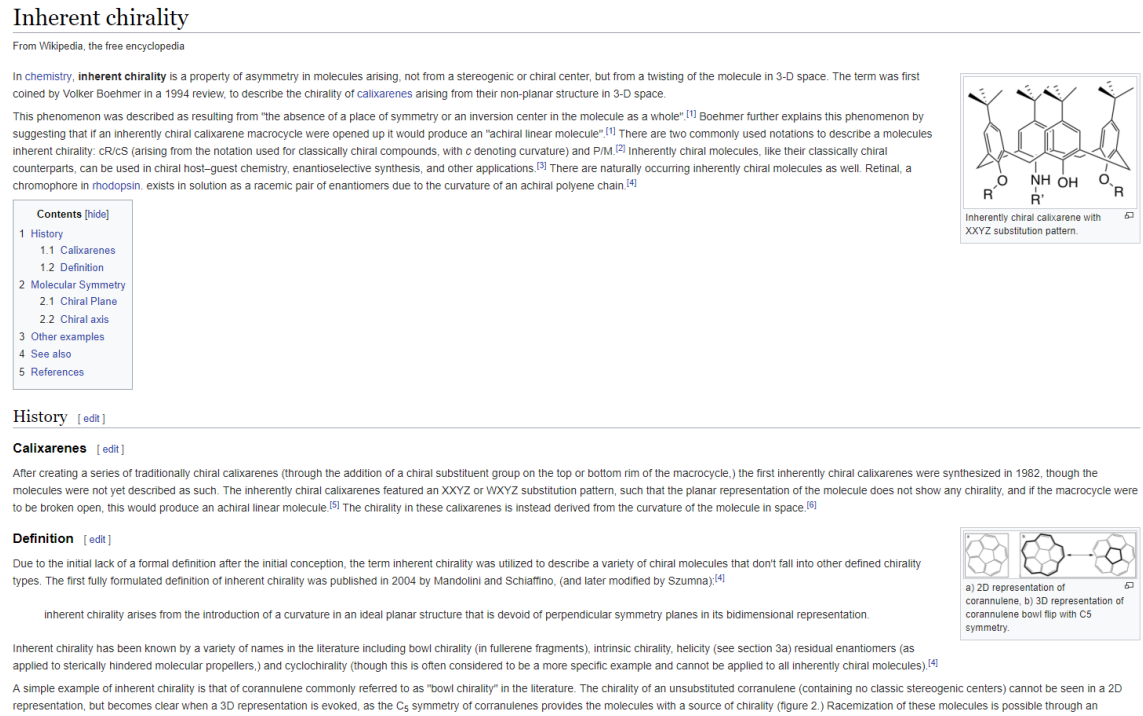

Figure 5. Screenshot of Inherent chirality Wikipedia page created by a student for this project. Screenshot taken March 2018.

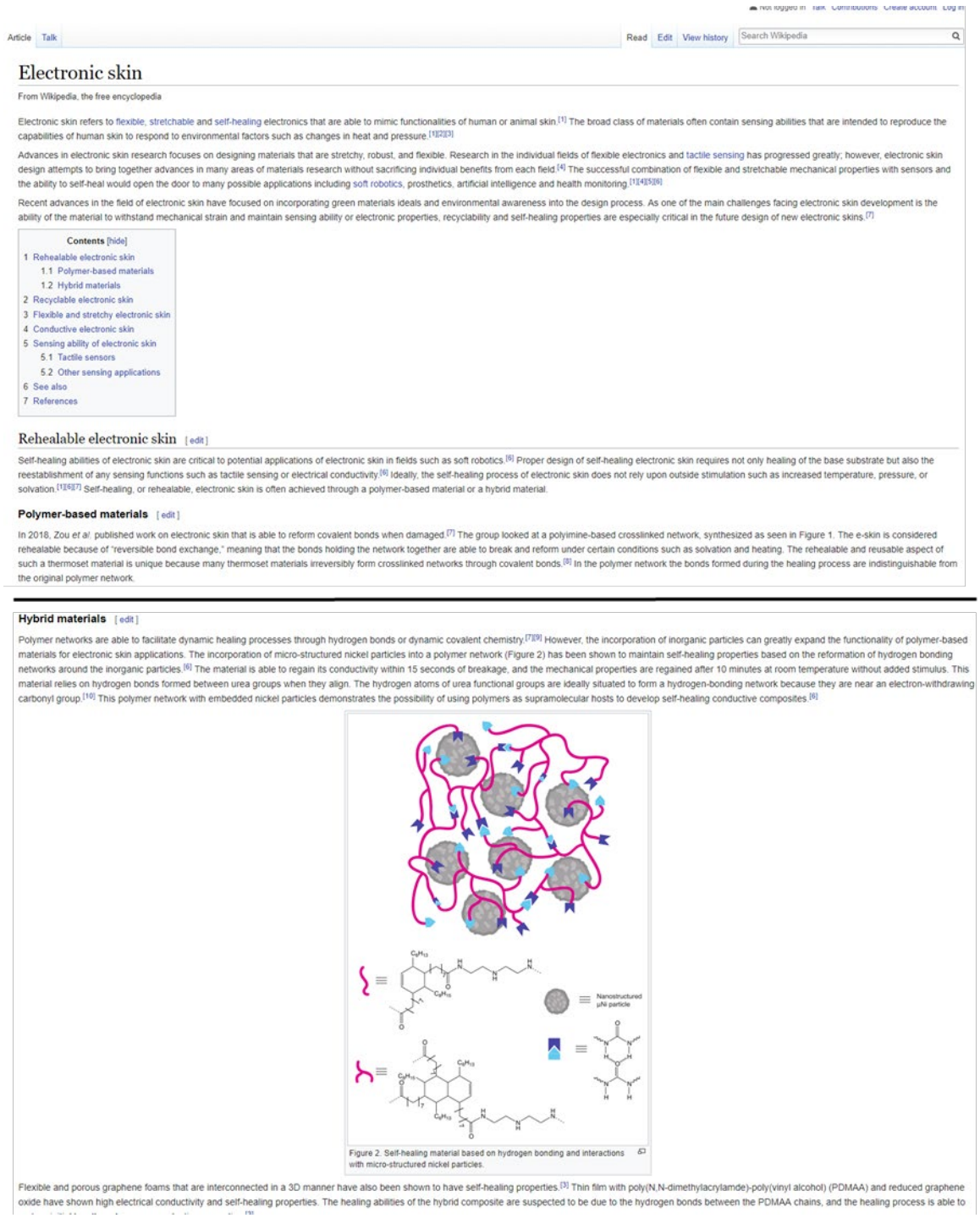

Article Talk Read Edit View history Search Wikipedia

Electronic skin

From Wikipedia, the free encyclopedia

Electronic skin refers to flexible, stretchable and self-healing electronics that are able to mimic functionalities of human or animal skin.[1] The broad class of materials often contain sensing abilities that are intended to reproduce the capabilities of human skin to respond to environmental factors such as changes in heat and pressure.[1][2][3]

Advances in electronic skin research focuses on designing materials that are stretchy, robust, and flexible. Research in the individual fields of flexible electronics and tactile sensing has progressed greatly; however, electronic skin design attempts to bring together advances in many areas of materials research without sacrificing individual benefits from each field.[4] The successful combination of flexible and stretchable mechanical properties with sensors and the ability to self-heal would open the door to many possible applications including soft robotics, prosthetics, artificial intelligence and health monitoring.[1][4][5][6]

Recent advances in the field of electronic skin have focused on incorporating green materials ideals and environmental awareness into the design process. As one of the main challenges facing electronic skin development is the ability of the material to withstand mechanical strain and maintain sensing ability or electronic properties, recyclability and self-healing properties are especially critical in the future design of new electronic skins.[7]

Contents [hide]

1 Rehealable electronic skin
  1.1 Polymer-based materials
  1.2 Hybrid materials
2 Recyclable electronic skin
3 Flexible and stretchy electronic skin
4 Conductive electronic skin
5 Sensing ability of electronic skin
  5.1 Tactile sensors
  5.2 Other sensing applications
6 See also
7 References

Rehealable electronic skin [edit]

Self-healing abilities of electronic skin are critical to potential applications of electronic skin in fields such as soft robotics.[6] Proper design of self-healing electronic skin requires not only healing of the base substrate but also the reestablishment of any sensing functions such as tactile sensing or electrical conductivity.[6] Ideally, the self-healing process of electronic skin does not rely upon outside stimulation such as increased temperature, pressure, or solvation.[1][6][7] Self-healing, or rehealable, electronic skin is often achieved through a polymer-based material or a hybrid material.

Polymer-based materials [edit]

In 2018, Zou *et al.* published work on electronic skin that is able to reform covalent bonds when damaged.[7] The group looked at a polyimine-based crosslinked network, synthesized as seen in Figure 1. The e-skin is considered rehealable because of "reversible bond exchange," meaning that the bonds holding the network together are able to break and reform under certain conditions such as solvation and heating. The rehealable and reusable aspect of such a thermoset material is unique because many thermoset materials irreversibly form crosslinked networks through covalent bonds.[8] In the polymer network the bonds formed during the healing process are indistinguishable from the original polymer network.

Hybrid materials [edit]

Polymer networks are able to facilitate dynamic healing processes through hydrogen bonds or dynamic covalent chemistry.[7][9] However, the incorporation of inorganic particles can greatly expand the functionality of polymer-based materials for electronic skin applications. The incorporation of micro-structured nickel particles into a polymer network (Figure 2) has been shown to maintain self-healing properties based on the reformation of hydrogen bonding networks around the inorganic particles.[6] The material is able to regain its conductivity within 15 seconds of breakage, and the mechanical properties are regained after 10 minutes at room temperature without added stimulus. This material relies on hydrogen bonds formed between urea groups when they align. The hydrogen atoms of urea functional groups are ideally situated to form a hydrogen-bonding network because they are near an electron-withdrawing carbonyl group.[10] This polymer network with embedded nickel particles demonstrates the possibility of using polymers as supramolecular hosts to develop self-healing conductive composites.[6]

Figure 2. Self-healing material based on hydrogen bonding and interactions with micro-structured nickel particles.

Flexible and porous graphene foams that are interconnected in a 3D manner have also been shown to have self-healing properties.[3] Thin film with poly(N,N-dimethylacrylamde)-poly(vinyl alcohol) (PDMAA) and reduced graphene oxide have shown high electrical conductivity and self-healing properties. The healing abilities of the hybrid composite are suspected to be due to the hydrogen bonds between the PDMAA chains, and the healing process is able to

Figure 6. Screenshot of Electronic skin Wikipedia page created by a student for this project. Screenshot taken March 2019.

REFERENCES CITED

Chapter I

1. M. F. Hossain, *Agric. Ecosyst. Environ.*, 2006, **113**, 1–16.

2. (a) S. Fields, *Environ. Health. Perspect.*, 2004, **112**, A556–A563; (b) U.S. Environmental Protection Agency Nutrient Pollution: The Problem, https://www.epa.gov/nutrientpollution/problem, (accessed November 2018); (c) J. F. Power and J. S. Schepers, *Agric. Ecosyst. Environ.*, 1989, **26**, 165–187; (d) W. H. M. Strebel, K. Wick, C. Heumesser and E. J. Schmid, *Environ. Manage.*, 2012, **111**, 178–186; (e) M. M. Mekonnen and A. Y. Hoekstra, *Water Resour. Res.*, 2018, **54**, 345–358.

3. B. A. Moyer, R. Custelcean, B. P. Hay, J. L. Sessler, K. Bowman-James, V. W. Day and S.-O. Kang, *Inorg. Chem.*, 2013, **52**, 3473–3490.

4. M. A. Gray, J. P. Winpenny, B. Verdon, H. McAlroy and B. E. Argent, *Biosci. Rep.* 1995, **15**, 531–541.

5. R. Wang, *Physiol. Rev.*, 2012, **92**, 791–896.

6. J. D. Coates and L. A. Achenbach, *Nat. Rev. Microbiol.*, 2004, **2**, 569–580.

7. (a) L. Ojha, M. B. Wilhelm, S. L. Murchie, A. S. McEwen, J. J. Wray, J. Hanley, M. Massé and M. Chojnacki, *Nat. Geosci*. 2015, **8**, 829–832; (b) R. A. Kerr, *Science*, 2013, **340**, 138; (c) While this comment is made with a bit of our tongues in our cheeks, we must acknowledge some inspiration from sci-fi extraterrestrial terraforming visions, such as that found in the *Mars Trilogy* by Kim Stanley Robinson.

8. (a) For an exhaustive review on approaches to anion recognition and an analysis of anion sizes, geometries, and interaction types, see: P. Molina, F. Zapata and A. Caballero, *Chem. Rev.*. 2017, **117**, 9907–9972; (b) J. L. Sessler, P. A. Gale and W.-S. Cho, *Anion Receptor Chemistry*, Royal Society of Chemistry, Cambridge, 2006; (c) P. A. Gale and W. Dehaen, *Anion Recognition in Supramolecular Chemistry*, Springer, Berlin, 2010.

9. For more comprehensive reviews of anion recognition see: (a) J. W. Steed and J. L. Atwood, *Supramol. Chem.,* John Wiley and Sons, 2nd edn, 2009; (b) P. A. Gale, E. N. W. Howe and X. Wu, *Chem.* 2016, **1**, 351–422; (c) J. Zhao, D. Yang, X.-J. Yang and B. Wu, *Coord. Chem. Rev.*, 2019, **378**, 415–444; (d) For a thorough review of CH hydrogen bond donors in anion recognition, see: J. Cai and J. L. Sessler, *Chem. Soc. Rev.,* 2014, **43**, 6198–6213.

10. For a comprehensive history and description of the weak hydrogen bond see: G. R. Desiraju and T. Steiner, *The Weak Hydrogen Bond: In Structural Chemistry and Biology*, Oxford University Press, Oxford, 1999.

11. (a) L. Pauling, *J. Am. Chem. Soc.*, 1935, **57**, 2680–2684; (b) L. Pauling and M. Delbrück, *Science*, 1940, **92**, 77–79; (c) The University of Oregon (Ducks) and Oregon State University (Beavers) have a productive collaboration and competition in educating students in our state, and we have many research collaborations (for instance, the NSF Center for Sustainable Materials Chemistry is a longstanding collaboration between many faculty at both institutions, e.g., B. L. Fulton, C. K. Perkins, R. H. Mansergh, M. A. Jenkins, V. Gouliouk, M. N. Jackson, Jr., J. C. Ramos, N. M. Rogovoy, M. T. Gutierrez-Higgins, S. W. Boettcher, J. F. Conley, D. A. Keszler, J. E. Hutchison and D. W. Johnson, *Chem. Mater.* **2017**, *29*, 7760–7765). On the athletics fields the Ducks and Beavers are fierce, fairly friendly, rivals.

12. Around the same time as Pauling's observations on the hydrogen bond, Kumler also noted its importance to dielectric constants, dipole moments, and hydrogen bonds in amides, among other functional groups. Of particular relevance to this *Feature Article*, Kumler likely offered the first observation of a CH HB between molecules of HCN; see: W. D. Kumler, *J. Am. Chem. Soc.*, 1935, **57**, 600–605.

13. (a) J. R. Quinn, S. C. Zimmerman, J. E. Del Bene and I. Shavitt, *J. Am. Chem. Soc.*, 2007, **129**, 934–941; (b) K. S. Jeong, T. Tjivikua, A. Muehldorf, G. Deslongchamps, M. Famulok and J. Rebek, Jr., *J. Am. Chem. Soc.*, 1991, **113**, 201–209.

14. L. Pauling, *The Nature of the Chemical Bond*, Cornell University Press, Ithaca, NY, 1939.

15. G. R. Desiraju, *Angew. Chem. Int. Ed*., 2011, **50**, 52–59.

16. (a) E. Arunan, G. R. Desiraju, R. A. Klein, J. Sadlej, S. Scheiner, I. Alkorta, D. C. Clary, R. H. Crabtree, J. J. Dannenberg, P. Hobza, H. G. Kjaergaard, A. C. Legon, B. Mennucci and D. J. Nesbitt, *Pure Appl. Chem.*, 2011, **83**, 1619–1636; (b) E. Arunan, G. R. Desiraju, R. A. Klein, J. Sadlej, S. Scheiner, I. Alkorta, D. C. Clary, R. H. Crabtree, J. J. Dannenberg, P. Hobza, H. G. Kjaergaard, A. C. Legon, B. Mennucci and D. J. Nesbitt, *Pure Appl. Chem.*, 2011, **83**, 1637–1641.

17. (a) D. J. Sutor, *Acta. Cryst.*, 1958, **11**, 453–458; (b) D. J. Sutor, *Nature*, 1962, **195**, 68–69; (c) D. J. Sutor, *J. Chem. Soc.*, 1963, 1105–1110.

18. J. Donohue in *Structural Chemistry and Molecular Biology,* ed. A. Rich and N. Davidson, W. H. Freeman, San Francisco, 1968, pp. 443–465.

19. R. Taylor and O. Kennard, *J. Am. Chem. Soc.*, 1982, **104**, 5063–5070.

20. C. H. Schawlbe, *Crystallogr. Rev.*, 2012, **18**, 191–206.

21. G. R. Desiraju, *Acc. Chem. Res.*, 1996, **29**, 441–449.

22. The first account of a solution-state quantification of the C–H···X$^-$ interaction was in fact published in 1990 but the next publication was over a decade later. See: W. B. Farnham, D. C. Roe, D. A. Dixon, J. C. Calabrese, R. L. Harlow, *J. Am. Chem. Soc.*, 1990, **112**, 7707–7718.

23. Some examples of solution-state quantifications of the CH hydrogen bond: (a) C. A. Ilioudis, D. A. Tocher and J. W. Steed, *J. Am. Chem. Soc.*, 2004, **126**, 12395–12402; (b) H. Maeda and Y. Kusunose, *Chem. Eur. J.*, 2005, **11**, 5661–5666; (c) I. E. D. Vega, P. A. Gale, M. E. Light and S. J. Loeb, *Chem. Commun.*, 2005, 4913–4915; (d) M. J. Chimielewski and J. Jurczak, *Chem. Eur. J.*, 2006, **12**, 7652–7667; (e) J. L. Adcock and H. Zhang, *J. Org. Chem.*, 1995, **60**, 1999–2002.

24. A selection of recent work not highlighted herein: (a) K. P. McDonald, R. O. Ramabhadran, S. Lee, K. Raghavachari and A. H. Flood, *Org. Lett.*, 2011, **13**, 6260–6263; (b) L. C. Gilday, N. G. White and P. D. Beer, *Dalton Trans.*, 2012, **41**, 7092–7097; (c) C. J. Massena, A. M. S. Riel, G. F. Neuhaus, D. A. Decato and O. B. Berryman, *Chem. Commun.*, 2015, **51**, 1417–1420; (d) Y. Hua, R. O. Ramabhadran, E. O. Uduehi, J. A. Karty, K. Raghavachari and A. Flood, *Chem. Eur. J.*, **2011**, 17, 312–321.

25. A. Bianchi, K. Bowman-James and E. Garcia-Espana, *Supramolecular Chemistry of Anions*, Wiley-VCH, New York, 1997.

26. O. B. Berryman, A. C. Sather, B. P. Hay, J. S. Meisner and D. W. Johnson, *J. Am. Chem. Soc.*, 2008, **130**, 10895–10897.

27. (a) B. P. Hay and V. S. Bryanstev, *Chem. Commun.*, 2008, 2417–2428; (b) O. B. Berryman, V. S. Bryanstev, D. P. Stay, D. W. Johnson and B. P. Hay, *J. Am. Chem. Soc.*, 2007, **129**, 48–58; (c) For an overview of related work, a snapshot of research at the time, and pictures of much younger versions of two of the guilty parties, see our earlier *Feature Article*: O. B. Berryman, D. W. Johnson, *Chem. Commun.* 2009, 3143–3153.

28. D.-W. Yoon, D. E. Gross, V. M. Lynch, J. L. Sessler, B. P. Hay and C.-H. Lee, *Angew. Chem. Int. Ed.*, 2008, **47**, 5038–5042.

29. C. Coletti and N. Re, *J. Phys. Chem. A*, 2009, **113**, 1578–1585.

30. O. B. Berryman, C. A. Johnson, II, L. N. Zakharov, M. M. Haley and D. W. Johnson, *Angew. Chem. Int. Ed.*, 2008, **47**, 117–120.

31. C. N. Carroll, O. B. Berryman, C. A. Johnson, II, L. N. Zakharov, M. M. Haley and D. W. Johnson, *Chem. Commun.*, 2009, 2520–2522.

32. B. W. Tresca, L. N. Zakharov, C. N. Carroll, D. W. Johnson and M. M. Haley, *Chem. Commun.*, 2013, **49**, 7240–7242.

33. (a) C. N. Carroll, B. A. Coombs, S. P. McClintock, C. A. Johnson II, O. B. Berryman, D. W. Johnson and M. M. Haley, *Chem. Commun.*, 2011, **47**, 5539–5541; (b) J. M. Engle, P. S. Lakshminarayanan, C. N. Carroll, L. N. Zakharov, M. M. Haley and D. W. Johnson, *Cryst. Growth Des.*, 2011, **11**, 5144–5152; (c) J. M. Engle, C. N. Carroll, D. W. Johnson and M. M. Haley, *Chem. Sci.*, 2012, **3**, 1105–1110; (d) M. M. Watt, L. N. Zakharov, M. M. Haley and D. W. Johnson, *Angew. Chem. Int. Ed.*, 2013, **52**, 10275–10280; (e) J. V. Gavette, N. S. Mills, L. N. Zakharov, C. A. Johnson II, D. W. Johnson and M. M. Haley, *Angew. Chem. Int. Ed.*, 2013, **52**, 10270–10274; (f) J. V. Gavette, C. J. Evoniuk, L. N. Zakharov, M. E. Carnes, M. M. Haley and D. W. Johnson, *Chem. Sci.*, 2014, **5**, 2899–2905; (g) L. M. Eytel, A. C. Brueckner, J. A. Lohrman, M. M. Haley, P. H.-Y. Cheong and D. W. Johnson, *Chem. Commun.*, 2018, **54**, 13208-13211.

34. For the sake of this review, we focus on receptors implementing aryl CH hydrogen bonds. For a comprehensive review on combined interactions, see ref. 8a.

35. Y. Li and A. H. Flood, *Angew. Chem. Int. Ed.*, 2008, **47**, 2649–2652.

36. A selection of triazolophane papers: (a) K. P. McDonald, Y. Hua, S. Lee and A. Flood, *Chem. Commun.*, 2012, **48**, 5065–5075; (b) Y. Li and A. H. Flood, *J. Am. Chem. Soc.*, 2008, **130**, 12111–12122; (c) R. O. Ramabhadran, Y. Hua, A. H. Flood and K. Raghavachari, *Chem. Eur. J.* 2011, **17**, 9123–9129; (d) I. Bandyopadhyay, K. Raghavachari and A. H. Flood, *Chem. Phys. Chem.*, 2009, **10**, 2535–2540; (e) E. M. Zahran, Y. Hua, Y. Li, A. H. Flood and L. G. Bachas, *Anal. Chem.*, 2010, **82**, 368–375.

37. S. Lee, B. E. Hirsch, Y. Liu, J. R. Dobscha, D. W. Burke, S. L. Tait and A. H. Flood, *Chem. Eur. J.*, 2016, **22**, 560–569.

38. (a) R. M. Meudtner and S. Hecht, *Angew. Chem. Int. Ed*., 2008, **47**, 4926–4930; (b) S. Lee, Y. Hua and A. H. Flood, *J. Org. Chem.*, 2014, **79**, 8383–8396; (c) Y. Hua and A. H. Flood, *J. Am. Chem. Soc.*, 2010, **132**, 12838–12840; (d) H. Juwarker, J. M. Lenhardt, D. M. Pham and S. L. Craig, *Angew. Chem. Int. Ed.*, 2008, **47**, 3740–3743.

39. J. L. Sessler, J. Cai, H.-Y. Gong, X. Yang, J. F. Arambula and B. P. Hay, *J. Am. Chem. Soc.*, 2010, **132**, 14058–14060.

40. M. G. Fisher, P. A. Gale, J. R. Hiscock, M. B. Hursthouse, M. E. Light, F. P. Schmidtchen and C. C. Tong, *Chem. Commun.*, 2009, 3017–3019.

41. (a) D. Curiel, A. Espinosa, M. Más-Montoya, G. Sánchez, A. Tárraga and P. Molina, *Chem. Commun.*, 2009, 7539–7541; (b) F. García, J. Aragó, R. Viruela, E. Ortí and L. Sánchez, *Org. Biomol. Chem.*, 2013, **11**, 765–772.

42. (a) Y. Hua and A. H. Flood, *Chem. Soc. Rev.*, 2010, **39**, 1262–1271; (b) B. Schulze and U. S. Schulbert*, Chem. Soc. Rev.*, 2014, **43**, 2522–2571.

43. M. A. Majewski, Y. Hong, T. Lis, J. Gregoliński, P. J. Chmielewski, J. Cybińska, D. Kim and M. Stępień, *Angew. Chem. Int. Ed.*, 2016, **55**, 14072–14076.

44. B. W. Tresca, R. J. Hansen, C. V. Chau, B. P. Hay, L. N. Zakharov, M. M. Haley and D. W. Johnson, *J. Am. Chem. Soc.*, 2015, **137**, 14959–14967.

45. S. Lee, C.-H. Chen and A. H. Flood, *Nat. Chem.*, 2013, **5**, 704–710.

46. A selection of cyanostar-related publications: (a) B. Qiao, J. R. Anderson, P. Pink and A. H. Flood, *Chem. Commun.*, 2016, **52**, 8683–8686; (b) E. M. Fatila, E. B. Twum, A. Sengupta, M. Pink, J. A. Karty, K. Raghavachari and A. H. Flood, *Angew. Chem. Int. Ed.*, 2016, **55**, 14057–14062; (c) C. R. Bensen, E. M. Fatila, S. Lee, M. G. Marzo, M. Pink, M. B. Mills, K. E. Preuss and A. H. Flood, *J. Am. Chem. Soc.*, 2016, **138**, 15057–15065; (d) E. M. Fatila, E. B. Twum, J. A. Karty and A. H. Flood, *Chem. Eur. J.*, 2017, **23**, 10652–10662.

47. W. V. Rossom, T. G. Terentyeva, K. Sodeyama, Y. Matsushita, Y. Tateyama, K. Ariga and J. P. Hill, *Org. Biomol. Chem.*, 2014, **12**, 5492–5499.

48. Y. Choi, T. Kim, S. Jang and J. Kang, *New. J. Chem.*, 2016, **40**, 794–802.

49. N. Lau, L. N. Zakharov and M. D. Pluth, *Chem. Commun*., 2018, **54**, 2337–2340.

50. Based on Pauling's electronegativity scale, the electrostatic difference between carbon and hydrogen is 0.35.

51. B. W. Tresca, A. C. Brueckner, M. M. Haley, P. H.-Y. Cheong and D. W. Johnson, *J. Am. Chem. Soc.*, 2017, **139**, 3962–3965.

52. Y. Liu, A. Sengupta, K. Raghavachari and A. H. Flood, *Chem*, 2017, **3**, 411–427.

53. P. S. Cremer, A. H. Flood, B. C. Gibb and D. L. Mobley, *Nat. Chem.*, 2018, **10**, 8–16.

54. A. Sengupta, Y. Liu, A. H. Flood and K. Raghavachari, *Chem. Eur. J.*, 2018, **24**, 14409–14417.

55. These solvation effects are well-recognized in the field of anion binding in general. For selected recent reviews on the thermodynamics of anion binding and discussions on solvation effects, see: (a) B. C. Gibb, *Isr. J. Chem.*, 2011, **51**, 798–806; (b) M. B. Hillyer and B. C. Gibb, *Annu. Rev. Phys. Chem.*, 2016, **67**, 307–329; (c) H. I. Okur, J. Hladíková, K. B. Rembert, Y. Cho, J. Heyda, J. Dzubiella, P. S. Cremer and P. Jungwirth, *J. Phys. Chem. B*, 2017, **121**, 1997–2014.

56. M. D. Hartle, R. J. Hansen, B. W. Tresca, S. S. Prakel, L. N. Zakharov, M. M. Haley, M. D. Pluth and D. W. Johnson, *Angew. Chem. Int. Ed.*, 2016, **55**, 11480–11484.

57. J. Vázquez and V. Sindelar, *Chem. Commun.*, 2018, **54**, 5859–5862.

58. (a) H. A. Fargher, N. Lau, L. N. Zakharov, M. M. Haley, D. W. Johnson and M. D. Pluth, *Chem. Sci.*, 2019, **10**, 67–72; (b) C.-L. Deng, J. P. Bard, J. A. Lohrman, J. E. Barker, L. N. Zakharov, D. W. Johnson, M. M. Haley, *Angew. Chem. Int. Ed.* 2019, **58**, 3934-3938, 10.1002/anie.201814431.

59. C. D. Sessler, M. Rahm, S. Becker, J. M. Goldberg, F. Wang and S. J. Lippard, *J. Am. Chem. Soc.*, 2017, **139**, 9325–9332.

60. D. Reniciuk, O. Blacque, M. Vorlickova and B. Spingler, *Nucl. Acids Res.*, 2013, **41**, 9891–9900.

Chapter II

1. a) J. L. Sessler, P. A. Gale, W.-S. Cho, *Anion Receptor Chemistry*, Royal Society of Chemistry, Cambridge, UK, **2006**; b) P. A. Gale, W. Dehaen, *Anion Recognition in Supramolecular Chemistry*, Springer, Berlin, Germany, **2010**.

2. a) M. Giese, M. Albrecht, K. Rissanen, *Chem. Rev.* **2015**, *115*, 8867; b) N. Busschaert, C. Caltagirone, W. Van Rossom, P. A. Gale, *Chem. Rev.* **2015**, *115*, 8038.

3. O. B. Berryman, D. W. Johnson, *Chem. Commun.* **2009**, 3143.

4. V. S. Bryantsev, B. P. Hay, *Org. Lett.* **2005**, *7*, 5031.

5. C. N. Carroll, J. J. Naleway, M. M. Haley, D. W. Johnson, *Chem. Soc. Rev.* **2010**, *39*, 3875.

6. C. L. Vonnegut, B. W. Tresca, D. W. Johnson, M. M. Haley, *Chem. Asian J.* **2015**, *10*, 522.

7. a) B. W. Tresca, L. N. Zakharov, C. N. Carroll, D. W. Johnson, M. M. Haley, *Chem. Commun.* **2013**, *49*, 7240; b) B. W. Tresca, R. J. Hansen, C. V. Chau, B. P. Hay, L. N. Zakharov, M. M. Haley, D. W. Johnson, *J. Am. Chem. Soc.* **2015**, *137*, 14959.

8. a) J. V. Gavette, C. J. Evoniuk, L. N. Zakharov, M. E. Carnes, M. M. Haley, D. W. Johnson, *Chem. Sci.* **2014**, *5*, 2899; b) C. N. Carroll, B. A. Coombs, S. P. McClintock, C. A. Johnson II, O. B. Berryman, D. W. Johnson, M. M. Haley, *Chem. Commun.* **2011**, *47*, 5539; c) J. V. Gavette, N. S. Mills, L. N. Zakharov, C. A. Johnson II, D. W. Johnson, M. M. Haley, *Angew. Chem.* **2013**, *125*, 10460; *Angew. Chem. Int. Ed.* **2013**, *52*, 10270; e) J. M. Engle, P. S. Lakshminarayanan, C. N. Carroll, L. N. Zakharov, M. M. Haley, D. W. Johnson, *Cryst. Growth Des.* **2011**, *11*, 5144; f) J. M. Engle, C. N. Carroll, D. W. Johnson, M. M. Haley, *Chem. Sci.* **2012**, *3*, 1105; g) M. M. Watt, J. M. Engle, K. C. Fairley, T. E. Robitshek, M. M. Haley, D. W. Johnson, *Org. Biomol. Chem.* **2015**, *13*, 4266; h) M. D. Hartle, R. J. Hansen, B. W. Tresca, S. S. Prakel, L. N. Zakharov, M. M. Haley, M. D. Pluth, D. W. Johnson, *Angew. Chem.* **2016**, *128*, 11652; *Angew. Chem. Int. Ed.* **2016**, *55*, 11480.

9. M. M. Watt, L. N. Zakharov, M. M. Haley, D. W. Johnson, *Angew. Chem.* **2013**, *125*, 10465; *Angew. Chem. Int. Ed.* **2013**, *52*, 10275.

10. a) P. de Hoog, P. Gamez, H. Mutikainen, U. Turpeinen, J. Reedijk, *Angew. Chem.* **2004**, *116*, 5939; *Angew. Chem. Int. Ed.* **2004**, *43*, 5815; b) S. Demeshko, S. Dechert, F. Meyer, *J. Am. Chem. Soc.* **2004**, *126*, 4508; c) Y. S. Rosokha, S. V. Lindeman, S. V. Rosokha, J. K. Kochi, *Angew. Chem.* **2004**, *116*, 4750; *Angew. Chem. Int. Ed.* **2004**, *43*, 4650; d) O. B. Berryman, F. Hof, M. J. Hynes, D. W. Johnson, *Chem. Commun.* **2006**, 506; e) P. Gamez, *Inorg. Chem. Front.* **2014**, ***1***, 35; f) M. Giese, M. Albrecht, K. Rissanen, *Chem. Commun.* **2016**, *52*, 1778; g) P. Ballester, *Acc. Chem. Res.* **2013**, *46*, 874.

11. O. B. Berryman, A. C. Sather, B. P. Hay, J. S. Meisner, D. W. Johnson, *J. Am. Chem. Soc.* **2008**, *130*, 10895.

12. Host concentration for titrations of **3** with TBA^+Cl^- was held constant at 0.4 mM. All other titrations were performed with host concentration of 1.0 mM.

13. a) P. Thordarson, *Chem. Soc. Rev.* **2011**, *40*, 1305; b) http://supramolecular.org/

14. a) Y. Li, M. Pink, J. A. Karty, A. H. Flood, *J. Am. Chem. Soc.* **2008**, *130*, 17293; b) H. Chen, H. Yang, W. Xu, Y. Ta, *RSC Adv.* **2013**, ***3***, 13311; c) M. Giese, M. Albrecht, A. Valkonen, K. Rissanen, *Eur. J. Org. Chem.* **2013**, 3247; d) H. Zhou, Y. Zhao, G. Gao, S. Li, J. Lan, J. You, *J. Am. Chem. Soc.* **2013**, *135*, 14908.

15. F. Ulatowski, K. Dąbrowa, T. Balakier, J. Jurczak, *J. Org. Chem.* **2016**, *81*, 1746.

16. During the titrations of **3**, the saturation point was determined by loss of signals of urea protons H^c and H^b. Further analysis with a 2-to-1 host-guest system indicates NMR-time-scale averaging across two asymmetric probes binding to a single guest. This is consistent with the conformation and stoichiometry found in the crystal structure in Figure 4.

17. Value is at the limit of detection provided by ^{1}H NMR titrations and would be more appropriately determined by UV-Vis spectroscopy.[10,11] The μM concentrations needed to obtain UV-Vis spectroscopy titration data dilute out the expected 2:1 host-guest model, however, leading to titrations only appropriately fit to a 1:1 host-guest model. Association constants determined by these UV-Vis titrations provided a K_a = 32800 M^{-1} (see Supporting Information).

18. K_{dimer} **3** = 500 M^{-1}. While the experiments were done in the same solvent system, it is important to note that the dimerization constants were determined in a solution with different ionic strengths compared to the titrations that produced the association constants. Additionally, the concentration at which the titrations were performed is low, leading to ca.10% of "free" (non-anion-bound) dimer formed in solution at any given time. Thermodynamic equilibria could drive more dimer to form in order to promote the sandwich-like interaction with the anion.

19. CCDC 1507418 contains the supplementary crystallographic data for this paper. These data are provided free of charge by The Cambridge Crystallographic Data Centre.

20. G. M. Sheldrick, *Bruker/Siemens Area Detector Absorption Correction Program*, Bruker AXS, Madison, WI, 1998.

21. G. M. Sheldrick, *Acta Cryst,* **2015**, *C71*, 3–8.

Chapter III

1. (a) J. F. Power, J. S. Schepers, *Agric. Ecosyst. Environ.* 1989, **26**, 165-187; (*b*) W. H. M. Strebel, K. Wick, C. Heumesser, E. J. Schmid, *Environ. Manage.* 2012, **111**, 178-186.

2. M. M. Mekonnen, A. Y. Hoekstra, *Water Resour. Res.* 2018, **54**, 345-358.

3. B. A. Moyer, R. Custelcean, B. P. Hay, J. L. Sessler, K. Bowman-James, V. W. Day, S.-O. Kang, *Inorg. Chem*. 2013, **52**, 3473-3490.

4. J. D. Coates, L. A. Achenbach, *Nat. Rev. Microbiol.* 2004, **2**, 569-580.

5. (*a*) J. L. Sessler, P. A. Gale, W.-S. Cho, *Anion Receptor Chemistry*, Royal Society of Chemistry, Cambridge, **2006**; (*b*) P. A. Gale, W. Dehaen, *Anion Recognition in Supramolecular Chemistry*, Springer, Berlin, **2010**; (*c*) P. Molina, F. Zapata, A. Caballero, *Chem. Rev.* 2017, **117**, 9907-9972.

6. (*a*) J. W. Steed, J. L. Atwood, *Supramolecular Chemistry*, John Wiley and Sons, 2nd edn, **2009**; (*b*) J. Cai, J. L. Sessler, *Chem. Soc. Rev.* 2014, **43**, 6198-6213; (*c*) G. T. Spence, P. D. Beer, *Acc. Chem. Res*. 2013, **46**, 571-586; (*d*) V. S. Bryantsev, B. P. Hay, *J. Am. Chem. Soc.* 2006, **128**, 2035-2042; (*e*) S. J. Brooks, P. A. Gale, M. E. Light, *Chem. Commun*. 2006, 4344-4346; (*e*) S. K. Kim, J. Lee, N. J. Williams, V. M. Lynch, B. P. Hay, B. A. Moyer, J. L. Sessler, *J. Am. Chem. Soc.* 2014, **136**, 15079-15085.

7. (*a*) J. K. Clegg, J. Cremers, A. J. Hogben, B. Breiner, M. M. J. Smulders, J. D. Thoburn, J. R. Nitschke, *Chem. Sci*. 2013, **4**, 68-76; (*b*) K. M. Mullen, P. D. Beer, *Chem. Soc. Rev*. 2009, **38**, 1701-1713; (*c*) B. Portis, A. Mirchi, M. E. Khansari, A. Pramanik, C. R. Johnson, D. R. Powell, J. Leszczynski, M. A. Hossain, *ACS Omega* 2017, **2**, 5840-5849; (*d*) A. Abebayehu, R. Dutta, S.-J. Kim, J. H. Lee, H. Hwang, C.-H. Lee, *Eur. J. Org. Chem*. 2016, 3959-3963; (*e*) C. A. Ilioudis, D. G. Georganopoulou, J. W. Steed, *J. Mater. Chem.* 2002, **4**, 26-36; (*f*) P. Blondeau, M. Segura, R. Pérez-Fernández, J. de Mendoza, *Chem. Soc. Rev.* 2007, **36**, 198-210; (*g*) J. Cai, B. P. Hay, N. J. Young, X. Yang, J. L. Sessler, *Chem. Sci.* 2013, **4**, 1560-1567.

8. (*a*) S.-O. Kang, T. S. Johnson, V. W. Day, K. Bowman-James, *Supramol. Chem.* 2018, **30**, 305-314; (*b*) E. M. Fatila, E. B. Twum, J. A. Karty, A. H. Flood, *Chem. Eur. J.* 2017, **23**, 10652-10662; (*c*) E. M. Fatila, M. Pink, E. B. Twum, J. A. Karty, A. H. Flood, *Chem. Sci.* 2018, **9**, 2863-2872; (*d*) W. Zhao, B. Qiao, C.-H. Chen, A. H. Flood, *Angew. Chem. Int. Ed.* 2017, **56**, 13083-13087; (*e*) S. Lee, B. E. Hirsch, Y. Liu, J. R. Dobscha, D. W. Burke, S. L. Tait, A. H. Flood*, Chem. Eur. J.* 2016, **22**, 560-569.

9. (*a*) C. N. Carroll, B. A. Coombs, S. P. McClintock, C. A. Johnson II, O. B. Berryman, D. W. Johnson, M. M. Haley, *Chem. Commun.* 2011, **47**, 5539-5541; (*b*) J. M. Engle, P. S. Lakshminarayanan, C. N. Carroll, L. N. Zakharov, M. M. Haley, D. W. Johnson, *Cryst. Growth Des.* 2011, **11**, 5144-5152; (*c*) J. M. Engle, C. N. Carroll, D. W. Johnson, M. M. Haley, *Chem. Sci.* 2012, **3**, 1105-1110; (*d*) M. M. Watt, J. M. Engle, K. C. Fairley, T. E. Robitshek, M. M. Haley, D. W. Johnson, *Org. Biomol. Chem.* 2015, **13**, 4266-4270; (*e*) M. M. Watt, L. N. Zakharov, M. M. Haley, D. W. Johnson, *Angew. Chem. Int. Ed.* 2013, **52**, 10275-10280; (*f*) B. W. Tresca, L. N. Zakharov, C. N. Carroll, D. W. Johnson, M. M. Haley, *Chem. Commun.* 2013, **49**, 7240-7242.

10. J. V. Gavette, N. S. Mills, L. N. Zakharov, C. A. Johnson II, D. W. Johnson, M. M. Haley, *Angew. Chem. Int. Ed.* 2013, **52**, 10270-10274.

11. J. V. Gavette, C. J. Evoniuk, L. N. Zakharov, M. E. Carnes, M. M. Haley, D. W. Johnson, *Chem. Sci.* 2014, **5**, 2899-2905.

12. L. M. Eytel, A. K. Gilbert, P. Görner, L. N. Zakharov, D. W. Johnson, M. M. Haley, *Chem. Eur. J.* 2017, **23**, 4051-4054.

13. (*a*) P. Thordarson, *Chem. Soc. Rev.* 2011, **40**, 1305-1323; (*b*) F. Ulatowski, K. Dąbrowa, T. Balakier, J. Jurczak, *J. Org. Chem.* 2016, **81**, 1746-1756; (*c*) http://supramolecular.org/

14. The change in ε at wavelengths attributed to the HG absorbing species (265, 290, and 345 nm for **3**) also resulted in similar association constants across all three anions.

15. D. H. Ripin, D. A. Evans, Evans pK_a Table. http://evans.rc.fas.harvard.edu/pdf/evans_pKa_table.pdf (accessed March 2018).

16. (*a*) Y. Marcus, *Chem. Rev.* 1988, **88**, 1475-1498; (*b*) Y. Marcus, H. D. B. Jenkins, L. Glasser, J. *Chem. Soc., Dalton Trans.* 2002, 3795-3798.

17. DFT (PBE/6-31G*) geometry optimizations were performed in gas phase, water, DMSO, and $CHCl_3$. Grimme's empirical dispersion correction (D3) with and without the Becke Johnson damping parameters (BJ) were also applied. Energy refinements were performed at the PBE and M06-2X in gas phase as well as in solvent using PCM for water, DMSO, and $CHCl_3$. All methods resulted in trends similar to the pK_a trend.

18. A. Jouyban, S. Soltanpour, *J. Chem. Eng. Data*, 2010, **55**, 2951-2963.

19. (a) J. P. Perdew, K. Burke, M. Ernzerhof, *Phys. Rev. Lett.* 1996, **77**, 3865–6868. (b) J. P. Perdew, K. Burke, M. Ernzerhof, *Phys. Rev. Lett.* 1997, **78**, 1396.

20. S. Grimme, S. Ehrlich, L. Goerigk. *J. Comput. Chem.* 2011, **32**, 1456–1465.

21. The PyMOL Molecular Graphics System, Version 1.7.4.2 Schrödinger, LLC.

Chapter IV

1. a) Umali, A. P.; Anslyn, E. V. *Curr. Opin. Chem. Bio.* **2010**, *14*, 685-692; b) Diehl, K. L.; Anslyn, E. V. *J. Am. Chem. Soc.* **2013**, *42*, 8596-8611; c) Anzenbacher, P.; Liu, Y.; Palacios, M. A.; Minami, T.; Wang, Z.; Nishiyabu, R. *Chem. Eur. J.* **2013,** *19*, 8497-8506.

2. Stewart, S.; Ivy, M. A.; Anslyn, E. V. Chem. Soc. Rev. **2014**, *43*, 70-84.

3. Examples of recent work: a) Gavette, J. V.; Evoniuk, C. J.; Zakharov, L. N.; Carnes, M. E.; Haley, M. M.; Johnson, D. W. *Chem. Sci.* **2014**, *5*, 2899-2905; b) Engle, J. M.; Carroll, C. N.; Johnson, D. W.; Haley, M. M. *Chem. Sci.* **2012**, *3*, 1105-1110; c) Watt, M. M.; Engle, J. M.; Fairley, K. C.; Robitshek, T. E.; Haley, M. M.; Johnson, D. W. *Org. Biomol. Chem.* **2015**, *13*, 4266-4270; d) Hartle, M. D.; Hansen, R. J.; Tresca, B. W.; Prakel, S. S.; Zakharov, L. N.; Haley, M. M.; Pluth, M. D.; Johnson, D. W. *Angew. Chem. Int. Ed.* **2016**, *55*, 11480-11484; e) Watt, M. M.; Zakharov, L. N.; Haley, M. M.; Johnson, D. W. *Angew. Chem. Int. Ed.* **2013**, *52*, 10275-10280; f) Tresca, B. W.; Hansen, R. J.; Chau, C. V.; Hay, B. P.; Zakharov, L. N.; Haley, M. M.; Johnson, D. W. *J. Am. Chem. Soc.* **2015**, *137*, 14959-14967; l) Eytel, L. M.; Brueckner, A. C.; Lohrman, J. A.; Haley, M. M.; Cheong, P. H.-Y.; Johnson, D. W. L. M. Eytel, A. C. Brueckner, J. A. Lohrman, M. M Haley, P. H.-Y. Cheong, and D. W. Johnson, *Chem. Commun.* **2018**, *54*, 13208-13211; k) Lohrman, J. A.; Deng, C.-L.; Shear, T. A.; Zakharov, L. N.; Haley, M. M.; Johnson, D. W. *Chem. Commun.* **2019**, *55*, 1919-1922.

4. Carroll, C. N.; Coombs, B. A.; McClintock, S. P.; Johnson II, C. A.; Berryman, O. B.; Johnson, D. W.; Haley, M. M. *Chem. Commun.* **2011**, *47*, 5539-5541.

5. Tresca, B. W. PhD. Dissertation, University of Oregon, 2016.

Chapter V

American Association for the Advancement of Science. *Vision and change in undergraduate biology education: A call to action.* Report edited by Brewer C & Smith D. Washington, D.C.: American Association for the Advancement of Science, 2011. Accessed March 2019: http://visionandchange.org/files/2011/03/Revised-Vision-and-Change-Final-Report.pdf

Anderson, M., Hitlin, P., & Atkinson, M. "Wikipedia at 15: Millions of readers in scores of languages." *Pew Research Center*. Last modified January 14, 2016. Accessed March 2019. https://www.pewresearch.org/fact-tank/2016/01/14/wikipedia-at-15/

Anslyn, E.V. & Dougherty, D.A. *Modern Physical Organic Chemistry.* Herndon, VA: University Science Books, 2006.

Association of American Medical Colleges & Howard Hughes Medical Institute. *Scientific foundations for future physicians.* Washington, D.C.: Association of American Medical Colleges, 2009. Accessed March 2019: https://www.aamc.org/download/271072/data/scientificfoundationsforfuturephysicians.pdf

Australian Learning & Teaching Council. *Learning and teaching academic standards project: Science learning and teaching academic standards statement.* Report prepared by Jones, S., Yates, B., & Kelder, J.A. New South Wales, Australia: 2011. Accessed March 2019: http://www.acds-tlcc.edu.au/wp-content/uploads/sites/14/2015/02/altc_standards_SCIENCE_240811_v3_final.pdf

Baram-Tsabari, A. & Lewenstein, B.V. "Science communication training: what are we trying to teach?" *International Journal of Science Education, Part B* 7, no. 3 (2017): 285-300. doi: 10.1080/21548455.2017.1303756

Baram-Tsabari, A. & Osborne, J. "Bridging science education and science communication research." *Journal of Research in Science Teaching* 52, no. 2 (2015): 135-144. doi: 10.1002/tea.21202

Blanchard, A. "The importance of science communication." *Optical Society of America*. Last modified October 11, 2017. Accessed March 2019. https://www.osa.org/en-us/the_optical_society_blog/2017/october/the_importance_of_science_communication/

Brownell, S.E., Price, J.V., & Steinman, L. "Science communication to the general public: Why we need to teach undergraduate and graduate students this skill as part of their formal scientific training." *The Journal of Undergraduate Neuroscience Education* 12, no. 1 (2013): E6-E10.

Burns, T.W., O'Connor, D.J., & Stocklmayer, S.M. "Science communication: A contemporary definition." *Public Understanding of Science* 12, no. 2 (2003): 183-202. doi: 10.1177/09636625030122004.

Gardner, G.E., Jones, M.G., Albe, V., Blonder, R., Laherto, A., Macher, D., & Paechter, M. "Factors influencing postsecondary STEM students' views of the public communication of an emergent technology: A cross-national study from five universities." *Research in Science Education* 47, 5 (2017): 1011-1029. doi: 10.1007/s11165-016-9537-7

Grange, I.R.-l. & Retief, L. "Action research: Integrating chemistry and scientific communication to foster cumulative knowledge building and scientific communication skills." *Journal of Chemical Education* 95, no. 8 (2018): 1284-1290. doi: 10.1021/acs.jchemed.7b00958

Higgins, P.A.T., Chan, K.M.A., & Porder, S. "Bridge over a philosophical divide." *Evidence & Policy* 2, no. 2 (2006): 249-255.

LLadós-Masllorens, J., Aibar, E., Meseguer-Artola, A., Minguillón, J., & Lerga, M. "Explaining teaching uses of Wikipedia through faculty personal and contextual features." *Online Information Review* 41, no. 5 (2017): 728-743. doi: 10.1108/OIR-10-2016-0298

Martineau, E. & Boisvert, L. “Using Wikipedia to develop students’ critical analysis skills in the undergraduate chemistry curriculum.” *Journal of Chemical Education* 88, no. 6 (2011): 769-771. doi: 10.1021/ed100017k.

Mandler, M.D. “Glaring chemical errors persist for years on Wikipedia.” *Journal of Chemical Education* 94 (2017): 271-272. doi: 10.1021/acs.jchemed.6b00478

Mercer-Mapstone, L. & Kuchel, L. “Teaching scientists to communicate: Evidence-based assessment for undergraduate science education.” *International Journal of Science Education* 37, no. 10 (2015): 1613-1638. doi: 10.1080/09500693.2015.1045959

Nadkarni, N.M. & Stasch, A.E. “How broad are our broader impacts? An analysis of the National Science Foundation’s ecosystem studies program and the broader impacts requirement.” *Frontiers in Ecology and the Environment* 11, no. 1 (2013): 13-19. doi: 10.1890/110106

National Science Board. *Communication science and technology in the public interest*. NSB-00-99. Alexandria, VA: National Science Foundation, 2000. Accessed March 2019 https://www.nsf.gov/nsb/documents/2000/nsb0099/nsb0099.pdf

Parkman, A. “The imposter phenomenon in higher education: Incidence and impact.” *Journal of Higher Education Theory and Practice* 16, no. 1 (2016): 51-60.

Sternberger, A. L. & Wyatt, S. E. “Wikipedia in the science classroom.” *CourseSource* 5 (2018): 1-7. doi: 10.24918/cs.2018.14